Title

Aspects of Conformal Field Theories: Entanglement, Tau Function and Black Hole Perturbation

Author

Jia, Hewei

Publication Date

2024

Peer reviewed|Thesis/dissertation

Aspects of Conformal Field Theories:
Entanglement, Tau Function and Black Hole Perturbation

By

HEWEI (FREDERIC) JIA
DISSERTATION

Submitted in partial satisfaction of the requirements for the degree of

DOCTOR OF PHILOSOPHY

in

Physics

in the

OFFICE OF GRADUATE STUDIES

of the

UNIVERSITY OF CALIFORNIA

DAVIS

Approved:

Veronika Hubeny, Chair

Mukund Rangamani

Jaroslav Trnka

Committee in Charge

2024

Contents

Abstract

The dissertation is concerned with various physical properties and mathematical applications of conformal field theories. The relevant conformal field theories include both holographic CFT_d with $d \geq 2$ and generic non-holographic CFT_2. The dissertation is divided into three parts.

In Part I, we study information-theoretic properties of entanglement entropies of holographic CFT_d. In particular, we study holographic entropy inequalities and their structural properties by making use of a judicious grouping of terms into certain multipartite information quantities. This results in the discovery of both new inequalities and considerably simpler forms for known inequalities. We also obtain a negative result on the interpretation of quantum information quantities associated with certain holographic entropy inequalities as correlation measures.

In Part II, we study twist operators in CFT_2 and their relation with both physical and mathematical objects. In Chapter 3, we formulate a generalized stress-tensor method for twist operator correlators (TOCs) and utilize it to establish a precise relation between TOCs and certain tau functions associated with branched covers of $\mathbb{P}^1$. This bypasses certain issues in the conventional stress-tensor method and further clarifies the mathematical nature of TOCs. In Chapter 4, we introduce a novel representation for TOCs and their associated tau functions by utilizing properties of ground state modular Hamiltonians in CFT_2. The connection with modular Hamiltonian originates from the formal path integral representation of the ground state reduced density matrix in CFT_2. For a class of genus-zero TOCs, we also argue an approximate factorization property, utilizing the known ground state correlation structure of large-c holographic CFT_2 and the universality of genus-zero TOCs. We provide numerical checks of our statements in various examples.

In Part III, we study an exact CFT_2 method for black hole perturbation problem in AdS_{d+1}, which is in turn dual to thermal correlators of holographic CFT_d. In particular, we refine and

further develop a recent exact analytic approach to black hole perturbation problem based on the semiclassical Virasoro blocks, or equivalently via AGT relation, the Nekrasov partition functions in the Nekrasov-Shatashvili limit. Focusing on asymptotically AdS_5 black hole backgrounds, we derive new universal exact expressions for holographic thermal two-point functions and quantization conditions for the associated quasinormal modes (QNMs). Our expressions for the holographic CFT_4 closely resemble the well-known results for 2d thermal CFTs on $\mathbb{R}^{1,1}$. This structural similarity stems from the locality of fusion transformation for Virasoro blocks. We provide numerical checks of our quantization conditions for QNMs. Additionally, we discuss the application of our results to understand specific physical properties of QNMs, including their near-extremal and asymptotic limits. The latter is related to a certain large-momentum regime of semiclassical Virasoro blocks dual to Seiberg-Witten prepotentials.

Attributions

The main contents of the dissertation are based on the following papers:

- Chapter 2 is based on [HHJ23], in collaboration with Sergio Hernández-Cuenca and Veronika Hubeny.
- Chapter 3 is based on [Jia23a].
- Chapter 4 is based on [Jia23b].
- Chapter 5 is based on [JR24], in collaboration with Mukund Rangamani.

Acknowledgments

I am grateful to my advisor Veronika Hubeny and other members of the FSG group for their support. I would also like to thank my collaborators, including Sergio Hernández-Cuenca, Veronika Hubeny and Mukund Rangamani, for sharing their insights on physics.

Common Acronyms

AdS$_d$ d-dimensional (asymptotically) anti-de Sitter spacetime

CFT$_d$ d-dimensional conformal field theory

HEC holographic entropy cone

HEI holographic entorpy inequality

MMI monogamy of mutual information

OPE operator product expansion

QFT quantum field theory

QI quantum information

QNM quasinormal mode

TOC twist operator correlator

1. Introduction

The dissertation is divided into three parts, dealing with the following distinct yet interrelated topics:

- Part I : Holographic Entanglement
- Part II : Twist Operators In CFT_2: From Entanglement To Tau Function
- Part III : Exact CFT_2 Method For Black Hole Perturbation

The aim of the current introduction is to provide a broader context to which these topics belong, complementary to the more specific introductions provided at the beginning of each chapter.

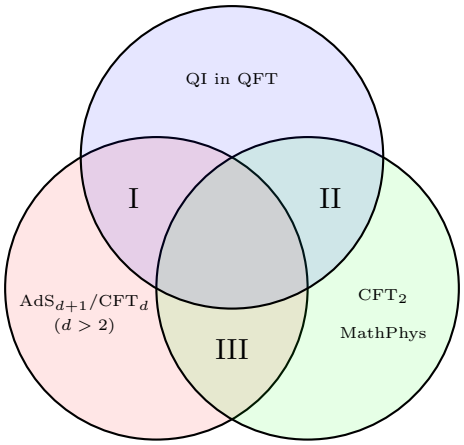

Figure 1.1.: Illustration of the different areas that the Parts I to III lie at intersections of.

As illustrated in Fig. 1.1, the Parts I to III lie at the intersections of the following three areas:

- AdS/CFT and its applications to strongly-coupled CFT
- CFT_2 and its applications in theoretical/mathematical physics
- Quantum information in QFT

In the following, we give a brief overview of the areas and explain the relation with our works. In particular, the part on "Quantum information in QFT" includes some additional motivations for Part II not explicitly stated there.

1.1. Background

AdS/CFT and its applications to strongly-coupled CFT: The celebrated AdS/CFT correspondence [Mal98] is a concrete realization of the holographic principle of [t H93; Sus95]. The canonical example is the case of $\mathrm{AdS}_5/\mathrm{CFT}_4$, which posits the equivalence between type IIB superstring theory on $\mathrm{AdS}_5 \times S^5$ and 4d $\mathcal{N} = 4$ SYM with gauge group $SU(N)$. The two dimensionless parameters on string theory side, the string coupling g_{s} and the ratio between AdS length scale and string length $\ell_{\mathrm{AdS}}/\ell_{\mathrm{s}}$, are identified with the 't Hooft coupling λ and the rank of gauge group N on gauge theory side, as follows:

$$g_{\mathrm{s}} \sim \frac{\lambda}{N}, \quad \frac{\ell_{\mathrm{AdS}}}{\ell_{\mathrm{s}}} \sim \lambda^{\frac{1}{4}}. \tag{1.1.1}$$

While the equivalence is expected to hold true for generic parameters, the precise dictionary is best understood in the $N, \lambda \to \infty$ regime, which is obtained as follows. One first takes the planar limit $N \to \infty$ at fixed λ, which corresponds to $g_{\mathrm{s}} \to 0$ and therefore reduces quantum string theory to classical string theory. One then takes the strong coupling limit $\lambda \to \infty$, which corresponds to $\ell_{\mathrm{s}}/\ell_{\mathrm{AdS}} \to 0$ and therefore reduces classical string theory to classical supergravity.

In this regime, a precise formulation of the correspondence is given by the GKPW dictionary [GKP98; Wit98]. Schematically, the dictionary reads:

$$\exp\Big[- I_{\mathrm{sugra}}\left(\Phi_i\right)\Big]\Big|_{\Phi_i|_{\mathrm{bdy}}=\phi_i} = \left\langle \exp\left(\int_{\partial \mathrm{AdS}} \phi_i\, \mathcal{O}_i\right)\right\rangle_{\mathrm{CFT}}. \tag{1.1.2}$$

The RHS denotes the CFT generating functional for correlation functions of operators $\mathcal{O}_i$ with sources ϕ_i. The CFT state is typically the vacuum state or thermal state. On LHS, Φ_i denotes the bulk field in AdS, obtained from Kaluza-Klein reduction on S^5, dual to the CFT operator $\mathcal{O}_i$. For instance, scalar operators in CFT are dual to scalar field perturbation in AdS, while conserved currents in CFT such as stress-tensor and R-symmetry current are dual to metric and

gauge field perturbation. The I_{sugra} denotes the on-shell action of the bulk fields Φ_i, subject to suitable boundary condition $\Phi_i|_{\text{bdy}}= \phi_i$, on certain asymptotically AdS background. For CFT vacuum state, the dual geometry is pure AdS. For thermal state, there exists a phase transition in the bulk at finite volume [HP83], with dual geometry being Schwarzchild-AdS (thermal AdS) above (below) the critical temperature. The also exists generalization of the dictionary to Lorentzian signature, as will be explained more in Part III.

The crucial feature of AdS/CFT is that it is a strong-weak duality: in the $N, \lambda \to \infty$ regime, properties of strongly-coupled CFT can be extracted from classical (super)gravity, which is relatively simpler to study. Indeed, many holographic results regarding strongly-coupled CFT have thus been obtained. Perhaps one of the most remarkable ones is the holographic calculation of shear viscosity of strongly-coupled $\mathcal{N} = 4$ SYM plasma [PSS01; KSS05], which is otherwise inaccessible from standard CFT method. The upshot is an universal ratio of shear viscosity over entropy density for holographic CFT dual to Einstein gravity:

$$\frac{\eta}{s} = \frac{1}{4\pi}. \tag{1.1.3}$$

The result is extracted from a small frequency limit of holographic stress-tensor thermal correlators, which is in turn governed by black hole perturbation in AdS_5. However, it turns out that away from such small frequency regime, even the holographic computation becomes less within reach. In Part III, we will present further progress on analytically studying such black hole perturbation problem associated with holographic thermal correlators.

Entanglement entropy is another example of a physical quantity that is hard to compute in CFT in general, but admits a simple holographic description. The holographic entanglement entropy formula relates the entanglement entropy of a subregion A in the boundary CFT to the area of a certain extremal surface in the dual bulk geometry [RT06a; HRT07a]:

$$S_A = \frac{\text{Area}\,[\mathcal{E}_A]}{4G_N}. \tag{1.1.4}$$

Here the appropriate extremal surface $\mathcal{E}_A$ is minimized over all extremal surfaces in the bulk geometry homologous to the boundary subregion A. The formula may be viewed as a gener-

alization of the Bekenstein-Hawking entropy formula. The holographic entanglement entropy formula can be derived from the GKPW dictionary via the replica method for computing entanglement entropy [LM13; DLR16], and is known to obey information-theoretic properties (HEIs) satisfied by entanglement entropy in general [HT07; Wal14]. Furthermore, holographic entanglement entropy also satisfies an infinite number of additional constraints, the holographic entropy inequalities, that entanglement entropy in generic quantum states wouldn't satisfy. It remains an open question to understand their information-theoretic meanings, and some further progress will be discussed in Part I.

CFT$_2$ and its applications in theoretical/mathematical physics: Since the seminal work of [BPZ84], two-dimensional conformal field theory has found numerous applications in distinct areas of theoretical and mathematical physics, ranging from statistical physics to string theory. In the absence of extended symmetry, the symmetry algebra of 2d CFT is given by the Virasoro algebra

$$[L_m, L_n] = (m-n)L_{m+n} + \frac{c}{12}m(m^2-1)\delta_{m+n,0}. \tag{1.1.5}$$

Physically, this is equivalent to the transformation property of stress-tensor, and the central charge c is related to conformal anomaly.

In general, two different types of data enter into physical observables in 2d CFT: i) theory-specific CFT data, viz., spectrum and OPE coefficients, and ii) universal data entirely determined by symmetry algebra such as conformal anomaly and Virasoro block. In CFT, the first type of data is subject to highly constrained self-consistent conditions from crossing symmetry and modular invariance. It is still an open problem to obtain its full classification, especially for $c > 1$.

It is the second type of data that will play a major role in our discussions in Parts II and III. Despite being fixed entirely by symmetry algebra, these universal data enjoy rather non-trivial mathematical properties. For instance, while the Virasoro block in general doesn't admit closed-form expression, the associated fusion matrix, which is essentially a change of basis in the space of conformal block, turns out to admit highly non-trivial closed-form expression. The finite-dimensional case is worked out in [MS89a] and the infinite-dimensional case in [PT99]. A recent application of the infinite-dimensional fusion matrix is to obtain universal OPE statistics

involving heavy operator [CMMT20], viz., the analog of Cardy's formula [Car86] for OPE coefficients. The finite-dimensional case, together with a semiclassical large-c limit, will play an important role in Part III.

Besides their intrinsic interests in relation with physical observables in CFT, these universal data also find applications in many other areas of theoretical and mathematical physics. For instance, there is a close relation between Virasoro blocks and mathematical topics such as Painlevé equation [ILT13; LLNZ14] and isomonodromic tau function [ILT15]. In Part II, we will discuss a relation between the conformal anomaly arising from certain path integral associated with branched covers of $\mathbb{P}^1$, a construction that arises in various physical contexts, and a notion of tau function associated with such branched covers [KK04].

Moreover, the AGT correspondence [AGT10], which relates Nekrasov partition function in certain 4d $\mathcal{N} = 2$ gauge theory to Virasoro block, provides yet another physical context where CFT_2 finds important applications. For instance, the known fusion transformation of Virasoro block has been utilized to verify S-duality transformation in the gauge theory side [Tes16]. We will also touch upon certain aspect of AGT relation in Part III.

Quantum information in QFT: Concepts in quantum information theory have recently found a wide range of applications in theoretical physics, both in the context of quantum many-body system [ZCZW19] and quantum field theory [Nis18]. Two of the most basic ingredients in quantum information theory are entanglement entropy and relative entropy, a special case of which is mutual information, a canonical correlation measure. While such quantum information quantities are straightforward to define and compute in quantum lattice systems, they turn out to be rather subtle in quantum field theory.

In fact, there exists two distinct definitions of QI quantities in QFT. One is based on the formal Euclidean path integral representation of the reduced density matrix, which eventually recasts the computation of certain one-parameter generalized, viz. Rényi , version of QI quantities to a QFT partition function, subject to a further analytic continuation procedure [CC04; Las14]. The other is based on the algebraic QFT definition in terms of von Neumann algebra [HS17; Wit18]. Both approaches have their shortcomings. While the path integral approach allows

explicit computation for Rényi QI quantities[1] in certain examples via standard QFT method, the analytic continuation in general poses a challenge [CCT09]. On the other hand, while the von Neumann algebra approach is rigorous and makes manifest important information-theoretic properties such as monotonicity of relative entropy, it typically resists explicit computation. Furthermore, there is no general understanding on if the two approaches are equivalent.

For instance, besides the large N holographic set-up relevant for the investigations in Part I, the only known exact result of mutual information of disjoint regions in QFT to date is in the case of 2d chiral free fermion [CH09], where in fact an alternative method suitable for free QFT, the continuum generalization of the correlation matrix method on lattice [Pes03], is utilized instead of the more general path integral method. The result in this case does turn out to be justifiable from the von Neumann algebra perspective [LX18].[2]

It is therefore the original motivation for the investigations in Part II to understand better the explicit computation of QI quantities, via the path integral approach, in one of the simplest yet non-trivial QFT set-up of CFT_2. The main obstacle for computing mutual information in CFT_2 is that the continuation in Rényi index would involve a continuation in the genus of CFT partition function [CCT09], which is challenging to perform. However, if one defines an appropriate Rényi mutual information [3] using suitable notions of Rényi relative entropy (see e.g. [KW20]), then for certain parameters the Rényi mutual information would only involve a partition function at fixed genus, e.g., $g = 1$, still with certain continuation to be performed. The tradeoff is that now the partition function is associated with a branched cover with non-abelian monodromy group, unlike the standard cyclic case, and one would need to perform certain continuation in the monodromy data of such branched cover.

This, unfortunately, also turns out to be a challenging problem. In fact, as will be elaborated more in Chapter 3, even in the genus-zero case which is of more relevance for some other physical context, there is no simple way of explicitly computing the partition function associated with prescribed non-abelian monodromy data. In such case, the quantum information

[1] These Rényi QI quantities usually lack important QI properties. For instance, the Rényi mutual information defined using Rényi entropy is not monotonic under region inclusion in general.

[2] There also exists a generalization of the result to free boson in physics literature [ACHP18], but a derivation from von Neumann algebra perspective has not yet appeared.

[3] A very preliminary discussion of this concept has since appeared in literature [Kud23], with no essential insight provided on the non-trivial situation with disjoint regions.

perspective turns out to yield a different method for computing such partition function, utilizing known universal property of modular Hamiltonian of single interval [CT16]. This is the content of Chapter 4.

1.2. Selected results

We point to the following results highlighted in the main text:

- A negative result on the interpretation of quantum information quantities associated with certain holographic entropy inequalities as correlation measures; see Theorem 2.4.1 in Chapter 2. This result precludes a certain information-theoretic interpretation for HEIs.

- A precise relation between correlation functions of twist operators in CFT_2 and a notion of tau functions associated with branched covers of $\mathbb{P}^1$; see Theorem 3.3.1 in Chapter 3. This result further clarifies the mathematical nature of TOC by associating it with a canonical algebro-geometric object.

- A novel way of computing certain TOCs in CFT_2 and their associated tau functions utilizing properties of ground state modular Hamiltonians; see Claim 4.3.1 in Chapter 4. This result provides a new physical perspective on these TOCs associated with branched covers.

- New exact universal expressions for holographic thermal correlators in AdS_5 and quantization conditions of the associated QNMs in terms of semiclassical Virasoro blocks; see (5.4.21) and (5.4.24) in Chapter 5. These results uncover new analytic structures of holographic thermal correlators and QNMs.

We refer to the main contents of each chapter for more complete summary of results and discussions.

Note: Statements/expressions highlighted with colored background indicates particularly important original results of our works. Some boxed expressions, on the other hand, are not original but emphasized due to their importance.

Part I.

Holographic Entanglement

2. Holographic entropy inequalities and multipartite entanglement

2.1. Introduction

Holographic entropy inequalities (HEIs) restrict the entanglement structure of geometric states of any holographic CFT, beyond what would be allowed for a generic quantum state. As such, HEIs provide some indirect insight into the emergence of spacetime and dynamical gravity, as well as the underlying workings of the holographic dictionary. Although presently we do not have the full set of HEIs for $\mathsf{N} \geq 6$ parties, in this work we have developed powerful heuristics which have allowed us to collect a set of 1877 HEI orbits for $\mathsf{N} = 6$. However, when written out in terms of subsystem entropies, these quantities appear rather lengthy and uninformative;[1] this is the case already for $\mathsf{N} = 5$, cf. table 2.1. Just by looking at these expressions, it is completely unclear what message they convey or what is the underlying principle they emerge from.

Recently the viewpoint that part of the complexity stems from fixing a definite value of N was suggested by [HHR22b], which showed that (subject to certain assumptions) these HEIs can be extracted from the solution to a much simpler problem (namely a part of the "holographic marginal independence problem" [HHRR19] of characterizing all the holographically admissible sets of simultaneously decorrelated subsystems) for a more refined partition $\mathsf{N}' \geq \mathsf{N}$. However, while conceptually appealing, the underlying construction utilized extreme rays of entropy cones, whereas the question of interest here concerns the facets of such cones. Since the passage between

[1] Other renditions, in the so-called I-basis (based on multipartite information quantities I_n) and K-basis (based on even-party perfect tensors) have been explored in [HHH19]. Although the I and K basis representations are more compact and have a number of advantages, they only reduce the number of terms appearing in the expressions by roughly a factor of two.

the representation of a polyhedral cone in terms of its extreme rays and the representation in terms of its facets is computationally hard, the insight of [HHR22b] does not directly address the initial question of what the individual N-party HEIs mean physically for a given fixed N. Correspondingly, it would be desirable to obtain a re-packaging which elucidates their physical meaning in a more manifest way. This motivated the present exploration, in which we do present a more compact form, but more importantly a no-go theorem for a certain natural interpretation.

The program of elucidating HEIs has proceeded primarily by examining the structural properties of the holographic entropy cone (HEC), first defined in [BNOSSW15] and subsequently explored from several different angles [MRW17; RW18; CHHHSW19; HRR18; BM18; HRR19; Her19; CD19; HHRR19; HHR20; BCHS20a; BCHS20b; AHR21; AH23; BCHS22; CW23; HHR22a; HHR23; HHK23]. The HEC can be naturally described as a convex hull of the most extremal holographic entropy vectors, namely the *extreme rays*, or equivalently in terms of the tightest HEIs that bound it, namely the *facets*. Inequalities which can be obtained as conical combinations of other HEIs are redundant and uninteresting. Facet-defining HEIs are a special set of non-redundant ones. To distinguish them one should consider the dimensionality of the space of saturating entropy vectors. More explicitly, any linear entropy inequality $Q \geq 0$ specifies a half-space bounded by the hyperplane $Q = 0$. A HEI defines a facet of the HEC if and only if there exists a codimension-1 set of linearly independent holographic entropy vectors for which $Q = 0$. The facets of the HEC thus single out a special set of such sign-definite objects in holography which is important to understand further.

From here on, we reserve the term HEI to indicate this facet-defining set of holographic inequalities, and we will refer to the associated sign-definite, non-redundant linear combinations of entropies as *information quantities*. Entropy vectors in the codimension-1 interior of any one facet will give strictly positive values for any other such information quantity. Because these information quantities are sign-definite and can all vanish independently of the others, it is tempting to view them as characterizing some sort of multipartite measures of correlations in holographic systems.

This expectation is of course borne out for a small but crucial subclass of HEIs, namely the mutual information quantities $I_2(\mathrm{X} : \mathrm{Y})$ measuring the total amount of correlation between

disjoint subsystems X and Y. The non-negativity of mutual information is the statement of subadditivity (SA),

$$I_2(\mathrm{X}:\mathrm{Y}) \equiv \mathtt{S}(\mathrm{X}) + \mathtt{S}(\mathrm{Y}) - \mathtt{S}(\mathrm{XY}) \geq 0 \ , \tag{2.1.1}$$

where $\mathtt{S}(\mathrm{X})$ denotes the entropy of X (and similarly for Y and $\mathrm{XY} := \mathrm{X} \cup \mathrm{Y}$). Structurally, the vanishing of the mutual information is indicative of the marginal independence property, that the common density matrix ρ_{XY} factorizes between the two subsystems, i.e. the marginals ρ_{X} and ρ_{Y}. The fact that the mutual information is a correlation measure not only justifies its non-negativity, but also the fact that this sign-definiteness is universal for any physical state.

Another universal statement, following from the mutual information being a correlation measure, is its monotonicity under inclusion. This property is known as strong subadditivity (SSA), and can be expressed as the non-negativity of conditional mutual information,

$$I_2(\mathrm{X}:\mathrm{Z}\,|\,\mathrm{Y}) \equiv I_2(\mathrm{X}:\mathrm{YZ}) - I_2(\mathrm{X}:\mathrm{Y}) \geq 0 \ . \tag{2.1.2}$$

Structurally, SSA saturation is associated with a quantum Markov chain [HJPW04], which plays a crucial role in quantum error correction. However, holographically, SSA is redundant, being superseded by the monogamy of mutual information (MMI), which can be expressed as the negativity of tripartite information, $I_3(\mathrm{X{:}Y{:}Z})$

$$-I_3(\mathrm{X{:}Y{:}Z}) \equiv I_2(\mathrm{X}:\mathrm{YZ}) - I_2(\mathrm{X}:\mathrm{Y}) - I_2(\mathrm{X}:\mathrm{Z}) \geq 0 \ . \tag{2.1.3}$$

While MMI can be violated by certain quantum states, it is satisfied by all geometric states in holography [HHM13], and thereby offers an intriguing insight about the entanglement structure of such states.

These simple classes of HEC facets prompt us to seek a similarly evocative explanation of the other facets, ideally as a correlation measure or perhaps as some conditional quantity to which one could give an operational interpretation. However, this quest is hindered by the structural complexity of the HEC growing rather quickly with the number of parties $\mathtt{N}$. The full HEC is symmetric under any relabeling of the parties including the purifier (referred to as permutations if they do not involve the purifier, and purifications if they do), so the set of

facets can be organized into symmetry orbits of a given representative instance of these HEIs. In absence of any symmetry structure for a given HEI, the number of instances of a given orbit grows factorially with N, and the number of facet orbits also grows rapidly: for $\mathsf{N} = 2, 3, 4, 5$ there are $1, 2, 3, 8$ orbits respectively, while for $\mathsf{N} = 6$ our search has yielded as many as 1877 facet orbits (including 11 distinct lifts from $\mathsf{N} \leq 5$), which gives a likely-modest lower bound on the actual number. Although a systematic constructive procedure for determining the full HEC by an iterative algorithm has been formulated in [AH23], the more fruitful method that has hitherto yielded all of these new HEIs has involved positing a structurally compact form for generating good candidate inequalities that we present in this chapter. For each such candidate one then uses the contraction map technique developed in [BNOSSW15] to check its validity, and then generates a suitable set of holographic entropy vectors to check if it is a facet.

To guess an obliging form for each HEI which might bring us closer to interpreting its information-theoretic meaning, we draw inspiration from the simple HEIs, namely the non-negativity of $I_2(\mathrm{X} : \mathrm{Y})$, $I_2(\mathrm{X} : \mathrm{Y} \,|\, \mathrm{Z})$, and $-I_3(\mathrm{X{:}Y{:}Z})$. In some sense, the next simplest form would be the conditional tripartite information $-I_3(\mathrm{X{:}Y{:}Z|W})$. Although as shown below, this quantity by itself is not sign-definite, it turns out that many HEIs do admit a rather compact form when decomposed into a combination of (conditional) tripartite information quantities for various composite subsystems, cf. table 2.1 for $\mathsf{N} = 5$ and table 2.2 for $\mathsf{N} = 6$. In one of the simplest cases, this recasting allows us to package a HEI into 2 terms as opposed to 13 terms when written in the S-basis. Besides providing a powerful heuristic for obtaining valid inequalities, we expect this efficient rendition of HEIs to bring us one step closer to a structural and qualitative understanding of their physical meaning.

To make this expectation more precise, we attempt to interpret the non-negative information quantities associated to HEIs as correlation measures, and explore whether they are monotonically non-increasing under partial-tracing (equivalently, non-decreasing under inclusion), as is the case with the mutual information. The main result of this chapter is a proof, in complete generality, that this is not possible. In particular, we prove that *none of the HEI information quantities besides the mutual information is monotonic under inclusion.* In other words, we can always find some holographic configuration for which shrinking some subsystem causes the information quantity to increase.

Our proof utilizes an important property of HEIs called *superbalance*. This was defined in [HRR19], and subsequently in [HHR20] it was shown that all non-SA HEIs must be superbalanced. This conveniently restricts the form that any HEI can take, so that when we consider the difference between the original information quantity and the corresponding quantity obtained by tracing out part of some subsystem, this difference can be shown to take either sign, even when restricted to the holographic context. More concretely, showing that it is not holographically sign-definite proceeds by expressing the difference in terms of a sum over conditional multipartite informations and by judicious sequential choice of states demonstrating that we can collapse this sum onto just a single term which itself can take either sign.

The outline of this chapter is as follows. In §2.2 we review the key properties of multipartite entanglement. We start in §2.2.1 by setting up our notation and terminology. Section 2.2.2 then defines the multipartite information I_n and presents a number of lemmas summarizing the properties which we will utilize below, while the short §2.2.3 analogously presents conditional multipartite information. All of these results can be derived straightforwardly from the basic definitions, but some of them simplify by using a certain structural property of the multipartite informations indicated in §2.A. In §2.3 we discuss the superbalance property of HEIs and its consequences, which paves the way to proving our main result in §2.4, namely that superbalance precludes monotonicity under inclusion. Having thus established that none of the higher HEIs act as correlation measures, we summarize our explorations of recasting the HEIs into a more compact form in §2.5, which also includes the tables of the non-uplift $\mathsf{N} = 5$ HEIs and selected representative subset of $\mathsf{N} = 6$ HEIs. This is accompanied by §2.B which explains how to obtain the compact forms starting from the standard representation. We end with a brief summary and discussion of future directions in §5.7.

2.2. Multipartite Entanglement

Hitherto, multipartite entanglement has remained a fascinating but poorly understood phenomenon at a quantitative level. The main obstacle resides already in the lack of meaningful measures of such correlations, or even a basic understanding of axiomatic properties these should reasonably satisfy. One of our goals in this chapter is to explore the possibility of interpreting

the information quantities associated to HEIs as multipartite correlation measures. To do so, in this section we begin by developing key aspects of the multipartite information and conditional multipartite information, which pave the way for a better reading of HEIs and their properties. To make the presentation notationally concise wherever possible, we will adopt several shorthand representations of the quantities of interest.

2.2.1. Notation and setup

The HEC is a geometrical construct in the entropy space $\mathbb{R}^{\mathsf{D}}$ with axes labeled by subsystem entropies. For N-party configuration, there are $\mathsf{D} = 2^{\mathsf{N}} - 1$ independent subsystems, consisting of all non-trivial collections of the individual parties.

We will label monochromatic subsystems (which we'll also refer to as *singletons*) by either letters $\mathrm{A}, \mathrm{B}, \mathrm{C}, \ldots$, or when we wish to enumerate them, a letter with subscript $\mathrm{A}_1, \mathrm{A}_2, \mathrm{A}_3$, etc.. As a notational shorthand, when working with N-party systems, we will denote the set of all parties by $[\mathsf{N}] \equiv \{1, 2, \ldots, \mathsf{N}\}$. A polychromatic system consisting of multiple monochromatic ones can be written out explicitly as e.g. AB. When referring to a general nonempty subsystem without needing to specify its singleton composition, our notation will be either a letter from the end of the alphabet such as $\mathrm{X}, \mathrm{Y}, \mathrm{Z}$ already employed above, or (for the sake of adhering to previously-established notation) $\mathcal{I}$, $\mathcal{J}$, ..., implicitly assumed to satisfy $\varnothing \neq \mathcal{I} \subseteq [\mathsf{N}]$. We can then use this index as a subscript on entropy, $\mathsf{S}_{\mathcal{I}}$, to denote the entropy of the joint polychromatic subsystem. Sometimes we will also wish to enumerate multiple polychromatic subsystems, in which case we will use a letter from the end of the alphabet with a subscript, e.g. $\mathrm{X}_1, \mathrm{X}_2, \mathrm{X}_3$, etc..

At times it will also be useful to refer to the complementary subsystem which purifies the state for N parties at hand. Labelling the purifier of an N-party system by $\mathsf{N}+1$, one may equivalently consider pure states on $\mathsf{N}+1$ parties. Subsystems which may involve the purifier will be decorated with an underline, $\underline{\mathcal{I}}$, $\underline{\mathcal{J}}$, ..., and throughout assumed to obey $\varnothing \neq \underline{\mathcal{I}} \subset [\mathsf{N}+1]$. An important property of the von Neumann entropy associated to this generalized notation is the fact that $\mathsf{S}_{\underline{\mathcal{I}}} = \mathsf{S}_{[\mathsf{N}+1]\setminus\underline{\mathcal{I}}}$ for all $\underline{\mathcal{I}}$, namely, that by purity of the full state, the entropy of a subsystem and that of its complement are identical.

The permutation symmetries that the HEC enjoys will be relevant to the study of general

information quantities as well. For N parties, the HEC is obviously symmetric under permutations of the party labels in $[\mathsf{N}]$, which are captured by the symmetric group Sym_{N}. These are referred to as the permutation symmetry of the HEC. In addition, by the purity property mentioned above, the full symmetry group of the HEC gets enhanced to $Sym_{\mathsf{N}+1}$ for permutations of $[\mathsf{N}+1]$ under the identification $\mathtt{S}_{\underline{\mathcal{I}}} = \mathtt{S}_{[\mathsf{N}+1]\setminus\underline{\mathcal{I}}}$ for all complementary subsystems. The set of permutations involving $\mathsf{N}+1$ are referred to as the purification symmetry of the HEC. Canonically, we will always use the purification symmetry to label entropies by the $2^{\mathsf{N}}-1$ subsets $\varnothing \neq \mathcal{I} \subseteq [\mathsf{N}]$ which do not involve $\mathsf{N}+1$.

When referring to multipartite information with n arguments, we write this abstractly as I_n; to indicate the explicit arguments, it is conventional to write them out explicitly as in $I_n(\mathrm{X}_1 : \mathrm{X}_2 : \ldots : \mathrm{X}_n)$ where the X_i's are mutually disjoint subsystems which can be monochromatic or polychromatic. When considering a collection of just monochromatic arguments, it will be notationally convenient to compress them into a single (decorated) polychromatic subsystem, which we will denote by an underdot like $\underset{\cdot}{\mathcal{I}}$ or a dotted underline as in $\underset{\cdot\cdot\cdot}{\mathrm{AB}}$. A further special case is when *all* the I_n arguments are monochromatic; since this is an important construct, we will use a dedicated notation and terminology for this case: we will call such an I_n a *singleton multipartite information* and emphasize this feature by a special font $\mathtt{I}_n$. Moreover if we want to specify the actual arguments, we can now use the combined polychromatic system as an index, in which case we drop the underdots and write simply $\mathtt{I}_{\mathcal{I}}$. (Note that in the latter case we can leave the number of arguments $n = |\mathcal{I}|$ implicit.) So for instance we can write interchangeably

$$\mathtt{I}_4(\mathrm{A} : \mathrm{B} : \mathrm{C} : \mathrm{D}) = \mathtt{I}_{\mathrm{ABCD}} = \mathtt{I}_4(\underset{\cdot\cdot\cdot}{\mathrm{AB}} : \mathrm{C} : \mathrm{D}) = \mathtt{I}_4(\mathrm{A} : \underset{\cdot\cdot\cdot\cdot}{\mathrm{BCD}}) \tag{2.2.1}$$

Although redundant, allowing ourselves this notational flexibility will enable us to present the arguments and HEI tables more cleanly.

2.2.2. Multipartite information

We now review the various salient properties of the multipartite information I_n. We start with the definition and structural aspects of these information quantities, and then proceed to discuss the values they can evaluate to for given classes of configurations.

I_n in terms of entropies: Using the notation established in §2.2.1, we can now write the multipartite information in terms of entanglement entropies quite compactly. Let us first specialize to the case where all the arguments are monochromatic. If the arguments comprise the polychromatic system $\mathcal{I}$, we can write the singleton multipartite information as

$$\mathtt{I}_{\mathcal{I}} = \sum_{\mathcal{K}\subseteq\mathcal{I}} (-1)^{|\mathcal{K}|+1}\, \mathtt{S}_{\mathcal{K}} \ , \tag{2.2.2}$$

where the usual sign convention is fixed so as to keep the singleton coefficients positive. For example, for the tripartite information this would give

$$\mathtt{I}_{\mathrm{ABC}} = \mathtt{S}_{\mathrm{A}} + \mathtt{S}_{\mathrm{B}} + \mathtt{S}_{\mathrm{C}} - \mathtt{S}_{\mathrm{AB}} - \mathtt{S}_{\mathrm{AC}} - \mathtt{S}_{\mathrm{BC}} + \mathtt{S}_{\mathrm{ABC}} \tag{2.2.3}$$

and so forth. Once written out in the form eq. (2.2.2), we can straightforwardly replace the monochromatic arguments by polychromatic ones, e.g.

$$I_3(\mathrm{A}:\mathrm{B}:\mathrm{CD}) = \mathtt{S}_{\mathrm{A}} + \mathtt{S}_{\mathrm{B}} + \mathtt{S}_{\mathrm{CD}} - \mathtt{S}_{\mathrm{AB}} - \mathtt{S}_{\mathrm{ACD}} - \mathtt{S}_{\mathrm{BCD}} + \mathtt{S}_{\mathrm{ABCD}} \tag{2.2.4}$$

(Note the change of font on the I_3 indicates that this is no longer a singleton multipartite information.)

$\mathtt{I}_n$ basis: Let us consider the set of all singleton multipartite informations $\mathtt{I}_{\mathcal{I}}$ (i.e. those with only monochromatic arguments). There are precisely D of them, the same as the number of independent entropies, and hence the dimensionality of the entropy space. Indeed, as argued in [HRR19; HHH19], the set of all $\mathtt{I}_{\mathcal{I}}$'s form a basis for the entropy space, referred to as the "I-basis", to distinguish it from the "S-basis" representation in terms of the entropies. This means that we can express any information quantity in terms of these multipartite informations. For example, the entropies themselves are obtained very simply by inverting eq. (2.2.2), which is in fact captured by an involutory matrix:

$$\mathtt{S}_{\mathcal{I}} = \sum_{\mathcal{K}\subseteq\mathcal{I}} (-1)^{|\mathcal{K}|+1}\, \mathtt{I}_{\mathcal{K}} \ . \tag{2.2.5}$$

I_n in terms of other I_m's: It will be useful to express the multipartite information with polychromatic arguments in the I-basis as well, and conversely, to express $\mathtt{I}_n$ in terms of I_m's with smaller m but polychromatic arguments. To obtain such relations, we will make use of the underlying symmetries of multipartite information. From eq. (2.2.2) we can easily see that any $\mathtt{I}_{\mathcal{I}}$ is symmetric under permuting its arguments. In fact it has a much larger symmetry since all the coefficients are ± 1 depending on the parity of the size of the term. Indeed, this has an iterative structure which is manifest in a "notationally-factorized" form presented in §2.A. This notation enables us to obtain the following relations straightforwardly.

First of all, we can build up higher multipartite informations, say I_{n+1}, from a combination of lower ones, say I_n's, but at the cost of invoking polychromatic arguments. In particular, using the shorthand notation indicated above in eq. (2.2.1) with $\dot{\mathcal{I}}$ comprising $n-1$ singletons distinct from A or B, we have, for any n,

$$\mathtt{I}_{n+1}(\mathrm{A}:\mathrm{B}:\dot{\mathcal{I}}) = \mathtt{I}_n(\mathrm{A}:\dot{\mathcal{I}}) + \mathtt{I}_n(\mathrm{B}:\dot{\mathcal{I}}) - I_n(\mathrm{AB}:\dot{\mathcal{I}}) \tag{2.2.6}$$

which by permutation symmetry on the arguments of I_n applies for any positions of A and B. We can furthermore "fine-grain" any singleton(s) into polychromatic subsystem(s), to obtain any I_{n+1} in terms of I_n's. We can then iterate eq. (2.2.6) further, to express any I_n in terms of a collection of I_m's for any smaller m, so in particular there is a multitude of ways we can express any I_m purely in terms of just mutual informations I_2 between various polychromatic subsystems. The special case of $n = 2$ was already utilized in eq. (2.1.3). Conversely, we can iterate eq. (2.2.6) to express multipartite information with polychromatic arguments in the I-basis. We will make explicit use of these relations to obtain a compact recasting of the HEIs in §2.B.

I_n values: Having defined the multipartite information I_n in the preceding subsection, we now consider the actual values it can take for a given configuration. Recall that by SA (eq. (2.1.1)), the mutual information I_2 for any two subsystems is always non-negative and vanishes when the subsystems are uncorrelated, and by MMI (eq. (2.1.3)) the tripartite information I_3 between any three subsystems is non-positive and likewise vanishes when the subsystems are uncorrelated.

In this subsection we will show that while the sign-definiteness does not extend to any higher n (for $n = 4, 5$ this was already observed in [HHM13] and noted for general n in [HRR19]), the feature of vanishing on decorrelated states does generalize to all I_n's.

We start with the latter part which is more immediate. Of course if all the n subsystems invoked by I_n were pairwise decorrelated from each other, then we could rewrite I_n in terms of just I_2's and apply the above SA saturation result to each term. We can however drastically relax the requirement to obtain a much stronger statement: for the n-partite information I_n to vanish, it suffices for any subsystem comprising a subcollection of its arguments to be decorrelated from the remainder.

Lemma 2.2.1. *$I_n(\mathrm{X}_1 : \ldots : \mathrm{X}_n)$ vanishes on any product state of the form*

$$\rho_{\mathrm{X}_1 \ldots \mathrm{X}_n} = \pi_{\mathcal{J}} \otimes \sigma_{\mathcal{K}},$$

with $\mathcal{J}$ and $\mathcal{K}$ composed of complementary subsets of the X_i subsystems.

Proof. For this proof, polychromatic subsystems X_i can be treated as irreducible monochromatic subsystems A_i, since the sub-parties of each X_i will play no role. Therefore, consider $I_{[n]}$ evaluated on some state $\rho_{[n]}$. A product state $\rho_{[n]}$ admits a bipartition, i.e., $[n] = \mathcal{J} \cup \mathcal{K}$ with $\mathcal{J} \cap \mathcal{K} = \varnothing$, such that

$$\rho_{[n]} = \pi_{\mathcal{J}} \otimes \sigma_{\mathcal{K}} \,. \tag{2.2.7}$$

Entropies evaluated on ρ then satisfy

$$\mathtt{S}(\mathcal{J} \cup \mathcal{K}) = \mathtt{S}(\mathcal{J}) + \mathtt{S}(\mathcal{K}), \qquad \forall \mathcal{J} \subseteq \mathcal{J}, \mathcal{K} \subseteq \mathcal{K}. \tag{2.2.8}$$

When substituted into eq. (2.2.2), it is easy to verify that $I_{[n]}$ reduces to

$$I_{[n]}\big|_{\rho} = \alpha(\mathcal{K})\, I_{\mathcal{J}}\big|_{\pi} + \alpha(\mathcal{J})\, I_{\mathcal{K}}\big|_{\sigma} \tag{2.2.9}$$

with coefficient $\alpha(\cdot)$ given by

$$\alpha(\mathcal{I}) = \sum_{k=0}^{|\mathcal{I}|} (-1)^k \binom{|\mathcal{I}|}{k} = 0 \,. \tag{2.2.10}$$

This shows that the multipartite information vanishes on any system whose density matrix can be written as a product between the density matrices of two systems. □

Let us now consider the case when the composite argument in I_n comprises a density matrix which does not factorize (or factorizes in a way which does not 'align' with the n-partition considered above). Does the sign of I_n get fixed for any $n > 3$? To see that the answer is *no*, it suffices to produce two configurations, one for which I_n is positive and another for which it is negative. While we could certainly do this with explicit holographic geometries, it is even easier to produce such examples using the toolkit of holographic graph models.[2]

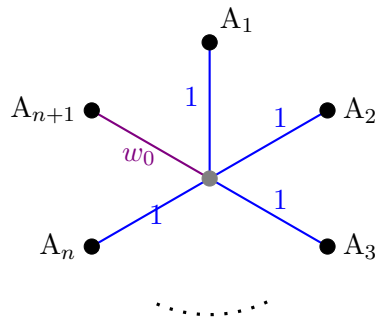

Figure 2.1.: Star graph with n edge weights fixed to 1 and the remaining edge weight to some $w_0 > 0$. Depending on the value of w_0, $\mathtt{I}_{[n]}$ evaluated on this graph can take either sign.

Lemma 2.2.2. *I_n with $n \geq 4$ is not holographically sign-definite.*

Proof. To prove this claim, it suffices to show that it holds on graphs for n parties. This is because for any larger number of parties, one could just assign the extra parties to the purifier, thereby effectively reducing it back to an n-party problem. Consider a star graph with $n + 1$ edges, involving all parties as well as the purifier. Assign weight w_0 to the purifier edge, and unit weight to the rest as indicated in Fig. 2.1.[3] The entropy of any nonempty subsystem $\mathcal{K} \subseteq [n]$

[2] As first done in [BNOSSW15], the problem of computing entropies using the Ryu-Takayanagi (RT) [RT06b] formula for arbitrary subsystems in a given holographic configuration can be concisely recast into a graph-theoretic language. Deploying the RT surfaces for all relevant subsystems altogether, they partition the bulk into a set of codimension-0 regions. One assigns a vertex to every such region, and connects them by an edge whenever they correspond to adjacent bulk regions. Each edge is given a weight corresponding to the area of the associated piece of RT surface they go through. Those vertices on regions reaching the conformal boundary are understood as capturing the boundary subsystems. This way, one ends up with a desiccation of the bulk geometry, where all results obtained from the RT prescription of minimizing areas can be efficiently reproduced by the prescription of minimizing cut weights on the resulting holographic graph model.

[3] This family of star graphs was also fruitful in proving structural properties of the HEC in [AH23; CS21; FH22].

on such a star graph is:

$$\mathtt{S}_{\mathcal{K}} = \min\{|\mathcal{K}|\,,\, w_0 + n - |\mathcal{K}|\}\,. \tag{2.2.11}$$

Since this only depends on the cardinality of $\mathcal{K}$, our quantity of interest $\mathcal{I}_n \equiv \mathtt{I}_{[n]}$ becomes

$$\begin{aligned}\mathcal{I}_n &= -\sum_{k=1}^{n} \binom{n}{k} (-1)^k \min\{k\,,\, w_0 + n - k\} \\ &= -\sum_{k=1}^{\lfloor \frac{w_0+n}{2} \rfloor} \binom{n}{k} (-1)^k\, k - \sum_{k=\lceil \frac{w_0+n}{2} \rceil}^{n} \binom{n}{k} (-1)^k\, (w_0 + n - k)\end{aligned} \tag{2.2.12}$$

Letting $w_0 = n - 1$, this evaluates to

$$\mathcal{I}_n = (-1)^n\, n - (-1)^n\, (n-1) = (-1)^n. \tag{2.2.13}$$

On the other hand, letting $w_0 = n - 3$ leads to

$$\mathcal{I}_n = -(-1)^n\, n(n-2) + (-1)^n\, (n(n-3) + 3) = -(-1)^n\, (n-3). \tag{2.2.14}$$

Hence $\mathcal{I}_n$ takes opposite signs in each of these star graphs, proving the claim.[4] □

Multipartite information for the entire system: The above two lemmas considered the typical case where the arguments of I_n comprise a polychromatic subsystem $\mathcal{I} \subseteq [\mathsf{N}]$. We now complete the characterization by considering what happens when the arguments comprise the entire purified system $[\mathsf{N}{+}1]$. For the mutual information ($n = 2$ case), the result is particularly simple: denoting the first argument by $\mathcal{I}$, the second argument is then its complement $\overline{\mathcal{I}} = [\mathsf{N}+1] \setminus \mathcal{I}$, so applying the definition in eq. (2.1.1) and using $\mathtt{S}_{\mathcal{I}} = \mathtt{S}_{\overline{\mathcal{I}}}$ and $\mathtt{S}_{[\mathsf{N}+1]} = 0$, we have

$$I_2(\mathcal{I} : \overline{\mathcal{I}}) = 2\, \mathtt{S}_{\mathcal{I}} \tag{2.2.15}$$

where we could think of the RHS as $2\, I_1(\mathcal{I})$. A similar result holds for every even n. Schematically, $I_n = 2\, I_{n-1}$, where any one of the arguments on the LHS gets dropped for the RHS expression (and therefore the latter is automatically purification-symmetric). The result for

[4] Note that the RHS vanishes for $n = 3$, consistent with MMI.

odd n is even simpler since there we have complete cancellation of terms, giving $I_n = 0$.

We summarize and prove these claims in the following lemma:

Lemma 2.2.3. *Consider the n-partite information I_n evaluated on n disjoint subsystems X_i comprising a full N-party system including the purifier, $\bigcup_i \mathrm{X}_i = [\mathsf{N}+1]$.*[5] *Then*

$$I_n(\mathrm{X}_1 : \ldots : \mathrm{X}_n) = \begin{cases} 2\, I_{n-1}(\mathrm{X}_1 : \ldots : \mathrm{X}_{n-1}) \ , & n \text{ even} \\ 0 \ , & n \text{ odd} \end{cases} \tag{2.2.16}$$

Proof. In both cases, one can show the result by direct evaluation. Since $\bigcup_i \mathrm{X}_i = [\mathsf{N}+1]$, one of the X_i's contains the purifier; w.l.o.g., let us assume that it is in X_n. Then we can replace $\mathrm{X}_n = [\mathsf{N}+1] \setminus \bigcup_{i=1}^{n-1} \mathrm{X}_i$, and similarly any subsystem containing X_n by the corresponding complementary subsystem. When we re-express $I_n(\mathrm{X}_1 : \ldots : \mathrm{X}_n)$ in terms of entropies using eq. (2.2.2), a given combination of X_i's with $i \in [n-1]$ appears twice in the resulting expression, with coefficient ± 1 depending on the number of terms combined for the original expression and for its complement. For odd n, these coefficients are opposite, and therefore all terms cancel (except for the entropy of the full system, which however vanishes by purity, $\mathsf{S}(\mathrm{X}_1 \ldots \mathrm{X}_n) = 0$). For even n both coefficients are the same, so they add constructively, giving the stated result. □

Geometrical significance of the I_n's: So far we have discussed various useful properties of the multipartite information quantities, which will come into play both for proving our no-go theorem in §2.4 as well as for presenting the HEIs in a more compact form in §2.5. As a further motivation for considering the I_n's, we note that they also provide a useful diagnostic of the basic geometrical features of the bulk configuration, in particular the connectivity of the entanglement wedges of the various subsystems. Let us characterize a bulk entanglement wedge of a composite subsystem AB as *connected* if there exists a continuous curve γ through the bulk joining the boundary regions A and B which stays entirely within their entanglement wedge.[6]

[5] We remark that here each X_i subsystem may involve more than one of the parties in $[\mathsf{N}+1]$, so that the statement applies to a general $n \leq \mathsf{N}+1$ and not just the $n = \mathsf{N}+1$ case where each X_i is a single party.

[6] By entanglement wedge we mean the full codimension-0 bulk region as originally defined in [HHLR14], namely the bulk domain of dependence of the corresponding homology region (bounded by the said boundary region and its HRT surface [HRT07b]). However, since the regions A and B must be spacelike-separated in order for $\mathtt{I}_{\mathrm{AB}}$ to be well-defined, it is simple to show that γ can be chosen to be spacelike, and the following connectivity statement can be reformulated to pertain to any Cauchy slice containing A and B on its boundary.

Then generically (i.e. when each subsystem has a unique HRT surface), the entanglement wedge of a composite subsystem AB is connected between A and B if and only if the two subsystems are correlated ($\mathtt{I}_{\mathrm{AB}} > 0$). This follows straightforwardly from the observation that $\mathtt{I}_{\mathrm{AB}} = 0$ iff the composite HRT surface for AB consists of the individual HRT surfaces for A and B, thereby disconnecting the joint entanglement wedge.

This statement can be suitably generalized to use I_n to characterize simultaneous connectivity of n-party entanglement wedges. We define an n-party entanglement wedge of $\mathrm{X}_1 \ldots \mathrm{X}_n$ as connected if there exists a bulk point p along with n continuous curves γ_{pi} from p to the respective boundary regions X_i, all contained entirely within the entanglement wedge.[7] Then as a consequence of Lemma 2.2.1, we have the following connectivity statement:

Proposition 2.2.1. *The multipartite information of n disjoint subsystems X_i in a generic[8] configuration is non-vanishing,*

$$I_n(\mathrm{X}_1 : \ldots : \mathrm{X}_n) \neq 0 \ , \tag{2.2.17}$$

if and only if the joint entanglement wedge of $\mathrm{X}_1 \ldots \mathrm{X}_n$ is connected.

Proof. To warm-up, let us first consider the simple case where each region X_i has a single entangling surface. Suppose the entanglement wedge of $\mathrm{X}_1 \ldots \mathrm{X}_n$ is disconnected. Then there exists a bipartition of the system $\bigcup_i \mathrm{X}_i = \mathcal{I} \cup \mathcal{K}$ such that the entanglement wedge of $\mathcal{I}\mathcal{K}$ is disconnected, and by the previous argument this means that $I_2(\mathcal{I} : \mathcal{K}) = 0$. Hence the corresponding density matrix $\rho_{\mathcal{I}\mathcal{K}}$ factorizes, and by Lemma 2.2.1, $I_n(\mathrm{X}_1 : \ldots : \mathrm{X}_n) = 0$.

However, there can be situations where the joint entanglement wedge is disconnected, but where all bipartitions have connected entanglement wedges. A simple example of this is if the configuration has the entanglement structure of a collection of Bell pairs, such as indicated in fig. 9 of [HRR18]. In this case, we can first fine-grain the full system so as to have the disjoint pieces of the entanglement wedge correspond to disjoint subsystems, and apply the above

[7] Note that according to this definition, a connected entanglement wedge may still consist of multiple disjoint pieces (which could happen if at least one of the regions X_i is comprised of multiple components), provided at least one of those pieces contains the full set $\{\gamma_{pi}\}$. If, on the other hand, each X_i admits only a single entangling surface, then the entanglement wedge consists of a single piece and connectivity is tantamount to the existence of a set of curves γ_{ij} joining all pairs of regions $\{\mathrm{X}_i, \mathrm{X}_j\}$ to each other within it.

[8] By "generic" we mean that we have not fine-tuned to a 'phase transition' when multiple extremal surfaces exchange dominance; in other words, each subsystem has a unique HRT surface, and these have independent areas with no accidental cancellations.

reasoning to derive the vanishing of the corresponding fine-grained multipartite information. Then by the same calculation as in Lemma 2.2.1, the coarse-grained $I_n(\mathrm{X}_1 : \ldots : \mathrm{X}_n)$ combines additively from the fine-grained one, leading to the desired result $I_n(\mathrm{X}_1 : \ldots : \mathrm{X}_n) = 0$. This proves (the contrapositive of) the "only if" ($\Rightarrow$) part of the statement.

Conversely, suppose the entanglement wedge of $\mathrm{X}_1 \ldots \mathrm{X}_n$ is connected. We can again bootstrap our argument. In the simple case where each region X_i is connected and has a single entangling surface, connectivity of the entanglement wedge implies that there is a connected HRT surface for $\mathrm{X}_1 \ldots \mathrm{X}_n$, whose area is therefore generically independent of the other HRT surfaces for the various subsystems, and therefore will not cancel in the I_n expression. In the more general case of the X_i's consisting of multiple components, even if the HRT surface for $\mathrm{X}_1 \ldots \mathrm{X}_n$ consists of multiple components, connectivity of the entanglement wedge guarantees that there is still at least one extremal surface which is anchored on at least one component of each X_i, and therefore again cannot be "canceled" by any of the subsystem HRT surfaces. This proves the "if" ($\Leftarrow$) part of the statement. □

In using the above arguments, it is important to realize that individual mutual information quantities are independent of the multipartite information; for example, there can be configurations for which

$$I_2(\mathrm{X}_i : \mathrm{X}_j) > 0 \quad \forall\ i, j \qquad \text{but} \qquad I_n(\mathrm{X}_1 : \ldots : \mathrm{X}_n) = 0\ , \tag{2.2.18}$$

as well as configurations for which

$$I_2(\mathrm{X}_i : \mathrm{X}_j) = 0 \quad \forall\ i, j \qquad \text{but} \qquad |I_n(\mathrm{X}_1 : \ldots : \mathrm{X}_n)| > 0\ . \tag{2.2.19}$$

(Examples of both of these cases were presented e.g. in [HRR18], but an analogous graph-based example is e.g. a collection of all ij Bell pairs for the former and a uniform star graph of Fig. 2.1 with $w_0 = 1$ for the latter.) It is the bipartitioning of the full system which is related to the multipartite information. The geometrical significance of the I_n is the simultaneous connectivity within the single entanglement wedge; in other words, $|I_n| > 0$ diagnoses the presence of a bulk region which lies inside the joint entanglement wedge but outside all possible

subsystem entanglement wedges.

2.2.3. Conditional multipartite information

Now that we have explored the properties of multipartite information I_n, let us consider a related but slightly more intricate construct, namely that of *conditional* multipartite information. The motivation for this comes from the observation that conditional quantities have a natural quantum information theoretic interpretation. The conditional entropy, where we condition $\mathtt{S}(\mathrm{X})$ on Y, is defined as $S(\mathrm{X}|\mathrm{Y}) \equiv \mathtt{S}(\mathrm{XY}) - \mathtt{S}(\mathrm{Y})$, and measures the amount of quantum communication needed to obtain complete quantum information contained in the joint state ρ_{XY} if we already know the marginal ρ_{Y}. Classically, this quantity is non-negative, but quantum mechanically it can take either sign.[9] On the other hand, for any quantum state the conditional mutual information is non-negative by SSA, cf. eq. (2.1.2). While we will show momentarily that the higher n conditional multipartite information is no longer sign definite, it nevertheless seems to provide a nicer packaging for the HEIs, as discussed in §2.5.

In general, a conditional information quantity (e.g. conditioned on subsystem A) can be obtained by writing it out as a linear combination of entropies $\mathtt{S}_{\mathcal{I}}$ with $\mathcal{I} \not\supseteq \mathrm{A}$ and replacing each entropy $\mathtt{S}(\mathcal{I})$ by the conditional entropy $S(\mathcal{I}|\mathrm{A})$. Using the notation from eq. (2.2.1), for $\dot{\mathcal{I}}$ comprising $n-2$ singletons distinct from A, B, or C, we have two useful identities for conditional multipartite information $I_n(\mathrm{B}:\dot{\mathcal{I}}|\mathrm{A})$, viewed as the multipartite information $I_n(\mathrm{B}:\dot{\mathcal{I}})$ conditioned on A:

$$\begin{aligned} I_n(\mathrm{B}:\dot{\mathcal{I}}|\mathrm{A}) &= I_n(\mathrm{AB}:\dot{\mathcal{I}}) - I_n(\mathrm{A}:\dot{\mathcal{I}}) \\ &= I_n(\mathrm{B}:\dot{\mathcal{I}}) - I_{n+1}(\mathrm{A}:\mathrm{B}:\dot{\mathcal{I}}) \end{aligned} \tag{2.2.20}$$

where we have used the definition of conditioning in the first line and eq. (2.2.6) in the second line. We now use these relations to show the following:

Lemma 2.2.4. *Conditional I_n with $n \geq 3$ is not holographically sign-definite.*

Proof. We first consider the case $n \geq 4$, where by a judicious choice of the state, we can reduce

[9] When this quantity is negative, its absolute value can be interpreted as the additional amount of quantum information which X can transmit to Y "for free" (i.e. using only classical communication).

the argument to that of Lemma 2.2.2. We rewrite conditional I_n as

$$I_n(\mathrm{A}_1 : \ldots : \mathrm{A}_n|\mathrm{A}_{n+1}) = \mathtt{I}_{[n]} - \mathtt{I}_{[n+1]} \tag{2.2.21}$$

and consider a product state

$$\rho_{\mathrm{A}_1\ldots\mathrm{A}_n\mathrm{A}_{n+1}} = \pi_{\mathrm{A}_1\ldots\mathrm{A}_n} \otimes \sigma_{\mathrm{A}_{n+1}}. \tag{2.2.22}$$

In such a state the last term of eq. (2.2.21) vanishes by Lemma 2.2.1, so we have

$$I_n(\mathrm{A}_1 : \ldots : \mathrm{A}_n|\mathrm{A}_{n+1})|_\rho = \mathtt{I}_{[n]}|_\pi \ . \tag{2.2.23}$$

Since we placed no restriction on $\pi_{\mathrm{A}_1\ldots\mathrm{A}_n}$, Lemma 2.2.2 then implies that the RHS of eq. (2.2.23) can take either sign, so conditional I_n with $n \geq 4$ is not holographically sign-definite.

Now we consider the $n = 3$ case. Consider w.l.o.g. a pure state on $\mathrm{A}_1 \ldots \mathrm{A}_5$. Purification symmetry of I_3 implies (cf. eq. (2.B.20))[10]

$$I_3(\mathrm{A}_1 : \mathrm{A}_2 : \mathrm{A}_3|\mathrm{A}_4) = -I_3(\mathrm{A}_1 : \mathrm{A}_2 : \mathrm{A}_3|\mathrm{A}_5)\,. \tag{2.2.24}$$

Therefore conditional I_3 being sign-definite would imply conditional I_3 vanishes on any state for any choice of regions, which is obviously not true.[11] □

2.3. HEIs and Superbalance

In this section we review a crucial property, dubbed superbalance, pertaining to all holographic information quantities describing the non-SA facets [HHR20].

A general information quantity Q can be written as a linear combination of subsystem entropies $\mathtt{S}_\mathcal{J}$, as

$$Q = \sum_{\mathcal{J}\subseteq[\mathsf{N}]} c_\mathcal{J}\, \mathtt{S}_\mathcal{J} \tag{2.3.1}$$

[10] Written out explicitly, $I_3(\mathrm{A}_1 : \mathrm{A}_2 : \mathrm{A}_3|\mathrm{A}_4) = I_3(\mathrm{A}_1 : \mathrm{A}_2 : \mathrm{A}_3\mathrm{A}_4) - I_3(\mathrm{A}_1 : \mathrm{A}_2 : \mathrm{A}_4) = I_3(\mathrm{A}_1 : \mathrm{A}_2 : \mathrm{A}_5) - I_3(\mathrm{A}_1 : \mathrm{A}_2 : \mathrm{A}_3\mathrm{A}_5) = -I_3(\mathrm{A}_1 : \mathrm{A}_2 : \mathrm{A}_3|\mathrm{A}_5)$.

[11] Since this argument only uses purification symmetry of I_3, it also works for all the odd n cases as a corollary of Lemma 2.2.3.

with some rational coefficients $c_{\mathcal{I}}$ which can take either sign.

Although the $\mathsf{D} = 2^{\mathsf{N}} - 1$ individual entropies $\mathsf{S}_{\mathcal{I}}$ in eq. (2.3.1) are independent of each other, it is interesting to consider a specific subset of terms which involve a given subsystem $\mathcal{J}$ by considering just the terms with $\mathcal{I} \supseteq \mathcal{J}$. We say that Q is *balanced in* $\mathcal{J}$ if the appearance of this subsystem "cancels out" in Q in the sense that

$$\sum_{\mathcal{I} \supseteq \mathcal{J}} c_{\mathcal{I}} = 0 \,. \tag{2.3.2}$$

Typically, we think of balance just in the singletons $\mathcal{J} = \{j\}$ for $j \in [\mathsf{N}]$, and say that Q is *balanced* if it is balanced for every $j \in [\mathsf{N}]$, i.e., if

$$\sum_{\mathcal{I} \ni j} c_{\mathcal{I}} = 0 \qquad \forall\ j \in [\mathsf{N}] \,. \tag{2.3.3}$$

This property is important when looking at entropy inequalities, in which case it corresponds to having each party showing up in the entropy terms on one side as many times as on the other when the inequality is canonically written involving only positive signs. The operational significance of balance is that for any configuration of boundary subsystems corresponding to non-adjoining regions, a balanced quantity is guaranteed to be UV-finite, since all the UV divergences cancel out.[12]

While well-defined on specific information quantities, the property of balance can be easily seen to be preserved under Sym_{N} but not under the purification symmetry in general.[13] This is undesirable since, given the $S_{\mathsf{N}+1}$ symmetry of the HEC, we would like to probe its structure using objects whose properties are invariants of $Sym_{\mathsf{N}+1}$ as well. A property of Q is invariant under $Sym_{\mathsf{N}+1}$ if every quantity in the symmetry orbit of Q is, in which case it becomes a property of the symmetry orbit itself. This originally motivated [HRR19] to upgrade balance to a property of symmetry orbits by demanding that it be preserved under the purification symmetry, which suggests the following definition:

[12] For adjoining regions the mutual information is no longer finite, though this UV divergence is well understood [CHMY15], and arises from the UV correlations across the joint entangling surface.

[13] For example, the mutual information $\mathsf{S}_{\mathrm{A}} + \mathsf{S}_{\mathrm{B}} - \mathsf{S}_{\mathrm{AB}}$ is clearly balanced. However, e.g. for $\mathsf{N} = 2$ we may use Sym_3 to exchange B with the purifier O. Then, using purity to canonically write $\mathsf{S}_{\mathrm{O}} = \mathsf{S}_{\mathrm{AB}}$ and $\mathsf{S}_{\mathrm{AO}} = \mathsf{S}_{\mathrm{B}}$, one ends up with $\mathsf{S}_{\mathrm{A}} + \mathsf{S}_{\mathrm{AB}} - \mathsf{S}_{\mathrm{B}}$ which is clearly not balanced.

Definition 2.3.1 (Superbalance)**.** *An information quantity is said to be superbalanced if every element in its $S_{\mathsf{N}+1}$ symmetry orbit is balanced.*

This property can be expressed algebraically in a way that is very analogous to eq. (2.3.3) for balance. Namely, as shown in Lemma 4 of [AH23], Q is superbalanced if and only if

$$\sum_{\mathcal{J}\supseteq\mathcal{I}} c_{\mathcal{J}} = 0 \qquad \forall\ \varnothing \neq \mathcal{I} \subseteq [\mathsf{N}] \ \text{ with } \ |\mathcal{I}| \leq 2\,. \tag{2.3.4}$$

In other words, Q is superbalanced if it is balanced not only in all singletons but also in all doubletons.

The I-basis is remarkably successful in making the properties of balance and superbalance manifest. To see this, consider re-expressing Q in this basis as

$$Q = \sum_{\mathcal{I}\subseteq[\mathsf{N}]} c_{\mathcal{I}}\, \mathtt{S}_{\mathcal{I}} = \sum_{\mathcal{J}\subseteq[\mathsf{N}]} q_{\mathcal{J}}\, \mathtt{I}_{\mathcal{J}}\,, \tag{2.3.5}$$

Using eq. (2.2.5), one can easily read off that the I-basis coefficients $q_{\mathcal{J}}$ can be written in terms of the S-basis coefficients $c_{\mathcal{I}}$ through[14]

$$q_{\mathcal{J}} = (-1)^{|\mathcal{J}|-1} \sum_{\mathcal{I}\supseteq\mathcal{J}} c_{\mathcal{I}}\,. \tag{2.3.6}$$

Up to signs, this is of course nothing but the left-hand side of eq. (2.3.2), whose vanishing appears in the definitions of both balance and superbalance. Hence we obtain the following result (cf. Definition 10 of [HRR19])

Proposition 2.3.1. *An information quantity is balanced if and only if its representation in the I-basis does not involve any $\mathtt{I}_1$ terms, and it is superbalanced if and only if it additionally does not involve any $\mathtt{I}_2$ terms.*

Proof. Writing Q as in eq. (2.3.5) and using eq. (2.3.6), the result follows from the defining properties of balance in eq. (2.3.3) and superbalance in eq. (2.3.4). □

In [HRR19], it was observed that any superbalanced information quantity is finite on all

[14] Using standard matrix notation so that eq. (2.3.5) and eq. (2.2.5) respectively read $c^T\mathtt{S} = q^T\mathtt{I}$ and $\mathtt{S} = M\,\mathtt{I}$ for M the transformation matrix between bases, one immediately finds $q = M^T c$.

smooth configurations, even those involving adjoining regions where a merely balanced quantity would diverge. To show this, it suffices to demonstrate finiteness for any I_3, since a superbalanced information quantity can be expressed as a finite sum of I_3's.[15] It is easy to check that the area divergences from common parts of entangling surface all cancel in the combination of entropies given by I_3. Indeed, since the subleading UV divergences (arising from corner terms etc. in higher-dimensional configurations) are local, they all likewise cancel (this was already argued for all $\mathtt{I}_n$'s with $n \geq 3$ in [HHM13]), which establishes finiteness in even greater generality.

A powerful property of HEIs that is also made manifest by the I-basis is the requirement that the coefficients of the I_n terms alternate in sign as follows [HRR19]:

Proposition 2.3.2. *An information quantity defines a valid HEI only if, written as in* (2.3.5)*, the I-basis coefficients satisfy*

$$(-1)^{|\mathcal{K}|}\, q_{\mathcal{K}} \geq 0 \ , \qquad \forall\ \mathcal{K} \subseteq [\mathsf{N}]\,.$$

Proof. Let Q be an N-party information quantity. Recall the star graphs of Fig. 2.1 introduced in the proof of Lemma 2.2.2. For any subsystem $\mathcal{K} \subset [\mathsf{N}]$, let $n = |\mathcal{K}|$ and consider a star graph with $n+1$ legs, n of which are assigned unit weight and connected to vertices labelled by the parties in $\mathcal{K}$, plus one of weight $w_0 = n-1$ for the purifier $\mathsf{N}+1$. Adding isolated vertices for any remaining parties in $[\mathsf{N}] \setminus \mathcal{K}$, this constitutes a graph model for N parties. Consider evaluating Q on such a model. We can do so by evaluating every $\mathtt{I}_{\mathcal{J}}$ on it and using eq. (2.3.5). Since the graph model factorizes between $\mathcal{K}$ and $[\mathsf{N}] \setminus \mathcal{K}$, it follows by Lemma 2.2.1 that $\mathtt{I}_{\mathcal{J}}$ vanishes for any $\mathcal{J} \supset \mathcal{K}$. Furthermore, for any $\mathcal{J} \subset \mathcal{K}$ one has $\mathsf{S}_{\mathcal{J}} = |\mathcal{J}|$ for all $\mathcal{J} \subseteq \mathcal{J}$ (and zero otherwise), which also implies the vanishing of $\mathtt{I}_{\mathcal{J}}$.[16] Lastly, for $\mathcal{J} = \mathcal{K}$, we obtained in eq. (2.2.13) that $\mathtt{I}_{\mathcal{K}} = (-1)^{|\mathcal{K}|}$. In other words, we have constructed a graph model for each $\mathcal{K} \subseteq [\mathsf{N}]$ that gives $\mathtt{I}_{\mathcal{J}} = 0$ for all $\mathcal{J} \neq \mathcal{K}$ and such that Q evaluates to

$$Q = (-1)^{|\mathcal{K}|}\, q_{\mathcal{K}}\,.$$

[15] This follows from Proposition 2.3.1, and the fact that all I-basis elements $\mathtt{I}_n$ for $n \geq 3$ can be spanned by I_3's with polychromatic arguments, as can be seen by applying eq. (2.2.6) recursively.

[16] Explicitly, $\mathtt{I}_{\mathcal{J}} = \sum_{\mathcal{J} \subseteq \mathcal{J}} (-1)^{|\mathcal{J}|} |\mathcal{J}| = \sum_{j=1}^{|\mathcal{J}|} \binom{|\mathcal{J}|}{j} (-1)^j j = 0$.

Since a valid HEI for Q would read $Q \geq 0$ for any graph model, the claim follows. □

What makes the superbalance property so crucial in understanding meaningful holographic information quantities and the structure of the HEC itself is the following result proven in [HHR20].

Theorem 1. Except for subadditivity, every facet of the HEC is superbalanced.

It follows from this and Proposition 2.3.1 that the set of normal vectors defining the facets of the HEC other than the ones for SA live in a proper subspace of entropy space. In particular, since there are N entropy terms $\mathtt{I}_1$ and $\binom{\mathsf{N}}{2}$ mutual information terms $\mathtt{I}_2$ which vanish for all of them, they all belong to a subspace of codimension $\frac{1}{2}\mathsf{N}(\mathsf{N}+1)$. Geometrically, what this means is that the HEC naturally decomposes into two complementary subspaces, an SA subspace (spanned by the normals of SA facets) and a superbalanced one (spanned by the normals of all other facets). From the viewpoint of extreme rays, this decomposition corresponds to a *bipartite* subspace of dimension $\frac{1}{2}\mathsf{N}(\mathsf{N}+1)$ spanned by all Bell-pair extreme rays (cf. the SA subspace), and a complementary *multipartite* subspace spanned by all other extreme rays.

2.4. Correlation Measures from HEIs?

Mutual information, corresponding to the total amount of correlation between two subsystems, is a prototypical correlation measure. It is non-negative $I_2(\mathrm{A}:\mathrm{B}) \geq 0$ and vanishes when bipartite correlation is absent, i.e., when the density matrix is in a product state $\rho_{\mathrm{AB}} = \rho_{\mathrm{A}} \otimes \rho_{\mathrm{B}}$. It also satisfies the monotonicity property $I_2(\mathrm{A}:\mathrm{BC}) \geq I_2(\mathrm{A}:\mathrm{B})$ by virtue of strong subadditivity.

We wish to abstract away these properties for more general measures. In particular, we require that any putative correlation measure cannot be negative and cannot increase as some part of the system is discarded. Therefore we posit the following as basic properties of any correlation measure, viewed as a measure of the amount of some type of correlation present in a system:

1. It should be a non-negative quantity and vanish when the correlation measured is absent.

2. It should be monotonically non-increasing under partial tracing.

Given that HEIs define non-negative information quantities on holographic states, it is natural to ask whether they can be viewed as multipartite correlation measures in holography. While such quantities are unlikely to satisfy the monotonicity property for general quantum states, one might hope that they are monotonic when restricted to holographic states. If so, this would elucidate some aspects of the structural form of the HEC. The main result of the present section is that this not the case. By theorem 1, apart from the mutual information, all information quantities corresponding to facets of the HEC are superbalanced. We now show that no superbalanced information quantity can be monotonic, even with the restriction to holographic states.

Theorem 2.4.1. *Superbalanced information quantities are non-monotonic in holography.*[a]

[a] It should not be surprising that superbalanced information quantities are non-monotonic for general quantum states, since these do not even obey any HEIs other than SA. The statement here is strictly stronger, and says that monotonicity is not respected even by the restricted class of holographic states.

Proof. Since here we discuss the effect of tracing out some subsystem, it will be convenient to generalize our framework to work with a mixed state on $\mathsf{N}+1$ parties, where the $(\mathsf{N}+1)^{\text{st}}$ party will be traced out. (Hence, for this proof only, the purifier will be left implicit.) Consider a mixed $(\mathsf{N}+1)$-party system with $[\mathsf{N}+1] = \{\mathrm{A}_1, \cdots, \mathrm{A}_\mathsf{N}, \mathrm{a}_\mathsf{N}\}$. We would like to show that any N-party superbalanced information quantity cannot be monotonic under tracing out a_N, i.e., for a generic superbalanced quantity $Q(\mathrm{A}_1 : \cdots : \mathrm{A}_\mathsf{N})$, the quantity

$$\Delta Q \equiv Q(\mathrm{A}_1 : \cdots : \mathrm{A}_\mathsf{N}\ \mathrm{a}_\mathsf{N}) - Q(\mathrm{A}_1 : \cdots : \mathrm{A}_\mathsf{N}) \tag{2.4.1}$$

cannot be non-negative for all states. By Proposition 2.3.1, we can expand the superbalanced quantity $Q(\mathrm{A}_1 : \cdots : \mathrm{A}_\mathsf{N})$ in terms of singleton I_n's with $n \geq 3$:

$$Q(\mathrm{A}_1 : \cdots : \mathrm{A}_\mathsf{N}) = \sum_{\mathcal{J} \subseteq [N-1] \,:\, |\mathcal{J}| \geq 2} \nu_\mathcal{J}\, \mathrm{I}_{|\mathcal{J}|+1}(\mathcal{J} : \mathrm{A}_\mathsf{N}) + (\text{terms independent of } \mathrm{A}_\mathsf{N}), \tag{2.4.2}$$

where $[\mathsf{N}-1] = \{\mathrm{A}_1, \cdots, \mathrm{A}_{\mathsf{N}-1}\}$. Using this expansion, the change ΔQ reads

$$\begin{aligned} \Delta Q &= \sum_{\mathcal{J} \subseteq [N-1] \,:\, |\mathcal{J}| \geq 2} \nu_\mathcal{J}\, \mathrm{I}_{|\mathcal{J}|+1}(\mathcal{J} : \mathrm{a}_\mathsf{N} | \mathrm{A}_\mathsf{N}) \\ &= \sum_{\mathcal{J} \subseteq [N-1] \,:\, |\mathcal{J}| \geq 2} \nu_\mathcal{J} \left(\mathrm{I}_{|\mathcal{J}|+1}(\mathcal{J} : \mathrm{a}_\mathsf{N}) - \mathrm{I}_{|\mathcal{J}|+2}(\mathcal{J} : \mathrm{a}_\mathsf{N} : \mathrm{A}_\mathsf{N}) \right), \end{aligned} \tag{2.4.3}$$

where we have used eq. (2.2.20). We now show that requiring ΔQ to be non-negative on every state forces all $\nu_{\mathcal{J}}$ to vanish, by sequentially choosing states that collapse the sum onto a single term, which is non-sign-definite unless its coefficient vanishes. To achieve this, consider a class of $(\mathsf{N}+1)$-party mixed states $\{\rho^{(\mathcal{J})}_{[\mathsf{N}+1]}\}_{\mathcal{J}\subseteq[\mathsf{N}-1]}$ with the following factorization structure

$$\rho^{(\mathcal{J})}_{[\mathsf{N}+1]} = \pi_{\mathcal{J}\mathrm{A}_\mathsf{N}\mathrm{a}_\mathsf{N}} \otimes \sigma_{[\mathsf{N}+1]\setminus\{\mathcal{J}\mathrm{A}_\mathsf{N}\mathrm{a}_\mathsf{N}\}} \tag{2.4.4}$$

with π, σ being arbitrary states. Then for any distinct pair $\mathcal{I}, \mathcal{J}' \subseteq [\mathsf{N}-1]$ with $\mathcal{J}' \not\subseteq \mathcal{I}$,

$$\mathrm{I}_{|\mathcal{J}'|+1}(\dot{\mathcal{J}}' : \mathrm{a}_\mathsf{N})|_{\rho^{(\mathcal{I})}} = \mathrm{I}_{|\mathcal{J}'|+2}(\dot{\mathcal{J}}' : \mathrm{A}_\mathsf{N} : \mathrm{a}_\mathsf{N})|_{\rho^{(\mathcal{I})}} = 0 \tag{2.4.5}$$

due to Lemma 2.2.1. Now, to collapse the sum in eq. (2.4.3) to a single term, pick any $\mathcal{I}$ with lowest cardinality in the sum such that $\mathcal{J}' \not\subseteq \mathcal{I}$ for any other $\mathcal{J}'$ in the sum; it follows by eq. (2.4.5) that

$$\Delta Q|_{\rho^{(\mathcal{I})}} = \nu_{\mathcal{I}}\, \mathrm{I}_{|\mathcal{I}|+1}(\dot{\mathcal{I}} : \mathrm{a}_\mathsf{N}|\mathrm{A}_\mathsf{N}). \tag{2.4.6}$$

Then, as we imposed no restriction on the state $\pi_{\mathcal{I}\mathrm{A}_\mathsf{N}\mathrm{a}_\mathsf{N}}$, requiring ΔQ to be non-negative on all states forces, for this particular $\mathcal{I}$, $\nu_{\mathcal{I}} = 0$ by virtue of Lemma 2.2.4. The same argument can then be applied to all other $\mathcal{I}$'s with the lowest cardinality, thereby setting $\nu_{\mathcal{J}} = 0$ for all lowest-cardinality-$\mathcal{J}$'s in the sum. Then the argument can be applied to $\mathcal{J}$'s with the lowest cardinality among the surviving terms in the sum. Iterating this argument sets $\nu_{\mathcal{J}} = 0$ for all $\mathcal{J}$'s, thereby proving the claim. □

This result shows that, besides the mutual information, none of the information quantities defined through HEIs admit an interpretation as a correlation measure in holography.

2.5. New $\mathsf{N} = 6$ HEIs and tripartite form

Having ascertained that the higher HEIs are not natural correlation measures, the task of understanding the physical significance of their form still remains. Often the operational meaning of a given quantity becomes more apparent when expressed in a better representation. We motivate a specific form for such a representation in §2.5.1, present a set of HEIs in this form

(cf. table 2.1 for $\mathsf{N} = 5$ quantities and table 2.2 for selected $\mathsf{N} = 6$ quantities) in §2.5.2, and offer some observations regarding their structure in §2.5.3.

2.5.1. Motivation for the tripartite form

We have already seen in [HHH19] that the I-basis representation is more convenient than the S-basis one for producing more compact expressions. Here we supplement this with some observations which allow us to propose a rather rigid structural form for information quantities which we speculate may be able to capture all HEIs.

We start by noting that there are structural similarities between distinct HEI orbits and across different N. One simple example of this is the MMI itself: while there is only a single orbit for $\mathsf{N} = 3$, there are two distinct orbits for $\mathsf{N} = 4, 5$, one of which ($-I_3(\text{A:B:C}) \geq 0$) can be viewed as a direct uplift from $\mathsf{N} = 3$, while the other ($-I_3(\text{A:B:CD}) \geq 0$) may be understood as a fine-graining thereof.[17] This motivates the consideration of multipartite information with polychromatic arguments to express HEIs. Moreover, we have seen that higher I_n's can be expressed in terms of smaller n ones by increasing the argument size. In principle, this means we could express all HEIs in terms of just mutual informations (with non-sign-definite coefficients), but such a recasting would manifest neither superbalance nor the I-basis sign-alternation required by Proposition 2.3.2. On the other hand, we might expect an efficient rewriting of HEIs to have these basic properties automatically built in.

To guarantee superbalance, by Proposition 2.3.1 it suffices to restrict the use of polychromatic I_n's to $n \geq 3$, while by iterating eq. (2.2.6), it is easy to check that the sign-alternation from Proposition 2.3.2 can be accomplished by demanding that any I_n, polychromatic or not, come with a coefficient sign $(-1)^n$, as extensively exemplified in §2.B. Moreover, because I_3 is the only sign-definite multipartite information quantity by MMI and Lemma 2.2.2, we also expect it to play a privileged role. Expressing information quantities only in terms of polychromatic I_3's would however fail to produce non-redundant HEIs; we need to supplement sign-definite terms with some non-sign-definite terms. We empirically observe that I_4's and I_3's appearing in HEIs naturally pair up to produce conditional (polychromatic) I_3's, and that such fortuitous

[17] At $\mathsf{N} = 5$, $I_3(\text{A:BC:DE})$ can be viewed as a purification and permutation of $I_3(\text{A:B:CD})$, while $I_3(\text{A:B:CDE})$ is similarly related to $I_3(\text{A:B:C})$. On the other hand, at $\mathsf{N} = 6$, there are 3 distinct orbits, generated by $I_3(\text{A:B:C})$, $I_3(\text{A:B:CD})$, and $I_3(\text{A:BC:DE})$.

groupings in fact extend to higher n as well. This motivates us to try expressing HEIs purely as combinations of I_3's and conditional I_3's, the latter being individually non-sign-definite by Lemma 2.2.4 as desired.[18] With these building blocks, it is also nicely straightforward to implement the desired sign-alternation property, by requiring that not just the I_3's, but also their conditional versions, must all come with a negative sign, independently of the argument size. This motivates the following ansatz for the form of information quantities corresponding to HEIs, which we dub the *tripartite form*.

Definition 2.5.1 (tripartite form)**.** *An information quantity Q is said to be in the* tripartite form *if it is expressed as*

$$Q = \sum_i -I_3(\mathrm{X}_i : \mathrm{Y}_i : \mathrm{Z}_i \,|\, \mathrm{W}_i) \tag{2.5.1}$$

where the arguments $\mathrm{X}_i, \mathrm{Y}_i, \mathrm{Z}_i, \mathrm{W}_i \subset [\mathsf{N}]$ are disjoint subsystems, the sum runs over any finite number of terms, and we allow for the conditioning to trivialize, $\mathrm{W}_i = \varnothing$, in which case $I_3(\mathrm{X}_i : \mathrm{Y}_i : \mathrm{Z}_i \,|\, \varnothing) \coloneqq I_3(\mathrm{X}_i : \mathrm{Y}_i : \mathrm{Z}_i)$.[19]

Each term in eq. (2.5.1) can be characterized as either tripartite information (when $\mathrm{W}_i = \varnothing$) or conditional tripartite information (when $\mathrm{W}_i \neq \varnothing$), which we will abbreviate as I and C, respectively. It will then be convenient to summarize the structural form of the HEI by a "word" made of I's and C's, one letter for each term, such as I, IC, IIC, etc.. The requirement of non-redundancy dictates that apart from SA and MMI, all higher HEIs must consist of at least two terms (since the single term C by itself is not sign-definite) and that at least one of the terms must be a C (because I itself is sign-definite, so multiple I's yield a redundant quantity). The minimal such expression would then be IC, i.e. consist of a single I_3 term and a single conditional I_3 term. And indeed, we find that there are HEIs of this form; cf. $Q^{[5]}$ of table 2.1 and $Q^{[12]}$ in table 2.2.

This is encouraging, and inspires a systematic method of looking for new HEIs: posit the requisite tripartite form, by specifying how many I's and C's a given information quantity should

[18] Of course, one could use eq. (2.2.20) to rewrite I_4 as a difference between I_3 and conditional I_3 in any information quantity, and similarly for higher I_n, but in general this would spoil the automatic $\mathtt{I}_n$ sign alternation, so it is non-trivial that such wrong-sign terms cancel out in the full expression for the HEIs as required by Proposition 2.3.2.

[19] Note that the tripartite form can account for arbitrary negative integer coefficients by simply repeating terms, though in practice they turn out to be distinct for vast majority of the HEIs we have found.

have, and then test all possible combinations of arguments $\{\mathrm{X}_i, \mathrm{Y}_i, \mathrm{Z}_i, \mathrm{W}_i\}$ (up to permutation symmetry between $\{\mathrm{X}_i, \mathrm{Y}_i, \mathrm{Z}_i\}$ for each i and overall permutation and purification symmetry). We refer to [HHJ23] for more details on this.

2.5.2. Presentation of HEIs

In this short subsection, we explain the HEI tables 2.1 and 2.2. By permutation symmetry, it suffices to list one instance from each symmetry orbit; since different choices may be convenient for different purposes, the given instance chosen for this section need not coincide with that listed in the ancillary file of [HHJ23]. On the other hand, it will be instructive to express each chosen instance in several alternative forms. In the following tables, we provide three separate forms: the conventional S-basis form, the I-basis representation, and the tripartite form motivated in the previous paragraph.[20] The HEI information quantities themselves are labeled by Q with the superscript indicating the position number of the HEI quantity (possibly permuted) as listed in the ancillary file of and the (optional) subscript consisting of the set of numbers $\{i_3, i_4, \ldots\}$, with i_n characterizing the number of $\mathtt{I}_n$'s when represented in the I-basis.[21] This decoration is mainly for convenience of providing immediate information about the quantity; when this information is not relevant for the discussion we omit it and simply quote the number n which is the unique identifier of the given orbit.[22] We employ the Q label to indicate the full equivalence class of instances along the permutation and purification orbit, so when we write $Q = \ldots$, we mean that there is an instance along the Q orbit which equals the given expression. Below the label, for convenience we also indicate the I..C.. form. For each HEI, we separate out the positive and negative entropy terms in the S-basis (the signs have no correlation with the subsystem size, but within each set we further order by subsystem size)

[20] We have also explored the corresponding quantities in the K-basis of [HHH19], which manifests the larger symmetry $Sym_{\mathsf{N}+1}$ including purifications, but since this representation did not yield substantially new insights, we omit it in the present summary.

[21] This turns out to be a useful characterization, which we dub the i# classification and utilize in §2.B; cf. table 2.3 for the i# classification for the individual building blocks. Note that for notational compactness, in this section we list only the non-zero values of i_n. This is unambiguous because for any tripartite form expression written in the I-basis, the absence of any $\mathtt{I}_m$ terms implies the absence of all $\mathtt{I}_n$ terms with $n \geq m$.

[22] The associated value of N is in fact uniquely determined from n. For $n = 1$, $N = 2$; for $n = 2, 3, 4$, $\mathsf{N} = 3$; for $5 \leq n \leq 11$, $\mathsf{N} = 5$; and for $n \geq 12$, $\mathsf{N} = 6$. On the other hand, there are several possible i# forms for the given orbit, due to the purification symmetry of I_3 implied by Lemma 2.2.3 (cf. eq. (2.B.19)). Hence its use allows for a further refinement of the specification, effectively fine-graining the equivalence class to Sym_{N} sub-orbit within the given $Sym_{\mathsf{N}+1}$ orbit.

and by n in the I-basis (with sign $(-1)^n$), and finally within each group lexicographically.

label	$\mathsf{N}=5$ HEI information quantities
$Q^{[5]}_{\{3,2\}}$	$-\mathsf{S}_{\mathrm{ABCD}}-\mathsf{S}_{\mathrm{ACDE}}-\mathsf{S}_{\mathrm{AB}}-\mathsf{S}_{\mathrm{AD}}-\mathsf{S}_{\mathrm{DE}}-\mathsf{S}_{\mathrm{C}}$ $+\mathsf{S}_{\mathrm{ABC}}+\mathsf{S}_{\mathrm{ABD}}+\mathsf{S}_{\mathrm{ACD}}+\mathsf{S}_{\mathrm{ADE}}+\mathsf{S}_{\mathrm{CDE}}$
IC	$\mathsf{I}_{\mathrm{ABCD}}+\mathsf{I}_{\mathrm{ACDE}}-\mathsf{I}_{\mathrm{ACD}}-\mathsf{I}_{\mathrm{ACE}}-\mathsf{I}_{\mathrm{BCD}}$ $-I_3(\mathrm{AB:C:D})-I_3(\mathrm{A:C:E\vert D})$
$Q^{[7]}_{\{4,2\}}$	$-\mathsf{S}_{\mathrm{ABCD}}-\mathsf{S}_{\mathrm{BCDE}}-\mathsf{S}_{\mathrm{ABE}}-\mathsf{S}_{\mathrm{BC}}-\mathsf{S}_{\mathrm{BD}}-\mathsf{S}_{\mathrm{A}}-\mathsf{S}_{\mathrm{C}}-\mathsf{S}_{\mathrm{D}}-\mathsf{S}_{\mathrm{E}}$ $+\mathsf{S}_{\mathrm{ABC}}+\mathsf{S}_{\mathrm{ABD}}+\mathsf{S}_{\mathrm{BCD}}+\mathsf{S}_{\mathrm{BCE}}+\mathsf{S}_{\mathrm{BDE}}+\mathsf{S}_{\mathrm{AE}}+\mathsf{S}_{\mathrm{CD}}$
IIC	$\mathsf{I}_{\mathrm{ABCD}}+\mathsf{I}_{\mathrm{BCDE}}-\mathsf{I}_{\mathrm{ABE}}-\mathsf{I}_{\mathrm{ACD}}-\mathsf{I}_{\mathrm{BCD}}-\mathsf{I}_{\mathrm{CDE}}$ $-I_3(\mathrm{AB:C:D})-I_3(\mathrm{A:B:E})-I_3(\mathrm{C:D:E\vert B})$
$Q^{[9]}_{\{4,3\}}$	$-\mathsf{S}_{\mathrm{ABCD}}-\mathsf{S}_{\mathrm{ACDE}}-\mathsf{S}_{\mathrm{BCDE}}-\mathsf{S}_{\mathrm{AB}}-\mathsf{S}_{\mathrm{AD}}-\mathsf{S}_{\mathrm{BC}}-\mathsf{S}_{\mathrm{CD}}-\mathsf{S}_{\mathrm{CE}}-\mathsf{S}_{\mathrm{DE}}$ $+\mathsf{S}_{\mathrm{ABC}}+\mathsf{S}_{\mathrm{ABD}}+\mathsf{S}_{\mathrm{ACD}}+\mathsf{S}_{\mathrm{ADE}}+\mathsf{S}_{\mathrm{BCD}}+\mathsf{S}_{\mathrm{BCE}}+2\mathsf{S}_{\mathrm{CDE}}$
ICC	$\mathsf{I}_{\mathrm{ABCD}}+\mathsf{I}_{\mathrm{ACDE}}+\mathsf{I}_{\mathrm{BCDE}}-\mathsf{I}_{\mathrm{ACD}}-\mathsf{I}_{\mathrm{ACE}}-\mathsf{I}_{\mathrm{BCD}}-\mathsf{I}_{\mathrm{BDE}}$ $-I_3(\mathrm{AB:C:D})-I_3(\mathrm{B:D:E\vert C})-I_3(\mathrm{A:C:E\vert D})$
$Q^{[10]}_{\{4,3\}}$	$-\mathsf{S}_{\mathrm{ABCE}}-\mathsf{S}_{\mathrm{ACDE}}-\mathsf{S}_{\mathrm{BCDE}}-\mathsf{S}_{\mathrm{ABD}}-\mathsf{S}_{\mathrm{AC}}-\mathsf{S}_{\mathrm{AE}}-\mathsf{S}_{\mathrm{BC}}-\mathsf{S}_{\mathrm{BE}}-\mathsf{S}_{\mathrm{CD}}-\mathsf{S}_{\mathrm{DE}}$ $+\mathsf{S}_{\mathrm{ABC}}+\mathsf{S}_{\mathrm{ABE}}+\mathsf{S}_{\mathrm{ACD}}+\mathsf{S}_{\mathrm{ACE}}+\mathsf{S}_{\mathrm{ADE}}+\mathsf{S}_{\mathrm{BCD}}+\mathsf{S}_{\mathrm{BCE}}+\mathsf{S}_{\mathrm{BDE}}+\mathsf{S}_{\mathrm{CDE}}$
ICCC	$\mathsf{I}_{\mathrm{ABCE}}+\mathsf{I}_{\mathrm{ACDE}}+\mathsf{I}_{\mathrm{BCDE}}-\mathsf{I}_{\mathrm{ABD}}-\mathsf{I}_{\mathrm{ACE}}-\mathsf{I}_{\mathrm{BCE}}-\mathsf{I}_{\mathrm{CDE}}$ $-I_3(\mathrm{A:B:D})-I_3(\mathrm{B:C:E\vert A})-I_3(\mathrm{C:D:E\vert B})-I_3(\mathrm{A:C:E\vert D})$
$Q^{[11]}_{\{8,6\}}$	$-2\mathsf{S}_{\mathrm{ABCD}}-\mathsf{S}_{\mathrm{ABCE}}-2\mathsf{S}_{\mathrm{ABDE}}-\mathsf{S}_{\mathrm{ACDE}}-2\mathsf{S}_{\mathrm{AB}}-\mathsf{S}_{\mathrm{AC}}-2\mathsf{S}_{\mathrm{AD}}-\mathsf{S}_{\mathrm{AE}}-2\mathsf{S}_{\mathrm{BC}}-\mathsf{S}_{\mathrm{BD}}-\mathsf{S}_{\mathrm{CE}}-2\mathsf{S}_{\mathrm{DE}}$ $+3\mathsf{S}_{\mathrm{ABC}}+3\mathsf{S}_{\mathrm{ABD}}+\mathsf{S}_{\mathrm{ABE}}+\mathsf{S}_{\mathrm{ACD}}+\mathsf{S}_{\mathrm{ACE}}+3\mathsf{S}_{\mathrm{ADE}}+\mathsf{S}_{\mathrm{BCD}}+\mathsf{S}_{\mathrm{BCE}}+\mathsf{S}_{\mathrm{BDE}}+\mathsf{S}_{\mathrm{CDE}}$
IICCCC	$2\mathsf{I}_{\mathrm{ABCD}}+\mathsf{I}_{\mathrm{ABCE}}+2\mathsf{I}_{\mathrm{ABDE}}+\mathsf{I}_{\mathrm{ACDE}}-\mathsf{I}_{\mathrm{ABD}}-2\mathsf{I}_{\mathrm{ABE}}-2\mathsf{I}_{\mathrm{ACD}}-\mathsf{I}_{\mathrm{ACE}}-\mathsf{I}_{\mathrm{BCD}}-\mathsf{I}_{\mathrm{BDE}}$ $-I_3(\mathrm{AB:C:D})-I_3(\mathrm{AE:B:D})-I_3(\mathrm{A:B:E\vert C})-I_3(\mathrm{A:B:E\vert D})-I_3(\mathrm{A:C:D\vert B})-I_3(\mathrm{A:C:E\vert D})$

Table 2.1.: HEI information quantities for $\mathsf{N}=5$ in the S-basis (white background), I-basis (blue background), and the tripartite form (pink background, with the specific I..C.. class indicated in the left column). We label the information quantities in the form $Q^{[n]}_{\{i\#\}}$, where n is the identifier in the ancillary files, and the $\{i\#\}$ lists the non-zero entries of $\{\#I_3,\#I_4,\#I_5,\#I_6\}$. The notational shorthand, explained in §2.2.1, is such that e.g. $\mathsf{S}_{\mathrm{ABCD}}\coloneqq\mathsf{S}(\mathrm{ABCD})$ and $\mathsf{I}_{\mathrm{ABCD}}\coloneqq\mathsf{I}_4(\mathrm{A:B:C:D})$.

In the rest of this section, we make a few observations regarding the actual expressions. These are mostly of a phenomenological nature; we relegate a more systematic analysis to future work.

2.5.3. Structural properties

Compactness: Evidently, the tripartite form has many fewer terms than the I-basis or S-basis forms, typically by a factor of 5 or so, though in some cases the reduction is from 47 terms in the I-basis to only 4 in the tripartite form. A priori, this was not guaranteed by the arguments that motivated these recastings (– one can certainly cook up information quantities for which this is not the case, or indeed those which do not admit tripartite form in the first place, such as single I_n for $n\neq 3$), so the very fact is intriguing. Moreover, we can see that many $\mathsf{N}=6$ HEIs are in fact simpler than some $\mathsf{N}=5$ HEIs, a feature we expect to prevail at higher N. However, while the original hope was that the recasting into the tripartite form would be sufficiently suggestive to explicate the operational meaning of these HEIs, this hope has not yet been realized. We therefore leave it as a challenge for the future.

label	Selected N = 6 HEI information quantities
$Q^{[12]}_{\{5,5,1\}}$	$-\mathrm{S}_{\mathrm{ABDEF}} - \mathrm{S}_{\mathrm{ABCF}} - \mathrm{S}_{\mathrm{AD}} - \mathrm{S}_{\mathrm{AF}} - \mathrm{S}_{\mathrm{BE}} - \mathrm{S}_{\mathrm{BF}} - \mathrm{S}_{\mathrm{CF}}$ $+\mathrm{S}_{\mathrm{ABDE}} + \mathrm{S}_{\mathrm{ABF}} + \mathrm{S}_{\mathrm{ACF}} + \mathrm{S}_{\mathrm{ADF}} + \mathrm{S}_{\mathrm{BCF}} + \mathrm{S}_{\mathrm{BEF}}$
	$-\mathrm{I}_{\mathrm{ABDEF}} + \mathrm{I}_{\mathrm{ABCF}} + \mathrm{I}_{\mathrm{ABDF}} + \mathrm{I}_{\mathrm{ABEF}} + \mathrm{I}_{\mathrm{ADEF}} + \mathrm{I}_{\mathrm{BDEF}} - \mathrm{I}_{\mathrm{ABC}} - \mathrm{I}_{\mathrm{ABF}} - \mathrm{I}_{\mathrm{AEF}} - \mathrm{I}_{\mathrm{BDF}} - \mathrm{I}_{\mathrm{DEF}}$
IC	$-I_3(\mathrm{AD:BE:F}) - I_3(\mathrm{A:B:C|F})$
$Q^{[24]}_{\{4,3\}}$	$-\mathrm{S}_{\mathrm{ABCF}} - \mathrm{S}_{\mathrm{ABDF}} - \mathrm{S}_{\mathrm{ABEF}} - \mathrm{S}_{\mathrm{AB}} - \mathrm{S}_{\mathrm{AD}} - \mathrm{S}_{\mathrm{AF}} - \mathrm{S}_{\mathrm{BE}} - \mathrm{S}_{\mathrm{BF}} - \mathrm{S}_{\mathrm{CF}}$ $+\mathrm{S}_{\mathrm{ABD}} + \mathrm{S}_{\mathrm{ABE}} + 2\mathrm{S}_{\mathrm{ABF}} + \mathrm{S}_{\mathrm{ACF}} + \mathrm{S}_{\mathrm{ADF}} + \mathrm{S}_{\mathrm{BCF}} + \mathrm{S}_{\mathrm{BEF}}$
	$\mathrm{I}_{\mathrm{ABCF}} + \mathrm{I}_{\mathrm{ABDF}} + \mathrm{I}_{\mathrm{ABEF}} - \mathrm{I}_{\mathrm{ABC}} - \mathrm{I}_{\mathrm{ABF}} - \mathrm{I}_{\mathrm{AEF}} - \mathrm{I}_{\mathrm{BDF}}$
ICC	$-I_3(\mathrm{AD:B:F}) - I_3(\mathrm{A:E:F|B}) - I_3(\mathrm{A:B:C|F})$
$Q^{[13]}_{\{5,3\}}$	$-\mathrm{S}_{\mathrm{ABCF}} - \mathrm{S}_{\mathrm{ABEF}} - \mathrm{S}_{\mathrm{CDEF}} - \mathrm{S}_{\mathrm{AF}} - \mathrm{S}_{\mathrm{BF}} - \mathrm{S}_{\mathrm{CD}} - \mathrm{S}_{\mathrm{CF}} - \mathrm{S}_{\mathrm{A}} - \mathrm{S}_{\mathrm{B}} - \mathrm{S}_{\mathrm{E}}$ $+\mathrm{S}_{\mathrm{ABF}} + \mathrm{S}_{\mathrm{ACF}} + \mathrm{S}_{\mathrm{AEF}} + \mathrm{S}_{\mathrm{BCF}} + \mathrm{S}_{\mathrm{BEF}} + \mathrm{S}_{\mathrm{CDE}} + \mathrm{S}_{\mathrm{CDF}} + \mathrm{S}_{\mathrm{AB}}$
	$\mathrm{I}_{\mathrm{ABCF}} + \mathrm{I}_{\mathrm{ABEF}} + \mathrm{I}_{\mathrm{CDEF}} - \mathrm{I}_{\mathrm{ABC}} - \mathrm{I}_{\mathrm{ABE}} - \mathrm{I}_{\mathrm{ABF}} - \mathrm{I}_{\mathrm{CEF}} - \mathrm{I}_{\mathrm{DEF}}$
IIC	$-I_3(\mathrm{CD:E:F}) - I_3(\mathrm{A:B:EF}) - I_3(\mathrm{A:B:C|F})$
$Q^{[14]}_{\{6,5,1\}}$	$-\mathrm{S}_{\mathrm{ABDEF}} - \mathrm{S}_{\mathrm{ABCF}} - \mathrm{S}_{\mathrm{CEF}} - \mathrm{S}_{\mathrm{AD}} - \mathrm{S}_{\mathrm{AF}} - \mathrm{S}_{\mathrm{BF}} - \mathrm{S}_{\mathrm{B}} - \mathrm{S}_{\mathrm{C}} - \mathrm{S}_{\mathrm{E}}$ $+\mathrm{S}_{\mathrm{ADEF}} + \mathrm{S}_{\mathrm{ABD}} + \mathrm{S}_{\mathrm{ABF}} + \mathrm{S}_{\mathrm{ACF}} + \mathrm{S}_{\mathrm{BCF}} + \mathrm{S}_{\mathrm{BEF}} + \mathrm{S}_{\mathrm{CE}}$
	$-\mathrm{I}_{\mathrm{ABDEF}} + \mathrm{I}_{\mathrm{ABCF}} + \mathrm{I}_{\mathrm{ABDE}} + \mathrm{I}_{\mathrm{ABDF}} + \mathrm{I}_{\mathrm{ABEF}} + \mathrm{I}_{\mathrm{BDEF}} - \mathrm{I}_{\mathrm{ABC}} - \mathrm{I}_{\mathrm{ABE}} - \mathrm{I}_{\mathrm{ABF}} - \mathrm{I}_{\mathrm{BDE}} - \mathrm{I}_{\mathrm{BDF}} - \mathrm{I}_{\mathrm{CEF}}$
IIC	$-I_3(\mathrm{C:E:F}) - I_3(\mathrm{AD:B:EF}) - I_3(\mathrm{A:B:C|F})$
$Q^{[17]}_{\{7,6,1\}}$	$-\mathrm{S}_{\mathrm{ABDEF}} - \mathrm{S}_{\mathrm{ABCF}} - \mathrm{S}_{\mathrm{CDEF}} - \mathrm{S}_{\mathrm{AD}} - \mathrm{S}_{\mathrm{AF}} - \mathrm{S}_{\mathrm{BF}} - \mathrm{S}_{\mathrm{CD}} - \mathrm{S}_{\mathrm{CF}} - \mathrm{S}_{\mathrm{B}} - \mathrm{S}_{\mathrm{E}}$ $+\mathrm{S}_{\mathrm{ADEF}} + \mathrm{S}_{\mathrm{ABD}} + \mathrm{S}_{\mathrm{ABF}} + \mathrm{S}_{\mathrm{ACF}} + \mathrm{S}_{\mathrm{BCF}} + \mathrm{S}_{\mathrm{BEF}} + \mathrm{S}_{\mathrm{CDE}} + \mathrm{S}_{\mathrm{CDF}}$
	$-\mathrm{I}_{\mathrm{ABDEF}} + \mathrm{I}_{\mathrm{ABCF}} + \mathrm{I}_{\mathrm{ABDE}} + \mathrm{I}_{\mathrm{ABDF}} + \mathrm{I}_{\mathrm{ABEF}} + \mathrm{I}_{\mathrm{BDEF}} + \mathrm{I}_{\mathrm{CDEF}}$ $-\mathrm{I}_{\mathrm{ABC}} - \mathrm{I}_{\mathrm{ABE}} - \mathrm{I}_{\mathrm{ABF}} - \mathrm{I}_{\mathrm{BDE}} - \mathrm{I}_{\mathrm{BDF}} - \mathrm{I}_{\mathrm{CEF}} - \mathrm{I}_{\mathrm{DEF}}$
IIC	$-I_3(\mathrm{CD:E:F}) - I_3(\mathrm{AD:B:EF}) - I_3(\mathrm{A:B:C|F})$
$Q^{[125]}_{\{6,4\}}$	$-\mathrm{S}_{\mathrm{ABCF}} - \mathrm{S}_{\mathrm{ABDE}} - \mathrm{S}_{\mathrm{ABEF}} - \mathrm{S}_{\mathrm{CDEF}} - \mathrm{S}_{\mathrm{AE}} - \mathrm{S}_{\mathrm{AF}} - \mathrm{S}_{\mathrm{BE}} - \mathrm{S}_{\mathrm{BF}} - \mathrm{S}_{\mathrm{CD}} - \mathrm{S}_{\mathrm{CF}} - \mathrm{S}_{\mathrm{DE}} - \mathrm{S}_{\mathrm{A}} - \mathrm{S}_{\mathrm{B}}$ $+\mathrm{S}_{\mathrm{ABE}} + \mathrm{S}_{\mathrm{ABF}} + \mathrm{S}_{\mathrm{ACF}} + \mathrm{S}_{\mathrm{ADE}} + \mathrm{S}_{\mathrm{AEF}} + \mathrm{S}_{\mathrm{BCF}} + \mathrm{S}_{\mathrm{BDE}} + \mathrm{S}_{\mathrm{BEF}} + \mathrm{S}_{\mathrm{CDE}} + \mathrm{S}_{\mathrm{CDF}} + \mathrm{S}_{\mathrm{AB}}$
	$\mathrm{I}_{\mathrm{ABCF}} + \mathrm{I}_{\mathrm{ABDE}} + \mathrm{I}_{\mathrm{ABEF}} + \mathrm{I}_{\mathrm{CDEF}} - \mathrm{I}_{\mathrm{ABC}} - \mathrm{I}_{\mathrm{ABD}} - \mathrm{I}_{\mathrm{ABE}} - \mathrm{I}_{\mathrm{ABF}} - \mathrm{I}_{\mathrm{CEF}} - \mathrm{I}_{\mathrm{DEF}}$
IICC	$-I_3(\mathrm{CD:E:F}) - I_3(\mathrm{A:B:EF}) - I_3(\mathrm{A:B:D|E}) - I_3(\mathrm{A:B:C|F})$
$Q^{[19]}_{\{8,8,2\}}$	$-\mathrm{S}_{\mathrm{ABCDF}} - \mathrm{S}_{\mathrm{ABDEF}} - \mathrm{S}_{\mathrm{BCDEF}} - \mathrm{S}_{\mathrm{BCE}} - \mathrm{S}_{\mathrm{CDF}} - \mathrm{S}_{\mathrm{AD}} - \mathrm{S}_{\mathrm{AF}} - \mathrm{S}_{\mathrm{BE}} - \mathrm{S}_{\mathrm{BF}} - \mathrm{S}_{\mathrm{D}} - \mathrm{S}_{\mathrm{F}}$ $+\mathrm{S}_{\mathrm{ABDE}} + \mathrm{S}_{\mathrm{ACDF}} + \mathrm{S}_{\mathrm{BCDE}} + \mathrm{S}_{\mathrm{BCDF}} + \mathrm{S}_{\mathrm{BCEF}} + \mathrm{S}_{\mathrm{ABF}} + \mathrm{S}_{\mathrm{ADF}} + \mathrm{S}_{\mathrm{BEF}} + \mathrm{S}_{\mathrm{DF}}$
	$-\mathrm{I}_{\mathrm{ABCDF}} - \mathrm{I}_{\mathrm{ABDEF}} - \mathrm{I}_{\mathrm{BCDEF}} + \mathrm{I}_{\mathrm{ABCD}} + \mathrm{I}_{\mathrm{ABCF}} + 2\mathrm{I}_{\mathrm{ABDF}} + \mathrm{I}_{\mathrm{ABEF}} + \mathrm{I}_{\mathrm{ADEF}} + \mathrm{I}_{\mathrm{BCDF}} + 2\mathrm{I}_{\mathrm{BDEF}}$ $+\mathrm{I}_{\mathrm{CDEF}} - \mathrm{I}_{\mathrm{ABC}} - \mathrm{I}_{\mathrm{ABD}} - \mathrm{I}_{\mathrm{ABF}} - \mathrm{I}_{\mathrm{AEF}} - 2\mathrm{I}_{\mathrm{BDF}} - \mathrm{I}_{\mathrm{CDF}} - 2\mathrm{I}_{\mathrm{DEF}}$
IIC	$-I_3(\mathrm{BCE:D:F}) - I_3(\mathrm{AD:BE:F}) - I_3(\mathrm{A:B:CD|F})$
$Q^{[21]}_{\{8,8,2\}}$	$-\mathrm{S}_{\mathrm{ABCDF}} - \mathrm{S}_{\mathrm{ABDEF}} - \mathrm{S}_{\mathrm{CDF}} - \mathrm{S}_{\mathrm{AD}} - \mathrm{S}_{\mathrm{AF}} - \mathrm{S}_{\mathrm{BC}} - \mathrm{S}_{\mathrm{BE}} - \mathrm{S}_{\mathrm{BF}} - \mathrm{S}_{\mathrm{D}} - \mathrm{S}_{\mathrm{F}}$ $+\mathrm{S}_{\mathrm{ABDE}} + \mathrm{S}_{\mathrm{ACDF}} + \mathrm{S}_{\mathrm{ABF}} + \mathrm{S}_{\mathrm{ADF}} + \mathrm{S}_{\mathrm{BCD}} + \mathrm{S}_{\mathrm{BCF}} + \mathrm{S}_{\mathrm{BEF}} + \mathrm{S}_{\mathrm{DF}}$
	$-\mathrm{I}_{\mathrm{ABCDF}} - \mathrm{I}_{\mathrm{ABDEF}} + \mathrm{I}_{\mathrm{ABCD}} + \mathrm{I}_{\mathrm{ABCF}} + 2\mathrm{I}_{\mathrm{ABDF}} + \mathrm{I}_{\mathrm{ABEF}} + \mathrm{I}_{\mathrm{ADEF}} + \mathrm{I}_{\mathrm{BCDF}} + \mathrm{I}_{\mathrm{BDEF}}$ $-\mathrm{I}_{\mathrm{ABC}} - \mathrm{I}_{\mathrm{ABD}} - \mathrm{I}_{\mathrm{ABF}} - \mathrm{I}_{\mathrm{AEF}} - 2\mathrm{I}_{\mathrm{BDF}} - \mathrm{I}_{\mathrm{CDF}} - \mathrm{I}_{\mathrm{DEF}}$
IIC	$-I_3(\mathrm{BC:D:F}) - I_3(\mathrm{AD:BE:F}) - I_3(\mathrm{A:B:CD|F})$
$Q^{[23]}_{\{10,11,3\}}$	$-\mathrm{S}_{\mathrm{ABCDE}} - \mathrm{S}_{\mathrm{ABCDF}} - \mathrm{S}_{\mathrm{ABDEF}} - \mathrm{S}_{\mathrm{CDF}} - \mathrm{S}_{\mathrm{AD}} - \mathrm{S}_{\mathrm{AF}} - \mathrm{S}_{\mathrm{BC}} - \mathrm{S}_{\mathrm{BE}} - \mathrm{S}_{\mathrm{BF}} - \mathrm{S}_{\mathrm{DE}} - \mathrm{S}_{\mathrm{A}}$ $+\mathrm{S}_{\mathrm{ABDE}} + \mathrm{S}_{\mathrm{ACDF}} + \mathrm{S}_{\mathrm{BCDE}} + \mathrm{S}_{\mathrm{BCDF}} + \mathrm{S}_{\mathrm{ABC}} + \mathrm{S}_{\mathrm{ABF}} + \mathrm{S}_{\mathrm{ADE}} + \mathrm{S}_{\mathrm{ADF}} + \mathrm{S}_{\mathrm{BEF}}$
	$-\mathrm{I}_{\mathrm{ABCDE}} - \mathrm{I}_{\mathrm{ABCDF}} - \mathrm{I}_{\mathrm{ABDEF}} + 2\mathrm{I}_{\mathrm{ABCD}} + \mathrm{I}_{\mathrm{ABCE}} + \mathrm{I}_{\mathrm{ABCF}} + \mathrm{I}_{\mathrm{ABDE}} + 2\mathrm{I}_{\mathrm{ABDF}} + \mathrm{I}_{\mathrm{ABEF}} + \mathrm{I}_{\mathrm{ACDE}}$ $+\mathrm{I}_{\mathrm{ADEF}} + \mathrm{I}_{\mathrm{BDEF}} - \mathrm{I}_{\mathrm{ABC}} - 2\mathrm{I}_{\mathrm{ABD}} - \mathrm{I}_{\mathrm{ABE}} - \mathrm{I}_{\mathrm{ABF}} - \mathrm{I}_{\mathrm{ACD}} - \mathrm{I}_{\mathrm{ACE}} - \mathrm{I}_{\mathrm{AEF}} - \mathrm{I}_{\mathrm{BDF}} - \mathrm{I}_{\mathrm{DEF}}$
IIC	$-I_3(\mathrm{A:BC:DE}) - I_3(\mathrm{AD:BE:F}) - I_3(\mathrm{A:B:CD|F})$
$Q^{[35]}_{\{8,6,1\}}$	$-\mathrm{S}_{\mathrm{ABCDF}} - \mathrm{S}_{\mathrm{ACEF}} - \mathrm{S}_{\mathrm{BDEF}} - \mathrm{S}_{\mathrm{CDF}} - 2\mathrm{S}_{\mathrm{AF}} - \mathrm{S}_{\mathrm{DE}} - \mathrm{S}_{\mathrm{EF}} - \mathrm{S}_{\mathrm{A}} - \mathrm{S}_{\mathrm{B}} - 2\mathrm{S}_{\mathrm{C}} - \mathrm{S}_{\mathrm{D}}$ $+\mathrm{S}_{\mathrm{BCDF}} + \mathrm{S}_{\mathrm{ABF}} + \mathrm{S}_{\mathrm{ACF}} + \mathrm{S}_{\mathrm{ADF}} + \mathrm{S}_{\mathrm{AEF}} + \mathrm{S}_{\mathrm{BDE}} + \mathrm{S}_{\mathrm{CEF}} + \mathrm{S}_{\mathrm{DEF}} + \mathrm{S}_{\mathrm{AC}} + \mathrm{S}_{\mathrm{CD}}$
	$-\mathrm{I}_{\mathrm{ABCDF}} + \mathrm{I}_{\mathrm{ABCD}} + \mathrm{I}_{\mathrm{ABCF}} + \mathrm{I}_{\mathrm{ABDF}} + \mathrm{I}_{\mathrm{ACDF}} + \mathrm{I}_{\mathrm{ACEF}} + \mathrm{I}_{\mathrm{BDEF}}$ $-\mathrm{I}_{\mathrm{ABC}} - \mathrm{I}_{\mathrm{ABD}} - \mathrm{I}_{\mathrm{ACD}} - \mathrm{I}_{\mathrm{ACE}} - \mathrm{I}_{\mathrm{ACF}} - \mathrm{I}_{\mathrm{BDF}} - \mathrm{I}_{\mathrm{BEF}} - \mathrm{I}_{\mathrm{CDF}}$
IIIC	$-I_3(\mathrm{AF:C:D}) - I_3(\mathrm{B:DE:F}) - I_3(\mathrm{A:C:EF}) - I_3(\mathrm{A:B:CD|F})$
$Q^{[46]}_{\{9,8,2\}}$	$-2\mathrm{S}_{\mathrm{ABCDF}} - \mathrm{S}_{\mathrm{ACEF}} - \mathrm{S}_{\mathrm{BDEF}} - \mathrm{S}_{\mathrm{CDF}} - \mathrm{S}_{\mathrm{AF}} - \mathrm{S}_{\mathrm{DE}} - \mathrm{S}_{\mathrm{EF}} - \mathrm{S}_{\mathrm{A}} - \mathrm{S}_{\mathrm{B}} - 2\mathrm{S}_{\mathrm{C}} - \mathrm{S}_{\mathrm{D}}$ $+\mathrm{S}_{\mathrm{ABCF}} + \mathrm{S}_{\mathrm{ABDF}} + \mathrm{S}_{\mathrm{ACDF}} + \mathrm{S}_{\mathrm{BCDF}} + \mathrm{S}_{\mathrm{AEF}} + \mathrm{S}_{\mathrm{BDE}} + \mathrm{S}_{\mathrm{CEF}} + \mathrm{S}_{\mathrm{DEF}} + \mathrm{S}_{\mathrm{AC}} + \mathrm{S}_{\mathrm{CD}}$
	$-2\mathrm{I}_{\mathrm{ABCDF}} + 2\mathrm{I}_{\mathrm{ABCD}} + \mathrm{I}_{\mathrm{ABCF}} + \mathrm{I}_{\mathrm{ABDF}} + \mathrm{I}_{\mathrm{ACDF}} + \mathrm{I}_{\mathrm{ACEF}} + \mathrm{I}_{\mathrm{BCDF}} + \mathrm{I}_{\mathrm{BDEF}}$ $-\mathrm{I}_{\mathrm{ABC}} - \mathrm{I}_{\mathrm{ABD}} - \mathrm{I}_{\mathrm{ACD}} - \mathrm{I}_{\mathrm{ACE}} - \mathrm{I}_{\mathrm{ACF}} - \mathrm{I}_{\mathrm{BCD}} - \mathrm{I}_{\mathrm{BDF}} - \mathrm{I}_{\mathrm{BEF}} - \mathrm{I}_{\mathrm{CDF}}$
IIIC	$-I_3(\mathrm{ABF:C:D}) - I_3(\mathrm{B:DE:F}) - I_3(\mathrm{A:C:EF}) - I_3(\mathrm{A:B:CD|F})$

Table 2.2.: HEI information quantities for N = 6, with the same notational conventions as in table 2.1.

Structural similarities: Upon closer examination of the tripartite form expressions for the HEIs, we find that many HEIs are very similar to each other, sometimes differing by only a single letter in a single argument. Such structural similarities between distinct HEI orbits may suggest a common origin, in the sense of modifying the same lower-N HEI in combinatorially distinct ways. For example, let us compare the compact form for $Q^{[7]}$, $Q^{[13]}$, $Q^{[14]}$, and $Q^{[17]}$ (the first from table 2.1 and the other three from table 2.2, for convenience reproduced here):

$$\begin{aligned}
Q^{[7]}_{\{4,2\}} &= -I_3(\mathrm{C}:\mathrm{E}:\mathrm{F}) - I_3(\mathrm{A}:\mathrm{B}:\mathrm{EF}) - I_3(\mathrm{A}:\mathrm{B}:\mathrm{C}|\mathrm{F}) \\
Q^{[13]}_{\{5,3\}} &= -I_3(\mathrm{CD}:\mathrm{E}:\mathrm{F}) - I_3(\mathrm{A}:\mathrm{B}:\mathrm{EF}) - I_3(\mathrm{A}:\mathrm{B}:\mathrm{C}|\mathrm{F}) \\
Q^{[14]}_{\{6,5,1\}} &= -I_3(\mathrm{C}:\mathrm{E}:\mathrm{F}) - I_3(\mathrm{AD}:\mathrm{B}:\mathrm{EF}) - I_3(\mathrm{A}:\mathrm{B}:\mathrm{C}|\mathrm{F}) \\
Q^{[17]}_{\{7,6,1\}} &= -I_3(\mathrm{CD}:\mathrm{E}:\mathrm{F}) - I_3(\mathrm{AD}:\mathrm{B}:\mathrm{EF}) - I_3(\mathrm{A}:\mathrm{B}:\mathrm{C}|\mathrm{F})
\end{aligned} \tag{2.5.2}$$

We see that the last three ($\mathsf{N} = 6$) quantities build up on the first ($\mathsf{N} = 5$) one by augmenting a single argument in, respectively, the first, second, and both, I_3 terms, by a new party D which did not appear in the $\mathsf{N} = 5$ quantity. Since the two I_3 terms in the $\mathsf{N} = 5$ quantity ($Q^{[7]}$) had arguments with different cardinalities, all four quantities have different number of terms when expanded in the I-basis (as indicated by the i# subscripts). Hence the structural relation between these four expressions would have been difficult to discover without the compact form. Moreover, the originally obtained quantities might be in different orbits, making their relations even more obscure. On the other hand, in the tripartite form with only a few terms, it is much easier to obtain a permutation that aligns the quantities for direct comparison as above, which is particularly convenient when the arguments have different cardinalities.[23]

Another type of structural relation is illustrated by the following triplet:

$$\begin{aligned}
Q^{[35]}_{\{8,6,1\}} &= -I_3(\mathrm{AF}:\mathrm{C}:\mathrm{D}) - I_3(\mathrm{B}:\mathrm{DE}:\mathrm{F}) - I_3(\mathrm{A}:\mathrm{C}:\mathrm{EF}) - I_3(\mathrm{A}:\mathrm{B}:\mathrm{CD}|\mathrm{F}) \\
Q^{[33]}_{\{8,6,1\}} &= -I_3(\mathrm{BF}:\mathrm{C}:\mathrm{D}) - I_3(\mathrm{B}:\mathrm{DE}:\mathrm{F}) - I_3(\mathrm{A}:\mathrm{C}:\mathrm{EF}) - I_3(\mathrm{A}:\mathrm{B}:\mathrm{CD}|\mathrm{F}) \\
Q^{[46]}_{\{9,8,2\}} &= -I_3(\mathrm{ABF}:\mathrm{C}:\mathrm{D}) - I_3(\mathrm{B}:\mathrm{DE}:\mathrm{F}) - I_3(\mathrm{A}:\mathrm{C}:\mathrm{EF}) - I_3(\mathrm{A}:\mathrm{B}:\mathrm{CD}|\mathrm{F})
\end{aligned} \tag{2.5.3}$$

[23] Indeed, the specific instance of each permutation orbit was chosen precisely so as to render the compact expressions conveniently aligned. In particular, we condition on F, with the last term always being $I_3(\mathrm{A}:\mathrm{B}:\mathrm{C}|\mathrm{F})$, and the remaining freedom in permuting is used to obtain as much similarity as possible on the other terms.

The only difference between these three expressions is in the first argument of the first term, where F is augmented by A, B, and AB, respectively.[24] On the other hand, this type of 'merging' of a pair of HEIs does not always produce the third. For example, while there is a structurally analogous companion to $Q^{[17]}_{\{7,6,1\}}$ (cf. eq. (2.5.2)), where the first argument of the first term changes from CD to AC, the 'merged' version, with the first argument becoming ACD, is not an HEI.[25]

There are several other types of near-complete similarities between certain pairs of HEIs. One rather common type is when one singleton gets 'transferred' between two arguments in a single I term, such as

$$\begin{aligned} Q^{[219]}_{\{9,9,2\}} &= -I_3(\text{BF}:\text{C}:\text{D}) - I_3(\text{AC}:\text{B}:\text{DE}) - I_3(\text{A}:\text{B}:\text{C}|\text{D}) - I_3(\text{A}:\text{CE}:\text{F}|\text{B}) \\ Q^{[222]}_{\{9,9,2\}} &= -I_3(\text{B}:\text{CF}:\text{D}) - I_3(\text{AC}:\text{B}:\text{DE}) - I_3(\text{A}:\text{B}:\text{C}|\text{D}) - I_3(\text{A}:\text{CE}:\text{F}|\text{B}) \end{aligned} \tag{2.5.4}$$

where in the 1st term, the F gets transferred from B to C. Often, but not always, this in fact constitutes a pair of augmentations; in this case, the expression without the F on either argument in the 1st term is indeed another HEI, namely $Q^{[19]}$. It would be interesting to understand such structural relations more systematically; we leave this for future explorations.

Building up HEIs: One particularly useful outcome of a systematic understanding of the structural relations between the HEIs would be a more direct solution-generating technique for higher-N HEIs, by bootstrapping successive augmentations or other modifications. To exemplify the idea, consider MMI (uplifted from $\mathsf{N}=3$), $Q^{[2]}_{\{1\}} = -\mathtt{I}_{\text{A:B:C}}$. We can augment one argument, say C $\to$ CD, to get a fine-grained version of MMI,[26] which is in fact $Q^{[3]}_{\{2,1\}} = -I_3(\text{A:B:CD})$. Using eq. (2.2.20), this can be recast as $Q^{[3]}_{\{2,1\}} = -I_3(\text{A:B:D}) - I_3(\text{A:B:C}|\text{D})$. Now, we can view this as the starting point and augment one argument in the first term, say B $\to$ BE. (Note that this is no longer a mere fine-graining, since other occurrences of B which appear elsewhere in the quan-

[24] Note that the first two expressions, while having the same number of I-basis terms, belong to distinct orbits, since A and B play different roles in the remaining terms.

[25] In this case it is a valid holographic inequality, but it does not define a facet, because it is redundant (in fact it is the sum of two different permutations of an uplift of the simplest $\mathsf{N}=5$ HEI, $Q^{[5]}_{\{3,2\}}$).

[26] Equivalently, we can obtain this by considering the original MMI at $\mathsf{N}=4$, using eq. (2.B.19) to replace one argument by complement of the union of the original ones, uplifting to $\mathsf{N}=6$, and permuting to get the desired form.

tity are left un-augmented.) Although such an augmentation was not a-priori guaranteed to lead to a valid HEI, nevertheless, it is indeed one, namely $Q^{[5]}_{\{3,2\}} = -I_3(\mathrm{A}:\mathrm{BE}:\mathrm{D}) - I_3(\mathrm{A}:\mathrm{B}:\mathrm{C}|\mathrm{D})$. Since F does not appear, this is intrinsically an $\mathsf{N} = 5$ HEI. However, we can also augment two of the I_3 arguments by different subsystems, resulting in a genuine $\mathsf{N} = 6$ HEI, namely $Q^{[12]}_{\{5,5,1\}} = -I_3(\mathrm{AF}:\mathrm{BE}:\mathrm{D}) - I_3(\mathrm{A}:\mathrm{B}:\mathrm{C}|\mathrm{D})$. Note that had we merely fine-grained $\mathrm{A} \to \mathrm{AF}$ in $Q^{[5]}_{\{3,2\}}$, we would have obtained an uplift of $Q^{[5]}_{\{3,2\}}$ which in our search for $\mathsf{N} = 6$ HEIs indeed showed up, as another instance in the orbit of $Q^{[6]}_{\{5,5,1\}}$.

A distinct way of building up new HEIs at a fixed N is to leave the arguments in the individual tripartite terms unmodified, but add more tripartite terms. Non-redundancy requires that each new term is a C rather than I. We can then obtain a chain of HEIs, such as I - IC - ICC - ICCC, which has a realization already at $\mathsf{N} = 5$:

$$\begin{aligned}
Q^{[3]}_{\{2,1\}} &= -I_3(\mathrm{A}:\mathrm{BE}:\mathrm{D}) \\
Q^{[5]}_{\{3,2\}} &= -I_3(\mathrm{A}:\mathrm{BE}:\mathrm{D}) \quad -I_3(\mathrm{A}:\mathrm{B}:\mathrm{C}|\mathrm{D}) \\
Q^{[9]}_{\{4,3\}} &= -I_3(\mathrm{A}:\mathrm{BE}:\mathrm{D}) \quad -I_3(\mathrm{A}:\mathrm{B}:\mathrm{C}|\mathrm{D}) \quad -I_3(\mathrm{C}:\mathrm{D}:\mathrm{E}|\mathrm{A}) \\
Q^{[6]}_{\{5,5,1\}} &= -I_3(\mathrm{A}:\mathrm{BE}:\mathrm{D}) \quad -I_3(\mathrm{A}:\mathrm{B}:\mathrm{C}|\mathrm{D}) \quad -I_3(\mathrm{C}:\mathrm{D}:\mathrm{E}|\mathrm{A}) \quad -I_3(\mathrm{B}:\mathrm{C}:\mathrm{E}|\mathrm{AD})
\end{aligned} \tag{2.5.5}$$

For both types of building up new HEIs from simpler ones, the crucial question is what are the necessary and sufficient conditions for its applicability; in other words, what characterizes the augmentations which produce another HEI.

2.6. Discussion

Our main result is that the non-negative information quantities associated to HEIs cannot at face value be understood as measures of correlations, as they lack the basic property of monotonicity under partial tracing. This does not preclude the existence of useful multipartite measures of holographic correlations, but does eliminate the only natural candidates arising from the polyhedral structure of the holographic entropy cone.[27] Besides this negative result,

[27] Since measures of multipartite correlations are famously poorly understood, it is also conceivable that our requirement of monotonicity simply be too strong. Our result would then potentially motivate a search for weaker, non-bipartite notions of monotonicity, or for a more relational requirement on correlations among subsystems, rather than a one-directional comparison between competing terms under partial tracing.

throughout this chapter we have proved several structural properties of HEIs, as well as explored a fruitful rewriting thereof in terms of I_3 and conditional I_3 quantities. This tripartite form has proven to be a powerful heuristic ansatz for the discovery of a plethora of novel HEIs which constitute facets of the $\mathsf{N} = 6$ holographic entropy cone.

While we have not proved that every HEI must necessarily be expressible in tripartite form, it is natural to conjecture that this is indeed the case. One encouraging piece of evidence comes from the fact that all the known HEIs for $\mathsf{N} \leq 6$ can be recast in this form. Even the new $\mathsf{N} = 7$ HEI introduced by [CW23] (cf. their eq. (2.1), which has the $\mathtt{I}_n$-multiplicities $\{10, 15, 6\}$) can likewise be recast in the tripartite form, as ICCCCCC. This seems a highly-nontrivial check, since it has the minimal number of $\mathtt{I}_3$'s possible to 'soak up' all the higher $\mathtt{I}_n$ terms. Indeed, [CW23] motivated this inequality by positing "oxidation" of $\mathsf{N} = 5$ HEI, built so as to guarantee that upon trivializing any subsystem, the HEI necessarily remains valid. The building blocks of the tripartite form partly incorporate this, in the sense that when the oxidized party is conditioned on, the C term reduces to I, while if it is one of the other arguments, the term trivializes, in both cases ensuring sign-definiteness. However this by itself does not guarantee sign-definiteness when only a subset of an argument in a C term trivializes. It would be interesting to see whether this observation could be utilized to further constrain the possible combinations of arguments in multiple terms of the tripartite form.

The challenge of understanding and classifying HEIs remains open. Besides recasting HEIs in tripartite form, one could try to extract structural properties of HEIs by exploring their symmetries. Naively characterizing the symmetry group of HEIs is however not a fruitful venue: most $\mathsf{N} = 6$ HEIs have no symmetries at all. Instead, a more promising pursuit consists of decomposing HEIs into representations of the symmetric group [CW23], an idea that generalizes the intriguing results looking at symmetric invariants of [CS21; FH22].

In a parallel series of works [HHRR19; HHR22b; HHR22a; HHR23; HHR24] which focus on extreme rays, rather than the facets, of the HEC, a more primal structure plays a prominent role: One can define the subadditivity cone (SAC) for any number of parties as the intersection of half-spaces given by all instances of SA, cf. eq. (2.1.1). Since this region of entropy space merely restricts the entropy vector to have a non-negative amount of correlation between any pair of subsystems, it contains the HEC (strictly for all $\mathsf{N} \geq 3$). Nevertheless, subject to a

certain conjecture, [HHR22b] showed that the HEC extreme rays can be obtained from the set of holographically-realizable extreme rays of the SAC of a more fine-grained system, by a suitable coarse-graining procedure.[28] In other words, subadditivity fundamentally underlies the emergence of the HEC. It would be interesting to explore whether the relevant SAC extreme rays can be repackaged to directly determine the HEIs, perhaps as a combination of polychromatic mutual information quantities. This would then elucidate the role of HEIs and their relation to correlation measures.

Another recurring theme, present in both facet and extreme ray representations, is the structural relation between different values of N. It was already emphasized in [HHR22b] that since the holographic system can be refined arbitrarily, fixing a specific value of N is artificial. It would be useful to formulate a more algorithmic way of 'bootstrapping' from smaller N to larger N. In the case of extreme rays, the graphical representation of larger-N extreme rays typically resembles some gluing of smaller-N extreme rays.[29] For facets, we have seen that they admit structural similarities when presented in the tripartite form which persist across N. Again, it would be interesting to examine whether these two observations are connected in some natural way.

Finally, recall that the multipartite information quantities, apart from their convenience in presenting the HEIs, also provide a useful diagnostic of the basic geometrical features of the bulk configuration. In particular, they diagnose the connectivity of the entanglement wedges of the various subsystems, cf. Proposition 2.2.1. This connectivity has operational implications for the HEIs. In the case of mutual information, [MPS20] used focusing arguments in general relativity to argue for existence of efficient non-local quantum computation protocols, which was further generalized by [MSY22] in "n-to-n connected wedge theorem". In fact, the consequence of theorem 19 in [MSY22] on the non-vanishing mutual information across any bipartition of the full system might be more naturally rephrased as simply the non-vanishing of I_n. It would be interesting to see if this can provide any insight towards formulating a more operational meaning of the higher-party HEIs.

[28] Operationally, while finding all the extreme rays of the SAC is prohibitively difficult for larger N, obtaining the vastly smaller set of SSA-compatible ones can be performed much more efficiently, and in fact can be used to obtain the full set of holographically realizable extreme rays of the SAC for $\mathsf{N} = 6$ [HHR].

[29] This can be observed in fig. 12 of [HHR22b]. We thank Bogdan Stoica for some early explorations and conversations about this idea.

2.A. Factorized notation for $\mathtt{I}_n$'s

Here we briefly describe a powerful notational simplification, which serves to motivate interesting relational properties of the multipartite informations. Let us start with the entropy basis representation shorthand $\mathtt{S}_{\mathrm{AB}} \doteq \mathrm{AB}$ etc., where we can then rewrite a given expression in a 'factorized' form, for example, $\mathrm{AB} + \mathrm{BC} = (\mathrm{A} + \mathrm{C})\mathrm{B}$, where the 'multiplication' is to be understood purely at the level of notation (i.e., presenting the expression in a compact form) rather than pertaining to the actual values of the entropy itself; we will use the $\doteq$ sign to remind ourselves of this fact. It will further be convenient to use the notation $\varnothing \doteq 1$, which implements the relation $\mathrm{X} \cup \varnothing = \mathrm{X}$. Any residual instances of 1 in the resulting expression then represent the empty set and can be ignored (or inserted at will). To avoid ambiguity, we will put a tilde, $\tilde{\mathrm{X}} \equiv -1 + \mathrm{X}$. This factorized form becomes particularly compact for the $\mathtt{I}_n$'s, which (up to an overall sign) can be written as n simple factors of $\tilde{\mathrm{X}}$ for each argument X. For example,

$$\widetilde{\mathtt{I}}_2(\mathrm{A}_1 : \mathrm{A}_2) \doteq -1 + \mathrm{A}_1 + \mathrm{A}_2 - \mathrm{A}_1\,\mathrm{A}_2 = -(-1 + \mathrm{A}_1)\,(-1 + \mathrm{A}_2) = -\tilde{\mathrm{A}}_1\,\tilde{\mathrm{A}}_2 \tag{2.A.1}$$

and more generally[30]

$$\widetilde{\mathtt{I}}_n(\mathrm{A}_1 : \ldots : \mathrm{A}_n) \doteq (-1)^{n+1}\,\tilde{\mathrm{A}}_1 \cdots \tilde{\mathrm{A}}_n \tag{2.A.2}$$

This shorthand factorized form allows us to prove interesting relations between the multipartite informations. Particularly useful one is

$$\widetilde{\mathtt{I}}_{n+m}(\mathrm{A}_1 : \ldots : \mathrm{A}_n : \mathrm{B}_1 : \ldots : \mathrm{B}_m) = -\widetilde{\mathtt{I}}_n(\mathrm{A}_1 : \ldots : \mathrm{A}_n)\,\widetilde{\mathtt{I}}_m(\mathrm{B}_1 : \ldots : \mathrm{B}_m) \tag{2.A.3}$$

for any $n, m \geq 0$. In terms of the untilded quantities, we can rewrite this as

$$\begin{aligned} &\mathtt{I}_{n+m}(\mathrm{A}_1 : \ldots : \mathrm{A}_n : \mathrm{B}_1 : \ldots : \mathrm{B}_m) \\ &\qquad = -\mathtt{I}_n(\mathrm{A}_1 : \ldots : \mathrm{A}_n)\,\mathtt{I}_m(\mathrm{B}_1 : \ldots : \mathrm{B}_m) + \mathtt{I}_n(\mathrm{A}_1 : \ldots : \mathrm{A}_n) + \mathtt{I}_m(\mathrm{B}_1 : \ldots : \mathrm{B}_m)\ . \end{aligned} \tag{2.A.4}$$

It is worth stressing that the 'multiplication' employed here does not commute with evaluating the actual entropy whereas the summation does.

[30] Since we define $I_1(\mathrm{A}) := \mathrm{A}$, we can set $\widetilde{I}_1(\mathrm{A}) := \tilde{\mathrm{A}}$ and $I_0 := 0$, sot that $\widetilde{I}_0 := -1$.

2.B. Obtaining tripartite form for HEIs

In §2.5 we have presented a number of new $\mathsf{N} = 6$ HEIs, as well as previously known $\mathsf{N} = 5$ HEIs, written in a tripartite form. We have seen that this compact recasting is especially convenient, not only to represent the information quantity efficiently, but also to extract structural relations with other information quantities. In this appendix we explain how we can obtain this compact form, starting from the I-basis representation. (In fact this is how we originally arrived at the compact form of the $\mathsf{N} = 5$ HEIs, which inspired the presently-utilized search strategy.)

Grouping $\mathtt{I}_n$ terms to compact expressions: Consider any information quantity writ- ten out (uniquely) in the I-basis. We can often group terms (non-uniquely) to re-write it in terms of fewer terms involving I_n's with polychromatic arguments or involving conditional I_n's. This will turn out to be particularly efficient for the information quantities associated to HEIs, where the final expression involves only $n = 3$, i.e. tripartite information and conditional tripartite information.

The conversion makes use of eq. (2.2.20), which for $n = 3$ can be written as

$$I_3(\mathrm{B} : \dot{\mathcal{J}}|\mathrm{A}) = I_3(\mathrm{AB} : \dot{\mathcal{J}}) - I_3(\mathrm{A} : \dot{\mathcal{J}}) = I_3(\mathrm{B} : \dot{\mathcal{J}}) - I_4(\mathrm{A} : \mathrm{B} : \dot{\mathcal{J}}) \ . \tag{2.B.1}$$

In particular we can group the pair $\mathtt{I}_3 - \mathtt{I}_4$ to get conditional I_3,

$$\mathtt{I}_{\mathrm{ABC}} - \mathtt{I}_{\mathrm{ABCD}} = I_3(\mathrm{A{:}B{:}C|D}) \ , \tag{2.B.2}$$

or we can group the triplet $\mathtt{I}_3 + \mathtt{I}_3 - \mathtt{I}_4$ to get polychromatic I_3,

$$\mathtt{I}_{\mathrm{ABC}} + \mathtt{I}_{\mathrm{ABD}} - \mathtt{I}_{\mathrm{ABCD}} = I_3(\mathrm{A{:}B{:}CD}) \ . \tag{2.B.3}$$

Furthermore, we can iterate to group more terms. For example, for I_3 having arguments with cardinalities $(1 : 1 : 3)$, we can write this out as the 7-term expression with 3 $\mathtt{I}_3$'s, 3 $\mathtt{I}_4$'s, and 1 $\mathtt{I}_5$,

$$\mathtt{I}_{\mathrm{ABC}} + \mathtt{I}_{\mathrm{ABD}} + \mathtt{I}_{\mathrm{ABE}} - \mathtt{I}_{\mathrm{ABCD}} - \mathtt{I}_{\mathrm{ABCE}} - \mathtt{I}_{\mathrm{ABDE}} + \mathtt{I}_{\mathrm{ABCDE}} = I_3(\mathrm{A{:}B{:}CDE}) \ , \tag{2.B.4}$$

so if the I-basis expression happens to include these 7 terms, we can compress them into the single $I_3(1:1:3)$ term. Notice that both singletons from the RHS (here A and B) appear as arguments in each term on the LHS. Similarly, if we have I_3 with argument cardinalities $(1:2:2)$, then this gets decomposed into 9 terms, namely 4 $\mathtt{I}_3$'s, 4 $\mathtt{I}_4$'s, and 1 $\mathtt{I}_5$,

$$\mathtt{I}_{\mathrm{ABD}} + \mathtt{I}_{\mathrm{ABE}} + \mathtt{I}_{\mathrm{ACD}} + \mathtt{I}_{\mathrm{ACE}} - \mathtt{I}_{\mathrm{ABCD}} - \mathtt{I}_{\mathrm{ABCE}} - \mathtt{I}_{\mathrm{ABDE}} - \mathtt{I}_{\mathrm{ACDE}} + \mathtt{I}_{\mathrm{ABCDE}} = I_3(\mathrm{A{:}BC{:}DE}) \ , \quad (2.B.5)$$

where the singleton argument on the RHS (here A) is the common subscript on all the $\mathtt{I}_n$ terms, and the grouping for the doubletons is such that its 'factorization' gives the given $\mathtt{I}_3$ terms.

In fact, this pattern continues for arbitrary cardinalities of the arguments. We have a de-facto 'factorization' between all arguments, which comes from the special structure of the $\mathtt{I}_n$'s explained in §2.A. Specifically, the colons separating the arguments act as multiplication, and within each argument composed of ℓ singletons, say $\mathrm{X} = \prod_i \mathrm{A}_i$ the factor is given by $[1 - \prod_i (1 - \mathrm{A}_i))]$. (Note that when $\ell = 1$, this factor reduces to just A_1.)

Moreover, this type of structure extends to the conditioning as well: there we simply replace $[1 - \Pi]$ by $[\Pi]$, which becomes the product $\prod_j (1 - \mathrm{B}_j)$ over each singleton B_j comprising the party conditioned on. For example, to extract the expression for conditioning on a doubleton, we can combine the following 4 $\mathtt{I}_n$ terms:

$$\mathtt{I}_{\mathrm{ABC}} - \mathtt{I}_{\mathrm{ABCD}} - \mathtt{I}_{\mathrm{ABCE}} + \mathtt{I}_{\mathrm{ABCDE}} = I_3(\mathrm{A{:}B{:}C|DE}) \ . \quad (2.B.6)$$

Notice that here ABC appears in all terms, while the arguments conditioned on (CD) appear in the combination $(1 - \mathrm{C})(1 - \mathrm{D})$. Similarly, we can of course also combine the rule for polychromatic rewriting with that for conditioning rewriting, with the 'factorization' combined accordingly; e.g.

$$\mathtt{I}_{\mathrm{ABC}} + \mathtt{I}_{\mathrm{ABD}} - \mathtt{I}_{\mathrm{ABCD}} - \mathtt{I}_{\mathrm{ABCE}} - \mathtt{I}_{\mathrm{ABDE}} + \mathtt{I}_{\mathrm{ABCDE}} = I_3(\mathrm{A{:}B{:}CD|E}) \ . \quad (2.B.7)$$

Conversely, one could likewise write a single $\mathtt{I}_n$ in terms of polychromatic and conditional

tripartite informations, but with non-sign-definite coefficients; for example:

$$\begin{aligned}&\mathtt{I}_{\mathrm{ABCDE}}\\&= I_3(\mathrm{A{:}D{:}E}) + I_3(\mathrm{B{:}D{:}E}) + I_3(\mathrm{C{:}D{:}E}) - I_3(\mathrm{AB{:}D{:}E}) - I_3(\mathrm{AC{:}D{:}E}) - I_3(\mathrm{BC{:}D{:}E}) + I_3(\mathrm{ABC{:}D{:}E})\\&= I_3(\mathrm{C{:}D{:}E}) - I_3(\mathrm{C{:}D{:}E|A}) - I_3(\mathrm{C{:}D{:}E|B}) + I_3(\mathrm{C{:}D{:}E|AB})\ .\end{aligned} \tag{2.B.8}$$

Notice that in the first expression, the first argument from each term groups to a form of $\mathtt{I}_{\mathrm{ABC}}$ with $\underset{\cdot\cdot\cdot}{\mathrm{DE}}$ in the other two arguments coming along for the ride, while in the second expression the conditioning is on parties grouped effectively as $(1-\mathrm{A})(1-\mathrm{B})$, now with $\underset{\cdot\cdot\cdot\cdot\cdot}{\mathrm{CDE}}$ coming along for the ride.

Finally, note that we can also rewrite the polychromatic I_3 in terms of conditional and monochromatic ones; for example,

$$I_3(\mathrm{A{:}B{:}CD}) = I_3(\mathrm{A{:}B{:}C|D}) + I_3(\mathrm{A{:}B{:}D}) \tag{2.B.9}$$

$$I_3(\mathrm{A{:}B{:}CDE}) = I_3(\mathrm{A{:}B{:}C|DE}) + I_3(\mathrm{A{:}B{:}D|E}) + I_3(\mathrm{A{:}B{:}E}) \tag{2.B.10}$$

and so forth, so we could in principle reduce all polychromatic tripartite form quantities to expressions involving just singleton I_3's conditioned on polychromatic arguments (with the singleton $\mathtt{I}_3$ terms regarded as conditioned on zero-cardinality subsystem).

Simple example, $Q^{[24]}_{\{4,3\}}$: In the I-basis, the expression for some specific instance along the orbit is

$$Q^{[24]}_{\{4,3\}} = +\mathtt{I}_{\mathrm{ABCD}} + \mathtt{I}_{\mathrm{ABCE}} + \mathtt{I}_{\mathrm{ABCF}} - \mathtt{I}_{\mathrm{ABC}} - \mathtt{I}_{\mathrm{ABF}} - \mathtt{I}_{\mathrm{ACE}} - \mathtt{I}_{\mathrm{BCD}}$$

which involves 3 $\mathtt{I}_4$'s and 4 $\mathtt{I}_3$'s. Examining the subscripts, we see that we can group one of the $\mathtt{I}_4$'s with two of the $\mathtt{I}_3$'s to get a polychromatic I_3 and the remaining 2 $\mathtt{I}_4$'s each with a single $\mathtt{I}_3$ to get conditional I_3. Since ABC is included in each of the three $\mathtt{I}_4$ subscripts, whereas the remaining 3 $\mathtt{I}_3$ subscripts are contained in precisely one of the $\mathtt{I}_4$ subscripts, using eq. (2.B.2)

and eq. (2.B.3), we have three options at the above-specified grouping:

$$\begin{aligned} Q^{[24]}_{\{4,3\}} &= (\mathtt{I}_{\mathrm{ABCD}} - \mathtt{I}_{\mathrm{ABC}} - \mathtt{I}_{\mathrm{BCD}}) + (\mathtt{I}_{\mathrm{ABCE}} - \mathtt{I}_{\mathrm{ACE}}) + (\mathtt{I}_{\mathrm{ABCF}} - \mathtt{I}_{\mathrm{ABF}}) \\ &= -I_3(\mathrm{B{:}C{:}AD}) - I_3(\mathrm{A{:}C{:}E|B}) - I_3(\mathrm{A{:}B{:}F|C}) \\ &= (\mathtt{I}_{\mathrm{ABCD}} - \mathtt{I}_{\mathrm{BCD}}) + (\mathtt{I}_{\mathrm{ABCE}} - \mathtt{I}_{\mathrm{ABC}} - \mathtt{I}_{\mathrm{ACE}}) + (\mathtt{I}_{\mathrm{ABCF}} - \mathtt{I}_{\mathrm{ABF}}) \\ &= -I_3(\mathrm{B{:}C{:}D|A}) - I_3(\mathrm{A{:}C{:}BE}) - I_3(\mathrm{A{:}B{:}F|C}) \\ &= (\mathtt{I}_{\mathrm{ABCD}} - \mathtt{I}_{\mathrm{BCD}}) + (\mathtt{I}_{\mathrm{ABCE}} - \mathtt{I}_{\mathrm{ACE}}) + (\mathtt{I}_{\mathrm{ABCF}} - \mathtt{I}_{\mathrm{ABC}} - \mathtt{I}_{\mathrm{ABF}}) \\ &= -I_3(\mathrm{B{:}C{:}D|A}) - I_3(\mathrm{A{:}C{:}E|B}) - I_3(\mathrm{A{:}B{:}CF}) \end{aligned} \tag{2.B.11}$$

Note that all three compact expressions have the same structural form (not just as ICC, or even more specifically as a single tripartite information with argument cardinalities $(1:1:2)$ along with two $(1:1:1\,|\,1)$ conditional tripartite informations, but also relationally between the various arguments); in other words, they can be rotated into each other under permutations.

Another simple example, $Q^{[12]}_{\{5,5,1\}}$: Here we start with a longer expression in the I-basis (though shorter than $Q^{[24]}_{\{4,3\}}$ in the S-basis), which has 1 $\mathtt{I}_5$, 5 $\mathtt{I}_4$'s, and 5 $\mathtt{I}_3$'s:

$$Q^{[12]}_{\{5,5,1\}} = -\mathtt{I}_{\mathrm{ABCEF}} + \mathtt{I}_{\mathrm{ABCD}} + \mathtt{I}_{\mathrm{ABCE}} + \mathtt{I}_{\mathrm{ABCF}} + \mathtt{I}_{\mathrm{ABEF}} + \mathtt{I}_{\mathrm{ACEF}} - \mathtt{I}_{\mathrm{ABC}} - \mathtt{I}_{\mathrm{ABF}} - \mathtt{I}_{\mathrm{ACE}} - \mathtt{I}_{\mathrm{AEF}} - \mathtt{I}_{\mathrm{BCD}}$$

Since the $\mathtt{I}_5$ argument is missing a D, the first $\mathtt{I}_4$ cannot be combined with it naturally, whereas the other 4 can. Guessing that the first $\mathtt{I}_4$ and last $\mathtt{I}_3$ terms pair (into conditional tripartite information) and the remaining 9 terms group according to eq. (2.B.5) (into a polychromatic $(1:2:2)$ tripartite information), we can readily rewrite this as

$$Q^{[12]}_{\{5,5,1\}} = -I_3(\mathrm{A{:}BE{:}CF}) - I_3(\mathrm{B{:}C{:}D|A})$$

Non-uniqueness: Permutation symmetry of the arguments of I_n's imply that groupings of polychromatic and/or conditional multipartite informations are non-unique. For example, if we write $\mathtt{I}_{\mathrm{ABCD}}$ using eq. (2.2.6) in form of 3 $\mathtt{I}_3$'s, change which two arguments get grouped together, and cancel terms (or equivalently if we use permutation symmetry in the first group

of arguments in I_3(B:C:D|A)), we have

$$I_3(\text{B:C:D}|\text{A}) = \mathtt{I}_{\text{BCD}} - \mathtt{I}_{\text{ABCD}} = I_3(\text{AB:C:D}) - I_3(\text{A:C:D}) = I_3(\text{AC:B:D}) - I_3(\text{A:B:D}) \tag{2.B.12}$$

which can be re-cast into an identity of the form

$$I_3(\text{AB:C:D}) + I_3(\text{A:B:D}) = I_3(\text{AC:B:D}) + I_3(\text{A:C:D}) \tag{2.B.13}$$

Note that this is generalizable to any I_n, replacing D by any $\dot{\mathcal{J}}$ (or even the empty set).

As a more complicated example, from eq. (2.B.2) and eq. (2.B.3) we can re-express

$$\begin{aligned} \mathtt{I}_{\text{ACD}} &= I_3(\text{AB:C:D}) - I_3(\text{B:C:D}|\text{A}) \\ &= I_3(\text{A:BC:D}) - I_3(\text{A:B:D}|\text{C}) \\ &= I_3(\text{A:C:BD}) - I_3(\text{A:B:C}|\text{D}) \end{aligned} \tag{2.B.14}$$

where the separate lines interchange which argument the extra party B not appearing in the LHS gets added on. A seemingly different kind of identity is apparent in the triplet of compact expressions of eq. (2.B.11) which were obtained by re-grouping terms. However, all such relations are ultimately rooted in the permutation symmetry of I_n.

Signs and term counting: Given the multitude of identical expressions, it is useful to have some structural organizing principle which would facilitate determining what kind of a simplification of a given HEI is possible. First of all, recall (cf. Proposition 2.3.2) that in any HEI written in the I-basis, the $\mathtt{I}_n$ terms have coefficient of sign determined by n, namely $(-1)^n$. By eq. (2.2.20), we see that any conditional or polychromatic I_n with sign $(-1)^n$ preserves this structure when decomposed in the I-basis. This observation suggests that we can characterize each quantity in terms of how many $(-1)^n I_n$ terms it has for each n. For superbalanced HEI quantities, we start at $n = 3$, and if we only consider $\mathsf{N} \leq 6$, we only need to go up to $n = 6$. However, in all the HEIs we use for examples, the $\mathtt{I}_6$ term is absent. So each term is characterized by a triplet of integer coefficients, given by $\{i_3, i_4, i_5\}$ where i_n is the number of $(-1)^n I_n$ terms.

IQ	$i\#$ classification	equation
$-I_{(1:1:1)}$	$\{1,0,0\}$	defn.
$I_{(1:1:1:1)}$	$\{0,1,0\}$	defn.
$-I_{(1:1:2)}$	$\{2,1,0\}$	eq. (2.B.3)
$-C_{(1:1:1\|1)}$	$\{1,1,0\}$	eq. (2.B.2)
$-I_{(1:1:1:1:1)}$	$\{0,0,1\}$	defn.
$-I_{(1:1:3)}$	$\{3,3,1\}$	eq. (2.B.4)
$-I_{(1:2:2)}$	$\{4,4,1\}$	eq. (2.B.5)
$-C_{(1:1:1\|2)}$	$\{1,2,1\}$	eq. (2.B.6)
$-C_{(1:1:2\|1)}$	$\{2,3,1\}$	eq. (2.B.7)

Table 2.3.: $i\#$ classification for (conditional) multipartite information depending in size of arguments.

Let us now establish a more refined shorthand for conditional and polychromatic I_n's based on the size of the argument: $I_{(1:1:1)}$ is the singleton tripartite information while $I_{(1:1:2)}$ has doubleton for one of the arguments, and $C_{(1:1:1|1)}$ etc. indicates the corresponding conditional tripartite informations. Table 2.3 shows how these decompose in the $i\#$ classification. This classification allows us to take a given HEI and immediately extract the various possibilities for writing it out in various polychromatic combinations. Note that correct $i\#$ decomposition is necessary but not sufficient condition for being able to rewrite a given HEI, since it suppresses the finer structural details.

In the above two simple examples, we can see the implementation straightforwardly. $Q^{[24]}_{\{4,3\}}$ can be decomposed as $\{4,3,0\} = \{2,1,0\} + 2\{1,1,0\}$, giving the form $-I_{(1:1:2)} - C_{(1:1:1|1)} - C_{(1:1:1|1)}$ (cf. the second row block in table 2.2). Even more simply, $Q^{[12]}_{\{5,5,1\}}$ can be decomposed as $\{5,5,1\} = \{4,4,1\} + \{1,1,0\}$, giving the form $-I_{(1:2:2)} - C_{(1:1:1|1)}$. On the other hand, we can easily find examples where the simplest decomposition doesn't work. Below we examine one such case in full detail.

Cyclic inequality and purification: Consider $Q^{[5]}_{\{3,2\}}$ in the first row block of table 2.1. In this form,

$$Q^{[5]}_{\{3,2\}} = \mathtt{I}_{\mathrm{ABCD}} + \mathtt{I}_{\mathrm{ABCE}} - \mathtt{I}_{\mathrm{ABC}} - \mathtt{I}_{\mathrm{ABE}} - \mathtt{I}_{\mathrm{ACD}}$$

has the suggestive decomposition as $\{3,2,0\} = \{2,1,0\}+\{1,1,0\}$, namely as $-I_{(1:1:2)}-C_{(1:1:1|1)}$, which can in fact be achieved in two different ways (by alternate groupings), giving

$$\begin{aligned} Q^{[5]}_{\{3,2\}} &= -I_3(\text{A:B:CE}) - I_3(\text{A:C:D}|\text{B}) \\ &= -I_3(\text{A:C:BD}) - I_3(\text{A:B:E}|\text{C}) \end{aligned} \tag{2.B.15}$$

If however we use the corresponding S-basis expression,

$$Q^{[5]}_{\{3,2\}} = -\mathtt{S}_{\text{ABCD}} - \mathtt{S}_{\text{ABCE}} - \mathtt{S}_{\text{BC}} - \mathtt{S}_{\text{BD}} - \mathtt{S}_{\text{CE}} - \mathtt{S}_{\text{A}} + \mathtt{S}_{\text{ABC}} + \mathtt{S}_{\text{ABD}} + \mathtt{S}_{\text{ACE}} + \mathtt{S}_{\text{BCD}} + \mathtt{S}_{\text{BCE}}$$

and purify on A, under additionally replacing $\{\text{E},\text{O},\text{D},\text{B},\text{C}\} \to \{\text{A},\text{B},\text{C},\text{D},\text{E}\}$, we obtain the cyclic (dihedral) HEI in the canonical form,

$$Q^{[5]}_{\{5,5,1\}} = -\mathtt{S}_{\text{ABCDE}} - \mathtt{S}_{\text{AB}} - \mathtt{S}_{\text{BC}} - \mathtt{S}_{\text{CD}} - \mathtt{S}_{\text{DE}} - \mathtt{S}_{\text{EA}} + \mathtt{S}_{\text{ABC}} + \mathtt{S}_{\text{BCD}} + \mathtt{S}_{\text{CDE}} + \mathtt{S}_{\text{DEA}} + \mathtt{S}_{\text{EAB}}$$

which now has a longer form in the I-basis,

$$Q^{[5]}_{\{5,5,1\}} = -\mathtt{I}_{\text{ABCDE}} + \mathtt{I}_{\text{ABCD}} + \mathtt{I}_{\text{ABCE}} + \mathtt{I}_{\text{ABDE}} + \mathtt{I}_{\text{ACDE}} + \mathtt{I}_{\text{BCDE}} - \mathtt{I}_{\text{ABD}} - \mathtt{I}_{\text{ACD}} - \mathtt{I}_{\text{ACE}} - \mathtt{I}_{\text{BCE}} - \mathtt{I}_{\text{BDE}}$$

This demonstrates the important fact that the $i\#$ classification is not purification-invariant (though it is of course invariant under the smaller color permutation group; cf. footnote 22).

Let us now try to obtain a compact form for this expression. One natural decomposition that suggests itself is $\{5,5,1\} = \{4,4,1\} + \{1,1,0\}$, giving the form $-I_{(1:2:2)} - C_{(1:1:1|1)}$ (which is what we utilized for $Q^{[12]}_{\{5,5,1\}}$). However, the specific form of the present $Q^{[5]}_{\{5,5,1\}}$ does not allow such a decomposition. This is because the $-I_{(1:2:2)}$ term requires all 4 $\mathtt{I}_3$'s to have a common argument, whereas in $Q^{[5]}_{\{5,5,1\}}$ only groups of 3 $\mathtt{I}_3$'s have a common argument. To get around this, we could add and subtract a spurious $\mathtt{I}_3$ so as to complete the requisite form. This would give $Q^{[5]}_{\{5,5,1\}} = -I_3(\text{BC:DE:A}) - I_3(\text{CD:B:E}) + I_3(\text{A:B:E})$, which is still compact, but has the wrong sign, and therefore is not of the tripartite form: Its $i\#$ decomposition is $\{5,5,1\} = \{4,4,1\} + \{2,1,0\} - \{1,0,0\}$. Similarly, if we try the potential decomposition $\{5,5,1\} = \{3,3,1\} + \ldots$, we find that this likewise does not have the structurally necessary form, which requires all 3 of the $\mathtt{I}_3$'s to have two arguments in common.

A more complicated possibility is to use the decomposition $\{5,5,1\} = \{1,2,1\} + \{2,1,0\} + 2\{1,1,0\}$, which now does admit the corresponding tripartite form; in particular,

$$Q^{[5]}_{\{5,5,1\}} = -I_3(\text{A:B:D}|\text{CE}) - I_3(\text{AB:C:E}) - I_3(\text{A:C:D}|\text{E}) - I_3(\text{B:D:E}|\text{C}) \tag{2.B.16}$$

This now has correct signs, but at the expense of a longer expression.

In fact, noting that $\{5,5,1\} = \{1,1,0\} + \{2,3,1\} + \{2,1,0\}$, we might seek a combination of the form $-C_{(1:1:1|1)} - C_{(1:1:2|1)} - I_{(1:1:2)}$, and we leave it to the reader as an exercise to check that indeed a suitable regrouping gives the requisite form,[31]

$$Q^{[5]}_{\{5,5,1\}} = -I_3(\text{A:C:D}|\text{B}) - I_3(\text{AB:C:E}|\text{D}) - I_3(\text{AE:B:D}) \tag{2.B.17}$$

Transmutation of I_3's under purifications: Motivated by the previous example, it is clear that to extract the full power of groupings, we need to understand how the I_3's transform under purifications, which will allow us to rewrite and recombine the compact expressions in various ways. While we leave the full exploration for future work, two useful observations pertaining to the tripartite information, which follow as a direct consequence of Lemma 2.2.3, are the following. For any (possibly composite) subsystems $\text{X}, \text{Y}, \ldots$, the tripartite information for any tripartition of the full system vanishes,

$$I_3(\text{X} : \text{Y} : \overline{\text{XY}}) = 0 \ , \tag{2.B.18}$$

while for any quadripartition, we can swap any of the arguments for the missing one,

$$I_3(\text{X} : \text{Y} : \text{Z}) = I_3(\text{X} : \text{Y} : \overline{\text{XYZ}}) \ . \tag{2.B.19}$$

Furthermore, we can use this to build up the analogous relation for conditional tripartite information:

$$I_3(\text{X} : \text{Y} : \text{Z} \,|\, \text{W}) = -I_3(\text{X} : \text{Y} : \text{Z} \,|\, \overline{\text{XYZW}}) \tag{2.B.20}$$

[31] In fact, originally this was obtained by purifying the tripartite form of $Q^{[5]}_{\{3,2\}}$ and using the relevant identities.

which follows by expanding out the LHS in terms of polychromatic I_3's, e.g.

$$I_3(\mathrm{X}:\mathrm{Y}:\mathrm{Z}\,|\,\mathrm{W}) = I_3(\mathrm{X}:\mathrm{Y}:\mathrm{ZW}) - I_3(\mathrm{X}:\mathrm{Y}:\mathrm{W}) \tag{2.B.21}$$

applying eq. (2.B.19) on each term, and finally recombining to get the RHS of eq. (2.B.20). Notice however that we have now broken the automatic I_n sign alternation. In particular, when the purifier appears explicitly in one of the arguments of a conditional tripartite information, its I-basis expansion will not have each $\mathtt{I}_n$ term with the sign given by $(-1)^n$. Hence if the purifier were to appear in some conditional I_3 in the expression for a HEI, it must be the case by Proposition 2.3.2 that any 'wrong-sign' $\mathtt{I}_n$ terms in the I-basis are cancelled out by other terms in the HEI.

For a more involved example of seeing this in operation, consider e.g. $Q^{[1716]}_{\{12,14,4\}}$,

$$-I_3(\mathrm{A}:\mathrm{BD}:\mathrm{CF}) - I_3(\mathrm{AE}:\mathrm{BO}:\mathrm{C}) - I_3(\mathrm{A}:\mathrm{B}:\mathrm{DE}|\mathrm{C}) - I_3(\mathrm{BF}:\mathrm{D}:\mathrm{O}|\mathrm{A}) \tag{2.B.22}$$

This involves the purifier O, so it's not in the tripartite form yet. If we convert this expression directly to the I-basis and then collect terms, we find that we can indeed recast this into tripartite form, but a 6-term (IICCCC) one:

$$-I_3(\mathrm{A}:\mathrm{B}:\mathrm{F})-I_3(\mathrm{AE}:\mathrm{C}:\mathrm{DF})-I_3(\mathrm{B}:\mathrm{C}:\mathrm{D}|\mathrm{A})-I_3(\mathrm{A}:\mathrm{BD}:\mathrm{C}|\mathrm{F})-I_3(\mathrm{AD}:\mathrm{B}:\mathrm{E}|\mathrm{C})-I_3(\mathrm{CE}:\mathrm{D}:\mathrm{F}|\mathrm{B}) \tag{2.B.23}$$

However, if we first permute O with F, we can directly regroup terms, and obtain a shorter tripartite form IICCC,

$$-I_3(\mathrm{CE}:\mathrm{D}:\mathrm{F}) - I_3(\mathrm{AE}:\mathrm{BF}:\mathrm{C}) - I_3(\mathrm{A}:\mathrm{B}:\mathrm{DE}|\mathrm{C}) - I_3(\mathrm{A}:\mathrm{D}:\mathrm{E}|\mathrm{F}) - I_3(\mathrm{A}:\mathrm{B}:\mathrm{EF}|\mathrm{D}) \tag{2.B.24}$$

This illustrates that, even if we have a given HEI in the tripartite form, there might in principle be a purification which can yield an even more compact tripartite form expression. Our search strategy guarantees that the tripartite form we have found for all HEIs involves the minimal number of terms possible.

Part II.

Twist Operators In CFT_2: From Entanglement To Tau Function

3. Twist operator correlators revisited and tau functions on Hurwitz space

3.1. Introduction and summary of results

The twist operator correlator is a natural quantity of interest in two-dimensional conformal field theory (2d CFT) due to the well-known relation between 2d CFT and Riemann surfaces and the classical fact that a Riemann surface Σ can generally be realized as a branched cover of $\mathbb{CP}^1$ via a meromorphic function $\phi : \Sigma \to \mathbb{CP}^1$. Twist operator correlator admits a path integral definition [LM01; CC04]:

Definition 3.1.1 (Twist operator correlator)**.** *A monodromy data is a pair* $\mathbf{m} = (\boldsymbol{\sigma}, \boldsymbol{z}) \in S_N^M \times \mathbb{C}^M$*. Twist operator correlator/partition function with prescribed monodromy* $\mathbf{m}$ *for a generic 2d CFT* $\mathcal{C}$ *is defined by path integral for* N *copies of* $\mathcal{C}$ *with monodromy conditions for fundamental fields* $\{\varphi_I\}_{I=1,\cdots,N}$ *specified by* $\mathbf{m}$

$$\mathcal{Z}_{\mathbf{m}}(\boldsymbol{z}|\boldsymbol{\sigma}) = \left\langle \prod_i \sigma_i(z_i) \right\rangle \coloneqq \int\limits_{\varphi_I(\xi_i \circ z) = \varphi_{\sigma_i(I)}(z)} [D\varphi]\, e^{-\sum_I S[\varphi_I]} \tag{3.1.1}$$

where $\boldsymbol{\xi}$ *are generating loops in* $\pi_1\left(\mathbb{CP}^1 \setminus \boldsymbol{z}\right)$ *and* $\xi_i \circ z$ *denotes continuation along path* ξ_i*. The monodromy data* $\mathbf{m}$ *is naturally identified as the monodromy data of a branched cover*

$$\phi_{\mathbf{m}} : \Sigma \to \mathbb{CP}^1$$

with branch locus $\boldsymbol{z}$ *(i.e., critical values of* $\phi_{\mathbf{m}}$*) and corresponding permutation monodromies* $\boldsymbol{\sigma}$*. In other words, the twist operator correlator* $\mathcal{Z}_{\mathbf{m}}$ *is the partition function of* $\mathcal{C}$ *on* Σ *evaluated*

in the conformal frame where base $\mathbb{CP}^1$ has flat metric.[1]

Besides the formal reason mentioned above that justifies twist operator correlator as a natural quantity of interest in 2d CFT, there is indeed a rich literature on the quantity with motivations from various different physical contexts, such as orbifold CFT with motivation from string theory [DFMS87; Kni87; AF98], replica trick calculation of quantum information-theoretic quantities (e.g., entanglement entropy [CC04; CCT09; Har13], entanglement negativity [CCT12], reflected entropy [DF21], etc.), conformal bootstrap [CMM17; CCY19], symmetric product orbifold [LM01; PRR09; DE20] and the associated $\mathrm{AdS}_3/\mathrm{CFT}_2$ [EGG20; GGKM21]. For example, in the context of replica calculation of information-theoretic quantities, twist operator correlator with pairwise trivial monodromies admits density matrix interpretation. Famously, the twist operator correlator corresponding to $M = 2$ monodromy data $\mathbf{m}$ with $\boldsymbol{\sigma}$

$$\sigma_1 = \sigma_2^{-1} = (1 \dots N) \tag{3.1.2}$$

is related to the universal single interval Rényi entropy of ground state of CFT $\mathcal{C}$ [CC04]:

$$\mathcal{Z}_{\mathbf{m}} = \mathrm{Tr}\left(\rho_A^N\right) = z_{12}^{-2h}\bar{z}_{12}^{-2\bar{h}}, \quad A = [z_1, z_2], \quad h = \bar{h} = \frac{c}{24}(N - N^{-1}). \tag{3.1.3}$$

In the context of symmetric product orbifold (the N in below definition of symmetric product orbifold is in general different from the N as degree of branched cover; see footnote 2.)

$$\mathcal{C}^{\otimes \mathsf{N}}/S_{\mathsf{N}}, \tag{3.1.4}$$

the (connected) gauge-invariant twist operator correlator is a partition function with prescribed ramification data and admits a representation as summing over the gauge-dependent twist operators $\mathcal{Z}_{\mathbf{m}}$ over Hurwitz space (the moduli space of branched covers; see Definition 3.2.1) [PRR09; DE20]:

$$\mathcal{Z}_{\mathbf{r}}(\boldsymbol{z}|\boldsymbol{\lambda}) = \left\langle \prod_i \lambda_i(z_i) \right\rangle = \sum_g \mathcal{N}_{g,\mathsf{N}}(\boldsymbol{\lambda}) \sum_{\substack{\phi_{\mathbf{m}} \in \mathcal{H}_g(\boldsymbol{\lambda}) \\ \mathrm{br}(\phi_{\mathbf{m}}) = \boldsymbol{z}}} \mathcal{Z}_{\mathbf{m}}(\boldsymbol{z}|\boldsymbol{\sigma}). \tag{3.1.5}$$

[1] Technically, a cut-off is required at infinity on $\mathbb{CP}^1$; this gives trivial contribution to the $\boldsymbol{z}$-dependence of the twist operator correlator $\mathcal{Z}_{\mathbf{m}}$ [LM01].

Here ramification data is a pair $\mathbf{r} = (\boldsymbol{\lambda}, \boldsymbol{z}) \in P_{\mathsf{N}}^M \times \mathbb{C}^M$, with P_{N} being the set of integer partitions of N. $\mathcal{H}_g(\boldsymbol{\lambda})$ is Hurwitz space at genus g with ramification profile $\boldsymbol{\lambda}$ and $\mathrm{br}(\phi)$ denotes the branch locus of a branched cover ϕ. [2] $\mathcal{N}_{g,\mathsf{N}}(\boldsymbol{\lambda})$ is a combinatorial normalization constant whose precise form can be found in, e.g., [DE20], and in the large N limit the gauge-invariant twist operator has a genus expansion [LM01; PRR09; DE20]:[3]

$$\lim_{\mathsf{N}\to\infty} \mathcal{N}_{g,\mathsf{N}}(\boldsymbol{\lambda}) \sim \mathsf{N}^{1-g-\frac{M}{2}}. \tag{3.1.6}$$

The genus expansion of symmetric product orbifold at large N limit has motivated studies on its relation with gauge theory/string theory/holography. Despite the rich literature on the quantity, some aspects of the general structure of twist operator correlator, as will be explained below, are not fully understood. One goal of this chapter is to clarify the general structures of twist operator correlators associated with generic branched covers of genus zero and one.

A method of computing the twist operator correlator directly from its path integral definition is developed in [LM01], where one performs the path integral on the covering surface Σ and takes into account the Weyl anomaly due to the Weyl transformation induced by the covering map $\phi_{\mathbf{m}}$. It is clear from the path integral perspective that for branched cover of genus zero and one, twist operator correlator has the following general structure:

$$\mathcal{Z}_{\mathbf{m}} = \begin{cases} |\mathcal{W}_{\mathbf{m}}|^{2c} & g = 0 \\ |\mathcal{W}_{\mathbf{m}}|^{2c} \mathcal{Z}(\tau_{\mathbf{m}}, \bar{\tau}_{\mathbf{m}}) & g = 1 \end{cases} \tag{3.1.7}$$

where in general we use subscript in $\mathbf{m}$ to denote dependence on monodromy data as $F_{\mathbf{m}} = F_{\mathbf{m}}(\boldsymbol{z}|\boldsymbol{\sigma})$, $\mathcal{W}_{\mathbf{m}}$ is the holomorphic part of Weyl anomaly factor and $\mathcal{Z}(\tau, \bar{\tau})$ is the torus partition function of the CFT $\mathcal{C}$ with period τ. The Weyl anomaly factor is determined from branched

[2] As argument in $\mathcal{H}_g(\boldsymbol{\lambda})$, $\boldsymbol{\lambda}$ should be viewed as integer partitions of N, the degree of branched cover $\phi_{\mathbf{m}}$, instead of N, with $g + N$ fixed by total ramification orders via Riemann-Hurwitz formula. The degree of branched cover N is called the number of "active colors" among all the N color indices in [PRR09].

[3] This is derived in the case where each partition/cycle structure λ_i has only one non-trivial cycle.

cover by Liouville action

$$\log \mathcal{W}_{\mathbf{m}} + \log \overline{\mathcal{W}}_{\mathbf{m}} = \frac{1}{48\pi} S_L^{\text{reg}}[\Phi], \quad \Phi = \log \phi'_{\mathbf{m}}(w) + \log \bar{\phi}'_{\mathbf{m}}(\bar{w})$$
$$S_L[\Phi] = \int d^2w \sqrt{\hat{g}} \left(\hat{R}\Phi + \frac{1}{2} \hat{g}^{\mu\nu} \partial_\mu \Phi \partial_\nu \Phi \right), \quad \hat{ds}^2 = dw d\bar{w} \tag{3.1.8}$$

where w is the coordinate on covering space, and we refer to [LM01] for technical details such as regularization of Liouville action. While the path integral method is conceptually clean and makes clear the general structure of twist operator correlator, it has some disadvantages: i) The $\boldsymbol{z}$-dependence of $\mathcal{W}_{\mathbf{m}}$ and in turn $\mathcal{Z}_{\mathbf{m}}$ appears rather indirectly; the branch locus $\boldsymbol{z}$ come in as coefficients in $\phi_{\mathbf{m}}$, a rational function for $g = 0$ and elliptic function for $g = 1$, and one obtains $\mathcal{W}_{\mathbf{m}}$ as a function of $\boldsymbol{z}$ upon substituting $\phi_{\mathbf{m}}$ into the regularized Liouville action $S_L^{\text{reg}}[\Phi]$; ii) the calculation of Liouville action requires careful and somewhat tedious regularization procedure, even in the simple cases of two- and three-point function. One is therefore naturally led to ask if there is a direct characterization of the regularized part of $\mathcal{W}_{\mathbf{m}}$ and in turn $\mathcal{Z}_{\mathbf{m}}$ as a function of $\boldsymbol{z}$, without having to go through the indirect and involved Liouville action calculation.

Indeed, an alternative method exists and is known as the stress-tensor method of [DFMS87]. The method can be understood as first using conformal Ward identity to derive following differential equation for twist operator correlator

$$\partial_{z_i} \log \mathcal{Z}_{\mathbf{m}} = \text{Res}_{z=z_i} \langle T(z) \rangle_{\mathbf{m}} \,, \tag{3.1.9}$$

where

$$\langle \cdot \rangle_{\mathbf{m}} := \frac{\langle (\cdot) \prod_i \sigma_i(z_i) \rangle}{\langle \prod_i \sigma_i(z_i) \rangle} = \frac{\int_{\varphi_I(\xi_i \circ z) = \varphi_{\sigma_i(I)}(z)} [D\varphi] \, (\cdot) \, e^{-\sum_I S[\varphi_I]}}{\int_{\varphi_I(\xi_i \circ z) = \varphi_{\sigma_i(I)}(z)} [D\varphi] \, e^{-\sum_I S[\varphi_I]}} \tag{3.1.10}$$

and

$$T(z) = \sum_I T_I(z) \tag{3.1.11}$$

is the total stress tensor of N copies of CFT $\mathcal{C}$; one then proceeds by finding $\langle T(z) \rangle_{\mathbf{m}}$ and solving the differential equation. In standard orbifold CFT literature [DFMS87; AF98], $\langle T(z) \rangle_{\mathbf{m}}$ is found by using free field realization and therefore the argument is not universal for generic

2d CFTs.

However, in light of the universal structure (3.1.7) clear from the path integral perspective, one is naturally led to ask if the universal structure can be understood directly from the stress-tensor method. To the best of our knowledge, such a generalized formulation of the stress-tensor method for generic 2d CFTs that makes the universal structure transparent is lacking in literature. Moreover, a general expression of $\langle T(z)\rangle_{\mathbf{m}}$ directly in terms of branched cover data and torus partition function of a generic CFT $\mathcal{C}$ for generic branched cover of genus zero and one is also lacking.

We fill these gaps by generalizing the argument of Calabrese-Cardy [CC04] in the context of single interval Rényi entropy, i.e., genus zero branched cover with cyclic monodromy. The insight of [CC04] is that $\langle T(z)\rangle_{\mathbf{m}}$ may as well be found by first finding the stress tensor one-point function on the covering surface in the uniformizing coordinate and then transforming back to the base coordinate z. This argument is universal because it only relies on transformation property of stress-tensor. Employing a generalization of this argument, we have following universal expression of stress tensor one-point function associated with generic branched covers of genus zero and one:

$$\boxed{\begin{aligned} g=0: \quad \langle T(z)\rangle_{\mathbf{m}} &= \frac{c}{12}\sum_I \{\psi^I_{\mathbf{m}}, z\}, \\ g=1: \quad \langle T(z)\rangle_{\mathbf{m}} &= \frac{c}{12}\sum_I \{\psi^I_{\mathbf{m}}, z\} + 2\pi i \sum_I \left(\psi^I_{\mathbf{m}}\right)'^2(z)\,\partial_{\tau_{\mathbf{m}}}\log \mathcal{Z}(\tau_{\mathbf{m}}) \\ &= \frac{c}{12}\sum_I \{u(p^I_z), z\} + 2\pi i \sum_I v^2(p^I_z)\partial_{\tau_{\mathbf{m}}}\log \mathcal{Z}(\tau_{\mathbf{m}}) \end{aligned}} \tag{3.1.12}$$

where $\psi^I_{\mathbf{m}}$ is the inverse of $\phi_{\mathbf{m}}$, $u(p)$ is Abel map, $\omega(p) = v(p)dz$ is the differential on covering torus in base coordinate $z \in \mathbb{CP}^1$, p^I_z are pre-images of z under $\phi_{\mathbf{m}}$, and $\{\cdot, z\}$ denotes Schwarzian derivative with respect to z.

This indeed agrees with the general structure (3.1.7): the anomalous contributions to stress-tensor one-point function corresponds to the Weyl anomaly terms in (3.1.7) and the additional thermal energy term at genus one corresponds to the torus partition function term in (3.1.7). It is non-trivial to confirm that the logarithmic derivatives of Weyl anomaly and torus partition function with respect to branch locus $\boldsymbol{z}$ indeed agree with residues of the corresponding terms

in (3.1.12). The agreement for Weyl anomaly term is essentially explained in [KK03] by studying variation of Liouville action with respect to branch locus; we will explain that the agreement of torus partition function term follows from a special case of Rauch variation formula derived in [KK03; Kor03].

The generalized stress-tensor method for twist operator correlator allows us to recognize its close relation with the tau function on Hurwitz space of Kokotov-Korotkin [KK03]. In general, tau function is a central concept in the theory of integrable systems, with canonical examples including the ones associated with KP hierarchy and isomonodromic deformations; see, e.g., [BBT03; HB21] for introduction. The tau function on Hurwitz space of [KK03] is known as essentially a special case of the more general isomonodromic tau function [JMU81] associated with rank N matrix Fuchsian equations while specializing to quasi-permutation matrix monodromies [Kor03]. To give more motivation for the relation, we could have asked the following question: given that the Weyl anomaly contribution to twist operator correlator is universal (i.e., only depending on central charge not on other CFT data) and therefore purely a property of the associated branched cover, is it captured by some canonical algebro-geometric object where one associates a branched cover $\phi_{\mathbf{m}}$ with a function $F_{\mathbf{m}}(\boldsymbol{z}|\boldsymbol{\sigma})$ of its monodromy data? The tau function on Hurwitz space of [KK03] indeed provides such an object and can be thought of as being defined on a cross-section of Hurwitz space with fixed monodromies $\boldsymbol{\sigma}$ while varying branch locus $\boldsymbol{z}$. The tau function on Hurwitz space is defined as

$$\partial_{z_i} \log \tau_{\mathbf{m}} \coloneqq \frac{1}{12} \operatorname{Res}_{z=z_i} S_{\mathbf{m}}(z) \tag{3.1.13}$$

where $S_{\mathbf{m}}(z)$ is the sum of Bergman projective connection of $\phi_{\mathbf{m}}$ at pre-images p_z^I evaluated in base coordinate z.[4] While deferring the precise definition of Bergman projective connection to the main text, here we highlight the structural similarity of above definition for tau function with the defining equation (3.1.9) of twist operator correlator using stress-tensor method and admit the fact (see (3.2.27)) that the Bergman projective connection $S_{\mathbf{m}}(z)$ indeed takes the same form as $\langle T(z)\rangle_{\mathbf{m}}$ in (3.1.12), except that in the genus one case it has a "thermal energy" term generated by its own "partition function" $\eta^{-1}(\tau)$, which originates from the theta function with

[4] While this definition apparently differs from the original one in [KK03], its equivalence will be explained. Also we choose a different normalization for convenience to compare with CFT.

odd characteristics in the definition of Bergman kernel in terms of which Bergman projective connection is defined. We thereby have following relations between twist operator correlator $\mathcal{Z}_{\mathbf{m}}$ and tau function on Hurwitz space $\tau_{\mathbf{m}}$ (Theorem 3.3.1):

$$\boxed{\mathcal{Z}_{\mathbf{m}} = \begin{cases} |\tau_{\mathbf{m}}|^{2c} & g = 0 \\ |\tau_{\mathbf{m}}|^{2c} |\eta(\tau_{\mathbf{m}})|^{2c} \mathcal{Z}(\tau_{\mathbf{m}}, \bar{\tau}_{\mathbf{m}}) & g = 1 \end{cases}} \tag{3.1.14}$$

where c is the central charge of CFT $\mathcal{C}$, $\eta(\tau)$ is Dedekind eta function, $\mathcal{Z}(\tau, \bar{\tau})$ is torus partition function of $\mathcal{C}$, and the period $\tau_{\mathbf{m}} = \tau_{\mathbf{m}}(\boldsymbol{z}|\boldsymbol{\sigma})$ of covering torus is viewed as a function of branch locus $\boldsymbol{z}$ (not to be confused with the tau function $\tau_{\mathbf{m}}$). Conversely, the tau function on Hurwitz space admits a CFT interpretation as the holomorphic part of twist operator correlator of $c = 1$ free boson

$$\tau_{\mathbf{m}} = \mathcal{Z}^{\text{bos.}}_{\mathbf{m}}|_{\text{holo.}} \tag{3.1.15}$$

except with a non-modular-invariant partition function corresponding to trace over free boson Fock space. We also comment on the relation between twist operator correlator and isomonodromic tau function (see (3.3.48)) via the known relation between tau function on Hurwitz space and isomonodromic tau function [KK03; Kor03].

Note on notations/conventions: As we use different fonts to denote objects with different meanings, we give a quick reference for notations in Table 3.1 to avoid confusion. The subscripts in $\mathbf{m}$ for quantities in Table 3.1 are understood as shorthand to denote following dependence on (permutation) monodromy data: $F_{\mathbf{m}} = F_{\mathbf{m}}(\boldsymbol{z}|\boldsymbol{\sigma})$; similarly for matrix monodromy data $\mathfrak{m}$. Twist operator correlator as defined in Definition 3.1.1 is technically divergent and requires UV-cutoff around branched points (e.g., as in Liouville action calculation); it is understood that we always refer to its finite cut-off independent part. We also don't keep track of the overall normalization of twist operator correlator $\mathcal{Z}_{\mathbf{m}}$ and primarily concern with its dependence on branch locus $\boldsymbol{z}$; in fact, the related tau functions are only defined up to overall constant.

Notation	Meaning	Definition
$\mathbf{m}$	(permutation) monodromy data	Definition 3.1.1
$\mathcal{Z}_{\mathbf{m}}$	twist operator correlator	Definition 3.1.1
$\mathcal{W}_{\mathbf{m}}$	Weyl anomaly	eq. (3.3.4)
$\tau_{\mathbf{m}}$	tau function on Hurwitz space	eq. (3.2.31)
$\boldsymbol{\tau}_{\mathbf{m}}$	period matrix	eq. (3.2.13)
$\mathfrak{m}$	matrix monodromy data	below eq. (3.3.43)
$\tau_{\mathfrak{m}}$	isomonodromic tau function	eq. (3.3.45)
$\mathcal{Z}(\tau,\bar{\tau})$	torus partition function	eq. (3.3.6)

Table 3.1.: Quick reference for notations. The subscripts in $\mathbf{m}$ for quantities in the table are understood as shorthand to denote following dependence on (permutation) monodromy data: $F_{\mathbf{m}} = F_{\mathbf{m}}(\boldsymbol{z}|\boldsymbol{\sigma})$; similarly for matrix monodromy data $\mathfrak{m}$.

The chapter is organized as follows. In Section 3.2 we review aspects of Riemann surfaces and branched covers relevant for our purpose. In particular, we review the Bergman kernel and Bergman projective connection, and comment on their analogy with 2d CFT; we define the tau function on Hurwitz space in a way that makes manifest its relation with twist operator correlator and explain the equivalence of our definition with the original definition. In Section 3.3 we give a brief review of the path integral method for twist operator correlator, explain the standard stress-tensor method for twist operator correlator and derive the universal expression of stress-tensor one-point function (3.1.12) that generalizes the conventional stress-tensor method to generic 2d CFTs, and comment on, among other things, the consistency between path integral and stress-tensor method. We give the precise relation between twist operator correlator and tau function on Hurwitz space in Theorem 3.3.1 and in turn the relation with isomonodromic tau function in (3.3.48). In Section 3.4, we comment on the relation of our results with existing literature and mention some remaining questions/future directions.

3.2. Riemann surfaces, branched covers and tau function on Hurwitz space

In this section we review aspects of Riemann surfaces and branched covers relevant for our purpose and introduce the tau function on Hurwitz space of Kokotov-Korotkin [KK03] in a way that makes manifest the analogy with twist operator correlator.

3.2.1. Branched covers of Riemann surfaces

The monodromy data $\mathbf{m}$ in Definition 3.1.1 is naturally identified as the monodromy of a branched cover

$$\phi_{\mathbf{m}} : \Sigma \to \mathbb{CP}^1, \tag{3.2.1}$$

which is a meromorphic function on Σ. The monodromies $\boldsymbol{\sigma}$ of a branched cover $\phi_{\mathbf{m}}$ are required to satisfy

- The monodromy group generated by $\boldsymbol{\sigma}$ is a transitive subgroup of S_N
- Compositions of all permutations in $\boldsymbol{\sigma}$ equal identity: $\sigma_1 \cdots \sigma_M = \mathrm{id}$.

The first condition imposes w.l.o.g that the covering surface Σ is connected, as otherwise the partition function $\mathcal{Z}_{\mathbf{m}}$ would factorize and one can study each connected component individually. The second condition is necessary as the monodromy data $\mathbf{m}$ gives a representation of $\pi_1\left(\mathbb{CP}^1 \setminus \boldsymbol{z}\right)$.

The genus of a monodromy data $\mathbf{m}$, i.e., genus of covering surface Σ, is given by Riemann-Hurwitz formula

$$g = \sum_{\gamma \in \boldsymbol{\sigma}} \frac{l-1}{2} - N + 1 \tag{3.2.2}$$

where the sum is over all cycles γ in cycle decompositions of all permutations in $\boldsymbol{\sigma}$ and $l = |\gamma|$ denotes the length of a cycle.

As our notation suggests, we think of the branched cover $\phi_{\mathbf{m}}$ as parametrized by its monodromy data $\mathbf{m}$; this is justified by Riemann's existence theorem, which essentially states the bijection between the set of inequivalent branched covers/meromorphic functions on Σ and the set of monodromy data. Indeed, the twist operator correlator in Definition 3.1.1 would not be well-defined if one could find two inequivalent branched covers with, for example, different Liouville actions but same monodromy data.

Theorem 3.2.1 (Riemann's existence theorem[5])**.** *Given a monodromy data* $\mathbf{m} = (\boldsymbol{\sigma}, \boldsymbol{z})$*, there exists a compact Riemann surface* Σ *and a meromorphic function* $\phi_{\mathbf{m}} : \Sigma \to \mathbb{CP}^1$ *such that* $\boldsymbol{z}$

[5] Apparently related but different statements go by the name Riemann's existence theorem. The exact statement in the theorem can be found in, e.g., Theorem 1.8.14 of [LZ03].

are branch locus of $\phi_{\mathbf{m}}$ *and* $\boldsymbol{\sigma}$ *are the corresponding permutation monodromies. The branched cover* $\phi_{\mathbf{m}}$ *is unique up to isomorphism.*

We will focus on branched covers of genus zero and one. For genus zero, the meromorphic function $\phi_{\mathbf{m}}$ is a rational function, and the inverses $\psi^I_{\mathbf{m}}$ are solutions of a polynomial equation. For genus one, the meromorphic function $\phi_{\mathbf{m}}$ is an elliptic function, and the inverses are given by Abel map

$$\psi^I_{\mathbf{m}}(z) = u(p^I_z) = \int^{p^I_z} \omega(p) \tag{3.2.3}$$

where $\omega(p) = v(p)dz$ is the differential on covering torus in base coordinate $z \in \mathbb{CP}^1$, p^I_z is the I^{th} pre-image of z on covering torus, and

$$\left(\psi^I_{\mathbf{m}}\right)'(z) = v(p^I_z). \tag{3.2.4}$$

We will give explicit examples of branched covers with cyclic monodromy and their associated twist operator correlators in Sec. 3.3; some useful visualizations of branched covers are given in Figure 3.1, 3.2.

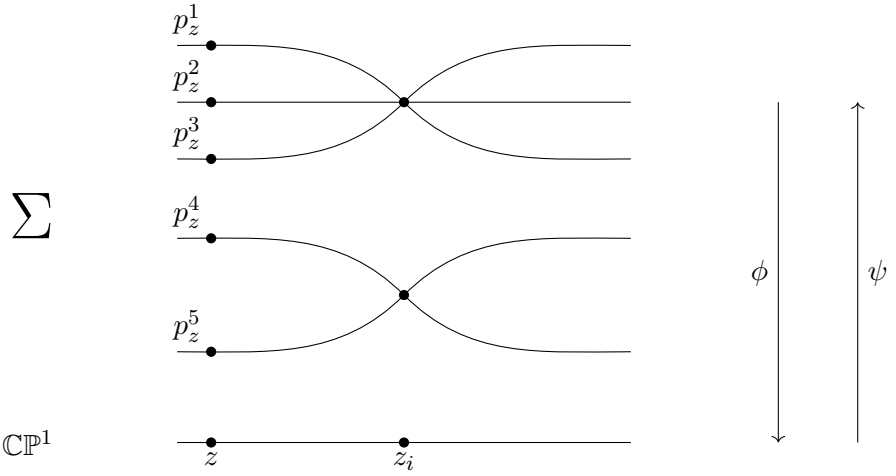

Figure 3.1.: Visualization of the local structure of a degree $N = 5$ branched cover near a branched point z_i with monodromy $\sigma_i = (123)(45)$. The branched cover ϕ is a projection and its inverse ψ a lift.

We will also need the concept of Hurwitz space, the moduli space of branched covers; more details can be found in, e.g., [CM16].

Definition 3.2.1 (Hurwitz space)**.** *Let* $\boldsymbol{\lambda} \in P_N^M$ *be a set of* M *integer partitions of* N*. The Hurwitz space* $\mathcal{H}_{g,N}(\boldsymbol{\lambda})$ *is the set of isomorphism classes of genus* g *degree* N *connected branched*

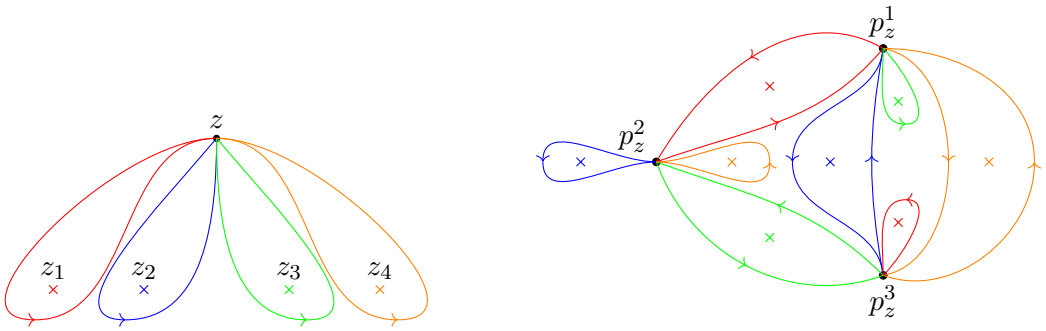

(a) Generating loops in $\pi_1(\mathbb{CP}^1 \setminus \boldsymbol{z})$ of base $\mathbb{CP}^1$.

(b) Lift of the generating loops in $\pi_1(\mathbb{CP}^1 \setminus \boldsymbol{z})$ of base $\mathbb{CP}^1$ to covering $\mathbb{CP}^1$.

Figure 3.2.: Visualization of the global structure of a genus zero $M = 4, N = 3$ branched cover with monodromies $\sigma_1 = (12), \sigma_2 = (13), \sigma_3 = (23), \sigma_4 = (13)$.

covers

$$\phi : \Sigma_g \to \mathbb{CP}^1 \tag{3.2.5}$$

with $\boldsymbol{\lambda}$ *being the ramification profiles at branch locus of* ϕ*. As the degree of branched cover is already determined from genus and ramification profiles via Riemann-Hurwitz formula, we simply denote Hurwitz space by* $\mathcal{H}_g(\boldsymbol{\lambda})$*.*

The branch locus $\boldsymbol{z}$ of ϕ are not fixed in the definition of Hurwitz space $\mathcal{H}_g(\boldsymbol{\lambda})$; the branch point map, br, is used in math literature to denote the branch locus $\boldsymbol{z}$ of a particular branched cover ϕ in Hurwitz space, i.e.,

$$\mathrm{br}(\phi) = \boldsymbol{z}. \tag{3.2.6}$$

The Hurwitz space $\mathcal{H}_g(\boldsymbol{\lambda})$ may be viewed as being parametrized by two set of coordinates: the branch locus $\boldsymbol{z}$ and monodromies $\boldsymbol{\sigma}$ (with cycle structures $\boldsymbol{\lambda}$).

3.2.2. Bergman kernel and Bergman projective connection

Here we review the Bergman kernel (also known as fundamental second kind differential, fundamental normalized bidifferential, etc.) in terms of which the Bergman projective connection is defined, and comment on their analogy with free boson 2d CFT. A classic reference on the material is [Fay73]; we largely follow the convention in [Eyn18]. The analogy with free boson is also observed in the context of hyperelliptic surfaces (cyclic degree two branched covers) in [Zam87]; see also [GM16].

Bergman kernel

Given a compact Riemann surface Σ, the Bergman kernel $B(p,q)$ is the unique meromorphic symmetric (1,1) form on $\Sigma \times \Sigma$ that has a normalized double pole as $p \to q$ and no other poles, i.e., in any local coordinate $x(p)$ it behaves as

$$B(p,q) = \frac{dx(p)dx(q)}{(x(p)-x(q))^2} + \text{analytic at } q, \tag{3.2.7}$$

and satisfies

$$B(p,q) = B(q,p) \tag{3.2.8}$$

$$\oint_{q\in\mathcal{A}_\alpha} B(p,q) = 0 \tag{3.2.9}$$

$$\oint_{q\in\mathcal{B}_\alpha} B(p,q) = 2\pi i \omega_\alpha(p) \tag{3.2.10}$$

where $\mathcal{A}_\alpha, \mathcal{B}_\alpha$ are usual homology cycles and $\omega_\alpha(p)$ basis of differentials. For $g=0$, the Bergman kernel is given by

$$B(z,z') = \frac{dzdz'}{(z-z')^2}, \quad z,z' \in \mathbb{CP}^1. \tag{3.2.11}$$

For $g \geq 1$, the Bergman kernel is given by

$$B(p,q) = d_p d_q \log \Theta_{\mathbf{c}}\left(\mathbf{u}(p) - \mathbf{u}(q)|\boldsymbol{\tau}\right) \tag{3.2.12}$$

where $\Theta_{\mathbf{c}}(\mathbf{u}|\boldsymbol{\tau})$ is Riemann theta function with a half-integer odd characteristics $\mathbf{c}$, $\boldsymbol{\tau}$ is the period matrix of Σ, $\mathbf{u}(p)$ is Abel map.[6] For our purpose we focus on the $g=1$ case, where the Abel map gives a uniformizing coordinate on torus $T_\tau = \mathbb{C}/(\mathbb{Z}+\tau\mathbb{Z})$, and the only odd

[6] See Appendix 3.A for review of definitions and conventions of theta functions. The period matrix is defined by

$$(\boldsymbol{\tau})_{\alpha\beta} = \oint_{\mathcal{B}_\alpha} \omega_\beta. \tag{3.2.13}$$

characteristics is $c = \frac{1}{2} + \frac{\tau}{2}$. For $g = 1$ the Bergman kernel can be explicitly written as

$$\begin{aligned} B(u,u') &= \partial_u \partial_{u'} \log \theta_1(u-u'|\tau) du du', \quad u, u' \in T_\tau \\ &= \left(\wp(u-u'|\tau) - \frac{1}{3} \frac{\theta_1'''(0|\tau)}{\theta_1'(0|\tau)} \right) du du' \\ &= \left(\wp(u-u'|\tau) - \frac{4\pi i}{3} \partial_\tau \log \theta_1'(0|\tau) \right) du du' \end{aligned} \tag{3.2.14}$$

where $\wp(u|\tau)$ is Weierstrass elliptic function

$$\wp(u|\tau) = \frac{1}{u^2} + \sum_{\lambda \in \Lambda \setminus \{0\}} \left(\frac{1}{(u-\lambda)^2} - \frac{1}{\lambda^2} \right), \quad \Lambda = \mathbb{Z} + \tau \mathbb{Z}, \tag{3.2.15}$$

second equality follows from identity

$$-\partial_u^2 \log \theta_1(u|\tau) = \wp(u|\tau) - \frac{1}{3} \frac{\theta_1'''(0|\tau)}{\theta_1'(0|\tau)}, \tag{3.2.16}$$

and third equality from heat equation

$$\theta_1''(u|\tau) = 4\pi i \partial_\tau \theta_1(u|\tau). \tag{3.2.17}$$

Remark 3.2.1 (Relation with free boson)**.** The weight (1,1) Bergman kernel at genus zero and one is analogous to the two point function of the weight $h = 1$ current operator $j(z) = i\partial X(z)$ in (uncompactified) free boson:

$$\begin{aligned} \left\langle j(z) j(z') \right\rangle_{\mathbb{CP}^1} &= \frac{1}{(z-z')^2} \\ \left\langle j(u) j(u') \right\rangle_{T_\tau} &= \wp(u-u'|\tau) - \frac{4\pi i}{3} \partial_\tau \log \theta_1'(0|\tau) - \frac{\pi}{\Im \tau} \end{aligned} \tag{3.2.18}$$

except without the zero mode contribution for genus one two point function.

Bergman projective connection for meromorphic function

Given a meromorphic function ϕ on Σ, the Bergman kernel can be used to define the Bergman projective connection of ϕ at a point p on Σ:

$$S_\phi(p) \coloneqq 6 \lim_{p' \to p} \left(\frac{B(p,p')}{d\phi(p) d\phi(p')} - \frac{1}{(\phi(p) - \phi(p'))^2} \right). \tag{3.2.19}$$

For our purpose, the meromorphic function ϕ will be the branched cover

$$\phi_{\mathbf{m}} : \Sigma \to \mathbb{CP}^1. \tag{3.2.20}$$

Viewing the projective connection as a function of base coordinate $z \in \mathbb{CP}^1$, we write

$$S^I_{\mathbf{m}}(z) \coloneqq S_{\phi_{\mathbf{m}}}(p^I_z) = 6 \lim_{z \to z'} \left(\frac{B\left(p^I_z, p^I_{z'}\right)}{dz dz'} - \frac{1}{(z-z')^2} \right) \tag{3.2.21}$$

where $p^I_z = \psi^I_{\mathbf{m}}(z) \coloneqq \left(\phi^I_{\mathbf{m}}\right)^{-1}(z)$ is the lift of the point z to the I^{th} sheet of covering surface Σ. In general under a change of coordinate $z \mapsto w(z)$, a projective connection transforms as

$$S(w) = \left(\frac{dw}{dz}\right)^{-2} \Big[S(z) + \{w, z\} \Big] \tag{3.2.22}$$

where $\{f, z\}$ is Schwarzian derivative

$$\{f, z\} = \frac{f'''(z)}{f'(z)} - \frac{3}{2} \left(\frac{f''(z)}{f'(z)} \right)^2. \tag{3.2.23}$$

For a genus zero branched cover $\phi_{\mathbf{m}}$, the associated Bergman projective connection is given by

$$\begin{aligned} S^I_{\mathbf{m}}(z) &= 6 \lim_{z' \to z} \left(\frac{\left(\psi^I_{\mathbf{m}}\right)'(z) \left(\psi^I_{\mathbf{m}}\right)'(z')}{\left(\psi^I_{\mathbf{m}}(z) - \psi^I_{\mathbf{m}}(z')\right)^2} - \frac{1}{(z-z')^2} \right) \\ &= \{\psi^I_{\mathbf{m}}, z\}. \end{aligned} \tag{3.2.24}$$

For a genus one branched cover $\phi_{\mathbf{m}}$, the associated Bergman projective connection is given by

$$\begin{aligned} S^I_{\mathbf{m}}(z) &= 6 \lim_{z'\to z} \left\{ \left[\wp\Big(\psi^I_{\mathbf{m}}(z) - \psi^I_{\mathbf{m}}(z')|\tau\Big) - \frac{4\pi i}{3}\partial_{\tau_{\mathbf{m}}} \log\theta_1'(0|\tau_{\mathbf{m}}) \right] \left(\psi^I_{\mathbf{m}}\right)'(z) \left(\psi^I_{\mathbf{m}}\right)'(z') - \frac{1}{(z-z')^2} \right\} \\ &= \{\psi^I_{\mathbf{m}}, z\} - 8\pi i \left(\psi^I_{\mathbf{m}}\right)'^2(z) \partial_{\tau_{\mathbf{m}}} \log\theta_1'(0|\tau_{\mathbf{m}}) \\ &= \{u\left(p^I_z\right), z\} - 8\pi i v^2(p^I_z) \partial_{\tau_{\mathbf{m}}} \log\theta_1'(0|\tau_{\mathbf{m}}). \end{aligned} \tag{3.2.25}$$

For convenience, we introduce following notation

$$S_{\mathbf{m}}(z) \coloneqq \sum_I S^I_{\mathbf{m}}(z) \tag{3.2.26}$$

and summarize

$$\boxed{\begin{aligned} g=0: \quad & S_{\mathbf{m}}(z) = \sum_I \{\psi^I_{\mathbf{m}}, z\}, \\ g=1: \quad & S_{\mathbf{m}}(z) = \sum_I \{\psi^I_{\mathbf{m}}, z\} - 8\pi i \sum_I \left(\psi^I_{\mathbf{m}}\right)'^2(z)\, \partial_{\tau_{\mathbf{m}}} \log\theta_1'(0|\tau_{\mathbf{m}}) \\ & \qquad = \sum_I \{u(p^I_z), z\} - 8\pi i \sum_I v^2(p^I_z) \partial_{\tau_{\mathbf{m}}} \log\theta_1'(0|\tau_{\mathbf{m}}). \end{aligned}} \tag{3.2.27}$$

Remark 3.2.2 (Relation with free boson)**.** The Bergman projective connection $S^I_{\mathbf{m}}(z)$ associated with a branched cover defined via regularizing diagonal part of Bergman kernel has close analogy with the one-point function of I^{th} copy of normal-ordered stress-tensor of free boson under monodromy conditions of branched cover. In light of previous remark, the Bergman kernel may be identified as (up to the difference in zero mode term at genus one)

$$\frac{B\left(p^I_z, p^I_{z'}\right)}{dzdz'} = \left\langle j_I(z) j_I(z') \right\rangle_{\mathbf{m}}, \tag{3.2.28}$$

and as the normal-ordered free boson stress-tensor is given by

$$T^{\text{bos.}}(z) = \lim_{z'\to z} j(z)j(z') - \frac{1}{(z-z')^2}, \tag{3.2.29}$$

the Bergman projective connection can therefore be identified, up to overall constant, as

$$S^I_{\mathbf{m}}(z) = \left\langle T_I^{\text{bos.}}(z) \right\rangle_{\mathbf{m}} \tag{3.2.30}$$

This is indeed in line with the usual stress-tensor method using free field realization in standard orbifold CFT literature [DFMS87; AF98]. It will be clear that similar analogy in fact holds for generic 2d CFTs.

3.2.3. Tau function on Hurwitz space

The tau function on Hurwitz space of [KK03] can be defined in terms of the Bergman projective connection $S^I_{\mathbf{m}}(z)$ associated with branched cover $\phi_{\mathbf{m}}$ as

$$\partial_{z_i} \log \tau_{\mathbf{m}} \coloneqq \frac{1}{12} \operatorname{Res}_{z=z_i} S_{\mathbf{m}}(z) \tag{3.2.31}$$

where we have chosen a different normalization for convenience to compare with CFT. The original definition in [KK03] corresponds to normalization

$$\partial_{z_i} \log \tau'_{\mathbf{m}} \coloneqq -\frac{1}{6} \operatorname{Res}_{z=z_i} S_{\mathbf{m}}(z). \tag{3.2.32}$$

While this in appearance differs from the original definition in [KK03]

$$\partial_{z_i} \log \tau'_{\mathbf{m}} \coloneqq -\frac{1}{6} \sum_{\gamma \in \sigma_i} \frac{1}{l(l-2)!} \partial_{x_i}^{l-2} S^{\gamma}_{\mathbf{m}}(x_i)|_{x_i=0} \tag{3.2.33}$$

where the sum is over cycles γ in the cycle decomposition of σ_i, $l = |\gamma|$ is the length of the cycle γ, x_i is the local uniformizing coordinate $x_i = (z - z_i)^{\frac{1}{l}}$ and $S^{\gamma}_{\mathbf{m}}(x_i)$ is Bergman projective connection in the local uniformizing coordinate x_i valid near the lift of branch point z_i corresponding to cycle γ, the two definitions agree and the equivalence can be seen as follows.

Consider the contribution of $\mathrm{Res}_{z=z_i} S_{\mathbf{m}}(z)$ associated with sheets glued in γ

$$\begin{aligned}
\mathrm{Res}_{z=z_i} \sum_{I\in\gamma} S^I_{\mathbf{m}}(z) &= \sum_{I\in\gamma} \oint_{\mathcal{C}(z_i)} dz S^I_{\mathbf{m}}(z) \\
&= \oint_{\mathcal{C}(0)} dx_i \frac{dz}{dx_i} \left[\left(\frac{dx_i}{dz}\right)^2 S^\gamma_{\mathbf{m}}(x_i) - \{x_i, z\} \right] \\
&= \oint_{\mathcal{C}(0)} dx_i \frac{dx_i}{dz} S^\gamma_{\mathbf{m}}(x_i) \\
&= \oint_{\mathcal{C}(0)} dx_i \frac{1}{l} \frac{1}{x_i^{l-1}} S^\gamma_{\mathbf{m}}(x_i) \\
&= \frac{1}{l(l-2)!} \partial_{x_i}^{l-2} S^\gamma_{\mathbf{m}}(x_i)|_{x_i=0}
\end{aligned} \tag{3.2.34}$$

where the second equality follows from joining the lifts of loop $\mathcal{C}(z_i)$ to x_i coordinate to obtain the loop $\mathcal{C}(0)$ in x_i coordinate and using transformation property (3.2.22) of projective connection, the third equality from that $\{x_i, z\}$ only has double pole in z_i and therefore doesn't contribute. The two definitions therefore agree upon summing over cycles γ.

The compatibility condition for the definition of tau function

$$\partial_{z_j} \mathrm{Res}_{z=z_i} S_{\mathbf{m}}(z) = \partial_{z_i} \mathrm{Res}_{z=z_j} S_{\mathbf{m}}(z) \tag{3.2.35}$$

can be verified using Rauch variation formula [KK03].

The tau function on Hurwitz space may be viewed as being defined on a cross-section of Hurwitz space with fixed monodromies $\boldsymbol{\sigma}$ while varying branch locus $\boldsymbol{z}$.

3.2.4. Rauch variation formula

In general the Rauch variation formula is concerned with the variation of basis of differentials and period matrix with respect to a Beltrami differential and we refer to [KK03; Kor03] and references therein for its most general form. We will need the following special case of the variation formula to verify the consistency between path integral and stress-tensor method for twist operator correlator.

Theorem 3.2.2 ([KK03; Kor03]). *The variation of the period matrix of a $g \geq 1$ Riemann*

surface Σ realized as branched cover

$$\phi_{\mathbf{m}} : \Sigma \to \mathbb{CP}^1$$

with respect to the change of branch locus $\boldsymbol{z}$ is given by

$$\partial_{z_i} \left(\boldsymbol{\tau}_{\mathbf{m}}\right)_{\alpha\beta} = 2\pi i \operatorname{Res}_{z=z_i} \sum_I v_\alpha \left(p_z^I\right) v_\beta \left(p_z^I\right) \tag{3.2.36}$$

where $\omega_\alpha(p) = v_\alpha(p)dz$ is the basis of differentials in base space coordinate $z \in \mathbb{CP}^1$ and p_z^I are pre-images of z under $\phi_{\mathbf{m}}$.

3.3. Twist operator correlator and tau function on Hurwitz space

In this section we give a brief review of the path integral method of [LM01] to highlight the general structure of twist operator correlator, generalize the stress-tensor method of [DFMS87] to generic 2d CFTs without relying on free field realization for generic branched covers of genus zero and one, comment on the consistency between two methods, and give the precise relation between twist operator correlator and tau function on Hurwitz space of [KK03] in Theorem 3.3.1 and in turn the relation with isomonodromic tau function.

3.3.1. Path integral method

The crucial observation underlying the path integral method of Lunin-Mathur [LM01] is that the defining path integral for twist operator correlator in Definition 3.1.1 can as well be performed in covering space for a single copy of CFT $\mathcal{C}$ where there's no longer non-trivial boundary conditions. This induces a Weyl transformation on covering space metric

$$dzd\bar{z} = e^{\Phi} dwd\bar{w}, \quad \Phi = \log \phi'_{\mathbf{m}}(w) + \log \bar{\phi}'_{\mathbf{m}}(\bar{w}) \tag{3.3.1}$$

with

$$g=0: \quad w \in \mathbb{CP}^1$$
$$g=1: \quad w \in T_\tau = \mathbb{C}/(\mathbb{Z}+\tau\mathbb{Z}). \tag{3.3.2}$$

The Weyl transformation leads to Weyl anomaly factor

$$\mathcal{Z}_{\mathbf{m}} = \mathcal{Z}\left[e^{\Phi}\hat{g}\right] = |\mathcal{W}_{\mathbf{m}}|^{2c}\mathcal{Z}\left[\hat{g}\right] \tag{3.3.3}$$

with the Weyl anomaly factor given by regularized Liouville action

$$\log \mathcal{W}_{\mathbf{m}} + \log \overline{\mathcal{W}}_{\mathbf{m}} = \frac{1}{48\pi} S_L^{\text{reg}}[\Phi], \quad \Phi = \log \phi'_{\mathbf{m}}(w) + \log \bar{\phi}'_{\mathbf{m}}(\bar{w})$$
$$S_L[\Phi] = \int d^2w\sqrt{\hat{g}}\left(\hat{R}\Phi + \frac{1}{2}\hat{g}^{\mu\nu}\partial_\mu\Phi\partial_\nu\Phi\right), \quad \hat{ds}^2 = dwd\bar{w}. \tag{3.3.4}$$

The path integral on the covering space $\mathcal{Z}[\hat{g}]$ is given by

$$\mathcal{Z}[\hat{g}] = \begin{cases} 1 & g=0 \\ \mathcal{Z}(\tau_{\mathbf{m}}, \bar{\tau}_{\mathbf{m}}) & g=1 \end{cases}. \tag{3.3.5}$$

Here in the genus zero case, $\mathcal{Z}[\hat{g}]$ has trivial dependence on branch locus $\boldsymbol{z}$; as we are only interested in the $\boldsymbol{z}$-dependence of $\mathcal{Z}_{\mathbf{m}}$, $\mathcal{Z}[\hat{g}]$ can be set to unity. In the genus one case, $\mathcal{Z}[\hat{g}]$ gives path integral on covering torus and contains non-trivial dependence on $\boldsymbol{z}$ via the dependence of the period of the covering torus on monodromy data $\mathbf{m}$, which we emphasize by writing $\tau_{\mathbf{m}} = \tau_{\mathbf{m}}(\boldsymbol{z}|\boldsymbol{\sigma})$, and $\mathcal{Z}(\tau)$ is the torus partition function of the CFT $\mathcal{C}$

$$\mathcal{Z}(\tau, \bar{\tau}) = \text{Tr}\left(q^{L_0 - \frac{c}{24}}\bar{q}^{\bar{L}_0 - \frac{c}{24}}\right), \quad q = e^{2\pi i\tau}, \quad \bar{q} = e^{-2\pi i\bar{\tau}}. \tag{3.3.6}$$

As mentioned in the introduction, the $\boldsymbol{z}$-dependence of $\mathcal{W}_{\mathbf{m}}$ in the path integral method appears rather indirectly: the branch locus $\boldsymbol{z}$ come in as coefficients in $\phi_{\mathbf{m}}$, a rational function for $g=0$ and elliptic function for $g=1$, and one obtains $\mathcal{W}_{\mathbf{m}}$ as a function of $\boldsymbol{z}$ upon substituting $\phi_{\mathbf{m}}$ into the regularized Liouville action $S_L^{\text{reg}}[\Phi]$. While referring to [LM01] for details on technicalities

such as regularization of Liouville action and examples of computations using the method, we highlight the general structure made clear by the path integral approach:

$$\mathcal{Z}_{\mathbf{m}} = \begin{cases} |\mathcal{W}_{\mathbf{m}}|^{2c} & g = 0 \\ |\mathcal{W}_{\mathbf{m}}|^{2c} \mathcal{Z}(\tau_{\mathbf{m}}, \bar{\tau}_{\mathbf{m}}) & g = 1 \end{cases} \tag{3.3.7}$$

where at genus zero the universal (i.e., only depending on central charge and not on other CFT data) Weyl anomaly contribution is the only non-trivial contribution, and at genus one there is an additional contribution from torus partition function of the CFT $\mathcal{C}$.

3.3.2. Stress-tensor method generalized

The stress-tensor method of [DFMS87] can be understood as follows. One starts by considering the stress-tensor one-point function $\langle T(z) \rangle_{\mathbf{m}}$ defined by

$$\langle \cdot \rangle_{\mathbf{m}} := \frac{\langle (\cdot) \prod_i \sigma_i(z_i) \rangle}{\langle \prod_i \sigma_i(z_i) \rangle} = \frac{\int\limits_{\varphi_I(\xi_i \circ z) = \varphi_{\sigma_i(I)}(z)} [D\varphi] \, (\cdot) \, e^{-\sum_I S[\varphi_I]}}{\int\limits_{\varphi_I(\xi_i \circ z) = \varphi_{\sigma_i(I)}(z)} [D\varphi] \, e^{-\sum_I S[\varphi_I]}}, \tag{3.3.8}$$

with

$$T(z) = \sum_I T_I(z) \tag{3.3.9}$$

being the sum of stress-tensor of N copies of the CFT $\mathcal{C}$. Then from conformal Ward identity

$$\left\langle T(z) \prod_i \sigma_i(z_i) \right\rangle = \sum_i \left(\frac{h_{\sigma_i}}{(z - z_i)^2} + \frac{1}{z - z_i} \partial_{z_i} \right) \left\langle \prod_i \sigma_i(z_i) \right\rangle$$

it follows that

$$\langle T(z) \rangle_{\mathbf{m}} = \sum_i \frac{h_{\sigma_i}}{(z - z_i)^2} + \frac{\partial_{z_i} \log \mathcal{Z}_{\mathbf{m}}}{z - z_i}. \tag{3.3.10}$$

This allows one to derive a differential equation directly characterizing $\mathcal{Z}_{\mathbf{m}}$ as functions of branch locus $\boldsymbol{z}$ from singularities of $\langle T(z) \rangle_{\mathbf{m}}$:

$$\partial_{z_i} \log \mathcal{Z}_{\mathbf{m}} = \mathrm{Res}_{z = z_i} \langle T(z) \rangle_{\mathbf{m}} \, . \tag{3.3.11}$$

We note that at this point the discussion is entirely general and in principle the differential equation holds for generic branched covers with arbitrary genus. To proceed one then needs to find the stress-tensor one-point function $\langle T(z)\rangle_{\mathbf{m}}$ to solve the differential equation and now we restrict the discussion to branched covers of genus zero and one. In standard orbifold CFT literature [DFMS87; AF98], the stress-tensor one-point function is obtained using free field realization of twist operators and the method relies on free-field-specific properties of stress-tensors. However, since the path integral method holds for generic 2d CFTs and makes clear the universal structure of twist operator correlator, one would expect that a correspondingly universal method should exist for finding the stress-tensor one-point function and makes clear the same universal structure. To achieve this, we employ a generalization of the argument in [CC04] in the context of single interval Rényi entropy (genus zero branched cover with cyclic monodromy). The key observation of [CC04] is that one can find the stress tensor one-point function by first evaluating it in the uniformizing coordinate and then transforming back to the base coordinate, which only relies on the universal transformation property of stress-tensor. Generalizing this argument to generic genus zero and one branched covers with non-abelian monodromy, we first find the stress-tensor one-point function of a copy of CFT in the uniformizing coordinate $\psi^I_{\mathbf{m}}(z)$

$$\left\langle T\left(\psi^I_{\mathbf{m}}(z)\right)\right\rangle = \begin{cases} 0 & g=0 \\ 2\pi i\partial_{\tau_{\mathbf{m}}}\log\mathcal{Z}\left(\tau_{\mathbf{m}}\right) & g=1 \end{cases} \tag{3.3.12}$$

where in the genus zero case it vanishes on covering sphere and in the genus one case it has a thermal energy on covering torus; then from transformation property of stress-tensor

$$T(w) = \left(\frac{dw}{dz}\right)^{-2}\left[T(z) - \frac{c}{12}\{w,z\}\right], \tag{3.3.13}$$

we obtain the stress-tensor one-point function of each copy of CFT in base coordinate

$$\begin{aligned} g=0: \quad \langle T_I(z)\rangle_{\mathbf{m}} &= \frac{c}{12}\{\psi^I_{\mathbf{m}}, z\}, \\ g=1: \quad \langle T_I(z)\rangle_{\mathbf{m}} &= \frac{c}{12}\{\psi^I_{\mathbf{m}}, z\} + 2\pi i \left(\psi^I_{\mathbf{m}}\right)'^2(z)\, \partial_{\tau_{\mathbf{m}}} \log \mathcal{Z}(\tau_{\mathbf{m}}) \\ &= \frac{c}{12}\{u(p^I_z), z\} + 2\pi i v^2(p^I_z) \partial_{\tau_{\mathbf{m}}} \log \mathcal{Z}(\tau_{\mathbf{m}}) \end{aligned} \tag{3.3.14}$$

where $\psi^I_{\mathbf{m}}$ is the inverse of $\phi_{\mathbf{m}}$, $u(p)$ is Abel map, $\omega(p) = v(p)dz$ is the differential on covering torus in base coordinate $z \in \mathbb{CP}^1$ and p^I_z are pre-images of z under $\phi_{\mathbf{m}}$. The expression (3.1.12) is obtained upon summing over copies of CFT. As will be remarked below, this indeed leads to the same universal structure of twist operator correlator as made clear in the path integral method.

Remark 3.3.1 (Twist operator dimension)**.** The universal twist operator dimension h_σ for a generic $\sigma \in S_N$,

$$h_\sigma = \frac{c}{24} \sum_{\gamma \in \sigma} l - l^{-1}, \tag{3.3.15}$$

where the sum is over cycles γ in the cycle decomposition of σ and $l = |\gamma|$ is the length of a cycle γ, can be read off from the genus zero case of (3.3.10)

$$\sum_i \frac{h_{\sigma_i}}{(z-z_i)^2} + \frac{\partial_{z_i} \log \mathcal{Z}_{\mathbf{m}}}{z - z_i} = \frac{c}{12} \sum_I \{\psi^I_{\mathbf{m}}, z\} \tag{3.3.16}$$

as follows. For a local coordinate of the form $\psi(z) = (z-z_i)^{\frac{1}{l}} f(z)$, the double pole term in Schwarzian derivative is fixed by local ramification order

$$\left\{(z-z_i)^{\frac{1}{l}} f(z), z\right\} = \frac{(1-l^{-2})/2}{(z-z_i)^2} + \mathcal{O}\left((z-z_i)^{-1}\right) \tag{3.3.17}$$

therefore in the Schwarzian derivative term of (3.3.16), the double pole contribution from a cycle γ is

$$\mathrm{Res}_{z=z_i}(z-z_i) \sum_{I \in \gamma} \{\psi^I_{\mathbf{m}}, z\} = l \cdot \frac{1-l^{-2}}{2} = \frac{l - l^{-1}}{2} \tag{3.3.18}$$

where the extra factor of l takes into account the number of sheets glued at a branch point. The total contribution sums over cycles and gives h_σ.

Remark 3.3.2 (Consistency between path integral and stress-tensor method)**.** Comparing between the path integral method and the generalized stress-tensor method leads to following consistency conditions

$$g=0: \quad \partial_{z_i}\log\mathcal{W}_{\mathbf{m}}=\frac{1}{12}\sum_I \mathrm{Res}_{z=z_i}\{\psi^I_{\mathbf{m}},z\}, \tag{3.3.19}$$

$$g=1: \quad \partial_{z_i}\log\mathcal{W}_{\mathbf{m}}=\frac{1}{12}\mathrm{Res}_{z=z_i}\sum_I\{\psi^I_{\mathbf{m}},z\}=\frac{1}{12}\sum_I \mathrm{Res}_{z=z_i}\{u(p^I_z),z\}, \tag{3.3.20}$$

$$\begin{aligned}\partial_{z_i}\log\mathcal{Z}(\tau_{\mathbf{m}})&=2\pi i\left(\mathrm{Res}_{z=z_i}\sum_I\left(\psi^I_{\mathbf{m}}\right)'^2(z)\right)\partial_{\tau_{\mathbf{m}}}\log\mathcal{Z}(\tau_{\mathbf{m}})\\&=2\pi i\left(\mathrm{Res}_{z=z_i}\sum_I v^2(p^I_z)\right)\partial_{\tau_{\mathbf{m}}}\log\mathcal{Z}(\tau_{\mathbf{m}})\end{aligned} \tag{3.3.21}$$

While above identifications are conceptually clear: the Weyl anomaly term in the path integral method corresponds to the anomalous contribution to stress-tensor one-point function in stress-tensor method and the torus partition function term to the thermal energy term, it is non-trivial to directly verify the consistency conditions. The consistency condition for the Weyl anomaly term is essentially verified by studying the variation of Liouville action with respect to branch locus $\boldsymbol{z}$ in [KK03] to which we refer for details. The consistency condition involving torus partition function is guaranteed by the $g=1$ case of the variation formula in Theorem 3.2.2:

$$\partial_{z_i}\tau_{\mathbf{m}}=2\pi i\,\mathrm{Res}_{z=z_i}\sum_I v^2(p^I_z). \tag{3.3.22}$$

Alternatively, one may interpret that requiring consistency between path integral and stress-tensor method gives a physical derivation of above variation formula.

Below we give concrete examples for calculation of twist operator correlators using the generalized stress-tensor method, to demonstrate its consistency with known results in cases associated with branched covers with cyclic monodromy and note its particular simplicity in the genus one case compared with usual derivation in literature [DFMS87; LM01].

Example 3.3.1 (Cyclic monodromy, genus zero [CC04]; N^{th} Rényi entropy of single interval)**.**

Consider genus zero $M = 2$ branched cover with monodromies $\boldsymbol{\sigma}$

$$\sigma_1 = \sigma_2^{-1} = (1 \dots N), \tag{3.3.23}$$

the covering map and uniformizing map can be written as

$$\begin{aligned} \phi_{\mathbf{m}}(w) &= \frac{z_2 w^N - z_1}{w^N - 1}, \\ \psi^I_{\mathbf{m}}(z) &= \left(\frac{z - z_1}{z - z_2}\right)^{\frac{1}{N}} e^{\frac{2\pi i}{N} I}, \quad I = 1, \cdots, N. \end{aligned} \tag{3.3.24}$$

In this case the stress-tensor method gives

$$\begin{aligned} \partial_{z_1} \log \mathcal{Z}_{\mathbf{m}} &= \frac{c}{12} \operatorname{Res}_{z=z_1} \sum_I \{\psi^I_{\mathbf{m}}, z\} \\ &= \frac{Nc}{12} \operatorname{Res}_{z=z_1} \left\{ \left(\frac{z - z_1}{z - z_2}\right)^{\frac{1}{N}}, z \right\} \\ &= -\frac{c}{12} \left(N - N^{-1}\right) z_{12}^{-1} \end{aligned} \tag{3.3.25}$$

with logarithmic derivative with respect to z_2 related by permutation; this therefore gives the usual two-point function

$$\mathcal{Z}_{\mathbf{m}} = z_{12}^{-2h} \times (\text{anti-holomorphic}), \quad h = \frac{c}{24}(N - N^{-1}). \tag{3.3.26}$$

Example 3.3.2 (Cyclic monodromy, genus one [DFMS87; LM01]; second Rényi entropy of two intervals)**.** Consider genus one $M = 4, N = 2$ branched cover with monodromies

$$\sigma_i = (12), \quad i = 1, \dots, 4. \tag{3.3.27}$$

The differential in base space coordinate is given by

$$\begin{aligned} \omega(p_z^I) &= (-1)^I v(z) dz, \quad I = 1, 2 \\ v(z) &= \left[\prod_{i=1}^4 (z - z_i)\right]^{-\frac{1}{2}}, \end{aligned} \tag{3.3.28}$$

and the period of covering torus is given by

$$\tau_{\mathbf{m}} = i\frac{{}_2F_1\left(\frac{1}{2},\frac{1}{2};1;1-r\right)}{{}_2F_1\left(\frac{1}{2},\frac{1}{2};1;r\right)}, \quad r = \frac{z_{12}z_{34}}{z_{14}z_{32}}. \tag{3.3.29}$$

Using stress-tensor method, the Weyl anomaly term satisfies

$$\begin{aligned}\partial_{z_i}\log\mathcal{W}_{\mathbf{m}} &= \frac{1}{12}\sum_I \mathrm{Res}_{z=z_i}\{u(p_z^I), z\} \\ &= \frac{1}{12}\cdot 2\cdot \mathrm{Res}_{z=z_i}\left[\frac{v''(z)}{v(z)} - \frac{3}{2}\left(\frac{v'(z)}{v(z)}\right)^2\right] \\ &= -\frac{1}{24}\sum_{j\neq i} z_{ij}^{-1},\end{aligned} \tag{3.3.30}$$

and therefore

$$\mathcal{W}_{\mathbf{m}} = \left(\prod_{i<j} z_{ij}\right)^{-\frac{1}{24}}. \tag{3.3.31}$$

The full answer for twist operator correlator is

$$\mathcal{Z}_{\mathbf{m}} = \left|\prod_{i<j} z_{ij}\right|^{-\frac{c}{12}} \mathcal{Z}(\tau_{\mathbf{m}}, \bar{\tau}_{\mathbf{m}}) \tag{3.3.32}$$

where the period $\tau_{\mathbf{m}}$ as function of branch locus $\boldsymbol{z}$ is given in (3.3.29) and we have used the consistency between path integral and stress-tensor method as remarked previously to obtain the partition function term. We note that unlike usual derivation in literature [DFMS87; LM01], we didn't need the elliptic function covering map $\phi_{\mathbf{m}}$, whose explicit form for special configuration of branch locus $\boldsymbol{z}$ can be found in [DFMS87; LM01] and generic configuration in [Ebe20].

3.3.3. Relation between twist operator correlator and tau function on Hurwitz space

We hope that at this point the structural similarity between the defining equation of twist operator correlator in stress-tensor method and the definition of tau function on Hurwitz space

in terms of Bergman projective connection

$$\begin{aligned}\partial_{z_i}\log\mathcal{Z}_{\mathbf{m}} &= \mathrm{Res}_{z=z_i}\,\langle T(z)\rangle_{\mathbf{m}}\,,\\ \partial_{z_i}\log\tau_{\mathbf{m}} &= \frac{1}{12}\,\mathrm{Res}_{z=z_i}\,S_{\mathbf{m}}(z),\end{aligned}\tag{3.3.33}$$

and the similar expressions, reproduced below for convenience of comparison, for stress-tensor one-point function $\langle T(z)\rangle_{\mathbf{m}}$

$$\begin{aligned}g=0:\quad \langle T(z)\rangle_{\mathbf{m}} &= \frac{c}{12}\sum_I\{\psi^I_{\mathbf{m}},z\},\\ g=1:\quad \langle T(z)\rangle_{\mathbf{m}} &= \frac{c}{12}\sum_I\{\psi^I_{\mathbf{m}},z\}+2\pi i\sum_I\left(\psi^I_{\mathbf{m}}\right)'^2(z)\,\partial_{\tau_{\mathbf{m}}}\log\mathcal{Z}(\tau_{\mathbf{m}})\\ &= \frac{c}{12}\sum_I\{u(p^I_z),z\}+2\pi i\sum_I v^2(p^I_z)\partial_{\tau_{\mathbf{m}}}\log\mathcal{Z}(\tau_{\mathbf{m}})\,,\end{aligned}\tag{3.3.34}$$

and Bergman projective connection $S_{\mathbf{m}}(z)$

$$\begin{aligned}g=0:\quad S_{\mathbf{m}}(z) &= \sum_I\{\psi^I_{\mathbf{m}},z\},\\ g=1:\quad S_{\mathbf{m}}(z) &= \sum_I\{\psi^I_{\mathbf{m}},z\}-8\pi i\sum_I\left(\psi^I_{\mathbf{m}}\right)'^2(z)\,\partial_{\tau_{\mathbf{m}}}\log\theta_1'(0|\tau_{\mathbf{m}})\\ &= \sum_I\{u(p^I_z),z\}-8\pi i\sum_I v^2(p^I_z)\partial_{\tau_{\mathbf{m}}}\log\theta_1'(0|\tau_{\mathbf{m}}),\end{aligned}\tag{3.3.35}$$

has made the relation between $\mathcal{Z}_{\mathbf{m}}$ and $\tau_{\mathbf{m}}$ transparent. In particular, the Bergman projective connection of branched cover $\phi_{\mathbf{m}}$ at I^{th} pre-image p^I_z evaluated in base coordinate z, $S^I_{\mathbf{m}}(z)=S_{\phi_{\mathbf{m}}}(p^I_z)$, is analogous to the stress-tensor one-point function of I^{th} copy of the CFT under monodromy conditions $\mathbf{m}$ of branched cover $\phi_{\mathbf{m}}$, $\langle T_I(z)\rangle_{\mathbf{m}}$; it contains an anomalous term responsible for "Weyl anomaly" and in the genus one case a "thermal energy" term generated by its own "partition function" $\theta_1'(0|\tau)^{-\frac{1}{3}}\propto\eta^{-1}(\tau)$, which originates from the theta function with odd characteristics in the definition of Bergman kernel.[7] We can therefore write the twist

[7] Recall Jacobi's identity $\theta_1'(0|\tau)=\theta_2(\tau)\theta_3(\tau)\theta_4(\tau)=2\eta^3(\tau)$.

operator correlator and tau function on Hurwitz space in a similar way

$$\begin{aligned} g=0: \quad & \mathcal{Z}_{\mathbf{m}} = |\mathcal{W}_{\mathbf{m}}|^{2c}, \\ & \tau_{\mathbf{m}} = \mathcal{W}_{\mathbf{m}}, \\ g=1: \quad & \mathcal{Z}_{\mathbf{m}} = |\mathcal{W}_{\mathbf{m}}|^{2c} \mathcal{Z}\left(\tau_{\mathbf{m}}, \bar{\tau}_{\mathbf{m}}\right), \\ & \tau_{\mathbf{m}} = \mathcal{W}_{\mathbf{m}} \eta^{-1}(\tau_{\mathbf{m}}), \end{aligned} \tag{3.3.36}$$

where we have used the compatibility conditions in Remark 3.3.2 to identify the Weyl anomaly $\mathcal{W}_{\mathbf{m}}$ and torus partition function $\mathcal{Z}\left(\tau_{\mathbf{m}}, \bar{\tau}_{\mathbf{m}}\right)$; also the genus one variation formula (3.3.22) again allows one to directly identify the "partition function" term $\theta_1'(0|\tau)^{-\frac{1}{3}} \propto \eta^{-1}(\tau)$ in $\tau_{\mathbf{m}}$ as explained in [KK03]. We then recognize that in the genus zero and one case the tau function on Hurwitz space is essentially the holomorphic part of the twist operator correlator of $c = 1$ free boson,

$$\tau_{\mathbf{m}} = \mathcal{Z}_{\mathbf{m}}^{\text{bos.}}|_{\text{holo.}}, \tag{3.3.37}$$

except with a non-modular-invariant partition function

$$\mathcal{Z}'_{\text{bos.}}(\tau, \bar{\tau}) = |\eta(\tau)|^{-2} \tag{3.3.38}$$

corresponding to trace over free boson Fock space, instead of the modular-invariant one

$$\mathfrak{Z}_{\text{bos.}}(\tau, \bar{\tau}) = (\Im\tau)^{-\frac{1}{2}} |\eta(\tau)|^{-2}. \tag{3.3.39}$$

This is indeed also expected from previous remarks on the analogy between Bergman kernel/projective connection and free boson.

We summarize the direct relation between twist operator correlator and tau function on Hurwitz space in following theorem, which can be immediately inferred from (3.3.36).

Theorem 3.3.1. *Let $\mathcal{Z}_{\mathbf{m}}$ be the twist operator correlator in Definition 3.1.1 and $\tau_{\mathbf{m}}$ be the tau function on Hurwitz space defined in (3.2.31), both associated with a branched cover $\phi_{\mathbf{m}} : \Sigma \to \mathbb{CP}^1$ with monodromy data $\mathbf{m}$; then for a generic branched cover $\phi_{\mathbf{m}}$ of genus zero and one,*

$$\mathcal{Z}_{\mathbf{m}} = \begin{cases} |\tau_{\mathbf{m}}|^{2c} & g = 0 \\ |\tau_{\mathbf{m}}|^{2c} |\eta(\tau_{\mathbf{m}})|^{2c} \mathcal{Z}(\tau_{\mathbf{m}}, \bar{\tau}_{\mathbf{m}}) & g = 1 \end{cases} \tag{3.3.40}$$

where c is the central charge of the CFT $\mathcal{C}$ in Definition 3.1.1, $\mathcal{Z}(\tau, \bar{\tau})$ is its torus partition function, $\eta(\tau)$ is Dedekind eta function and $\tau_{\mathbf{m}}$ is the period of the covering torus.

Remark 3.3.3 (Compatibility condition)**.** The relation between Bergman projective connection and stress-tensor one-point function also makes clear the compatibility condition of (3.1.9)

$$\partial_{z_j} \operatorname{Res}_{z=z_i} \langle T(z) \rangle_{\mathbf{m}} = \partial_{z_i} \operatorname{Res}_{z=z_j} \langle T(z) \rangle_{\mathbf{m}} \tag{3.3.41}$$

from the known compatibility condition (3.2.35) for Bergman projective connection $S_{\mathbf{m}}(z)$, as they essentially coincide in the genus zero case and only differ in the genus one case by terms that trivially satisfy the compatibility condition.

Remark 3.3.4 (Relation with isomonodromic tau function [Kor03])**.** The tau function on Hurwitz space is known essentially as special case of the more general isomonodromic tau function associated with rank N matrix Fuchsian equation with M singularities

$$\partial_z \Psi(z) = A(z)\Psi(z), \quad A(z) = \sum_i \frac{A_i}{z - z_i}, \quad A_i \in \mathrm{GL}(N, \mathbb{C}), \quad \mathrm{Tr}\,(A_i) = 0, \tag{3.3.42}$$

where the matrix function $\Psi(z) \in \mathrm{GL}(N, \mathbb{C})$ has monodromies

$$\Psi(\xi_i \circ z) = \Psi(z) M_i, \quad M_i \in \mathrm{SL}(N, \mathbb{C}) \tag{3.3.43}$$

with monodromy matrices satisfying $M_M \cdots M_1 = \mathbb{I}$ again because the matrix monodromy data $\mathfrak{m} = (\boldsymbol{M}, \boldsymbol{z}) \in \mathrm{SL}(N, \mathbb{C})^M \times \mathbb{C}^M$ gives a representation of $\pi_1\left(\mathbb{CP}^1 \setminus \boldsymbol{z}\right)$.

Isomonodromic deformation of such matrix Fuchsian equation is concerned with changing $A_i \in \boldsymbol{A}$ as function of $\boldsymbol{z}$ while keeping $\boldsymbol{M}$ fixed. The isomonodromic deformation is governed

by a set of non-linear PDEs known as Schlesinger equations

$$\begin{aligned}\partial_{z_j} A_i &= \frac{[A_i, A_j]}{z_{ij}}, \quad i \neq j \\ \partial_{z_i} A_i &= -\sum_{j \neq i} \frac{[A_i, A_j]}{z_{ij}},\end{aligned} \tag{3.3.44}$$

and given a solution to Schlesinger equation, the associated isomonodromic tau function is defined in terms of the solution as [JMU81]

$$\partial_{z_i} \log \tau_{\mathfrak{m}} (\boldsymbol{z}|\boldsymbol{M}) \coloneqq \frac{1}{2} \operatorname{Res}_{z=z_i} \operatorname{Tr} \left(A^2\right). \tag{3.3.45}$$

It is shown in [Kor03] that the tau function on Hurwitz space is essentially the isomonodromic tau function while specializing to quasi-permutation monodromy matrices

$$(M_i)_{IJ} = \pm \delta_{I,\sigma_i(J)} \tag{3.3.46}$$

where the minus signs arise from branch cuts on covering space and we refer to [Kor03] for details, and the two tau functions essentially coincide up to theta function

$$\tau_{\mathfrak{m}} = \tau_{\mathbf{m}} \Theta (0|\boldsymbol{\tau}_{\mathbf{m}}) \tag{3.3.47}$$

where $\boldsymbol{\tau}_{\mathbf{m}}$ is the period matrix of covering surface and at genus zero the two tau functions exactly coincide.[8] Therefore, by virtue of the relation in Theorem 3.3.1 we have following relation between twist operator correlator and isomonodromic tau function

$$\mathcal{Z}_{\mathbf{m}} = \begin{cases} |\tau_{\mathfrak{m}}|^{2c} & g = 0 \\ |\tau_{\mathfrak{m}}|^{2c} \left| \frac{\eta(\tau_{\mathbf{m}})}{\theta_3(\tau_{\mathbf{m}})} \right|^{2c} \mathcal{Z} (\tau_{\mathbf{m}}, \bar{\tau}_{\mathbf{m}}) & g = 1 \end{cases}. \tag{3.3.48}$$

We note that now conversely the isomonodromic tau function at genus zero and one admits a CFT interpretation as the holomorphic part of the associated twist operator correlator of two copies of $c = \frac{1}{2}$ free fermion with the non-modular-invariant torus partition function with

[8] The construction in [Kor03] in fact involves sets of additional parameters; the isomonodromic tau function we consider here corresponds to not turning on such parameters.

(NS,NS) boundary conditions

$$\mathcal{Z}_{\text{ferm.}}^{(\text{NS,NS})}(\tau,\bar{\tau}) = \left|\frac{\theta_3(\tau)}{\eta(\tau)}\right|. \tag{3.3.49}$$

Remark 3.3.5 (Integrable system interpretation)**.** The relation with tau function gives a quite different interpretation of the Weyl anomaly contribution to twist operator correlator: while in the context of twist operator correlator the branch locus are viewed as locations of operator insertions and monodromies as boundary conditions, in the context of isomonodromic deformation the branch locus can be viewed as "times" and the monodromies kept fixed during the deformation as "conserved quantities".

Remark 3.3.6 (Gauge-invariant twist operator)**.** As mentioned in introduction, the gauge-invariant twist operator correlator $\mathcal{Z}_{\mathbf{r}}(\boldsymbol{z}|\boldsymbol{\lambda})$ in symmetric product orbifold $\mathcal{C}^{\otimes \mathsf{N}}/S_{\mathsf{N}}$ admits a representation as summing over the gauge-dependent twist operators $\mathcal{Z}_{\mathbf{m}}$ over Hurwitz space and has a genus expansion in the large N limit. In light of the relation in Theorem 3.3.1 between gauge-dependent twist operator and tau function on Hurwitz space, the leading order genus zero and one contribution at large N limit of gauge-invariant twist operator therefore admits a representation as summing over tau functions on Hurwitz space:

$$\begin{aligned}\mathcal{Z}_{\mathbf{r}}(\boldsymbol{z}|\boldsymbol{\lambda}) = \mathcal{N}_{0,\mathsf{N}}(\boldsymbol{\lambda}) \sum_{\substack{\phi_{\mathbf{m}}\in\mathcal{H}_0(\boldsymbol{\lambda})\\ \mathrm{br}(\phi_{\mathbf{m}})=\boldsymbol{z}}} |\tau_{\mathbf{m}}(\boldsymbol{z}|\boldsymbol{\sigma})|^{2c} \\ + \mathcal{N}_{1,\mathsf{N}}(\boldsymbol{\lambda}) \sum_{\substack{\phi_{\mathbf{m}}\in\mathcal{H}_1(\boldsymbol{\lambda})\\ \mathrm{br}(\phi_{\mathbf{m}})=\boldsymbol{z}}} |\tau_{\mathbf{m}}(\boldsymbol{z}|\boldsymbol{\sigma})|^{2c} |\eta(\tau_{\mathbf{m}})|^{2c} \mathcal{Z}(\tau_{\mathbf{m}},\bar{\tau}_{\mathbf{m}}) + \cdots\end{aligned} \tag{3.3.50}$$

3.4. Discussions

We conclude by commenting on the relation between our results with existing literature and mentioning some open questions we hope to address in the future.

3.4.1. Relation with existing literature

- *Twist operator correlator and tau function on Hurwitz space.* The relation between twist operator correlator in 2d CFT and tau function on Hurwitz space is also studied in [GM16] in the context of interpreting tau function as twist operator conformal blocks of W-algebra

by utilizing free field realization of $c = N - 1$ W_N algebra. While similar technical details are discussed such as the analogy between Bergman projective connection and stress-tensor in 2d CFT, our purpose and perspective are quite different: we relate two independently well-defined objects, the universal Weyl anomaly contribution to twist operator correlator and tau function on Hurwitz space, and concern generic 2d CFTs without relying on free-field realization. Also the Liouville action associated with Weyl anomaly contribution to twist operator correlator is studied in the original paper [KK03] on tau function on Hurwitz space where it is observed that the Liouville action solves (the non-trivial part of) the defining differential equation for tau function (i.e., the Weyl anomaly part of consistency conditions in Remark 3.3.2); we clarify the physical origin of Liouville action in their tau function calculation by pointing out the relation between tau function and twist operator correlator.

- *Twist operator correlator and isomonodromic tau function.* The relation between twist operator correlator and isomonodromic tau function dates back to the holonomic quantum fields of [SMJ79] in the early studies of isomonodromic tau function, where solution of matrix Riemann-Hilbert problem with generic matrix monodromy data is constructed using twist operators in free fermion and the isomonodromic tau function is shown to be equal to twist operator correlator. Our result is specialized to matrix monodromy data with quasi-permutation monodromy matrices and generalize in this case the relation between twist operator correlator and isomonodromic tau function to generic 2d CFTs using universal arguments.

3.4.2. Remaining questions and future directions

- *Explicit evaluation of twist operator correlator/tau function.* While our expression for stress-tensor one-point function holds for generic branched covers with non-abelian monodromy, it is not explicit enough for direct evaluation of twist operator correlator using stress-tensor method as the uniformizing map in general is not known explicitly beyond the cyclic cases; this is also the case in the path integral method where the coefficients of covering map are in general not known explicitly as functions of branch locus. However, the

relation with tau function might provide a promising reformulation in light of the recent development in the CFT/isomonodromy correspondence [GIL12; ILT15; GIL19], which relates isomonodromic tau function associated with rank N matrix Fuchsian equation to Fourier-transformed W_N conformal blocks. The relation is made precise for generic $N = 2$ (Virasoro) cases but only certain semi-degenerate cases for arbitrary N due to technicalities in W_N conformal blocks and therefore the relation doesn't immediately apply for the isomonodromic tau function related to twist operator correlator.[9] A precise realization of the CFT/isomonodromy correspondence at arbitrary N for generic matrix monodromy data would give explicit evaluation of (the universal Weyl anomaly part of) twist operator correlator via its relation with isomonodromic tau function.

- *Generalization to higher genus $g \geq 2$.* A similar understanding, as in the genus zero and one case, of the general structure of twist operator correlator associated with generic branched covers with genus $g \geq 2$ for generic 2d CFTs has remained lacking in literature: in symmetric product orbifold context, most of the discussions have been focused on the lower genus cases motivated by their relevance for large N limit; in the context of replica trick calculation of quantum-information quantities, usually a single block domination prescription, valid for large c 2d CFT, is used to calculate twist operator correlator at higher genus [Har13; DF21]; there are also results on free theories [CCT09; DFMS87; Zam87]. While an explicit evaluation of twist operator correlator for generic 2d CFTs associated with generic branched covers is, as already in genus zero and one case, likely out of reach, one might hope to understand better its general structure such as i) the suitable formulation of path integral and stress-tensor method for generic 2d CFTs and their consistency in $g \geq 2$ cases and ii) the relation with tau function on Hurwitz space and isomonodromic tau function, which are indeed still well-defined at $g \geq 2$ [KK03; Kor03].

[9] The semi-degeneracy essentially means that all but two of the spectra of monodromy matrices have $N - 1$ degeneracies. While at first sight it seems that quasi-permutation matrices corresponding to transpositions satisfy this condition, the extra minus sign (needed for a cycle of even length [Kor03]) makes it actually have $N - 2$ degeneracy.

3.A. Theta function conventions

The genus g Riemann theta function is defined as

$$\Theta(\mathbf{u}|\boldsymbol{\tau}) = \sum_{\mathbf{n}\in\mathbb{Z}^g} e^{2\pi i \mathbf{n}\cdot\mathbf{u}} e^{\pi i \mathbf{n}\cdot\boldsymbol{\tau}\cdot\mathbf{n}}, \tag{3.A.1}$$

and the Riemann theta function with characteristics $\mathbf{c} = \frac{\mathbf{a}}{2} + \frac{\boldsymbol{\tau}\cdot\mathbf{b}}{2}$ can be defined as

$$\Theta_{\mathbf{c}}(\mathbf{u}|\boldsymbol{\tau}) = \Theta\begin{bmatrix}\mathbf{a}\\ \mathbf{b}\end{bmatrix}(\mathbf{u}|\boldsymbol{\tau}) = \exp\pi i\left(\frac{\mathbf{a}\cdot\boldsymbol{\tau}\cdot\mathbf{a}}{4} + \mathbf{a}\cdot\mathbf{u} + \frac{\mathbf{a}\cdot\mathbf{b}}{2}\right)\Theta(\mathbf{u}+\mathbf{c}|\boldsymbol{\tau}). \tag{3.A.2}$$

A characteristics $\mathbf{c} = \frac{\mathbf{a}}{2} + \frac{\boldsymbol{\tau}\cdot\mathbf{b}}{2}$ is called half-integer if $\mathbf{a}, \mathbf{b} \in \mathbb{Z}^g$ and even/odd if $\mathbf{a}\cdot\mathbf{b}$ is even/odd.

At $g = 1$, the Jacobi theta functions are related to Riemann theta function by

$$\begin{aligned}
\theta_1(u|\tau) &= -\theta\begin{bmatrix}1\\ 1\end{bmatrix}(u|\tau), \quad \theta_2(u|\tau) = \theta\begin{bmatrix}1\\ 0\end{bmatrix}(u|\tau),\\
\theta_3(u|\tau) &= \theta\begin{bmatrix}0\\ 0\end{bmatrix}(u|\tau), \quad \theta_4(u|\tau) = \theta\begin{bmatrix}0\\ 1\end{bmatrix}(u|\tau)
\end{aligned} \tag{3.A.3}$$

with $\theta_1(u|\tau)$ being the one with odd characteristics and others with even characteristics. Theta functions with argument $u = 0$ are abbreviated as

$$\theta_\nu(0|\tau) = \theta_\nu(\tau), \quad \nu = 1, \ldots, 4. \tag{3.A.4}$$

4. Twist operator correlators and isomonodromic tau functions from modular Hamiltonians

4.1. Introduction, summary of results and discussions

The goal of this chapter is to uncover novel representations and properties of the twist operator correlators (TOC) in two-dimensional conformal field theory (2d CFT) and the closely related tau functions of isomonodromic type, utilizing techniques and intuitions from quantum information theory.

We first recall the general path integral definition of TOCs in terms of the monodromy data of branched covers [LM01; CC04], and refer the reader to [Jia23a] and references therein for the relevance of TOCs in physical contexts such as symmetric product orbifold and string theory.

Definition 4.1.1 (Twist operator correlator)**.** *A monodromy data is a pair* $\mathbf{m} = (\boldsymbol{\sigma}, \boldsymbol{z}) \in S_N^M \times \bar{\mathbb{C}}^M$*. Twist operator correlator/partition function with prescribed monodromy* $\mathbf{m}$ *for a generic 2d CFT* $\mathcal{C}$ *is defined by path integral for* N *copies of* $\mathcal{C}$ *with monodromy conditions for fundamental fields* $\{\varphi_I\}_{I=1,\cdots,N}$ *specified by* $\mathbf{m}$

$$\mathcal{Z}_{\mathbf{m}}(\boldsymbol{z}|\boldsymbol{\sigma}) = \left\langle \prod_i \sigma_i(z_i) \right\rangle \coloneqq \int_{\varphi_I(\xi_i \circ z) = \varphi_{\sigma_i(I)}(z)} [D\varphi]\, e^{-\sum_I S[\varphi_I]} \tag{4.1.1}$$

where $\boldsymbol{\xi}$ *are generating loops in* $\pi_1\left(\mathbb{CP}^1 \setminus \boldsymbol{z}\right)$ *and* $\xi_i \circ z$ *denotes continuation along path* ξ_i*. The*

monodromy data $\mathbf{m}$ *is naturally identified as the monodromy data of a branched cover*

$$\phi_{\mathbf{m}} : \Sigma \to \mathbb{CP}^1$$

with branch locus $\boldsymbol{z}$ *(i.e., critical values of* $\phi_{\mathbf{m}}$*) and corresponding permutation monodromies* $\boldsymbol{\sigma}$*. In other words, the twist operator correlator* $\mathcal{Z}_{\mathbf{m}}$ *is the partition function of* $\mathcal{C}$ *on* Σ *evaluated in the conformal frame where base* $\mathbb{CP}^1$ *has flat metric.*[1]

The TOCs in physics literature are closely related to the tau functions of isomonodromic type in math literature. The tau function on Hurwitz space, the moduli space of branched covers, associated with a branched cover $\phi_{\mathbf{m}}$ is studied in [KK04] and is defined as

$$\partial_{z_i} \log \boldsymbol{\tau}_{\mathbf{m}} \coloneqq \frac{1}{12} \operatorname{Res}_{z=z_i} S_{\phi_{\mathbf{m}}}(z) \tag{4.1.2}$$

where $S_{\phi_{\mathbf{m}}}(z)$ is the sum of Bergman projective connections of $\phi_{\mathbf{m}}$ at pre-images of z evaluated in base coordinate z and we refer to [KK04; Jia23a] for more details. The tau functions on Hurwitz space are special cases of the more general isomonodromic tau functions [JMU81] associated with rank N matrix Fuchsian systems while specializing to quasi-permutation monodromies [Kor04].

We showed in [Jia23a] that for generic 2d CFT $\mathcal{C}$ and branched covers of genus zero and one, the following relation holds between TOCs and tau functions on Hurwitz space:

$$\mathcal{Z}_{\mathbf{m}} = \begin{cases} |\boldsymbol{\tau}_{\mathbf{m}}|^{2c} & g = 0 \\ |\boldsymbol{\tau}_{\mathbf{m}}|^{2c} |\eta(\tau_{\mathbf{m}})|^{2c} \mathcal{Z}(\tau_{\mathbf{m}}, \bar{\tau}_{\mathbf{m}}) & g = 1 \end{cases} \tag{4.1.3}$$

where c is the central charge of CFT $\mathcal{C}$, $\eta(\tau)$ is Dedekind eta function, $\mathcal{Z}(\tau, \bar{\tau})$ is torus partition function of $\mathcal{C}$, and the period $\tau_{\mathbf{m}} = \tau_{\mathbf{m}}(\boldsymbol{z}|\boldsymbol{\sigma})$ of covering torus is viewed as a function of branch locus $\boldsymbol{z}$. Physically, the universal, only central-charge-dependent part of TOC arises from the Weyl anomaly due to Weyl transformation induced by the covering map. In this chapter, we will focus on the genus-zero case where the tau functions are the holomorphic part of the $c = 1$ TOCs.

[1] Technically, a cut-off is required at infinity on $\mathbb{CP}^1$; this gives trivial contribution to the $\boldsymbol{z}$-dependence of the twist operator correlator $\mathcal{Z}_{\mathbf{m}}$ [LM01].

The relevance of quantum information theory for TOC/tau functions arises from the formal path integral representation of the reduced density matrix of the ground state in 2d CFT. As the representation is quite standard in physics literature, we refer readers unfamiliar with the idea to, e.g., the original paper [CC04] and the review [Nis18] for more details. In this introduction, we proceed by illustrating with a simple example associated with a branched cover with non-abelian monodromy group.

Consider a four-point TOC/tau function, associated with a degree-three genus-zero branched cover, with the following monodromy data (the meaning of the subscripts in the TOC/tau function will become clear):

$$\begin{aligned} &\mathcal{Z}_{(2,2)}(\boldsymbol{z}) = \left|\tau_{(2,2)}(\boldsymbol{z})\right|^{2c} \\ &\sigma_1 = \sigma_2 = (12), \quad \sigma_3 = \sigma_4 = (13). \end{aligned} \tag{4.1.4}$$

It follows from the standard path integral representation of ground state reduced density matrix in 2d CFT that the TOC admits the following identification as a density matrix/exponentiated modular Hamiltonian correlator:

$$\begin{aligned} &\mathcal{Z}_{(2,2)}(\boldsymbol{z}) = \mathrm{Tr}\left[\rho_R\left(\rho_{R_1}\otimes\rho_{R_2}\right)\right] = \left\langle \rho_{R_1}\rho_{R_2}\right\rangle, \\ &R = R_1 \cup R_2, \quad R_1 = (z_1, z_2), \quad R_2 = (z_3, z_4), \end{aligned} \tag{4.1.5}$$

where $\langle\cdot\rangle$ denotes ground state expectation value, and the density matrices are understood as those of the intervals R, R_1, R_2. The reason behind the identification is as follows. The formal path integral on the three sheets of the branched cover with cuts at R_1 and/or R_2 are understood as preparing the reduced density matrices $\rho_R, \rho_{R_1}, \rho_{R_2}$, and the trace in $\mathrm{Tr}\left[\rho_R\left(\rho_{R_1}\otimes\rho_{R_2}\right)\right]$ glues the sheets together and leads to the defining path integral for TOC in Definition 4.1.1. In particular, the first sheet of the branched cover corresponds to ρ_R, the second sheet to ρ_{R_1}, and the third sheet to ρ_{R_2}.

The example above is the $(n_1, n_2) = (2, 2)$ case of the class of genus-zero four-point TOC/tau

functions studied in this chapter:

$$\begin{aligned}
&\mathcal{Z}_{(n_1,n_2)} = \left|\tau_{(n_1,n_2)}\right|^{2c} = \mathrm{Tr}\left[\rho_R\left(\rho_{R_1}^{n_1-1}\otimes\rho_{R_2}^{n_2-1}\right)\right] = \left\langle \rho_{R_1}^{n_1-1}\rho_{R_2}^{n_2-1}\right\rangle \\
&\sigma_1 = \sigma_2^{-1} = (1\cdots n_1), \quad \sigma_3 = \sigma_4^{-1} = (1\ n_1+1\cdots n_1+n_2-1) \\
&R = R_1\cup R_2, \quad R_1 = (z_1,z_2), \quad R_2 = (z_3,z_4),
\end{aligned} \tag{4.1.6}$$

where the associated monodromy data can be easily read off from the path integral representation of reduced density matrices.

From the perspective of their identifications as density matrix correlators, the universality of the genus-zero TOC/tau functions above stems from their representations as ground state expectation value of single-interval density matrices, and the universality of single-interval modular Hamiltonian $\mathcal{H}_{R_i}$ [BW76; CHM11; CT16]:

$$\begin{aligned}
&\rho_{R_i} \propto e^{-\mathcal{H}_{R_i}}, \quad R_i = (a_i,b_i) \\
&\mathcal{H}_{R_i} = \int_{R_i} dz \frac{(z-a_i)(z-b_i)}{b_i-a_i} T(z) + \frac{c}{6}\log\frac{b_i-a_i}{\epsilon}\mathbb{1} + \text{anti-holo.},
\end{aligned} \tag{4.1.7}$$

where $T(z)$ is the holomorphic stress-tensor of the 2d CFT.

While in general genus-zero TOC/tau functions, including the ones in (4.1.6), can in principle be calculated from the Liouville action associated with the branched cover [LM01; KK04], or directly from the definition[2]

$$\partial_{z_i}\log\tau_{\mathbf{m}} = \frac{1}{12}\mathrm{Res}_{z=z_i}\sum_I \{\psi_{\mathbf{m}}^I, z\}, \tag{4.1.8}$$

where $\psi_{\mathbf{m}}^I$ are inverses of $\phi_{\mathbf{m}}$ and $\{\cdot,z\}$ denotes Schwarzian derivative with respect to z, to perform the calculation one needs the explicit knowledge of how branched cover $\phi_{\mathbf{m}}$ varies under deformation of branch locus $\boldsymbol{z}$, i.e., the explicit solution of an isomonodromic deformation problem. Such direct evaluation of TOC/tau functions is generally obstructed by the difficulty of explicitly constructing branched covers with prescribed monodromy, especially those with non-abelian monodromy group, and previous expressions for TOC/tau functions [KK04; LM01;

[2]Physically, this is equivalent to the stress-tensor method for TOC [DFMS87; Jia23a].

PRR09; DE20] generally leave implicit the dependence on branch locus $\boldsymbol{z}$ in terms of certain unknown coefficients in the rational function $\phi_{\mathbf{m}}$.

Interestingly, the density matrix representations of TOC/tau functions in (4.1.6) entirely avoid the need for explicit construction of the associated branched covers, and can be evaluated using techniques initially developed in the contexts of condensed matter/quantum information theory.

In particular, utilizing the universality of the genus-zero TOC/tau functions in (4.1.6), we may as well evaluate them in simple CFTs such as free fermions where the continuum answers can be extracted from the lattice set-up where the correlation matrix method of [Pes03] applies. The method facilitates the evaluation of the density matrix correlators relevant for our purpose by utilizing the simple relation between modular Hamiltonian kernel/matrix and correlation matrix in Gaussian states. This approach is adopted in §4.3.

Moreover, the universal continuum modular Hamiltonian expression (4.1.7) can also in principle be used to compute TOC/tau functions in (4.1.6). We discuss more details and subtleties on computing TOC/tau functions using the continuum modular Hamiltonians in §4.5.

Summary of results

Our main results are:

- A novel determinantal representation for the class of TOC/tau functions in (4.1.6). This is derived using the correlation matrix method for free fermions. We claim that the non-trivial part of the four-point tau function $\mathcal{T}_{(n_1,n_2)}$, defined by:

$$\tau_{(n_1,n_2)}(\boldsymbol{z}) = \mathcal{L}_{(n_1,n_2)}(\boldsymbol{z})\,\mathcal{T}_{(n_1,n_2)}(x), \quad x = \frac{z_{12}z_{34}}{z_{13}z_{24}}, \tag{4.1.9}$$

  where the leg factor $\mathcal{L}_{(n_1,n_2)}(\boldsymbol{z})$ is defined in § 4.2.1, admits the following determinantal representation in terms of free fermion correlation matrices (claim 4.3.1):

$$\left|\mathcal{T}_{(n_1,n_2)}(x)\right|^2 = \lim_{\substack{l_1,l_2,d\to\infty \\ x(l_1,l_2,d)\ \text{fixed}}} \mathcal{L}^{-2}_{(n_1,n_2)}(l_1,l_2,d)\det\left(\mathsf{M}^{(n_1,n_2)}_{R_1,R_2}\right) \tag{4.1.10}$$

where the equality is understood to hold up to x-independent overall constant. l_1, l_2 are the sizes of the intervals R_1, R_2 on the lattice and d their separation, $x(l_1, l_2, d)$ and $\mathcal{L}_{(n_1,n_2)}(l_1, l_2, d)$ are the appropriate cross-ratio and leg factor on lattice, and the l_1+l_2+2-dimensional square matrix $\mathsf{M}^{(n_1,n_2)}_{R_1,R_2}$ is defined in terms of correlation matrices of free fermions; see §4.3.2 for more details. In §4.4, we verify the claim in the $(n_1, n_2) = (2, 2)$ case where the exact tau function $\mathcal{T}_{(2,2)}(x)$ is known, and find very good agreement between the exact expression and continuum limit of lattice data. We also present a multi-interval generalization of the determinantal representation in claim 4.3.2.

- An approximate factorization property for the class of TOC/tau functions in (4.1.6):

  Claim. *There exists* $x^* \in \left(\frac{1}{2}, 1\right)$ *such that* $\forall x \in (0, x^*)$,

  $$\left|\frac{\mathcal{T}_{(n_1,n_2)}(x)}{\mathcal{T}^{\text{fac.}}_{(n_1,n_2)}(x)}\right| = 1 + \epsilon, \quad |\epsilon| \ll 1. \tag{4.1.11}$$

  where $\mathcal{T}^{\text{fac.}}_{(n_1,n_2)}(x)$ is associated with the factorized TOC/tau function; see §4.2.2 for more details. This is argued based on the known correlation structure of the ground state of large-c holographic CFT and the universality of the genus-zero TOCs. A priori, while the TOCs generally factorize in the $x \to 0$ limit, there is no reason to expect them to approximately factorize in a finite range of cross-ratios as the associated branched cover is connected. In §4.4, we verify the claim in the $(n_1, n_2) = (2, 2)$ case where the exact tau function $\mathcal{T}_{(2,2)}(x)$ is known, and present more evidence in other two-interval examples by comparing with lattice data.

We also study the class of TOC/tau function in (4.1.6) using the continuum modular Hamiltonian (4.1.7). This results in a formal integral representation for TOC/tau functions in terms of integrated stress-tensor correlators:

$$\frac{\mathfrak{T}_{(n_1,n_2)}(x)}{\mathfrak{T}^{\text{fac.}}_{(n_1,n_2)}(x)} = \prod_{\substack{l_1+l_2>1 \\ l_1,l_2\neq 0}} \exp\left\{\frac{\alpha_1^{l_1}\alpha_2^{l_2}}{l_1!\, l_2!}\mathfrak{T}_{(l_1,l_2)}(x)\right\}, \quad \alpha_i = n_i - 1, \quad x = \frac{z_{12}z_{34}}{z_{13}z_{24}}, \tag{4.1.12}$$

where $\mathfrak{T}_{(l_1,l_2)}(x)$ is defined by integrating connected stress-tensor correlators against entanglement temperatures of the associated intervals; see §4.5.3 for details. There are, however, sub-

tleties in making sense of the formal expression due to divergence of $\mathfrak{T}_{(l_1,l_2)}(x)$ from singularities at coincident insertion points in stress-tensor correlators and the potential need to analytically continue in α_i. We leave a more systematic study of the continuum modular Hamiltonian approach to future work.

Discussions

A few remarks are in order:

- In deriving our results, while we have relied on the formal manipulation of density matrices that technically don't exist in general in quantum field theory (see, e.g., [Wit18] and references therein), our claims are mathematically precise and concern well-defined mathematical objects such as isomonodromic tau functions.[3] It would be interesting to understand if the same results concerning TOC/tau functions can be derived without relying on the formal manipulations.

- We have focused on branched covers with monodromy data such that their associated TOCs can be identified as density matrix correlators involving disjoint intervals. More generic monodromy data can be obtained by taking the adjacent limit of the disjoint case, where the permutation monodromy in the limit is given by composition of monodromies at coincident endpoints. In fact, this implies that a generic genus-zero TOC/tau function can in principle be obtained from the class of multi-interval TOC/tau functions in (4.2.6) with $n_i = 2$; the reason is the following. As any permutation can be decomposed as composition of transpositions, generic genus-zero TOC/tau functions can be obtained by taking the coincident limit of higher-point genus-zero twist-two TOC/tau functions, i.e., those associated with *simple* branched covers. Furthermore, TOC/tau functions associated with branched covers with the same ramification profile are related by analytic continuation [PRR09; DE20], and therefore the desired twist-two TOC/tau functions can be obtained from the $n_i = 2$ case of (4.2.6) by continuation. Implementing this explicitly requires understanding better the regularization and monodromy property of the formal

[3] Modulo the issue of showing the existence of the limits in the determinantal representations and making sense of the formal integrals in the integral representation. The existence of the limits are supported by direct numerical calculations in §4.4.

integral representation, which we leave for future work.

- The correlation matrix method for free fermions has been generalized to continuum in cyclic cases (i.e., Rényi entropies) in [CH09; ACHP18] by generalizing the correlation matrix to an integral kernel and finding its spectrum and eigenfunctions. It would be interesting to understand if the non-abelian cases studied here can also be directly studied in the continuum using integral kernels.

- The relation between isomonodromic tau functions and CFT is also studied in [GIL12; ILT15; GM16; GIL19], where the tau functions studied here are conjectured to be related to W_N conformal blocks. To the best of our knowledge, the relation has not been made precise for the class of tau functions considered here due to technicalities in W_N conformal blocks. The modular Hamiltonian approach for isomonodromic tau functions initiated here might also shed more light on the CFT/isomonodromy correspondence.

Structure of the chapter. In §4.2, we discuss the general structures of TOC/tau functions and argue the approximate factorization property. In §4.3, we review the correlation matrix method for free fermions and derive the determinantal representation. In §4.4, we provide non-trivial checks of the determinantal representation and the approximate factorization property in several two-interval examples. In §4.5, we derive the formal integral representation and discuss some subtleties in the continuum modular Hamiltonian approach.

4.2. General structures and the approximate factorization property

In this section, we first discuss the general structures of TOC/tau functions and set up some notations used throughout the chapter. We then argue an approximate factorization property of a class of TOC/tau functions utilizing known correlation structure of the ground state of large-c holographic CFTs and the universality of genus-zero TOCs.

4.2.1. General structures of TOCs and tau functions

Two intervals

Recall the class of four-point TOCs mentioned in the introduction:

$$\begin{aligned}
&\mathcal{Z}_{(n_1,n_2)} = \left|\tau_{(n_1,n_2)}\right|^{2c} = \mathrm{Tr}\left[\rho_R\left(\rho_{R_1}^{n_1-1}\otimes\rho_{R_2}^{n_2-1}\right)\right] = \left\langle \rho_{R_1}^{n_1-1}\rho_{R_2}^{n_2-1}\right\rangle \\
&\sigma_1 = \sigma_2^{-1} = (1\cdots n_1), \quad \sigma_3 = \sigma_4^{-1} = (1\ n_1+1\cdots n_1+n_2-1) \\
&R = R_1\cup R_2, \quad R_i = (z_{2i-1}, z_{2i}).
\end{aligned} \tag{4.2.1}$$

where $\langle\cdot\rangle$ denotes ground state expectation value.

The tau function can be thought of as the holomorphic part of the $c=1$ four-point genus zero TOC; in general, four-point functions in CFT only contain non-trivial dependence on cross-ratio:

$$\begin{aligned}
\tau_{(n_1,n_2)}(\boldsymbol{z}) &= \mathcal{L}_{(n_1,n_2)}(\boldsymbol{z})\,\mathcal{T}_{(n_1,n_2)}(x) \coloneqq \prod_{i<j} z_{ij}^{\frac{h}{3}-h_i-h_j}\mathcal{T}_{(n_1,n_2)}(x), \quad x=\frac{z_{12}z_{34}}{z_{13}z_{24}} \\
&= z_{12}^{-\frac{4}{3}\hat{h}_{n_1}+\frac{2}{3}\hat{h}_{n_2}} z_{34}^{\frac{2}{3}\hat{h}_{n_1}-\frac{4}{3}\hat{h}_{n_2}} \left(z_{13}z_{14}z_{23}z_{24}\right)^{-\frac{1}{3}\left(\hat{h}_{n_1}+\hat{h}_{n_2}\right)} \mathcal{T}_{(n_1,n_2)}(x)
\end{aligned} \tag{4.2.2}$$

where $h=\sum_i h_i = 2\hat{h}_{n_1}+2\hat{h}_{n_2}$, and

$$\hat{h}_n = \frac{1}{24}\left(n-n^{-1}\right) \tag{4.2.3}$$

is the twist operator dimension with unit central charge. We denote the twist operator dimension for generic central charge by

$$h_n = c\hat{h}_n. \tag{4.2.4}$$

In some cases it is convenient to consider the tau function in special configuration $\boldsymbol{z}=(0,x,1,\infty)$:

$$\begin{aligned}
\tau_{(n_1,n_2)}(x) &\coloneqq \lim_{\boldsymbol{z}\to(0,x,1,\infty)} z_4^{2h_4}\tau_{(n_1,n_2)}(\boldsymbol{z}) \\
&= x^{-\frac{4}{3}\hat{h}_{n_1}+\frac{2}{3}\hat{h}_{n_2}}(1-x)^{-\frac{1}{3}\left(\hat{h}_{n_1}+\hat{h}_{n_2}\right)}\mathcal{T}_{(n_1,n_2)}(x).
\end{aligned} \tag{4.2.5}$$

Multi-intervals

We also consider the following more general class of genus-zero TOCs:

$$\mathcal{Z}_{(n_1,\cdots,n_r)} = \left|\tau_{(n_1,\cdots,n_r)}\right|^{2c} \coloneqq \mathrm{Tr}\left[\rho_R\left(\bigotimes_{i=1}^{r}\rho_{R_i}^{n_i-1}\right)\right] = \left\langle\prod_{i=1}^{r}\rho_{R_i}^{n_i-1}\right\rangle$$
$$R = \bigcup_{i=1}^{r} R_i = \bigcup_{i=1}^{r}(a_i,b_i) = \bigcup_{i=1}^{r}(z_{2i-1},z_{2i}). \tag{4.2.6}$$

The monodromies of the associated branched cover can be easily read off from the density matrix representation. In particular, the monodromies at endpoints of each interval R_i are n_i cycles, with different cycles for all the r intervals having only one common sheet index (i.e., the one corresponding to ρ_R).

The $2r$-point tau function now depends on $2r-3$ cross ratios:

$$\begin{aligned}\tau_{(n_1,\cdots n_r)}(\boldsymbol{z}) &= \mathcal{L}_{(n_1,\cdots,n_r)}(\boldsymbol{z})\,\mathcal{T}_{(n_1,\cdots,n_r)}(\boldsymbol{x})\\ &\coloneqq z_{ij}^{\delta_{ij}}\mathcal{T}_{(n_1,\cdots,n_r)}(\boldsymbol{x})\end{aligned} \tag{4.2.7}$$

with

$$\delta_{ij} = \frac{2}{2r-2}\left(\frac{\sum_k h_k}{2r-1} - h_i - h_j\right), \quad h_{2i-1} = h_{2i} = \hat{h}_{n_i}, \quad x_i = \frac{(z_i - z_{2r-2})(z_{2r-1}-z_{2r})}{(z_i-z_{2r-1})(z_{2r-2}-z_{2r})}. \tag{4.2.8}$$

4.2.2. Approximate factorization

Ground state correlation structure in large-c holographic CFTs

In quantum information theory, the amount of correlation between two subsystems R_1, R_2 can be measured by the mutual information between them. The mutual information is defined as

$$I(R_1:R_2) = S(R_1) + S(R_2) - S(R) = S_{\mathrm{rel}}(\rho_R|\rho_{R_1}\otimes\rho_{R_2}) \tag{4.2.9}$$

where $S(R)$ is the von Neumann entropy/entanglement entropy and S_{rel} the relative entropy. As the relative entropy is a distinguishability measure, the formulation of mutual information in terms of the relative entropy, i.e., as the distinguishability from a de-correlated state, makes

manifest its information-theoretic meaning as a correlation measure. In particular,

$$I(R_1 : R_2) = 0 \iff \rho_R = \rho_{R_1} \otimes \rho_{R_2}, \tag{4.2.10}$$

i.e., mutual information vanishes iff the state factorizes.

In large-c holographic CFTs, the mutual information in ground state ρ_R between R_1 and R_2 is known to vanish to leading order in central charge in a specific kinematic regime:

$$I(R_1 : R_2) = \begin{cases} \mathcal{O}(c^0) & x \in \left(0, \frac{1}{2}\right) \\ \frac{c}{3} \log\left(\frac{x}{1-x}\right) & x \in \left(\frac{1}{2}, 1\right) \end{cases}, \tag{4.2.11}$$

with a phase transition at $x = \frac{1}{2}$. The statement can be derived using holographic entanglement entropy formula [RT06b; HRT07b] in $\mathrm{AdS}_3/\mathrm{CFT}_2$ or directly using large-c CFT method [Har13]. This therefore implies that

$$\rho_R \simeq \rho_{R_1} \otimes \rho_{R_2}, \quad x \in \left(0, \frac{1}{2}\right) \text{ for large } c \text{ holographic CFT}. \tag{4.2.12}$$

Implication for TOC/tau functions

Now first consider the genus-zero TOCs $\mathcal{Z}_{(n_1,n_2)}$ in large-c holographic CFT. In light of the density matrix interpretation of $\mathcal{Z}_{(n_1,n_2)}$ and the approximate factorization of ρ_R in disconnected phase, we have

$$\begin{aligned} &\mathcal{Z}_{(n_1,n_2)}(\boldsymbol{z}) \simeq \mathcal{Z}^{\text{fac.}}_{(n_1,n_2)}(\boldsymbol{z}), \quad x \in \left(0, \frac{1}{2}\right) \text{ for large } c \text{ holographic CFT} \\ &\mathcal{Z}^{\text{fac.}}_{(n_1,n_2)}(\boldsymbol{z}) \coloneqq \mathcal{Z}_{(n_1)}(z_1, z_2)\mathcal{Z}_{(n_2)}(z_3, z_4), \quad \mathcal{Z}_{(n)}(z_1, z_2) = |z_{12}|^{-4h_n}. \end{aligned} \tag{4.2.13}$$

However, since the genus-zero TOCs $\mathcal{Z}_{(n_1,n_2)}$ have trivial dependence on central charge, we expect that the factorization approximation holds universally at the level of tau functions:

$$\begin{aligned} &\tau_{(n_1,n_2)}(\boldsymbol{z}) \simeq \tau^{\text{fac.}}_{(n_1,n_2)}(\boldsymbol{z}), \quad x \in \left(0, \frac{1}{2}\right) \\ &\tau^{\text{fac.}}_{(n_1,n_2)}(\boldsymbol{z}) \coloneqq \tau_{(n_1)}(z_1, z_2)\tau_{(n_2)}(z_3, z_4), \quad \tau_{(n)}(z_1, z_2) = z_{12}^{-2\hat{h}_n}, \end{aligned} \tag{4.2.14}$$

and furthermore that the restriction $x \in \left(0, \frac{1}{2}\right)$ can be relaxed as no phase transition is expected for tau functions. The factorized tau function $\tau^{\text{fac.}}_{(n_1,n_2)}$ corresponds to having the following cross-ratio dependent part:

$$\mathcal{T}^{\text{fac.}}_{(n_1,n_2)}(x) = \left(\frac{1-x}{x^2}\right)^{\frac{1}{3}\left(\hat{h}_{n_1}+\hat{h}_{n_2}\right)}. \tag{4.2.15}$$

We therefore have the following statement:

Claim 4.2.1 (Approximate factorization of tau functions)**.** *There exists* $x^* \in \left(\frac{1}{2}, 1\right)$ *such that* $\forall x \in (0, x^*)$,

$$\left|\frac{\mathcal{T}_{(n_1,n_2)}(x)}{\mathcal{T}^{\text{fac.}}_{(n_1,n_2)}(x)}\right| = 1 + \epsilon, \quad |\epsilon| \ll 1. \tag{4.2.16}$$

Remark 4.2.1. In general, the TOC/tau functions satisfy the factorization limit

$$\lim_{x\to 0} \mathcal{T}_{(n_1,n_2)}(x) = \mathcal{T}^{\text{fac.}}_{(n_1,n_2)}(x), \tag{4.2.17}$$

which can be used to fix the normalization of $\mathcal{T}_{(n_1,n_2)}(x)$. That the factorization should approximately hold in a finite range of cross-ratio is a non-trivial statement.

4.3. TOCs and tau functions from correlation matrices

In this section, we derive determinantal representations for TOC/tau functions using the correlation matrix method for free fermions. The correlation matrix method is first developed in [Pes03]; more details specific to discretization of free fermion CFT can be found in, e.g., [BC20].

4.3.1. Correlation matrix method for free fermion

Consider a theory of $\mathcal{N}$ fermions with algebra

$$\{\psi_i, \psi_j^\dagger\} = \delta_{ij}, \quad i = 1, \cdots, \mathcal{N} \tag{4.3.1}$$

and a quadratic Hamiltonian

$$\hat{H} = \sum_{i,j} \psi_i^\dagger M_{ij} \psi_j = \sum_i \lambda_i c_i^\dagger c_i, \quad \{c_i, c_j^\dagger\} = \delta_{ij} \tag{4.3.2}$$

where $\mathbf{M} = \mathbf{V}^\dagger \boldsymbol{\lambda} \mathbf{V}$ is a Hermitian matrix and $c_i = V_{ij}\psi_j, c_i^\dagger = \psi_j^\dagger \left(V^\dagger\right)_{ji}$.

The ground state is defined to be the state where negative energy modes are occupied and positive energy modes unoccupied:

$$c_i^\dagger |0\rangle = 0 \quad \text{for} \quad \lambda_i < 0, \qquad c_i |0\rangle = 0 \quad \text{for} \quad \lambda_i > 0. \tag{4.3.3}$$

Denote the ground state two-point function as

$$\mathsf{C}_{ij} = \left\langle \psi_i \psi_j^\dagger \right\rangle, \tag{4.3.4}$$

and it follows that

$$\mathsf{C} = \mathbf{V}^\dagger \theta(\boldsymbol{\lambda}) \mathbf{V} \tag{4.3.5}$$

where $\theta(\boldsymbol{\lambda})$ is diagonal with diagonal entries being ones for positive energy modes and zeros for negative energy modes.

We will be interested in the free fermion 2d CFT with Hamiltonian $-\frac{i}{2}\int dx \left(\psi^\dagger \partial\psi - \partial\psi^\dagger \psi\right)$, and therefore the discretized Hamiltonian

$$\begin{aligned} \hat{H} &= -\frac{i}{2}\sum_j \psi_j^\dagger \psi_{j+1} - \psi_{j+1}^\dagger \psi_j \\ M_{jl} &= -\frac{i}{2}\left(\delta_{l,j+1} - \delta_{l,j-1}\right). \end{aligned} \tag{4.3.6}$$

The corresponding correlation matrix is given by

$$\mathsf{C}_{jl} = \begin{cases} \frac{(-1)^{j-l}-1}{2\pi i(j-l)} & j \neq l \\ \frac{1}{2} & j = l. \end{cases} \tag{4.3.7}$$

Let R be a subset of the $\mathcal{N}$ indices, and define the correlation kernel by restriction to R:

$$(\mathsf{C}_R)_{ij} \coloneqq \mathsf{C}_{ij}|_{i,j\in R}. \tag{4.3.8}$$

Let ρ_R be the density matrix of R with a quadratic modular Hamiltonian given by a modular

Hamiltonian kernel H_R:

$$\rho_R = \mathcal{N}_R^{-1} e^{-\mathcal{Q}(\mathsf{H}_R)}, \quad \mathcal{Q}(\mathsf{H}_R) \coloneqq \sum_{i,j\in R} \psi_i^\dagger (\mathsf{H}_R)_{ij} \psi_j$$
$$\mathcal{N}_R = \operatorname{Tr} e^{-\mathcal{Q}(\mathsf{H}_R)} = \det\left(\mathbb{1} + e^{-\mathsf{H}_R}\right). \tag{4.3.9}$$

Requiring

$$(\mathsf{C}_R)_{ij} = \operatorname{Tr}\left(\rho_R \psi_i \psi_j^\dagger\right)|_{i,j\in R} \tag{4.3.10}$$

leads to following relation between modular Hamiltonian kernel and correlation kernel:

$$e^{-\mathsf{H}_R} = \mathsf{C}_R^{-1} - \mathbb{1}. \tag{4.3.11}$$

The relation allows one to write Rényi entropies directly in terms of correlation kernel. For example, the N^{th} Rényi entropy can be written as:

$$\operatorname{Tr}\rho_R^N = \frac{\det\left(\mathbb{1} + e^{-N\mathsf{H}_R}\right)}{\det^N\left(\mathbb{1} + e^{-\mathsf{H}_R}\right)} = \det\left((\mathbb{1} - \mathsf{C}_R)^N + \mathsf{C}_R^N\right). \tag{4.3.12}$$

For more general density matrix correlators involving different density matrices, the computation is facilitated by the fact, as can be verified using free fermion algebra, that the quadratic modular Hamiltonian $\mathcal{Q}(\mathsf{H}_R)$ gives a representation of matrix algebra

$$\left[\mathcal{Q}\left(\mathsf{H}_R^{(1)}\right), \mathcal{Q}\left(\mathsf{H}_R^{(2)}\right)\right] = \mathcal{Q}\left(\left[\mathsf{H}_R^{(1)}, \mathsf{H}_R^{(2)}\right]\right), \tag{4.3.13}$$

from which it follows that

$$e^{-\mathcal{Q}\left(\mathsf{H}_R^{(1)}\right)} e^{-\mathcal{Q}\left(\mathsf{H}_R^{(2)}\right)} = e^{-\mathcal{Q}\left(\mathsf{H}_R^{(3)}\right)}$$
$$e^{-\mathsf{H}_R^{(1)}} e^{-\mathsf{H}_R^{(2)}} = e^{-\mathsf{H}_R^{(3)}}. \tag{4.3.14}$$

The property above is also used in other contexts such as [BGZ14; CMST18]. In the following, we compute the density matrix correlators in (4.2.1) by taking advantage of this property.

4.3.2. Relation with TOCs and tau functions

Two intervals

For the density matrix correlators associated with the class of four-point TOC/tau functions in (4.2.1), we have

$$\begin{aligned}
&\mathrm{Tr}\left[\rho_R\left(\rho_{R_1}^{n_1-1}\otimes\rho_{R_2}^{n_2-1}\right)\right]\\
&=\det\left(\mathsf{C}_R\right)\det\left(\mathsf{C}_{R_1}\right)^{n_1-1}\det\left(\mathsf{C}_{R_2}\right)^{n_2-1}\mathrm{Tr}\left(e^{-\mathcal{Q}(\mathsf{H}_R)}e^{-\mathcal{Q}\left[(n_1-1)\mathsf{H}_{R_1}\oplus(n_2-1)\mathsf{H}_{R_2}\right]}\right)\\
&=\det\left(\mathsf{C}_R\right)\det\left(\mathsf{C}_{R_1}\right)^{n_1-1}\det\left(\mathsf{C}_{R_2}\right)^{n_2-1}\det\left[\mathbb{1}+e^{-\mathsf{H}_R}\left(e^{-(n_1-1)\mathsf{H}_{R_1}}\oplus e^{-(n_2-1)\mathsf{H}_{R_2}}\right)\right]\\
&=\det\left(\mathsf{C}_R\right)\det\left(\mathsf{C}_{R_1}^{n_1-1}\oplus\mathsf{C}_{R_2}^{n_2-1}\right)\det\left\{\mathbb{1}+\left(\mathsf{C}_R^{-1}-\mathbb{1}\right)\left[\left(\mathsf{C}_{R_1}^{-1}-\mathbb{1}\right)^{n_1-1}\oplus\left(\mathsf{C}_{R_2}^{-1}-\mathbb{1}\right)^{n_2-1}\right]\right\}\\
&=\det\left(\mathsf{M}_{R_1,R_2}^{(n_1,n_2)}\right),
\end{aligned}\tag{4.3.15}$$

with

$$\mathsf{M}_{R_1,R_2}^{(n_1,n_2)}\coloneqq\mathsf{C}_R\left(\mathsf{C}_{R_1}^{n_1-1}\oplus\mathsf{C}_{R_2}^{n_2-1}\right)+\bar{\mathsf{C}}_R\left(\bar{\mathsf{C}}_{R_1}^{n_1-1}\oplus\bar{\mathsf{C}}_{R_2}^{n_2-1}\right),\quad\bar{\mathsf{C}}\coloneqq\mathbb{1}-\mathsf{C},\tag{4.3.16}$$

where we have used relations in (4.3.9), (4.3.11) and (4.3.14).

Now let R_1,R_2 be intervals with sizes l_1,l_2, respectively, and their separation being d. In terms of discrete indices on lattice, this corresponds to $R_1=\{1,\cdots,l_1+1\}$, $R_2=\{l_1+d+1,\cdots,l_1+l_2+d+1\}$; the total number of fermions is $\mathcal{N}=l_1+l_2+d+1$, and $\mathsf{M}_{R_1,R_2}^{(n_1,n_2)}$ is a l_1+l_2+2 dimensional square-matrix. For this configuration, the leg factor and cross-ratio read:

$$\begin{aligned}
&\mathcal{L}_{(n_1,n_2)}(l_1,l_2,d)=l_1^{-\frac{4}{3}\hat{h}_{n_1}+\frac{2}{3}\hat{h}_{n_2}}l_2^{\frac{2}{3}\hat{h}_{n_1}-\frac{4}{3}\hat{h}_{n_2}}\left(d\,(l_1+d)\,(l_2+d)\,(l_1+l_2+d)\right)^{-\frac{1}{3}\left(\hat{h}_{n_1}+\hat{h}_{n_2}\right)},\\
&x(l_1,l_2,d)=\frac{l_1l_2}{(l_1+d)(l_2+d)}.
\end{aligned}\tag{4.3.17}$$

Due to the doubling of degree of freedom on lattice (cf., e.g., [BC20]), the density matrix correlators computed using correlation matrices above in fact correspond to $c=1$ instead of $c=\frac{1}{2}$ TOCs. Recalling the general structure of TOC/tau functions discussed in §4.2.1, we can therefore extract the non-trivial part of TOC/tau functions $\mathcal{T}_{(n_1,n_2)}(x)$ as follows:

Claim 4.3.1 (Determinantal representation of tau functions, two intervals)**.** *The non-trivial part of the class of TOC/tau functions in* (4.2.1) *are related to the continuum limit of the determinant of free fermion correlation matrices by*

$$\left|\mathcal{T}_{(n_1,n_2)}(x)\right|^2 = \lim_{\substack{l_1,l_2,d\to\infty \\ x(l_1,l_2,d) \text{ fixed}}} \mathcal{L}^{-2}_{(n_1,n_2)}(l_1,l_2,d) \det\left(\mathsf{M}^{(n_1,n_2)}_{R_1,R_2}\right) \tag{4.3.18}$$

where the equality is understood to hold up to x-independent overall constant.

Multi-interval

The generalization to the $2r$-point TOC and tau functions in (4.2.6) involving r-intervals is straightforward, and we simply state the result. We now consider r intervals R_i each with sizes l_i, with the separation between R_i and R_{i+1} being d_i. We can again translate the set-up to lattice similar to the two-interval case with l_i, d_i being integers and R_i being subsets of $\{1,\cdots\mathcal{N}\}$ with $\mathcal{N} = \sum_i l_i + \sum_i d_i + r - 1$. The associated leg factor $\mathcal{L}_{(n_1,\cdots,n_r)}(\boldsymbol{l},\boldsymbol{d})$ and cross-ratios $\boldsymbol{x}(\boldsymbol{l},\boldsymbol{d})$ can be easily determined from the general discussion in §4.2.1. Define the following $\sum_i l_i + r$-dimensional square matrix from correlation matrices:

$$\mathsf{M}^{(n_1,\cdots,n_r)}_{R_1,\cdots R_r} := \mathsf{C}_R\left(\bigoplus_{i=1}^{r}\mathsf{C}^{n_i-1}_{R_i}\right) + \bar{\mathsf{C}}_R\left(\bigoplus_{i=1}^{r}\bar{\mathsf{C}}^{n_i-1}_{R_i}\right). \tag{4.3.19}$$

The multi-interval generalization of our statement reads:

Claim 4.3.2 (Determinantal representation of tau functions, multi-interval.)**.** *The non-trivial part of the class of TOC/tau functions in* (4.2.6) *are related to the continuum limit of the determinant of free fermion correlation matrices by*

$$\left|\mathcal{T}_{(n_1,\cdots,n_r)}(\boldsymbol{x})\right|^2 = \lim_{\substack{\boldsymbol{l},\boldsymbol{d}\to\infty \\ \boldsymbol{x}(\boldsymbol{l},\boldsymbol{d}) \text{ fixed}}} \mathcal{L}^{-2}_{(n_1,\cdots,n_r)}(\boldsymbol{l},\boldsymbol{d}) \det\left(\mathsf{M}^{(n_1,\cdots,n_r)}_{R_1,\cdots,R_r}\right) \tag{4.3.20}$$

where the equality is understood to hold up to $\boldsymbol{x}$-independent overall constant.

4.4. Examples

In this section, we provide non-trivial checks of our claims 4.2.1 and 4.3.1 in several examples of two intervals. In the case of $n_1 = n_2 = 2$, the exact TOC/tau function is known analytically,

and we will verify both claims 4.2.1 and 4.3.1 explicitly. For other examples of two intervals, we don't have the explicit knowledge of exact TOC/tau functions. Instead, in those examples, we will assume the validity of the claim 4.3.1 to verify the claim 4.2.1 by comparing $\mathcal{T}^{\text{fac.}}_{(n_1,n_2)}(x)$ with lattice data.

4.4.1. $n_1 = n_2 = 2$

The monodromy data in this case is given by

$$\sigma_1 = \sigma_2 = (12), \quad \sigma_3 = \sigma_4 = (13). \tag{4.4.1}$$

The associated tau function has known exact expression [GM16] in the special configuration $\boldsymbol{z} = (0, x, 1, \infty)$ (derivation reviewed in §4.A):

$$\begin{aligned}
\tau_{(2,2)}(x) &= \frac{(3-\alpha)^{\frac{1}{3}}}{\sqrt{2}\,(1-\alpha)^{\frac{1}{8}}\left(\alpha\,(3+\alpha)\right)^{\frac{1}{24}}}, \quad x = \frac{(3+\alpha)^3\,(1-\alpha)}{(3-\alpha)^3\,(1+\alpha)}, \quad \alpha \in (0,1) \\
\mathcal{T}_{(2,2)}(x) &= (x(1-x))^{\frac{1}{24}}\,\tau_{(2,2)}(x).
\end{aligned} \tag{4.4.2}$$

The factorization approximation is given by

$$\begin{aligned}
\tau^{\text{fac.}}_{(2,2)}(x) &= x^{-\frac{1}{8}} \\
\mathcal{T}^{\text{fac.}}_{(2,2)}(x) &= (x(1-x))^{\frac{1}{24}}\,\tau^{\text{fac.}}_{(2,2)}(x) = \left(\frac{1-x}{x^2}\right)^{\frac{1}{24}}.
\end{aligned} \tag{4.4.3}$$

The normalization in $\mathcal{T}_{(2,2)}(x)$ was fixed by the factorization limit $\lim_{x\to 0}\mathcal{T}_{(2,2)}(x) = \mathcal{T}^{\text{fac.}}_{(2,2)}(x)$.

Verification of claim 4.2.1. The correction to $\mathcal{T}^{\text{fac.}}_{(2,2)}(x)$ in the exact tau function $\mathcal{T}_{(2,2)}(x)$ is quite small for finite x; the small cross-ratio expansion of $\mathcal{T}_{(2,2)}(x)$ reads:

$$\frac{\mathcal{T}_{(2,2)}(x)}{\mathcal{T}^{\text{fac.}}_{(2,2)}(x)} = 1 + \frac{1}{2^9}x^2 + \frac{1}{2^9}x^3 + \frac{3^2\cdot 103}{2^{19}}x^4 + \cdots \tag{4.4.4}$$

At $x = \frac{1}{2}$, the deviation from factorization approximation is

$$\frac{\mathcal{T}_{(2,2)}(\frac{1}{2})}{\mathcal{T}^{\text{fac.}}_{(2,2)}(\frac{1}{2})} \simeq 1 + 9.3 \times 10^{-4}. \tag{4.4.5}$$

The comparison between $\mathcal{T}_{(2,2)}(x)$ and $\mathcal{T}^{\text{fac.}}_{(2,2)}(x)$ in the full range of cross-ratio is given in Fig. 4.1. The deviation from factorization approximation increases with cross-ratio x, and the error is around 1% for $x \simeq .9$. This verifies the approximate factorization property in the claim 4.2.1 for the $n_1 = n_2 = 2$ case.

Verification of claim 4.3.1. The comparison between lattice data and $\mathcal{T}_{(2,2)}(x)$ is given in Fig. 4.2. The lattice data compute (the logarithm of) RHS of (4.3.18). Each data point with a particular cross-ratio x is computed by choosing l_1, l_2, d as described in §4.3.2 and increasing their sizes while keeping x fixed until convergence is reached. An overall shift in $\log \mathcal{T}_{(2,2)}(x)$ is required to match the lattice data. We observe very good agreement between the exact expression for tau function $\mathcal{T}_{(2,2)}(x)$ and our lattice data. This verifies the determinantal representation of TOC/tau functions in claim 4.3.1 for the $n_1 = n_2 = 2$ case.

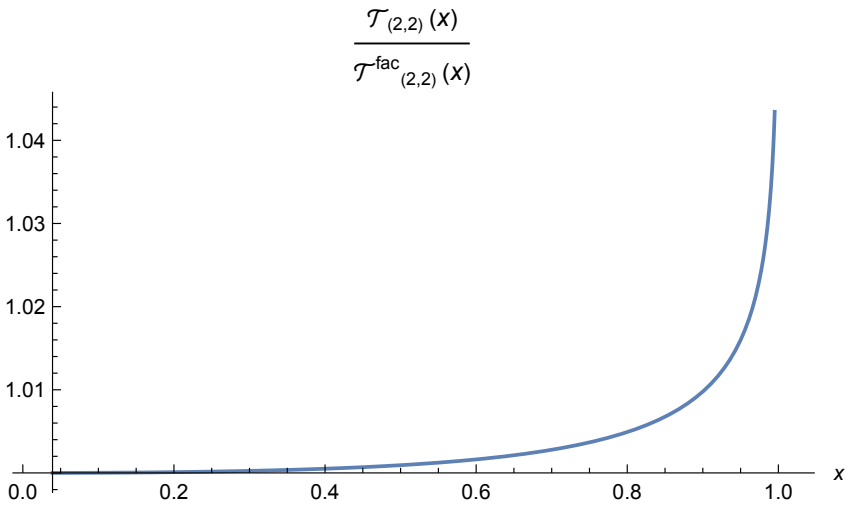

Figure 4.1.: Comparison between $\mathcal{T}_{(2,2)}(x)$ and $\mathcal{T}^{\text{fac.}}_{(2,2)}(x)$. The deviation from factorization approximation increases with cross-ratio x, and the error is around 1% for $x \simeq .9$. This verifies the approximate factorization property in the claim 4.2.1 for the $n_1 = n_2 = 2$ case.

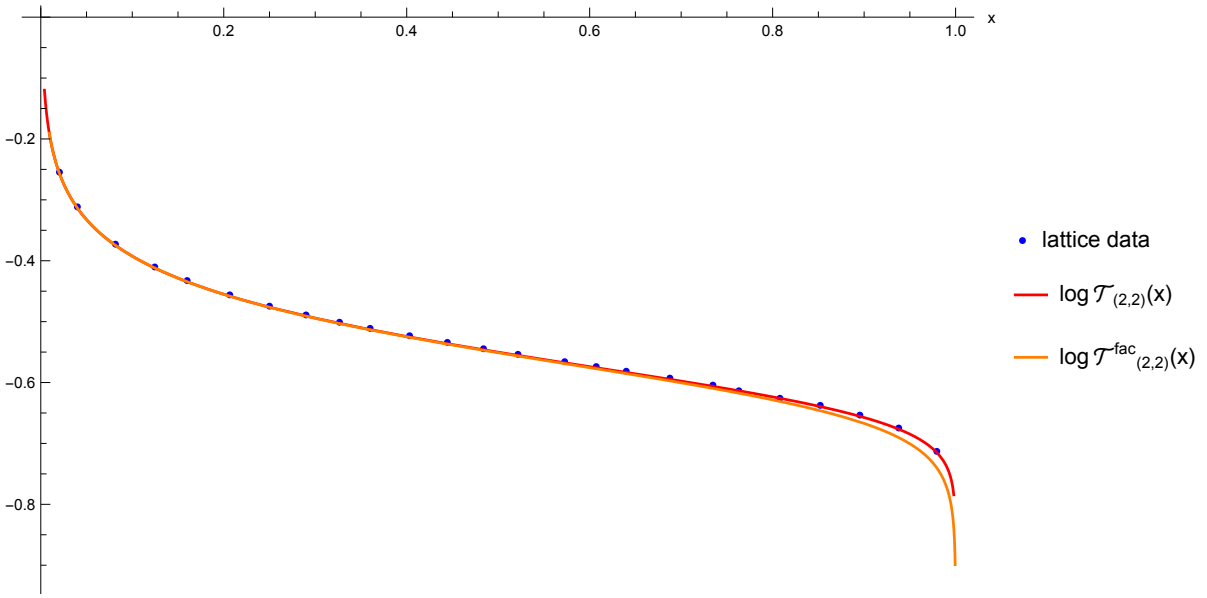

Figure 4.2.: Comparison between lattice data and $\mathcal{T}_{(2,2)}(x)$. The lattice data compute (the logarithm of) RHS of (4.3.18). An overall shift in $\log \mathcal{T}_{(2,2)}(x)$ is required to match the lattice data. We observe very good agreement between the exact expression for tau function $\mathcal{T}_{(2,2)}(x)$ and our lattice data. This verifies the determinantal representation of TOC/tau functions in claim 4.3.1 for the $n_1 = n_2 = 2$ case.

4.4.2. Other two-interval examples

Here we consider two other two-interval examples, with $(n_1, n_2) = (3, 2), (3, 3)$. As we don't know the exact TOC/tau functions in those cases, we will assume the validity of claim 4.3.1 that the lattice data compute the exact tau function $\mathcal{T}_{(n_1,n_2)}(x)$ and compare the factorized approximation $\mathcal{T}^{\text{fac.}}_{(n_1,n_2)}(x)$ with the lattice data. In the two examples, the factorized tau functions read:

$$\mathcal{T}^{\text{fac.}}_{(3,2)}(x) = \left(\frac{1-x}{x^2}\right)^{\frac{25}{432}},$$
$$\mathcal{T}^{\text{fac.}}_{(3,3)}(x) = \left(\frac{1-x}{x^2}\right)^{\frac{2}{27}}. \tag{4.4.6}$$

The comparisons between the factorized TOC/tau functions and lattice data are given in Fig.4.3. The lattice data are computed similarly to the case $(n_1, n_2) = (2, 2)$. The overall shifts in $\log \mathcal{T}^{\text{fac.}}_{(n_1,n_2)}(x)$ needed to compare with lattice data are determined by the factorization limit, i.e., by matching $\log \mathcal{T}^{\text{fac.}}_{(n_1,n_2)}(x)$ with lattice data at small cross-ratios. In both cases, we observe that, similar to the $(n_1, n_2) = (2, 2)$ case, the factorized tau functions give good approximation to lattice data in an extended range of cross ratio. This gives more evidence to the claim 4.2.1.

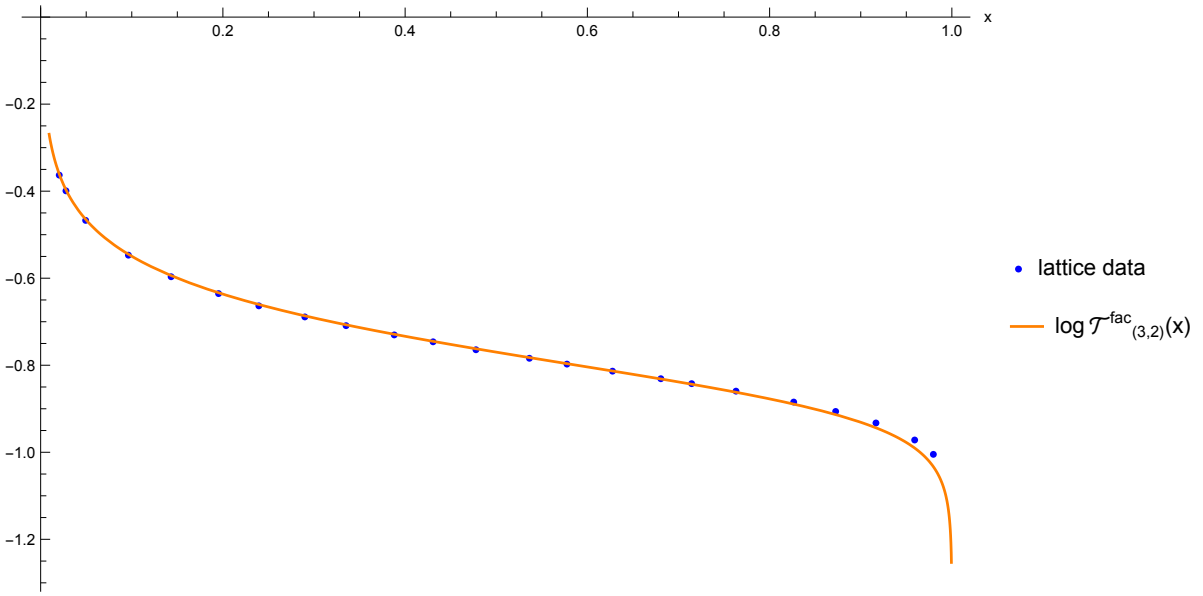

(a) $(n_1, n_2) = (3, 2)$.

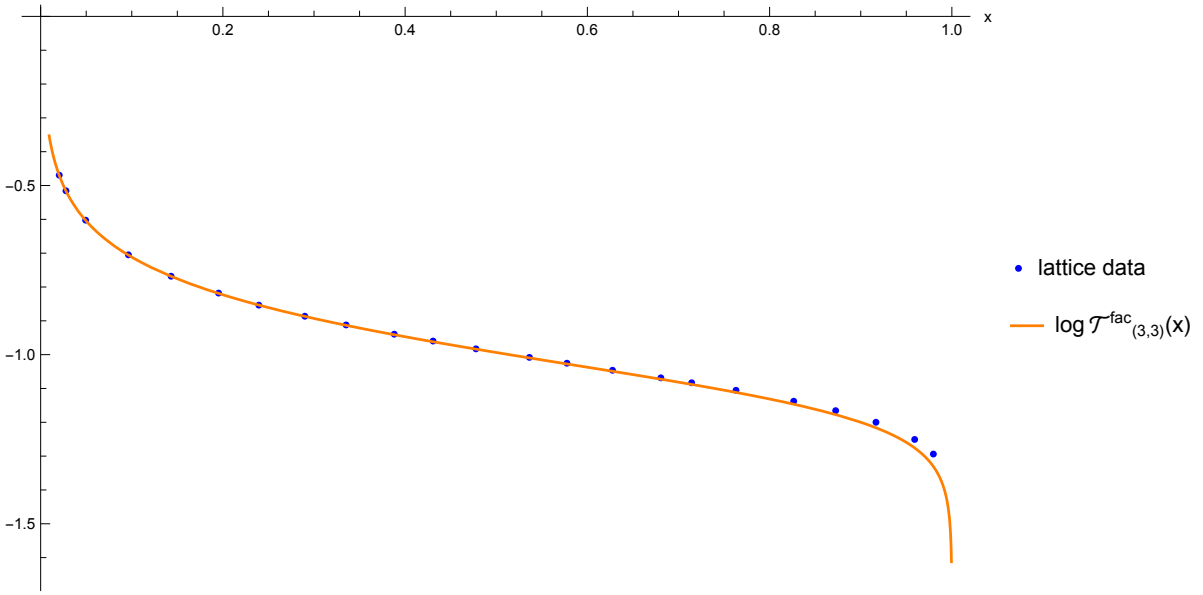

(b) $(n_1, n_2) = (3, 3)$.

Figure 4.3.: The comparisons between the factorized TOC/tau functions and lattice data in cases $(n_1, n_2) = (3, 2), (3, 3)$. The overall shifts in $\log \mathcal{T}^{\text{fac.}}_{(n_1,n_2)}(x)$ needed to compare with lattice data are determined by the factorization limit. In both cases, we observe that the factorized tau functions give good approximation to lattice data in an extended range of cross ratio. This gives more evidence to the claim 4.2.1.

4.5. Towards a representation from continuum modular Hamiltonian

In this section, we study TOC/tau functions using the continuum expression for modular Hamiltonian of single interval [BW76; CHM11; CT16]. This results in a formal integral representation in terms of integrated stress-tensor correlators for the class of TOC/tau functions in

(4.2.1). We leave more careful study for certain subtleties/technicalities for future work.

Note. It is understood that the expressions for TOCs in this section are only their holomorphic parts.

4.5.1. Generalities

As mentioned in the introduction, the class of TOCs in (4.2.1) can in principle be computed from the universal expression for single-interval modular Hamiltonian $\mathcal{H}_{R_i}$:

$$\begin{aligned}
&\rho_{R_i} \propto e^{-\mathcal{H}_{R_i}}, \quad R_i = (a_i, b_i) \\
&\mathcal{H}_{R_i} = \int_{R_i} dz \frac{(z-a_i)(z-b_i)}{b_i - a_i} T(z) + \frac{c}{6} \log \frac{b_i - a_i}{\epsilon} \mathbb{1} + \text{anti-holo.}.
\end{aligned} \tag{4.5.1}$$

where the constant term in $\mathcal{H}_{R_i}$ is fixed by requiring the von Neumann entropy $S(R_i) = \langle \mathcal{H}_{R_i} \rangle$ has the known answer $S(R_i) = \frac{c}{3} \log \frac{b_i - a_i}{\epsilon}$. For convenience we write

$$\begin{aligned}
&\rho_{R_i} = (b_i - a_i)^{-\frac{c}{6}} e^{\mathcal{K}_{R_i}} \times \text{anti-holo.} \\
&\mathcal{K}_{R_i} = \int_{R_i} dz \beta_i(z) T(z), \quad \beta_i(z) \coloneqq \frac{(z-a_i)(z-b_i)}{a_i - b_i}.
\end{aligned} \tag{4.5.2}$$

The quantity $\beta_i(z)$ is sometimes referred to as "entanglement temperature" in literature.

The density matrix correlators in (4.2.1) can then be evaluated as sum of integrated stress-tensor correlators, which are fixed by the Ward identity:

$$\begin{aligned}
\left\langle T(z) \prod_{i=1}^{n} T(z_i) \right\rangle &= \left(\sum_i \frac{2}{(z-z_i)^2} + \frac{\partial_{z_i}}{z - z_i} \right) \left\langle \prod_{i=1}^{n} T(z_i) \right\rangle \\
&+ \sum_i \langle T(z) T(z_i) \rangle \langle T(z_1) \cdots T(z_{i-1}) T(z_{i+1}) \cdots T(z_n) \rangle, \quad \langle T(z) T(z_i) \rangle = \frac{c/2}{(z-z_i)^4}
\end{aligned} \tag{4.5.3}$$

In other words, the Ward identity recursively defines higher-point stress-tensor correlators from the initial conditions of trivial one-point function $\langle T(z) \rangle = 0$ and two-point function $\langle T(z_1) T(z_2) \rangle = \frac{c/2}{z_{12}^4}$. The Ward identity guarantees that the recursively-defined stress-tensor

correlators have the expected structure of splitting into connected part and disconnected part:

$$\left\langle \prod_i T(z_i) \right\rangle = \left\langle \prod_i T(z_i) \right\rangle_{\text{c}} + \left\langle \prod_i T(z_i) \right\rangle_{\text{disc}} , \tag{4.5.4}$$

with connected part given by the $\mathcal{O}(c)$ term:

$$\left\langle \prod_i T(z_i) \right\rangle_{\text{c}} = \left\langle \prod_i T(z_i) \right\rangle \Big|_{\mathcal{O}(c)} . \tag{4.5.5}$$

The connected, $\mathcal{O}(c)$ parts of the stress-tensor correlators can be recursively obtained from the usual weight-two, anomaly-free part of the Ward identity:

$$\left\langle T(z) \prod_{i=1}^{n} T(z_i) \right\rangle_{\text{c}} = \left(\sum_i \frac{2}{(z-z_i)^2} + \frac{\partial_{z_i}}{z-z_i} \right) \left\langle \prod_{i=1}^{n} T(z_i) \right\rangle_{\text{c}} . \tag{4.5.6}$$

Diagrammatic notations. We introduce following convenient diagrammatic notations for stress-tensor correlators:

$$\left\langle \prod_i T(z_i) \right\rangle = \quad \left\langle \prod_i T(z_i) \right\rangle_{\text{c}} = \quad , \tag{4.5.7}$$

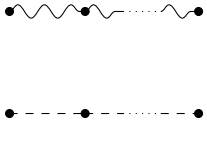

and the non-trivial part of modular Hamiltonian $\mathcal{K}_{R_i}$:

$$\mathcal{K}_{R_i} = \int_{R_i} dz \beta_i(z) T(z) = \quad . \tag{4.5.8}$$

4.5.2. Single interval

As a consistency check of the method, first consider single interval $R = (a, b)$ case where the two-point TOC is known. In this case the TOC is given by:

$$\begin{aligned} \mathcal{Z}_{(n)} &= \left\langle \rho_R^{n-1} \right\rangle = (b-a)^{-\frac{\alpha c}{6}} \left\langle e^{\alpha \mathcal{K}_R} \right\rangle, \quad \alpha = n-1 \\ \left\langle e^{\alpha \mathcal{K}_R} \right\rangle &= \sum_l \frac{\alpha^l}{l!} \left\langle \mathcal{K}_R^l \right\rangle \\ &= 1 + \sum_{l>1} \frac{\alpha^l}{l!} \end{aligned}$$

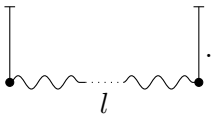

(4.5.9)

Consistency with the universal Weyl-anomaly structure of genus-zero TOCs requires the following exponentiation structure:

$$\left\langle e^{\alpha \mathcal{K}_R} \right\rangle = \exp\left(\left\langle e^{\alpha \mathcal{K}_R} \right\rangle \Big|_{\mathcal{O}(c)} \right), \tag{4.5.10}$$

or more explicitly,

$$1 + \sum_{l>1} \frac{\alpha^l}{l!}$$

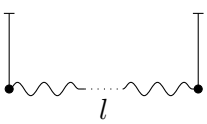

$$= \exp\left(\sum_{l>1} \frac{\alpha^l}{l!} \right.$$

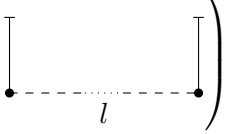

$$\left. \right).$$

(4.5.11)

The multiplicities of distinct terms on LHS equal the number of partitions of a set with size l with distinct partition structures (with partitions with size one excluded). The combinatorial structure is similar to the generating function of Bell number B_n (the number of partitions of a set of size n):

$$\sum_n \frac{B_n}{n!} x^n = e^{e^x - 1}. \tag{4.5.12}$$

For convenience, define the following notation for integrated connected stress-tensor correlator

$$\mathfrak{K}_{(l)} = \left\langle \mathcal{K}_R^l \right\rangle \Big|_{\mathcal{O}(c)} =$$

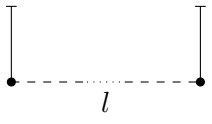

, (4.5.13)

the two-point TOC in the continuum modular Hamiltonian approach is therefore given by

$$\mathcal{Z}_{(n)} = (b-a)^{-\frac{\alpha c}{6}} \prod_{l>1} \exp\left(\frac{\alpha^l}{l!}\mathfrak{K}_{(l)}\right). \tag{4.5.14}$$

Comparing with known answer for two-point TOC

$$\mathcal{Z}_{(n)} = (b-a)^{-2h_n} = (b-a)^{-\frac{c}{12}\left(2\alpha-\alpha^2+\alpha^3-\alpha^4+\cdots\right)}, \tag{4.5.15}$$

implies that the integrated connected stress-tensor correlator should evaluate to

$$\mathfrak{K}_{(l)} = (-1)^l l!\,\frac{c}{12}\log(b-a) \tag{4.5.16}$$

where the equality is understood to hold up to cut-off in regularization of the associated integrals.

We verified by brute-force that the regularized integrals $\mathfrak{K}_{(l)}$ do agree with the expected expression above up to $l=4$, and leave more systematic checks taking advantage of the recursion structure of stress-tensor correlators for future work. However, we observe the following subtlety: the expression (4.5.14) in fact would not converge for $\alpha \geq 1$ or $n \geq 2$. The correct answer for two-point TOC is only recovered when contributions from all $\mathfrak{K}_{(l)}$ are summed in (4.5.14) for $\alpha < 1$ and then analytically continued to $\alpha \geq 1$.

4.5.3. Two intervals

For the four-point TOCs in (4.2.1), we have

$$\mathcal{Z}_{(n_1,n_2)} = \left\langle \rho_{R_1}^{n_1-1}\rho_{R_2}^{n_2-1}\right\rangle = \left(\prod_{i=1}^{2}(b_i-a_i)^{-\frac{\alpha_i c}{6}}\right)\left\langle e^{\alpha_1\mathcal{K}_{R_1}}e^{\alpha_2\mathcal{K}_{R_2}}\right\rangle, \quad \alpha_i = n_i - 1$$

$$\left\langle e^{\alpha_1\mathcal{K}_{R_1}}e^{\alpha_2\mathcal{K}_{R_2}}\right\rangle = \sum_{l_1,l_2}\frac{\alpha_1^{l_1}\alpha_2^{l_2}}{l_1!\,l_2!}\left\langle \mathcal{K}_{R_1}^{l_1}\mathcal{K}_{R_2}^{l_2}\right\rangle$$

$$= 1 + \sum_{l_1+l_2>1}\frac{\alpha_1^{l_1}\alpha_2^{l_2}}{l_1!\,l_2!}$$

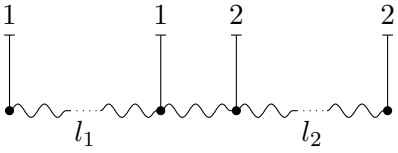

. (4.5.17)

The universal Weyl anomaly structure of genus-zero TOC again requires

$$\left\langle e^{\alpha_1 \mathcal{K}_{R_1}} e^{\alpha_2 \mathcal{K}_{R_2}} \right\rangle = \exp\left(\left\langle e^{\alpha_1 \mathcal{K}_{R_1}} e^{\alpha_2 \mathcal{K}_{R_2}} \right\rangle \Big|_{\mathcal{O}(c)} \right), \tag{4.5.18}$$

i.e., the following combinatorial structure holds:

$$1 + \sum_{l_1+l_2>1} \frac{\alpha_1^{l_1}\alpha_2^{l_2}}{l_1!\,l_2!}$$

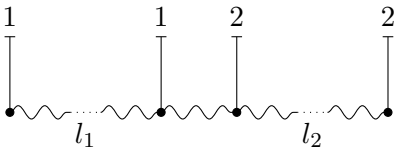

$$= \exp\left(\sum_{l_1+l_2>1} \frac{\alpha_1^{l_1}\alpha_2^{l_2}}{l_1!\,l_2!} \right.$$

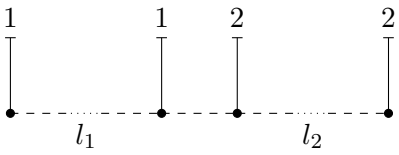

$$\left. \right). \tag{4.5.19}$$

For convenience, we now define, similar to the single interval case, the following notation for integrated connected stress-tensor correlators:

$$\mathfrak{K}_{(l_1,l_2)} \coloneqq \left\langle \mathcal{K}_{R_1}^{l_1} \mathcal{K}_{R_2}^{l_2} \right\rangle \Big|_{\mathcal{O}(c)} =$$

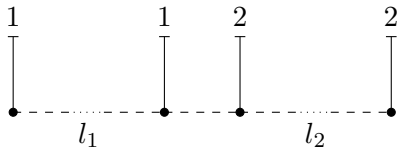

$$, \tag{4.5.20}$$

and the four-point TOC in the continuum modular Hamiltonian approach is therefore given by:

$$\mathcal{Z}_{(n_1,n_2)} = \left(\prod_{i=1}^{2} (b_i - a_i)^{-\frac{\alpha_i c}{6}} \right) \prod_{l_1+l_2>1} \exp\left\{ \frac{\alpha_1^{l_1}\alpha_2^{l_2}}{l_1!\,l_2!} \mathfrak{K}_{(l_1,l_2)} \right\}. \tag{4.5.21}$$

Interestingly, the resulting expression from the continuum modular Hamiltonian approach manifestly splits into the factorized answer and its correction: the $l_1 = 0$ and $l_2 = 0$ parts of the previous expression give $\mathcal{Z}^{\text{fac.}}_{(n_1,n_2)} \coloneqq \mathcal{Z}_{(n_1)}\mathcal{Z}_{(n_2)}$. We therefore have, for the class of four-point TOCs in (4.2.1):

$$\frac{\mathcal{Z}_{(n_1,n_2)}(\boldsymbol{z})}{\mathcal{Z}^{\text{fac.}}_{(n_1,n_2)}(\boldsymbol{z})} = \prod_{\substack{l_1+l_2>1 \\ l_1,l_2\neq 0}} \exp\left\{ \frac{\alpha_1^{l_1}\alpha_2^{l_2}}{l_1!\,l_2!} \mathfrak{K}_{(l_1,l_2)}(x) \right\}, \quad \alpha_i = n_i - 1, \quad x = \frac{z_{12}z_{34}}{z_{13}z_{24}}. \tag{4.5.22}$$

To make contact with our previous tau function notations, we define the $c = 1$ version of the

integrated stress-tensor correlators:

$$\mathfrak{T}_{(l_1,l_2)} \coloneqq \mathfrak{K}_{(l_1,l_2)}|_{c=1}, \tag{4.5.23}$$

and we have (the common leg factor has been canceled below):

$$\frac{\mathfrak{T}_{(n_1,n_2)}(x)}{\mathfrak{T}^{\text{fac.}}_{(n_1,n_2)}(x)} = \prod_{\substack{l_1+l_2>1 \\ l_1,l_2\neq 0}} \exp\left\{ \frac{\alpha_1^{l_1}\alpha_2^{l_2}}{l_1!\, l_2!}\mathfrak{T}_{(l_1,l_2)}(x) \right\}, \quad \alpha_i = n_i - 1, \quad x = \frac{z_{12}z_{34}}{z_{13}z_{24}}. \tag{4.5.24}$$

In particular, our claim 4.2.1 states that the (appropriately regularized) RHS of previous expression should be very close to one in a finite range of cross-ratio.

We have the following symmetry property for $\mathfrak{T}_{(l_1,l_2)}(x)$ due to its dependence on cross-ratio:

$$\mathfrak{T}_{(l_1,l_2)}(x) = \mathfrak{T}_{(l_2,l_1)}(x), \tag{4.5.25}$$

as the cross-ratio is unchanged after exchanging the two intervals.

We warn the reader that the integral representations for TOC/tau functions in preceding expressions involving $\mathfrak{K}_{(l_1,l_2)}$ are formal due to singularities in stress-tensor correlators at coincident insertion points, and the associated integrals need to be properly regularized. For explicit evaluation, it is enough to consider special configuration $R_1 = (0, x), R_2 = (1, \infty)$. A convenient change of variable yields:

$$\begin{aligned}
\mathfrak{K}_{(l_1,l_2)}(x) = & \int_{[0,1]^{(l_1+l_2)}} \left[\prod_{i=1}^{l_1} \hat{\beta}_1\left(\mathtt{z}_i\right) d\mathtt{z}_i\right] \left[\prod_{j=1}^{l_2} \hat{\beta}_2\left(\mathtt{w}_j\right) d\mathtt{w}_j\right] \left\langle \prod_{i=1}^{l_1} T\left(x\mathtt{z}_i\right) \prod_{j=1}^{l_2} T\left(\frac{1}{\mathtt{w}_j}\right) \right\rangle_{\text{c}} \\
& \hat{\beta}_1\left(\mathtt{z}\right) = x^2\mathtt{z}(1-\mathtt{z}), \quad \hat{\beta}_2\left(\mathtt{w}\right) = \frac{1-\mathtt{w}}{\mathtt{w}^3}.
\end{aligned} \tag{4.5.26}$$

For example,

$$\begin{aligned}\mathfrak{K}_{(1,1)}(x) &= \frac{cx^2}{2}\int\limits_{[0,1]^2} d\mathtt{z}d\mathtt{w}\frac{\mathtt{z}\,(1-\mathtt{z})\,\mathtt{w}\,(1-\mathtt{w})}{(1-x\mathtt{z}\mathtt{w})^4}\\ &= -\frac{c}{12}\left[2+\left(\frac{2}{x}-1\right)\log(1-x)\right], \qquad (4.5.27)\\ \mathfrak{K}_{(2,1)}(x) &= cx^2 \text{ reg.}\int\limits_{[0,1]^3} d\mathtt{z}_1 d\mathtt{z}_2 d\mathtt{w}\frac{\mathtt{z}_1\,(1-\mathtt{z}_1)\,\mathtt{z}_2\,(1-\mathtt{z}_2)\,\mathtt{w}\,(1-\mathtt{w})}{(\mathtt{z}_1-\mathtt{z}_2)^2\,(1-x\mathtt{z}_1\mathtt{w})^2\,(1-x\mathtt{z}_2\mathtt{w})^2}\\ &= \frac{c}{4}\left[2+\left(\frac{2}{x}-1\right)\log(1-x)\right], \qquad (4.5.28)\end{aligned}$$

where $\mathfrak{K}_{(2,1)}$ is technically divergent, and we have regularized by imposing cut-offs at end-points. The quantity $\mathfrak{K}_{(l_1,l_2)}$ at small l_i is also studied in [Lon19].

As noted in [Lon19], brute-force evaluation of $\mathfrak{K}_{(l_1,l_2)}$ quickly becomes cumbersome with increasing l_i, and we leave for future work to systematically study their properties such as proper regularization and efficient evaluation. Moreover, another concern is the convergence in the sum over l_i and whether continuation in α_i is required as in the single interval case. We also leave a careful study of the issue to future work.

It is clear that the continuum modular Hamiltonian approach can be also generalized to the multi-interval set-up (4.2.6), and that similar issues regarding regularization arise. We therefore also leave a more explicit discussion of the multi-interval case for future work.

4.A. Derivation of (4.4.2)

Here we review the derivation of (4.4.2) in [GM16], where a one-parameter family of genus zero branched covers

$$\begin{aligned}\phi : \mathbb{CP}^1 &\to \mathbb{CP}^1\\ w &\mapsto z \qquad (4.A.1)\end{aligned}$$

with monodromy data

$$\begin{aligned} &\boldsymbol{z} = (0, x(\alpha), 1, \infty), \quad \alpha \in (0,1) \\ &\sigma_1 = \sigma_2 = (12), \quad \sigma_3 = \sigma_4 = (13) \end{aligned} \tag{4.A.2}$$

is constructed, with

$$\begin{aligned} \phi(w) &= \frac{\left(2w - \alpha^2 + 1\right)^2 (w-4)}{(\alpha-3)^2 (\alpha+1) w} \\ x(\alpha) &= \frac{(3+\alpha)^3 (1-\alpha)}{(3-\alpha)^3 (1+\alpha)}. \end{aligned} \tag{4.A.3}$$

We will need the pre-images of the branched point $x(\alpha)$,

$$\phi^{-1}(x(\alpha)) = \{w_2^{\text{br.}}, w_2^{\text{non.br.}}\} = \{1-\alpha, (1+\alpha)^2\}. \tag{4.A.4}$$

Among the two pre-images, one of them is branched corresponding to the two-cycle, and the other is not branched corresponding to the trivial cycle.

The associated tau function is given by (below ψ^I denotes inverses of ϕ, and residues are understood as residues of one-forms)

$$\begin{aligned} \partial_x \log \tau_{(2,2)} &= \frac{1}{12} \operatorname{Res}_{z=x} \sum_I \{\psi^I, z\} dz \\ &= -\frac{1}{12} \operatorname{Res}_{z=x} \sum_I \left(\frac{d\psi^I}{dz}\right)^2 \{\phi, w\}|_{w=\psi^I(z)} dz \\ &= -\frac{1}{12} \left(\operatorname{Res}_{w=w_2^{\text{br.}}} + \operatorname{Res}_{w=w_2^{\text{non.br.}}}\right) \frac{\{\phi, w\}}{\phi'(w)} dw \\ &= -\frac{1}{12} \operatorname{Res}_{w=w_2^{\text{br.}}} \frac{\{\phi, w\}}{\phi'(w)} dw \\ &= -\frac{(\alpha-3)^3(\alpha+1)^3\left(\alpha^2+6\alpha-3\right)}{128(\alpha-1)\alpha^3(\alpha+3)^3} \equiv f(\alpha) \end{aligned} \tag{4.A.5}$$

Solving the equation

$$\partial_\alpha \log \tau_{(2,2)} = x'(\alpha) f(\alpha) \tag{4.A.6}$$

yields

$$\tau_{(2,2)} \propto \frac{(3-\alpha)^{\frac{1}{3}}}{(1-\alpha)^{\frac{1}{8}}\left(\alpha\,(3+\alpha)\right)^{\frac{1}{24}}}. \tag{4.A.7}$$

Part III.

Exact CFT_2 Method For Black Hole Perturbation

5. Holographic thermal correlators and quasinormal modes from semiclassical Virasoro blocks

5.1. Introduction

Recently, an exact analytic approach to black hole perturbations has been developed, based on the semiclassical Virasoro block. Equivalently, one can view this as an application of techniques used to analyze 4d supersymmetric field theories, in particular the Nekrasov partition function (in the so called Nekrasov-Shatashvili limit) to the black hole context. Our aim here is to exploit these developments to achieve the following:

- First, to provide some further insights into the connection, refining the general method, and extending it to incorporate some physically motivated generalizations.
- Second, to utilize this framework to analyze the matter and graviton fluctuations around asymptotically AdS black hole backgrounds. We are motivated here by the AdS/CFT correspondence, and, as we shall demonstrate, these techniques can be applied to study thermal correlators of generic operators and conserved currents of strongly coupled CFTs.

In the rest of the introduction, we elaborate on the physical motivations and technical background, and summarize the results we obtain.

5.1.1. Background

Quasinormal modes and holographic real-time thermal correlators: Perturbation around black hole spacetime, due to the existence of horizon, features characteristic damped oscillations

known as quasinormal modes (QNMs). The study of QNMs is an important subject of long history due to their relevance for distinct branches of physics, ranging from gravitational wave astronomy to gauge/gravity duality. We refer to the comprehensive reviews [KS99; BCS09; KZ11] for more background; see also [HK21] for a review specialized to the exact WKB method.

In the gauge/gravity context where black holes are generically dual to thermal field theory (at least above the deconfinement transition in compact volume), QNMs are related to the relaxation to thermal equilibrium [HH00]. The retarded thermal two-point function, is meromorphic, and has poles at QNMs. This observable can be extracted from the wave equations associated with black hole perturbation using the prescription of [SS02]. In fact, up to an overall constant, the two-sided thermal two-point function is entirely fixed by QNMs [DIKZ24].

Recently, a systematic approach for computing real-time holographic thermal correlators has since been developed. This not only justifies the prescription of [SS02], which is aimed at thermal two-point functions, but also provides a framework for computing arbitrary higher-point correlators. In general, real-time correlators in QFT should be computed using the Schwinger-Keldysh formalism. In the holographic context, the Schwinger-Keldysh contour is represented as a complexified two-sheeted geometry introduced in [GCL18] (for important prior work, see [SR09; SR08]). This prescription was analyzed and refined further in [CCCJLS19; JLR20; LRV22; LRV23; LM24]. Specifically, these works argued for the efficacy of the contour integral prescription demonstrating that one could compute correlation functions using Witten diagrams on a complexified spacetime, dubbed the *grSK geometry*. (for related work see [LRSS21; LRS20; CP21]). The upshot of this analysis is that a general correlator is obtained as a single integral over the exterior region of the black hole. The integrand is a multiple discontinuity of a non-analytic function, obtained by suitable convolution of a set of Green's functions in the grSK geometry. Employing this new formulation, it is demonstrated in [JLR20; LRV22] that, higher-point thermal correlators are also meromorphic – they have poles at QNMs or anti-QNMs.[1] In this work, we will primarily focus on thermal two-point functions, which are amenable to analysis via the prescription of [SS02], though we shall comment briefly on higher-point functions.

[1]The anti-QNMs are the poles of the advanced Green's function, and are complex conjugates of the QNMs. We also note that higher-point functions could additionally have poles at (kinematic) Matsubara frequencies.

Holographic open quantum systems: Apart from their intrinsic interest, a secondary motivation for analyzing holographic thermal correlators is to further our understanding of effective field theories of open quantum dynamics.

The study of open quantum systems, viz., systems coupled to an environment, has wide-ranging relevance in many physical problems. The key question here is to integrate out the environmental degrees of freedom, and to derive the (non-unitary) effective dynamics of the open system. The basic paradigm for analyzing such systems was explained in [FV63], and has been extensively applied in 1d quantum mechanical systems (see [BP02] for an overview). The analysis in the quantum field theoretic context, however, has been less developed, see [BJLR17].

In general, thermal correlators form the basic data for constructing the open EFT of a probe coupled to a thermal environment. As thermal correlators in generic QFT are difficult to compute, holographic environment, whose thermal correlators admit dual gravitational descriptions, provides a valuable avenue for explicitly determining the open EFT [JLR20; LRV22]. More concretely, the idea is to use a strongly coupled holographic field theory as a thermal environment, and probe it with a quantum system. Integrating out the holographic degrees of freedom, one obtains the open effective dynamics of the probe quantum system. An exact description of holographic thermal correlators will therefore be a useful tool in understanding such open quantum systems.

Black hole wave equations in AdS and Heun-type opers: Despite their physical significance and long history of study, QNMs and the associated thermal two-point functions have long resisted exact analytic understanding. In a way that aligns with our subsequent discussions, the reason can be explained as follows. The differential operator governing the (complexified) radial wave equations, for a mode with definite frequency ω and momentum k, on black hole background can generally be recast to certain $SL(2,\mathbb{C})$ opers on $\mathbb{P}^1$, viz.,

$$\partial_z^2 + \mathtt{T}(z|\omega,k) \tag{5.1.1}$$

with meromorphic $\mathtt{T}(z)dz^2$. The poles/punctures in the quadratic differential corresponds to special locations in black hole geometry, in particular including asymptotic boundary and hori-

zon.

An immediate consequence of the definition of QNMs and the prescription in [SS02] is that, solving QNMs and thermal two-point functions amounts to understanding certain global property of such oper, viz., the *connection problem* between asymptotic boundary and horizon. This turns out to be rather non-trivial beyond the well-understood three-puncture hypergeometric oper: standard exact results on QNMs, in particular the case of BTZ black hole in AdS_3 [BSS02], indeed all correspond to opers of this type.

We will focus on asymptotically AdS black hole backgrounds, where the associated oper generically has regular punctures [LRV23], viz., $\mathtt{T}(z)dz^2$ with double poles. In more elementary term, differential equations associated with such opers are referred to as Fuchsian equations. Other asymptotics will generically involve opers with irregular punctures, viz., $\mathtt{T}(z)dz^2$ with poles beyond second order. We refer to opers with more than three regular punctures as Heun-type opers.

Heun-type opers and semiclassical Virasoro blocks: The new feature of Heun-type opers compared to the hypergeometric opers is the presence of *accessory parameters*. It has been known since [Zam86] that accessory parameters in Heun-type opers are directly related to semiclassical Virasoro blocks; see also [LLNZ14]. There exists a long list of applications of this relation to various topics in theoretical and mathematical physics, ranging from AdS_3/CFT_2 [Har13; FKW14] to isomonodromic deformation [Tes17].

A recent breakthrough was made in [BIPT23] to utilize, among other things, this relation to solve the connection coefficients of Heun-type opers in terms of semiclassical Virasoro blocks.[2] The original derivation in [BIPT23] involves using crossing symmetry of Liouville correlators and the DOZZ formula. The resulting expression involves a degenerate fusion matrix and the semiclassical Virasoro block. Subsequently, it was clarified in [CFMP22; LN22] that the result of [BIPT23] directly follows from examining the fusion transformation of degenerate Virasoro block in the semiclassical limit.

Semiclassical Virasoro block and black hole perturbation: The result of [BIPT23] relating connection coefficients of Heun-type opers to semiclassical Virasoro blocks, for previously ex-

[2] Connection coefficients in presence of irregular punctures are also derived in [BIPT23].

plained reasons, is immediately applicable to obtain new exact analytic characterizations of QNMs and thermal two-point functions in $\text{AdS}_{d>3}$. There already exists a considerable amount of literature on applying semiclassical Virasoro blocks to black hole perturbation problems based on the relation with connection coefficients, either in AdS or flat spacetime asymptotics. Moreover, there have also emerged, in recent years, other new exact analytic approach based on distinct methods such as quantum Seiberg-Witten period [AGH22], ODE/IM correspondence [FG21], exact WKB [HK21], some of which also involve semiclassical Virasoro block for reasons besides the relation with connection coefficients. We refer to [AABGT23] for a quite extensive list of references.

While previous works such as [DGIPZ22] have analyzed thermal two-point functions (for scalar operators) in AdS_5 using the semiclassical Virasoro block approach, we will provide a new and considerably simpler exact analytic description. As we describe, previous work in this context utilizes what we refer to as the t-channel connection formula. However, a simpler s-channel connection formula for the *same* connection coefficients exists. The explicit dependence on the choice of channel of the semiclassical Virasoro block has remained rather underappreciated in the literature. As will be made clear later, the t-channel expression does have its merit that the t-channel OPE limit corresponds to physical limits in the black hole perturbation problem, while the s-channel one does not.

These considerations motivate our analysis. We were inspired by exploiting this technology to compute conserved current correlators of holographic CFTs. Thanks to large N, these results are universal for all holographic CFTs. For instance, the energy-momentum tensor correlators obtained holographically remain valid for all d-dimensional CFTs with a dual AdS_{d+1} gravitational description. We will focus on $d = 4$ for simplicity. A few additional comments are in order:

Additional comments

- A large part of the existing literature on applying semiclassical Virasoro block to black hole perturbation involves using the gauge theory side of AGT correspondence [AGT10], which relates semiclassical Virasoro blocks to Nekrasov instanton partition functions in the Nekrasov-Shatashvili limit. We would like to emphasize that the connection coefficients approach to

black hole perturbation problems can be purely, and arguably more simply, understood in CFT terms, without the need for AGT relation. For example, the gauge-theoretic derivation of BPZ equation, which is crucial for deriving the connection coefficients for Heun-type opers, was only understood rather recently in [Nek17; JN20]. We have therefore chosen to phrase our discussions exclusively in CFT language. The only exception to this is the analysis in §5.5 on the WKB regime of QNMs.

- We would like to clarify explicitly that there exists two distinct notions of CFTs in our discussions: one being the CFT_4 whose thermal correlators are holographically dual to black hole perturbations in AdS_5, the other being the auxiliary CFT_2 whose semiclassical Virasoro blocks are used to analyze the Heun-type opers arising from perturbation equations in AdS_5. Which notion of CFT is referred to in our subsequent discussions should be clear from context.

5.1.2. Summary of results

We give a brief summary of our salient results, with pointers to the appropriate part of the chapter for further details.

Universal exact descriptions: Our central results are universal exact analytic characterizations of QNMs and holographic thermal two-point functions in AdS_5, described in terms of the auxiliary data of spherical four-point semiclassical Virasoro blocks, in both s-channel (cf. (5.4.21) and (5.4.24)) and t-channel (cf. (5.4.32) and (5.4.35)). These are different descriptions of the same physical objects. The universality of the results refers to their applicability to a wide range of examples in AdS_5.[3]

As alluded to previously, while the t-channel expressions have appeared in the earlier literature in certain examples. The s-channel expressions, having a considerably simpler analytic structure, are new to the best of our knowledge. In particular, they resemble the formal structure of the answers for BTZ black hole in AdS_3 dual to thermal correlator for holographic CFT_2.[4]

[3] Here we refer to distinct types of perturbations (scalar, electromagnetic, gravitational) on different asymptotically AdS_5 backgrounds, both uncharged and charged black holes with planar or spherical horizon topology.
[4] The form of thermal 2-point function in CFT_2 on $\mathbb{R}^{1,1}$ is independent of the central charge, and thus holds even for non-holographic CFTs.

Certain examples do require extension of the aforementioned results. In particular, the extension involves adding one more regular puncture (non-scalar perturbations on charged planar black hole background; cf. §5.4.4), or taking into account punctures with trivial monodromy (scalar channel of metric perturbation; cf. §5.4.5). The latter corresponds to certain heavy degenerate operator in the auxiliary CFT_2. The aforementioned s-channel exact expressions admit straightforward extension to these cases, thanks to the locality of fusion transformation of the (degenerate) Virasoro blocks.

Specific properties: Besides the universal exact expressions, we also discuss their specific physical aspects illustrated in various examples, including

- *Computing QNMs using s-channel exact quantization condition:* The simplicity of the analytic structure of s-channel expressions facilitates explicit computation of QNMs using semiclassical Virasoro block data. This is illustrated in Example 5.4.1 for different types of perturbations on planar Schwarzschild-AdS_5 black hole background.

- *WKB regime of QNMs from Seiberg-Witten limit of s-channel exact quantization condition.* The WKB regime of QNMs, where QNMs become equally spaced, is also more transparent from the s-channel exact quantization condition. It corresponds to certain large-momenta limit of semiclassical Virasoro block, which is related to Seiberg-Witten prepotential from gauge theory side of AGT relation. This is discussed in §5.5.

- *Physical limits of QNMs from the OPE limit of t-channel exact quantization condition.* Compared to their s-channel counterpart, the t-channel exact quantization condition does have the advantage that its OPE limit corresponds to physical limits in the black hole perturbation problems. In particular, in Example 5.4.3, we obtain new analytic expressions for purely decaying QNMs in near-extremal planar black hole.

5.1.3. Outline

The outline of the chapter is as follows. In §5.2 we introduce the black hole perturbation problem, and the holographic computation of thermal observables. We take the opportunity here to give an algorithm for the real-time computations. We then turn in §5.3 to a broad

overview of connection formulae for Heun type opers using 2d CFT techniques, specifically developing the relation to the semiclassical Virasoro blocks. These results are used in §5.4 to derive properties of thermal correlation functions in holographic CFTs. In §5.5 we explain how the connection with supersymmetric field theory observables can aid our understanding of the WKB asymptotics. The reader interested in explicit results for energy-momentum tensor correlators of 4d CFTs can find them compiled in §5.6. We conclude in §5.7 with a discussion of open questions and future directions.

5.2. Black holes and holographic CFTs

Consider a CFT in d spacetime dimensions, $\Sigma_{d-1} \times \mathbb{R}$. We will primarily focus on the cases where the spatial manifold Σ_{d-1} is either the round sphere $\mathbf{S}^{d-1}$ or flat Euclidean space R^{d-1}, corresponding to placing the CFT on the Einstein Static Universe, or Minkowski spacetime, respectively. We work at finite temperature $T = \frac{1}{\beta}$. We will also allow ourselves the freedom to turn on chemical potentials for conserved global currents, should the CFT admit any.

Focusing on holographic CFTs, which have a large number of degrees of freedom, and a sparse low-lying spectrum, the thermal ensemble at high enough temperatures is described by a black hole in the dual gravitational theory. For thermal equilibrium, we will be interested in static black holes with AdS_{d+1} asymptotics. Working in ingoing coordinates, the line element takes the form

$$ds^2 = -r^2\, f(r)\, dv^2 + 2\, dv\, dr + r^2\, ds^2_{\Sigma_{d-1}}\,, \tag{5.2.1}$$

where $ds^2_{\Sigma_{d-1}}$ is the round metric on $\mathbf{S}^{d-1}$ or the flat Euclidean metric on $\mathbb{R}^{d-1}$, depending on the case of interest. The black hole horizon is at r_+, the largest real root of $f(r)$, $f(r_+) = 0$. The temperature of the black hole and the dual CFT is

$$T = \frac{r_+^2\, f'(r_+)}{4\pi}\,. \tag{5.2.2}$$

In the absence of any chemical potentials, viz., in the canonical ensemble, the duals are the Schwarzschild-AdS_{d+1} black holes. The explicit metric functions in the coordinates chosen

above are

$$f(r) = \begin{cases} \frac{\ell_{\rm AdS}^2}{r^2}\left[1 + \frac{r^2}{\ell_{\rm AdS}^2} - \frac{r_+^{d-2}}{r^{d-2}}\left(1 + \frac{r_+^2}{\ell_{\rm AdS}^2}\right)\right], & \Sigma_{d-1} = \mathbf{S}^{d-1}\,, \\ 1 - \frac{r_+^d}{r^d}\,, & \Sigma_{d-1} = \mathbb{R}^{d-1}\,. \end{cases} \tag{5.2.3}$$

The ingoing coordinates are regular at the future horizon, and the radial derivative adapted to this choice is

$$\mathbb{D}_+ \equiv r^2 f \frac{\partial}{\partial r} + \frac{\partial}{\partial v}\,. \tag{5.2.4}$$

5.2.1. Quasinormal modes and thermal Green's functions

We would like to compute real-time thermal correlators using the holographic description. A single trace, gauge invariant CFT operator $\mathcal{O}(x)$, where x coordinatizes $\mathbb{R} \times \Sigma_{d-1}$ is dual to a field $\Phi(r, x)$. We are suppressing the representation labels of the operator for simplicity. The field $\Phi(r, x)$ has a classical action in the AdS black hole background, with a kinetic term, and a potential, which characterizes its interactions (both with itself and other fields). The basic ingredient for our analysis will be the linear wave equation arising from the kinetic term, which schematically takes the form

$$\mathfrak{D}\Phi + V(r)\,\Phi = 0\,, \qquad \mathfrak{D} = -\frac{1}{\sqrt{-g}\,e^{\chi(r)}}\partial_A\left(\sqrt{-g}\,e^{\chi(r)}\,g^{AB}\,\partial_B\right). \tag{5.2.5}$$

Here $V(r)$ and $\chi(r)$ are some auxiliary functions that depend on the nature of the kinetic operator for the field Φ. We will outline some examples below in §5.4.1.

The CFT correlation functions of interest will be real-time thermal correlators. Per se, these should be evaluated using the Schwinger-Keldysh contour, which computes the generating function $\mathrm{Tr}\big(U[J_{\rm R}]\,\rho_\beta\,(U[J_{\rm L}])^\dagger\big)$. Such observables probe the thermal state and can be viewed as characterizing the retarded response, and associated stochastic fluctuations. Sources $J_{\rm R}$ and $J_{\rm L}$ are inserted in the forward and backward evolution segments of the contour. We give a quick overview of implementing this in holography in §5.2.2. For the present, we will give a somewhat simpler characterization (which we justify below).

The wave equation (5.2.5) has two linearly independent solutions. For non-extremal black

holes, the solutions near the horizon are ingoing or outgoing. Using the Killing symmetry ∂_v to pass to the frequency domain,[5] the local solutions, near the horizon $r \sim r_+$, are $\Phi(r) = c_1 + c_2 (r - r_+)^{i\beta\omega}$. The constant mode is the ingoing solution that is analytic at the horizon. At the asymptotic AdS boundary, we have as usual normalizable and non-normalizable modes, the latter corresponding to the sources we can turn on for the boundary operator.

The asymptotically normalizable solution to the wave equation with ingoing boundary conditions at the horizon exists only for a discretuum of frequencies. These are the quasinormal modes (henceforth QNMs) of the black hole. One way to extract them is to examine the retarded 2-point function of the dual boundary operator (spatial dependence suppressed for simplicity),

$$K(\omega) = \langle \mathcal{O}(\omega)\, \mathcal{O}(-\omega) \rangle_\beta \ . \tag{5.2.6}$$

In holographic theories $K(\omega)$ is meromorphic, with poles at the quasinormal frequencies.

A prescription for computing $K(\omega)$ was given in [SS02]. The essential idea was to phrase the calculation in terms of a connection problem for (5.2.5). Consider turning on the non-normalizable asymptotic mode for Φ (to activate a source for $\mathcal{O}$) and imposing ingoing boundary condition at the horizon. The solution defines the ingoing boundary-bulk Green's function $G_{\rm in}(r, \omega)$. The 2-point function is determined in terms of the ratio of normalizable and non-normalizable modes of $G_{\rm in}$, viz.,

$$K(\omega) = \frac{\text{Normalizable}(G_{\rm in})}{\text{Non-normalizable}(G_{\rm in})}. \tag{5.2.7}$$

This prescription, which was argued for in [HS03] has the virtue of being simple, but does not readily generalize to computing higher point functions. The more natural way to proceed is to directly implement the real-time Schwinger-Keldysh computation in gravity. As noted above, this has been achieved recently [GCL18] (see also [Ree09]). For completeness, we give a brief synopsis of this development, and argue for how to recover (5.2.14).

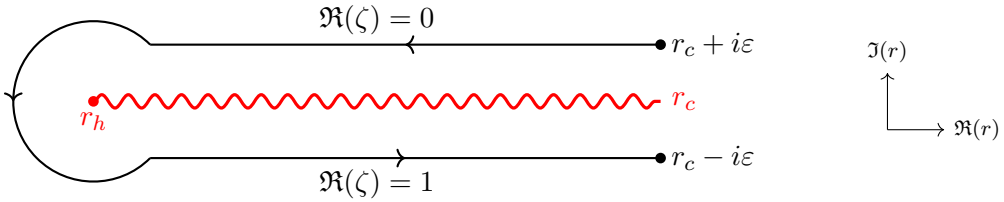

Figure 5.1.: The complex r plane, with the locations of the two boundaries and the horizon marked. The grSK contour is a codimension-1 surface in this plane (drawn at fixed v). The direction of the contour is as indicated counter-clockwise, encircling the branch point at the horizon.

5.2.2. Real-time observables in thermal holographic CFTs

The Schwinger-Keldysh contour is implemented in gravity by a complex two-sheeted geometry obtained from (5.2.1). Following [JLR20] introduce the complexified (mock) tortoise coordinate

$$d\zeta = \frac{2}{i\,\beta}\,\frac{dr}{r^2 f}\,. \tag{5.2.8}$$

The one form $\frac{dr}{f(r)}$ has a branch-point at the horizon/ We avoid this by working on a keyhole contour encircling the horizon, see Fig. 5.1.

The algorithm for computation of the CFT correlators on this geometry can be summarized as follows:

- First, we obtain the ingoing boundary to bulk propagator $G_{\rm in}(r,\omega)$ for (5.2.5). It satisfies

$$\lim_{r\to\infty} G_{\rm in} = 1\,, \qquad \left.\frac{{\rm d}G_{\rm in}}{{\rm d}r}\right|_{r_+} = 0\,. \tag{5.2.9}$$

- Next, we uplift the fluctuations of fields in the gravitational theory to the grSK contour. The bulk dynamics is then prescribed by a contour integral

$$S_{\rm bulk} = \oint d\zeta \int d^d x\,\sqrt{-g}\,\mathcal{L}[g_{AB},\Phi]\,, \tag{5.2.10}$$

- $G_{\rm in}(r,\omega)$is regular at the horizon, and therefore is insensitive to the branch cut in ζ. Therefore, the ingoing grSK propagator $G_{\rm in}(\zeta,\omega)$ is obtained by replacing $r \to r(\zeta)$.

- The solution for Φ with L and R Schwinger-Keldysh sources on the respective boundaries is

[5] We work in the frequency domain with wavefunctions having temporal dependence $e^{-i\omega v}$.

obtained by exploiting the time-reversal involution of the static solution. One finds

$$\begin{aligned}\Phi(\zeta,\omega) &= G_{\rm in}(\zeta,\omega)\left((1+n_\omega)\,J_{\rm R}-n_\omega\,J_{\rm L}\right)-G_{\rm in}(\zeta,-\omega)\,e^{\beta\,\omega\,(1-\zeta)}\,n_\omega\Big(J_{\rm R}-J_{\rm L}\Big)\,,\\ &\equiv -G_{\rm in}(\zeta,\omega)\,J_F+G_{\rm in}(\zeta,-\omega)\,e^{\beta\omega\,(1-\zeta)}\,J_P\,.\end{aligned} \tag{5.2.11}$$

Here $n_\omega=(e^{\beta\omega}-1)^{-1}$ is the Bose-Einstein function. In the second line, we introduced the retarded/advanced sources J_F and J_P as linear combinations of the R and L sources.

- Finally, the propagation of the field between two bulk spacetime points is captured by the bulk-bulk propagator ($\mathcal{N}(\omega)$ is a normalization factor)

$$G_{\rm bulk}(\zeta,\zeta';\omega)=\mathcal{N}(\omega)\,e^{\beta\omega\,\zeta'}\Big[\Theta(\zeta-\zeta')\,G_L(\zeta,k)\,G_R(\zeta',k)+\Theta(\zeta'-\zeta)\,G_L(\zeta',k)\,G_R(\zeta,k)\Big]\,. \tag{5.2.12}$$

Here $\Theta(\zeta-\zeta')$ is a contour-ordered step function along the contour depicted in Fig. 5.1, while

$$\begin{aligned}G_R(\zeta,\omega)&=e^{\beta\,\omega}\,n_\omega\left(G_{\rm in}(\zeta,\omega)-e^{-\beta\omega\,\zeta}\,G_{\rm in}(\zeta,-\omega)\right),\\ G_L(\zeta,\omega)&=-n_\omega\left(G_{\rm in}(\zeta,k)-e^{\beta\omega\,(1-\zeta)}\,G_{\rm in}(\zeta,-\omega)\right).\end{aligned} \tag{5.2.13}$$

The functions G_R and G_L have source on the right ($\zeta=1$) and left ($\zeta=0$) boundaries, respectively, and are normalizable at the other end.

Real-time correlators are computed by Witten diagrams on the grSK geometry. Any such diagram comprises a set of propagators, vertex functions, and radial-ordering step-functions. This constructs the integrand for the contour integral over the contour depicted in Fig. 5.1. The non-analytic parts of the integrand come from the factors $e^{-\beta\omega\,\zeta}$ and $\Theta(\zeta-\zeta')$. Accounting for these, the final result for an n-point function can be expressed as an integral of (multiple) discontinuities of the original integrand in the region exterior of the black hole (in the original radial coordinate $r\in[r_+,\infty)$, cf. [JLR20; LRV22; LM24] for details.[6]

The essential data necessary for real-time observables is the ingoing boundary to bulk Green's function for Φ. Since this Green's function has a source at the boundary, and is infalling at the horizon, it should be meromorphic, with poles at the quasinormal frequencies. Factoring out

[6] As noted in [CCL19; LRV22] one may also have localized contributions at the horizon in certain situations.

the contribution from the quasinormal modes, one can write

$$G_{\rm in}(\zeta,\omega) = K(\omega)\,\widetilde{G}_{\rm in}(\zeta,\omega)\,. \tag{5.2.14}$$

The function $K(\omega)$ is the boundary 2-point introduced in (5.2.6). This can be seen by computing the corresponding Witten diagram. The contour integral picks out the discontinuity proportional to $J_F\,J_P$ (the other combinations vanish as they have no discontinuities consistent with Schwinger-Keldysh and KMS constraints). Since the field is on-shell in the bulk, the result simply reduces to the product of the boundary value of the field and its conjugate momentum. The latter is the normalizable mode of the field. Accounting for the fact that $G_{\rm in}$ was defined with a unit boundary source, we recover (5.2.7). This recovers the prescription of [SS02] quoted above.

For purposes of computing the 2-point function $K(\omega)$, it suffices to phrase the calculation as a connection problem. We will use this language, since it allows us to reframe the question of computing the thermal real-time correlation functions using semiclassical conformal blocks of an auxiliary two-dimensional CFT. However, the grSK perspective will be useful, since the ingoing bulk-boundary propagator itself can be reinterpreted as a conformal block. Thus, all correlation functions can in principle determined from the data of this auxiliary two-dimensional CFT.

5.3. Connection formulae for Heun-type opers from semiclassical Virasoro blocks

The wave equations of interest in AdS_{d+1} black hole backgrounds are generically Fuchsian differential equations [AGH22; LRV23]. These equations are characterized by having regular singular points or punctures. By a suitable choice of coordinates, one may bring the equations to the canonical form of Heun-type opers. We will assume this has been achieved for the present discussion. Some well-known examples are the hypergeometric equation that arises in the case of $d = 2$, i.e., for wave equations in the BTZ background. Our focus will be on the case $d = 4$, relevant to 4d CFTs such as $\mathcal{N} = 4$ SYM. In this case, the equations of interest (for neutral black holes) turn out to have 4 punctures. Such equations are usually referred to as Heun's equation.

For the case of a charged black hole, we will also encounter an equation with 5 punctures, which we shall also comment on.

We revisit the large-c CFT derivation of the connection formula for Heun's equation, largely following the presentation of [LN22]. As explained in [LN22], the generalization to equations with more singular points is immediate. In CFT parlance, this follows from the locality of fusion transformation. We therefore primarily focus on AdS_5 black holes, and the associated Heun's equations, for simplicity in presentation.

The connection between (5.2.5) and 2d CFTs can be motivated as follows. Consider a degenerate Virasoro block, involving the insertion of n-heavy operators and one light degenerate operator. Here, heavy/light refers to conformal weights being $\mathcal{O}(c^1)$ or $\mathcal{O}(c^0)$, respectively, in the large-c limit. The BPZ equation satisfied by such degenerate blocks reduces to Fuchsian equation in the large-c limit. The heavy operators correspond to the punctures. The fusion of the light degenerate operator with different heavy operators corresponds to different Frobenius solutions. The change of basis of the Frobenius solutions is then directly related to the degenerate fusion transformation of these degenerate Virasoro blocks, from which one directly reads off the connection formula. Eventually, the connection matrix depends on degenerate fusion matrix and classical Virasoro block of the heavy operators.

The above derivation can be carried out by starting with degenerate Virasoro block in *any* channel and then performing degenerate fusion transformation. The resulting connection matrix will be apparently different for different choices of channel. As we shall see, for the connection problem in the Heun case (4 punctures), there will be a distinction between s- and t- channel connection formulae. The s-channel one takes a simpler form than the t-channel one (the reason being the former is derived from using one fusion transformation, whereas the latter a composition of two).

This important point, to the best of our knowledge, has not been explicitly explained or emphasized in literature. We will use the simpler s-channel connection formula for application to QNMs and thermal 2-point functions of 4d holographic CFTs. The t-channel connection formula is equivalent to the one employed in [DGIPZ22]. Details of this will become clear in the sequel.

Notation: The following convenient notation will be used throughout our subsequent discussions:

$$\Gamma(\alpha \pm \beta) \coloneqq \Gamma(\alpha+\beta)\,\Gamma(\alpha-\beta)\,. \tag{5.3.1}$$

5.3.1. Elements of 2d CFT

We first give a brief review of elements of 2d CFT relevant for our subsequent discussions. We refer to, e.g., [DMS97; Rib14] for more comprehensive background.

Liouville parametrization: The Liouville parametrization of central charge and conformal weights is, in general, convenient for understanding representations of Virasoro algebra. The central charge is parametrized by

$$c = 1 + 6\,Q^2\,, \qquad Q = b + \frac{1}{b}\,. \tag{5.3.2}$$

Primary operators V_P are labeled by Liouville momenta P, and have conformal weight

$$h = \frac{Q^2}{4} - P^2\,. \tag{5.3.3}$$

Degenerate representations: The Verma module atop V_P is obtained by acting with Virasoro raising generators L_{-n} with $n \geq 1$. For generic P, such a module is non-degenerate in the sense that no null vectors appear in the module. Degenerate modules occur for a discrete set of momenta characterized by two integers

$$P_{\langle r,s\rangle} = \frac{1}{2}\left(r\,b + \frac{s}{b}\right)\,. \tag{5.3.4}$$

The corresponding degenerate primary is $V_{\langle r,s\rangle}$, and it has conformal weight

$$h_{\langle r,s\rangle} = \frac{1}{4}\left[\left(b+\frac{1}{b}\right)^2 - \left(r\,b+\frac{s}{b}\right)^2\right]. \tag{5.3.5}$$

The fusion rules for the degenerate operators with a generic primary operator with Liouville momentum P is given by

$$V_{\langle r,s\rangle} \times V_P = \sum_{m=-\frac{r-1}{2}}^{\frac{r-1}{2}} \sum_{n=-\frac{s-1}{2}}^{\frac{s-1}{2}} V_{P+m\,b+\frac{n}{b}}\,. \tag{5.3.6}$$

Virasoro blocks and their semiclassical limits: The spherical four-point Virasoro block in s-channel is defined via a series expansion in cross-ratio:

$$\begin{aligned} \mathcal{F}^s\left(x|\boldsymbol{P},P_\sigma\right) &\coloneqq x^{h_\sigma-h_0-h_x}\left(1+\sum_{k=1}^{\infty}\mathcal{F}_k^s\left(\boldsymbol{P},P_\sigma\right)x^k\right), \\ \mathcal{F}_1^s\left(\boldsymbol{P},P_\sigma\right) &= \frac{\left(h_\sigma-h_0+h_x\right)\left(h_\sigma-h_\infty+h_1\right)}{2\,h_\sigma}, \quad \text{etc.} \end{aligned} \tag{5.3.7}$$

The expansion coefficients, $\mathcal{F}_k^s\left(\boldsymbol{P},P_\sigma\right)$, are entirely fixed by Virasoro algebra, and their precise definitions can be found in standard references such as [DMS97; Rib14]. The relation between conformal weights and Liouville momenta is understood. We use $\boldsymbol{P}$ to collectively denote $\{P_i\}_{i=0,x,1,\infty}$. The expansion coefficients also admit closed-form combinatorial expression from instanton counting thanks to the AGT relation [AGT10]. A standard graphical notation is

$\mathcal{F}^s(x) =$ 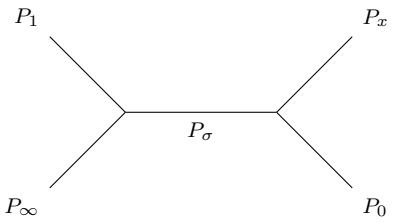

(5.3.8)

An alternative t-channel expansion, corresponding to a different pair-of-pants decomposition of the four-punctured sphere, can be performed for the same set of external momenta $\boldsymbol{P}$. This is

graphically represented by

$\mathcal{F}^t(x) =$ 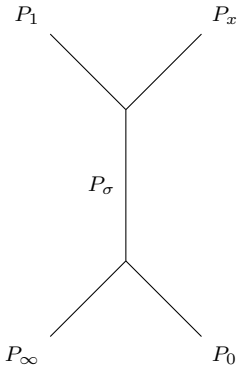

(5.3.9)

The blocks in the two channels are related by

$$\mathcal{F}^t(x) = \mathcal{F}^s(1-x)\Big|_{P_0 \leftrightarrow P_1} . \tag{5.3.10}$$

Now consider the following semiclassical limit:

$$\text{S.C.} : b \to 0, \quad P_i,\, P_\sigma \to \infty, \quad b\, P_i \to \theta_i, \quad b\, P_\sigma \to \sigma. \tag{5.3.11}$$

The semiclassical Virasoro block $\mathcal{W}(x)$,[7] in either channel, is then defined by

$$\mathcal{W}\left(x|\boldsymbol{\theta},\sigma\right) \coloneqq \lim_{\text{S.C.}} b^2 \, \log \mathcal{F}\left(x|\boldsymbol{P},P_\sigma\right). \tag{5.3.12}$$

The limit is understood to be taken term by term in the cross-ratio expansion of $\log \mathcal{F}(x)$. For s-channel, the explicit expansion reads:

$$\begin{aligned} \mathcal{W}^s(x) &= \left(\delta_\sigma - \delta_0 - \delta_x\right) \log x + \sum_{k=1}^{\infty} \mathcal{W}^s_k\left(\boldsymbol{\theta},\sigma\right) x^k \,, \\ \mathcal{W}^s_1\left(\boldsymbol{\theta},\sigma\right) &= \frac{\left(\delta_\sigma - \delta_0 + \delta_x\right)\left(\delta_\sigma - \delta_\infty + \delta_1\right)}{2\,\delta_\sigma}, \quad \text{etc.} \end{aligned} \tag{5.3.13}$$

where $\delta_i = \frac{1}{4} - \theta_i^2$ is (semi)classical conformal weight, and by convention $\theta_\sigma = \sigma$. The existence of the defining large-c limit of semiclassical Virasoro block is non-trivial beyond $k = 1$: it requires cancellation between all the $\mathcal{O}\big(c^2\big), \ldots, \mathcal{O}\big(c^k\big)$ terms in the x^k term of $\log \mathcal{F}^s(x)$ expansion. The

[7] This notation comes from the gauge theory side of AGT relation, where semiclassical Virasoro block is related to effective twisted superpotential. We find that it does more justice to the significance of the object, compared to the frequently-used notation $f(x)$.

exponentiation of Virasoro block is originally conjectured in [Zam86] and usually motivated by saddle-point argument in Liouville theory; a proof is recently claimed in [BDK20].

The definitions of Virasoro blocks and their semiclassical limits also extend to cases with more punctures, which will also be relevant in our subsequent discussions.

Degenerate fusion transformation and its locality property: The infinite-dimensional fusion transformation relating generic Virasoro blocks at different channels is, in general, known in closed form [PT99]. For our purpose, we only need the simplest two-dimensional case involving Virasoro block with the insertion of a degenerate operator $V_{\langle 2,1\rangle}$, whose fusion with V_P results in $V_{P\pm\frac{b}{2}}$. In graphical notation, such degenerate fusion transformation is represented as:

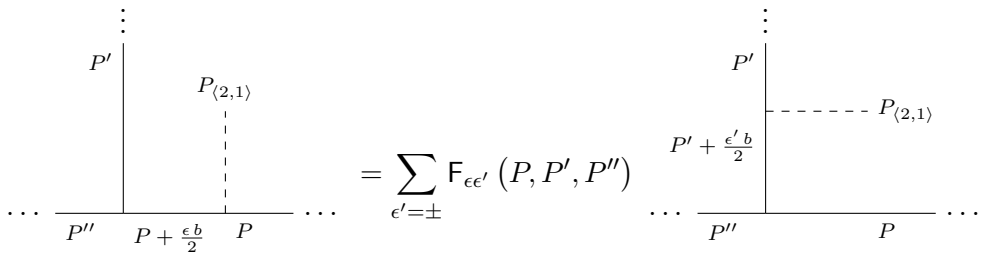

(5.3.14)

with

$$\mathsf{F}_{\epsilon\epsilon'}\left(P,P',P''\right)=\frac{\Gamma\left(1-2\,\epsilon\,b\,P\right)\Gamma\left(2\,\epsilon'\,b\,P'\right)}{\Gamma\left(\frac{1}{2}-\epsilon\,b\,P+\epsilon'\,b\,P'\,\pm\,b\,P''\right)}\,. \tag{5.3.15}$$

The crucial property is the *locality* of such transformation [MS89a; MS89b]: the omitted dots above could represent arbitrary conformal block diagrams with additional external operators/punctures. The degenerate block in the case with three non-degenerate external operators is the well-known hypergeometric block, and the above transformation is equivalent to the classically-known connection formulae for hypergeometric functions. As will be seen with more details later, the locality of such transformation allows using CFT method to obtain connection formulae beyond the hypergeometric case.

The only necessary ingredients we haven't introduced thus far are the BPZ equation satisfied by the degenerate Virasoro block, and the relation between accessory parameters in Heun-type opers and semiclassical Virasoro blocks. These will be introduced along with the derivation of connection coefficients.

For much of the discussion, we will be interested in a five-point degenerate Virasoro block where four of the operators V_{P_i} are generic, and the fifth corresponds to the degenerate representation $V_{\langle 2,1\rangle}$. This will turn out to be sufficient for understanding thermal 2-point functions of scalar operators, and tensor and vector polarizations of the energy-momentum tensor in 4d holographic CFTs. The scalar polarization of the energy-momentum tensor will, however, require an additional insertion of $V_{\langle 1,3\rangle}$. The reason for this will be the presence of an apparent singular point in the associated differential equation [LRV23].

5.3.2. Prelude: The connection problem for Heun-type opers and subtleties in logartihmic cases

For concreteness, consider Heun's equation, which is the most general second order ODE with four punctures. The generalization of subsequent discussions to generic Heun-type opers with more punctures is immediate. For Heun's equation, the location of punctures can always be set to $\{0, x, 1, \infty\}$ via Möbius transformation. The equation in normal form reads

$$\begin{aligned}
&\psi''(z) + \mathtt{T}(z)\,\psi(z) = 0\,,\\
&\mathtt{T}(z) = \frac{\delta_0}{z^2} + \frac{\delta_1}{(z-1)^2} + \frac{\delta_x}{(z-x)^2} + \frac{\delta_\infty - \delta_0 - \delta_1 - \delta_x}{z\,(z-1)} + \frac{(x-1)\,\mathcal{E}}{z\,(z-1)\,(z-x)}\,,\\
&\delta_i = \frac{1}{4} - \theta_i^2\,.
\end{aligned} \tag{5.3.16}$$

The characteristic exponents at each puncture are $\frac{1}{2} \pm \theta_i$, and $\mathcal{E}$ is the accessory parameter.

We focus on the connection problem between the punctures at 0 and x. It will be clear that the CFT method can be used to derive the connection formula between any other pair of punctures. Assume $\theta_0, \theta_x \notin \frac{\mathbb{Z}}{2}$ so that there exists unique normalized Frobenius bases

$$\begin{aligned}
\psi_\epsilon^{[0]}(z) &= z^{\frac{1}{2}-\epsilon\,\theta_0}\left(1 + \sum_{k=1}^{\infty} \psi_{\epsilon,k}^{[0]}\, z^k\right),\\
\psi_\epsilon^{[x]}(z) &= (z-x)^{\frac{1}{2}-\epsilon\,\theta_x}\left(1 + \sum_{k=1}^{\infty} \psi_{\epsilon,k}^{[x]}\, (z-x)^k\right), \qquad \epsilon = \pm\,.
\end{aligned} \tag{5.3.17}$$

The connection problem is the problem of finding the connection matrix C such that

$$\psi_{\epsilon}^{[0]}(z) = \sum_{\epsilon'=\pm} \mathsf{C}_{\epsilon\epsilon'}\, \psi_{\epsilon'}^{[x]}(z). \tag{5.3.18}$$

While the case of exponent being half-integer appears rather non-generic mathematically, for many physical examples in black hole perturbation problems we will encounter $\theta_x \in \mathbb{Z}/2$, which is related to the fall-off behavior at AdS boundary. In the half-integer cases, one of the local solutions is logarithmic and there are additional subtleties on the appropriate generalization of the connection problem. While eventually we will claim that the connection coefficient in the logarithmic cases relevant for defining QNMs can be obtained via a suitable continuation of the CFT answer in the non-logarithmic case, we find it important to first give a direct mathematical characterization of the logarithmic cases. This requires a more careful examination of the local Frobenius expansion.

Details on Frobenius expansion: subtleties in logarithmic cases

Here we give more details on the local Frobenius expansion, in particular in the logarithmic cases. We follow the presentation in [IKSY91], adapting to our set-up and convention. We would like to find local Frobenius solutions to Fuchsian equation $\left(\partial_z^2 + \mathtt{T}(z)\right)\psi(z)$ at $z = 0$, where $\mathtt{T}(z)$ has a double pole. It is convenient to rewrite the equation in the following manner:

$$0 = \left[z^2\partial_z^2 + z^2\,\mathtt{T}(z)\right]\psi(z) = \left[\mathtt{d}_z^2 - \mathtt{d}_z + z^2\,\mathtt{T}(z)\right]\psi(z) \equiv \mathfrak{D}_z\psi(z). \tag{5.3.19}$$

Here $\mathtt{d}_z := z\partial_z$, and we have used $z^k\partial_z^k = \mathtt{d}_z\,(\mathtt{d}_z - 1)\cdots(\mathtt{d}_z - k + 1)$. Consider the normalized Frobenius expansion

$$\Psi(z) = z^{\lambda}\left(1 + \sum_{k=1}^{\infty}\Psi_k\, z^k\right). \tag{5.3.20}$$

One then reads off from (5.3.19):

$$\begin{aligned}
\mathfrak{D}_z\Psi(z) &= z^{\lambda}\sum_{k=0}^{\infty}\mathtt{R}_k\left(\Psi_0,\cdots,\Psi_k|\lambda\right)\, z^k \\
\mathtt{R}_k\left(\Psi_0,\cdots,\Psi_k|\lambda\right) &= \Psi_k\,(\lambda+k)\,(\lambda+k-1) + \sum_{p=0}^{k}\Psi_p\,\mathfrak{l}_{p-k}.
\end{aligned} \tag{5.3.21}$$

Here the $\mathfrak{l}$ operators are expansion coefficients in $z^2\,\mathtt{T}(z) = \sum_{k=0}^{\infty} \mathfrak{l}_{-k}\, z^k$. In particular, $\mathfrak{l}_0 = \frac{1}{4} - \theta^2$ with sign convention $\Re(\theta) \geq 0$. Also $\Psi_0 = 1$ by convention. The coefficients $\mathtt{R}_k$ can be more conveniently written as

$$\begin{aligned} \mathtt{R}_k\left(\Psi_0, \cdots, \Psi_k | \lambda\right) &= \Psi_k\, f_k(\lambda) + \sum_{p=0}^{k-1} \Psi_p\, \mathfrak{l}_{p-k} \\ f_k(\lambda) &= \prod_{\epsilon=\pm} \Big[\lambda - (\lambda_\epsilon - k)\Big]. \end{aligned} \tag{5.3.22}$$

Here $\lambda_\pm = \frac{1}{2} \pm \theta$, with $f_0(\lambda) = 0$ being the characteristic equation. Now define

$$\begin{aligned} &\Psi_k(\lambda) \coloneqq \text{solution to recursion relation } \; \mathtt{R}_k\left(\Psi_0, \cdots, \Psi_k | \lambda\right) = 0\,, \quad k \geq 1 \\ &\Psi(z|\lambda) \coloneqq z^\lambda \left(1 + \sum_{k=1}^{\infty} \Psi_k(\lambda)\, z^k\right). \end{aligned} \tag{5.3.23}$$

Eventually we will set $\lambda = \lambda_\pm$. But when $\lambda_\pm = \frac{1 \pm n}{2} \equiv \lambda_\pm^{(n)}$ with $n \in \mathbb{Z}_{>0}$ (viz., $\theta = n/2$), the recursive solutions $\Psi_k(\lambda_-^{(n)})$ are not well-defined at all k. In particular, the coefficient $f_n(\lambda_-)$ for Ψ_n in $\mathtt{R}_n\left(\Psi_0, \cdots, \Psi_n | \lambda_-^{(n)}\right)$ vanishes due to $\lambda_-^{(n)} = \lambda_+^{(n)} - n$. In this case, define $\Psi_k\left(\lambda_-^{(n)}\right)$ in the following way. With the coefficients $\Psi_0\left(\lambda_-^{(n)}\right), \ldots, \Psi_{n-1}\left(\lambda_-^{(n)}\right)$ still defined from solving the recursion relation, choose $\Psi_n\left(\lambda_-^{(n)}\right)$ arbitrarily. Then $\Psi_{k>n}\left(\lambda_-^{(n)}\right)$ can be solved for recursively starting from this arbitrary choice. This then defines the associated $\Psi\left(z|\lambda_-^{(n)}\right)$.

One then has

$$\mathfrak{D}_z \Psi(z|\lambda) = z^\lambda \left(f_0(\lambda) + z^n \delta_{\lambda, \lambda_-^{(n)}} \sum_{p=0}^{n-1} \Psi_p\left(\lambda_-^{(n)}\right) \mathfrak{l}_{p-n}\right), \quad n \in \mathbb{Z}_{>0}. \tag{5.3.24}$$

Therefore, for all θ, $\Psi(z|\lambda_+)$ is one of the solutions:

$$\mathfrak{D}_z \Psi(z|\lambda_+) = 0. \tag{5.3.25}$$

Case I ($\theta \notin \mathbb{Z}/2$): In this case there is no ambiguity. The two independent solutions are

$$\psi_\pm(z) = \Psi(z|\lambda_\pm) = z^{\lambda_\pm} \left(1 + \sum_{k=1}^{\infty} \Psi_k(\lambda_\pm)\, z^k\right). \tag{5.3.26}$$

To find the other solution in the remaining cases, consider taking derivative w.r.t. λ on both sides of (5.3.24) at $\lambda = \lambda_+$, which is allowed since the discontinuities are only at $\lambda_-^{(n)}$. This gives:

$$\begin{aligned} \mathfrak{D}_z \Phi(z|\lambda_+) &= z^{\lambda_+} f_0'(\lambda_+) \\ \Phi(z|\lambda_+) &:= \partial_\lambda \Psi(z|\lambda)|_{\lambda=\lambda_+} = \log(z)\, \Psi(z|\lambda_+) + z^{\lambda_+} \sum_{k=1}^{\infty} \Psi_k'(\lambda_+)\, z^k. \end{aligned} \tag{5.3.27}$$

Case II ($\theta = 0$): In this case $\lambda_\pm = \lambda_* = 1/2$. Since $f_0'(\lambda_*) = 0$, $\Phi(z|\lambda_*)$ is another independent solution. A basis of solutions is therefore given by

$$\begin{aligned} \psi_{\text{nlog}}(z) &= \Psi(z|\lambda_*) \\ \psi_{\log}(z) &= \Phi(z|\lambda_*). \end{aligned} \tag{5.3.28}$$

Case III ($\theta = \frac{n}{2}$, $n \in \mathbb{Z}_{>0}$): In this case, one first observes that

$$\mathfrak{D}_z \Psi\left(z|\lambda_-^{(n)}\right) = z^{\lambda_+^{(n)}} \sum_{p=0}^{n-1} \Psi_p\left(\lambda_-^{(n)}\right) \mathfrak{l}_{p-n}. \tag{5.3.29}$$

Therefore another independent solution is given by a suitable linear combination of $\Psi\left(z|\lambda_-^{(n)}\right)$ and $\Phi\left(z|\lambda_+^{(n)}\right)$. Explicitly, a basis of solution is:

$$\begin{aligned} \psi_{\text{nlog}}(z) &= \Psi\left(z|\lambda_+^{(n)}\right) \\ \psi_{\log}(z) &= \Psi\left(z|\lambda_-^{(n)}\right) - \frac{\sum_{p=0}^{n-1} \Psi_p\left(\lambda_-^{(n)}\right) \mathfrak{l}_{p-n}}{f_0'(\lambda_+^{(n)})} \Phi\left(z|\lambda_+^{(n)}\right). \end{aligned} \tag{5.3.30}$$

Remark 5.3.1. Recall that only the $\Psi_{k<n}\left(\lambda_-^{(n)}\right)$ coefficients in the Frobenius expansion $\Psi\left(z|\lambda_-^{(n)}\right)$ are unambiguously determined, whereas the coefficients $\Psi_{k>n}\left(\lambda_-^{(n)}\right)$ depend on the arbitrary choice of $\Psi_n\left(\lambda_-^{(n)}\right)$. This arbitrary choice corresponds to shifting $\psi_{\log}(z)$ by an arbitrary multiple of $\psi_{\text{nlog}}(z)$. Therefore, there is an ambiguity in the non-logarithmic part of $\psi_{\log}(z)$, whereas the logarithmic part of $\psi_{\log}(z)$, which only involves $\Phi\left(z|\lambda_+^{(n)}\right)$ and $\Psi_{k<n}\left(\lambda_-^{(n)}\right)$, has no ambiguity.

Remark 5.3.2. The apparent singularity condition ASC_n is thus given by

$$\mathsf{ASC}_n = \sum_{p=0}^{n-1} \Psi_p\left(\lambda_-^{(n)}\right) \mathfrak{l}_{p-n} = 0\,, \tag{5.3.31}$$

with $\Psi_p\left(\lambda_-^{(n)}\right)$ understood to be defined via (5.3.23). This is alternative to the method discussed in §5.A. The first few expressions for ASC_n are listed in table 5.1.

Connection coefficients in logarithmic cases

We will be interested in the situation where θ_0 is generic while $\theta_x \in \mathbb{Z}/2$. In the logarithmic cases, we seek generalization of (5.3.18) to

$$\psi_\epsilon^{[0]}(z) = \mathsf{C}_{\epsilon\,\mathrm{log}}\,\psi_{\mathrm{log}}^{[x]}(z) + \mathsf{C}_{\epsilon\,\mathrm{nlog}}\,\psi_{\mathrm{nlog}}^{[x]}(z)\,. \tag{5.3.32}$$

Case II ($\theta_x = 0$): In this case, both $\psi_{\mathrm{log}}^{[x]}(z)$ and $\psi_{\mathrm{nlog}}^{[x]}(z)$ are unambiguously defined. So the connection coefficients $\mathsf{C}_{\epsilon\,\mathrm{log}}$ and $\mathsf{C}_{\epsilon\,\mathrm{nlog}}$ have no ambiguity.

Case III ($\theta_x = \frac{n}{2}$, $n \in \mathbb{Z}_{>0}$): In this case, as discussed in Remark 5.3.1, there is an ambiguity of shifting the non-logarithmic part of $\psi_{\mathrm{log}}^{[x]}(z)$ by arbitrary multiple of $\psi_{\mathrm{nlog}}^{[x]}(z)$. Therefore, only the connection coefficient $\mathsf{C}_{\epsilon\,\mathrm{log}}$ is unambiguously defined, with $\mathsf{C}_{\epsilon\,\mathrm{nlog}}$ subject to arbitrary shift.

Therefore, in both logarithmic cases, the connection coefficient $\mathsf{C}_{\epsilon\,\mathrm{log}}$ is unambiguously defined. It is only this type of connection coefficient that will appear in the definition of QNMs.

Fall-off coefficients

While the notion of connection coefficients is sufficient for defining QNMs, it will be necessary to use *fall-off coefficients* to define the thermal two-point function in one of the logarithmic cases due to the aforementioned ambiguity in connection coefficient. The fall-off coefficients are defined as follows in the three cases.

Case I ($\theta_x \notin \mathbb{Z}/2$):

$$\mathcal{C}_{\epsilon\,\mathrm{nor/nnor}} \;:=\; \psi_\epsilon^{[0]}(z)\Big|_{\mathrm{coeff}\left[(\mathsf{z}_x)^{\lambda_\pm}\right]} = \mathsf{C}_{\epsilon\pm}. \tag{5.3.33}$$

Here coeff$(\cdot)$ denotes the coefficient of $(\cdot)$ in the expansion near $z = x$, with $\mathtt{z}_x = z - x$.

Case II ($\theta_x = 0$):

$$\begin{aligned} \mathcal{C}_{\epsilon\,\mathrm{nor}} &:= \psi_\epsilon^{[0]}(z)\Big|_{\mathrm{coeff}\left[(\mathtt{z}_x)^{\lambda_*}\right]} = \mathsf{C}_{\epsilon\,\mathrm{nlog}}\,, \\ \mathcal{C}_{\epsilon\,\mathrm{nnor}} &:= \psi_\epsilon^{[0]}(z)\Big|_{\mathrm{coeff}\left[(\mathtt{z}_x)^{\lambda_*}\log \mathtt{z}_x\right]} = \mathsf{C}_{\epsilon\ \log}\,. \end{aligned} \tag{5.3.34}$$

Case III ($\theta_x = \frac{n}{2}$, $n \in \mathbb{Z}_{>0}$):

$$\begin{aligned} \mathcal{C}_{\epsilon\,\mathrm{nor}} &:= \psi_\epsilon^{[0]}(z)\Big|_{\mathrm{coeff}\left[(\mathtt{z}_x)^{\lambda+}\right]} = \mathsf{C}_{\epsilon\,\mathrm{nlog}} + \Psi_n\left(\lambda_-^{(n)}\right)\mathsf{C}_{\epsilon\,\log}\,, \\ \mathcal{C}_{\epsilon\,\mathrm{nnor}} &:= \psi_\epsilon^{[0]}(z)\Big|_{\mathrm{coeff}\left[(\mathtt{z}_x)^{\lambda-}\right]} = \mathsf{C}_{\epsilon\,\log}\,. \end{aligned} \tag{5.3.35}$$

Note that, despite the appearance, there is no ambiguity in $\mathcal{C}_{\epsilon\,\mathrm{nor}}$ by definition.

5.3.3. The connection formula in the s-channel expansion

We now proceed to the derivation of the s-channel connection formula, closely following [LN22]. The relevant object is the five-point Virasoro block with four non-degenerate vertex operators V_{P_i} and one degenerate vertex operator $V_{\langle 2,1\rangle}$. Without loss of generality, we can place the four non-degenerate vertex operators at 0, x, 1, and ∞. We will label the momenta by these loci for simplicity. The degenerate vertex operator will be inserted at z.

The fusion transformation and BPZ equation: Consider the five-point Virasoro blocks with insertion of degenerate representation $V_{\langle 2,1\rangle}(z)$ in the following channels:

$\mathcal{F}_\epsilon^{s,[0]}(z,x) :=$

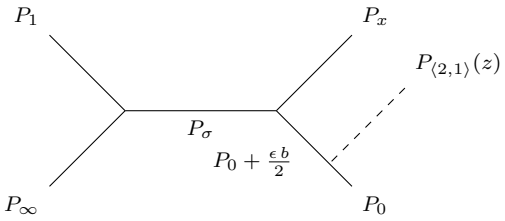

(5.3.36)

$$\mathcal{F}_{\epsilon}^{s,[x]}(z,x) :=$$

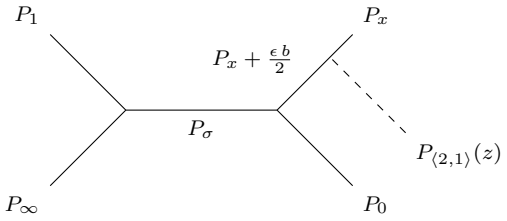

(5.3.37)

Here $\epsilon = \pm 1$ to succinctly account for the fusion relations (5.3.6). We will use P_σ to denote the momentum in the internal leg. This sets up our notation for the blocks in question.

By considering the OPE limits, $z \to 0$ and $z \to x$, respectively, we can simplify the above, and recover a leading behavior,

$$\mathcal{F}_{\epsilon}^{s,[0]}(z,x) \quad \xrightarrow{z\to 0} \quad z^{\frac{1+b^2}{2} - \epsilon\, b\, P_0}$$

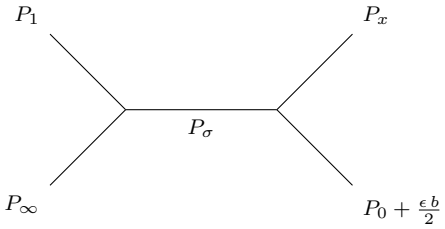

(5.3.38)

$$\mathcal{F}_{\epsilon}^{s,[x]}(z,x) \quad \xrightarrow{z\to x} \quad (z-x)^{\frac{1+b^2}{2} - \epsilon\, b\, P_x}$$

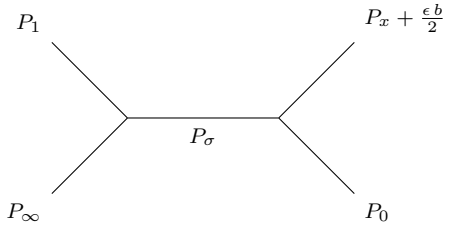

(5.3.39)

We already see the features of interest, viz., there are two scaling behaviors in this OPE limit as $z \to \{0, x\}$, which should be reminiscent of the local Frobenius basis of Heun's equation.

To make the connection precise, let us further recall that the degenerate blocks in the two channels are related by the degenerate fusion matrix,

$$\mathcal{F}_{\epsilon}^{s,[0]}(z,x) = \sum_{\epsilon'=\pm} \mathsf{F}_{\epsilon\epsilon'}\left(P_0, P_x, P_\sigma\right) \mathcal{F}_{\epsilon'}^{s,[x]}(z,x)\,, \tag{5.3.40}$$

where the fusion matrix $\mathsf{F}_{\epsilon\epsilon'}$ is as defined in (5.3.14). The final piece of data we need is that these degenerate blocks satisfy a BPZ decoupling equation (in any channel). This reads

$$\Big(b^{-2}\,\partial_z^2 + \mathcal{L}_{-2}\Big)\mathcal{F}(z,x) = 0\,, \tag{5.3.41}$$

with the differential operator $\mathcal{L}_{-2}$ being given by

$$\begin{aligned}\mathcal{L}_{-2} = \frac{h_0}{z^2} + \frac{h_1}{(z-1)^2} + \frac{h_x}{(z-x)^2} + \frac{h_\infty - h_{\langle 2,1\rangle} - h_0 - h_1 - h_x}{z\,(z-1)} \\ + \frac{x\,(x-1)}{z\,(z-1)\,(z-x)}\partial_x - \left(\frac{1}{z} + \frac{1}{z-1}\right)\partial_z\,.\end{aligned} \tag{5.3.42}$$

We now have all the ingredients necessary for relating the connection matrix of Heun's differential equation to these degenerate conformal blocks. The final step involves taking a suitable semiclassical limit.

The connection formula from semiclassical limit: Recall the previously-introduced semiclassical limit where we scale $b \to 0$, and let the momenta diverge as b^{-1}, cf. (5.3.11). The notation in (5.3.11) is suggestively intended to make the connection with (5.3.16) transparent. In such semiclassical limit, there are two important simplifications: Firstly, the degenerate blocks are expected to obey heavy-light factorization. Secondly, the heavy part is expected to exponentiate in the central charge c. Altogether, this implies

$$\mathcal{F}_\epsilon^{s,[i]}(z,x) \xrightarrow{\text{S.C.}} \mathcal{N}_\epsilon^{[i]}\,\psi_\epsilon^{[i]}(z)\,\exp\left[b^{-2}\,\mathcal{W}^s(x)\right], \quad i = 0, x\,. \tag{5.3.43}$$

Here $\mathcal{W}^s$ is the classical Virasoro block in s-channel, viz.,

$\mathcal{W}^s(x) :=$ 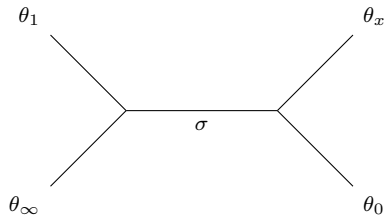

(5.3.44)

The normalization factor $\mathcal{N}_\epsilon^{[i]}$ comes from considering the OPE limits (5.3.38) and taking into account the shift in conformal weights due to fusion with the light degenerate operator,

$$\mathcal{N}_\epsilon^{[i]} = \exp\left[\frac{\epsilon}{2}\,\partial_{\theta_i}\mathcal{W}^s(x)\right]\,. \tag{5.3.45}$$

We are now in a position to state the connection formula. Note that the wave functions $\psi_\epsilon^{[i]}(z)$, with exponents $\frac{1}{2} - \epsilon\,\theta_i$ in the semiclassical limit, can be identified with the normalized Frobe-

nius solutions of Heun's equation. This is straightforward to see from the OPE limit (5.3.38). Moreover, one recovers Heun's equation (5.3.16) to leading order, $\mathcal{O}\big(b^{-2}\big)$, upon substituting the classical limit (5.3.43) into BPZ equation (5.3.41). In this limit, the accessory parameter is identified to be related to the classical Virasoro block, viz.,

$$\mathcal{E} = x\,\partial_x \mathcal{W}^s(x). \tag{5.3.46}$$

This is sometimes referred to as the *Zamolodchikov relation*.

The connection formula for $\psi_\epsilon^{[i]}(z)$ can then be derived from taking the semiclassical limit of (5.3.40). The degenerate fusion matrix has an obvious classical limit using (5.3.15),

$$\mathsf{F}_{\epsilon\epsilon'}\left(P_0, P_x, P_\sigma\right) \quad \xrightarrow{\text{S.C.}} \quad \mathsf{F}^{\text{cl}}_{\epsilon\epsilon'}\left(\theta_0, \theta_x, \sigma\right) = \frac{\Gamma\left(1-2\,\epsilon\,\theta_0\right)\,\Gamma\left(2\,\epsilon'\,\theta_x\right)}{\Gamma\left(\frac{1}{2}-\epsilon\,\theta_0+\epsilon'\,\theta_x\pm\sigma\right)}. \tag{5.3.47}$$

From this expression, we arrive at our sought for s-channel connection formula

$$\boxed{\begin{aligned}\mathsf{C}_{\epsilon\epsilon'} &= \mathsf{F}^{\text{cl}}_{\epsilon\epsilon'}\left(\theta_0, \theta_x, \sigma\right)\,\frac{\mathcal{N}_{\epsilon'}^{[x]}}{\mathcal{N}_{\epsilon}^{[0]}} \\ &= \frac{\Gamma\left(1-2\,\epsilon\,\theta_0\right)\Gamma\left(2\,\epsilon'\,\theta_x\right)}{\Gamma\left(\frac{1}{2}-\epsilon\,\theta_0+\epsilon'\,\theta_x\pm\sigma\right)}\,\exp\left[\frac{1}{2}\left(\epsilon'\,\partial_{\theta_x}-\epsilon\,\partial_{\theta_0}\right)\mathcal{W}^s(x)\right].\end{aligned}} \tag{5.3.48}$$

The key point to note is that the Liouville momentum σ appearing in the connection matrix is only defined implicitly through the Zamolodchikov relation (5.3.46). The connection matrix is clearly meromorphic; the poles arise from the Gamma functions. To understand the structure of this formula, we need to have a better handle on σ. We therefore turn to take a closer look at the Zamolodchikov relation.

Inverting the Zamolodchikov relation using semiclassical Virasoro block: Since the Zamolodchikov relation gives us a link between the accessory parameter and the classical Virasoro block, we can use it to obtain σ as an expansion in x. To this end, introduce

$$\sigma = \mathfrak{s} + \sum_{k=1}^{\infty} \sigma_k\, x^k\,, \qquad \sigma^{(n)} := \mathfrak{s} + \sum_{k=1}^{n} \sigma_k\, x^k\,, \tag{5.3.49}$$

where $\mathfrak{s}$ is the leading Liouville momentum. It is fixed by the leading OPE term in the classical Virasoro block

$$\mathfrak{s}^2 = \theta_0^2 + \theta_x^2 - \mathcal{E} - \frac{1}{4}\,. \tag{5.3.50}$$

From the Zamolodchikov relation, we further have,

$$\sigma^2 = \mathfrak{s}^2 + \sum_{k=1}^{\infty} k\,\mathcal{W}_k(\boldsymbol{\theta},\sigma)\,x^k\,. \tag{5.3.51}$$

This can be exploited to obtain the following recursion relation for σ_k:

$$\sigma_n = (2\mathfrak{s})^{-1}\left(\sum_{k=1}^{n} k\,\mathcal{W}_k\left(\boldsymbol{\theta},\sigma^{(n-1)}\right)\,x^k\Big|_{\text{coeff}[x^n]} - \sum_{k=1}^{n-1}\sigma_k\,\sigma_{n-k}\right), \tag{5.3.52}$$

where $|_{\text{coeff}[x^n]}$ denotes taking coefficient of x^n. For instance, first two terms read

$$\begin{aligned}\sigma_1 &= \frac{\mathcal{W}_1^s(\boldsymbol{\theta},\mathfrak{s})}{2\,\mathfrak{s}}\,,\\ \sigma_2 &= -\frac{\mathcal{W}_1^s(\boldsymbol{\theta},\mathfrak{s})^2 - 8\,\mathfrak{s}^2\,\mathcal{W}_2^s(\boldsymbol{\theta},\mathfrak{s}) - 2\,\mathfrak{s}\,\mathcal{W}_1^s(\boldsymbol{\theta},\mathfrak{s})\,\partial_\sigma\mathcal{W}_1^s(\boldsymbol{\theta},\mathfrak{s})}{8\,\mathfrak{s}^3}\,.\end{aligned} \tag{5.3.53}$$

The upshot is that the internal classical Liouville momentum σ is entirely fixed by external Liouville momenta, accessory parameter and Virasoro block data. We will use this in our analysis below to deduce properties of the thermal 2-point function.

To wrap up our discussion of the s-channel connection formula, let us record the behavior in the OPE limit $x \to 0$. We simply retain the leading terms in the above to find

$$\begin{aligned}&\sigma \to \mathfrak{s}\,,\\ &\mathsf{C}_{\epsilon\epsilon'} \to \frac{\Gamma\left(1-2\,\epsilon\,\theta_0\right)\Gamma\left(2\,\epsilon'\,\theta_x\right)}{\Gamma\left(\frac{1}{2}-\epsilon\,\theta_0+\epsilon'\,\theta_x\pm\mathfrak{s}\right)}x^{-\epsilon\,\theta_0+\epsilon'\,\theta_x}\,.\end{aligned} \tag{5.3.54}$$

The s-channel connection formula (5.3.48) is a particularly simple expression, especially when we compare with the t-channel expression, which we turn to next.

5.3.4. The connection formula in the t-channel expansion

While we already have the result using the s-channel conformal blocks, we can equivalently derive an expression in the t-channel. The t-channel expression will be useful for comparing with

the literature, and does have its own merits in application to black hole perturbation problems. The logic, however, is similar to the above, where we make use of the semiclassical limit of a degenerate Virasoro block.

To obtain the result we seek, we again consider the following three five-point degenerate Virasoro blocks:

$\mathcal{F}_{\epsilon}^{t,[0]}(z,x) \coloneqq$

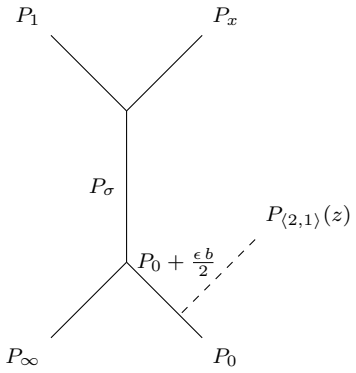

(5.3.55)

$\mathcal{F}_{\epsilon}^{t,[\sigma]}(z,x) \coloneqq$

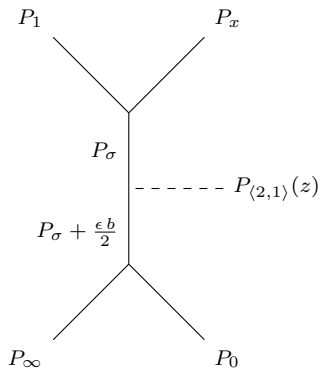

(5.3.56)

$\mathcal{F}_{\epsilon,\epsilon'}^{t,[x]}(z,x) \coloneqq$

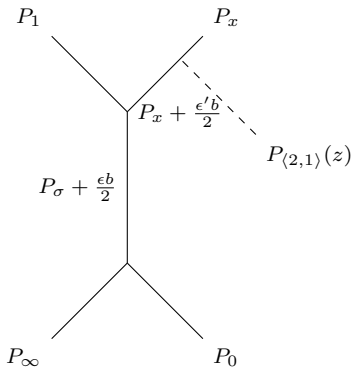

(5.3.57)

These degenerate blocks are related by the following fusion transformations

$$\begin{aligned}\mathcal{F}_{\epsilon}^{t,[0]} &= \sum_{\kappa=\pm} \mathsf{F}_{\epsilon\kappa}\left(P_0, P_\sigma, P_\infty\right) \mathcal{F}_{\kappa}^{t,[\sigma]}\,,\\ \mathcal{F}_{\kappa}^{t,[\sigma]} &= \sum_{\epsilon'=\pm} \mathsf{F}_{\bar{\kappa}\epsilon'}\left(P_\sigma + \frac{\kappa\, b}{2}, P_x, P_1\right) \mathcal{F}_{\kappa,\epsilon'}^{t,[x]}\,.\end{aligned} \tag{5.3.58}$$

In the second fusion, the convention relating the blocks is $\bar{\kappa} = -\kappa$. Putting the two together, we can relate the fusion between the degenerate operator and P_0 to that between the operator and P_x. All told, this gives

$$\mathcal{F}_{\epsilon}^{t,[0]} = \sum_{\kappa,\epsilon'=\pm} \mathsf{F}_{\epsilon\kappa}\left(P_0, P_\sigma, P_\infty\right) \mathsf{F}_{\bar{\kappa}\epsilon'}\left(P_\sigma + \frac{\kappa\, b}{2}, P_x, P_1\right) \mathcal{F}_{\kappa,\epsilon'}^{t,[x]} \,. \tag{5.3.59}$$

The connection formula we seek is derived by taking the semiclassical limit of (5.3.59). In the semiclassical limit, exploiting the heavy-light factorization and exponentiation of Virasoro lock, we obtain

$$\begin{aligned} \mathcal{F}_{\epsilon}^{t,[0]}(z,x) &\xrightarrow{\text{S.C.}} \mathcal{N}_{\epsilon}^{[0]}\, \psi_{\epsilon}^{[0]}(z)\, \exp\left[b^{-2}\, \mathcal{W}^t(x)\right] \,, \\ \mathcal{F}_{\kappa,\epsilon'}^{t,[x]}(z,x) &\xrightarrow{\text{S.C.}} \mathcal{N}_{\kappa,\epsilon'}^{[x]}\, \psi_{\epsilon'}^{[x]}(z)\, \exp\left[b^{-2}\, \mathcal{W}^t(x)\right] \,. \end{aligned} \tag{5.3.60}$$

Now $\mathcal{W}^t$ is the t-channel semiclassical Virasoro block,

$\mathcal{W}^t(x) \coloneqq$ 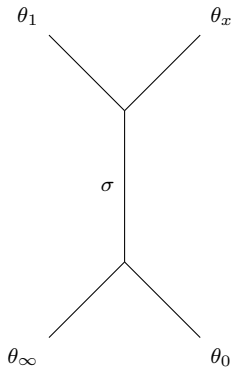

(5.3.61)

The normalization factors are determined by considering OPE limits similar to the s-channel case, and are given by

$$\mathcal{N}_{\epsilon}^{[0]} = \exp\left[\frac{\epsilon}{2}\, \partial_{\theta_0} \mathcal{W}^t(x)\right] , \qquad \mathcal{N}_{\kappa,\epsilon'}^{[x]} = \exp\left[\frac{1}{2}\left(\kappa\, \partial_\sigma + \epsilon'\, \partial_{\theta_x}\right) \mathcal{W}^t(x)\right] . \tag{5.3.62}$$

The degenerate blocks $\mathcal{F}(z,x)$ satisfy the BPZ equation in any channel. Therefore, for the same reason as in the s-channel case, the wave functions $\psi_{\epsilon}^{[i]}$ can be identified as normalized Frobenius solutions of Heun's equation. The accessory parameter is still identified via Zamolod-

chikov relation

$$\mathcal{E} = x\,\partial_x \mathcal{W}^t(x)\,. \tag{5.3.63}$$

Armed with this data, one then reads off the t-channel connection formula by taking the classical limit of (5.3.59). This results in

$$\boxed{\begin{aligned}\mathsf{C}_{\epsilon\epsilon'} &= \sum_{\kappa=\pm} \mathsf{F}^{\rm cl}_{\epsilon\kappa}\left(\theta_0,\sigma,\theta_\infty\right)\,\mathsf{F}^{\rm cl}_{\bar\kappa\epsilon'}\left(\sigma,\theta_x,\theta_1\right)\,\frac{\mathcal{N}^{[x]}_{\kappa,\epsilon'}}{\mathcal{N}^{[0]}_{\epsilon}}\,,\\ &= \sum_{\kappa=\pm}\frac{\Gamma\left(1-2\,\epsilon\,\theta_0\right)\Gamma\left(2\,\kappa\,\sigma\right)}{\Gamma\left(\frac{1}{2}-\epsilon\,\theta_0+\kappa\,\sigma\pm\theta_\infty\right)}\frac{\Gamma\left(1-2\,\bar\kappa\,\sigma\right)\Gamma\left(2\,\epsilon'\,\theta_x\right)}{\Gamma\left(\frac{1}{2}-\bar\kappa\,\sigma+\epsilon'\,\theta_x\pm\theta_1\right)}\\ &\qquad\qquad\times\exp\left[\frac{1}{2}\left(\kappa\,\partial_\sigma+\epsilon'\,\partial_{\theta_x}-\epsilon\,\partial_{\theta_0}\right)\mathcal{W}^t(x)\right].\end{aligned}} \tag{5.3.64}$$

Once again, the internal classical Liouville momentum σ appearing in the connection matrix is defined via the Zamolodchikov relation. This is a slightly more involved expression than the s-channel counterpart (5.3.48) because we had to convolve two successive fusion transformations.

Finally, let us record the behavior in the t-channel OPE limit $x \to 1$. Now the internal Liouville momentum simplifies to

$$\sigma \to \mathfrak{s}, \qquad \mathfrak{s}^2 = \theta_1^2+\theta_x^2+(1-x)\,\mathcal{E}-\frac{1}{4}\,. \tag{5.3.65}$$

We note that $(1-x)\mathcal{E}$ is finite as per the convention in (5.3.16).

When $\Re(\mathfrak{s}) \neq 0$, the sum over signs κ in $\mathsf{C}_{\epsilon\epsilon'}$ simplifies. The leading OPE part of t-channel block $\mathcal{W}^t(x)$ gives a factor $(1-x)^{-\kappa\mathfrak{s}}$. Choosing w.l.o.g. a sign convention such that $\Re(\mathfrak{s}) > 0$, the leading OPE contribution comes from the $\kappa = +$ term. One finds

$$\mathsf{C}_{\epsilon\epsilon'} \;\to\; \frac{\Gamma(1-2\,\epsilon\,\theta_0)\Gamma(2\,\mathfrak{s})}{\Gamma\left(\frac{1}{2}-\epsilon\,\theta_0+\mathfrak{s}\pm\theta_\infty\right)}\,\frac{\Gamma(1+2\,\mathfrak{s})\Gamma(2\,\epsilon'\,\theta_x)}{\Gamma\left(\frac{1}{2}+\mathfrak{s}+\epsilon'\,\theta_x\pm\theta_1\right)}(1-x)^{-\mathfrak{s}+\epsilon'\,\theta_x}+\mathcal{O}((1-x)^{\mathfrak{s}})\,. \tag{5.3.66}$$

5.3.5. The connection formula in the five-punctured case

We will also have occasion to need the generalization of (5.3.16) to five punctures. In this case, the normal form for the function $\mathtt{T}(z)$ is

$$\begin{aligned}\mathtt{T}(z) = \frac{\delta_0}{z^2} + \frac{\delta_1}{(z-1)^2} + \frac{\delta_x}{(z-x)^2} + \frac{\delta_{x'}}{(z-x')^2} + \frac{\delta_\infty - \delta_0 - \delta_1 - \delta_x - \delta_{x'}}{z\,(z-1)} \\ + \frac{(x-1)\,\mathcal{E}_x}{z\,(z-1)\,(z-x)} + \frac{(x'-1)\,\mathcal{E}_{x'}}{z\,(z-1)\,(z-x')}\,.\end{aligned} \tag{5.3.67}$$

We are still interested in the connection problem between $0, x$, which is as defined earlier. As explained in [LN22], thanks to locality of fusion transformation, the derivation of s-channel connection formula in the previous section can be immediately generalized to yield

$$\boxed{\mathsf{C}_{\epsilon\epsilon'} = \frac{\Gamma\left(1-2\,\epsilon\,\theta_0\right)\Gamma\left(2\,\epsilon'\,\theta_x\right)}{\Gamma\left(\frac{1}{2}-\epsilon\,\theta_0+\epsilon'\,\theta_x \pm \sigma\right)}\exp\left[\frac{1}{2}\left(\epsilon'\,\partial_{\theta_x} - \epsilon\,\partial_{\theta_0}\right)\mathcal{W}(x,x')\right]} \tag{5.3.68}$$

The semiclassical Virasoro block encountered here is

$\mathcal{W}(x,x') :=$ 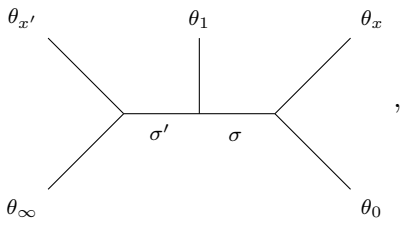

, (5.3.69)

Now the accessory parameters σ, σ' are defined implicitly by

$$\mathcal{E}_x = x\,\partial_x \mathcal{W}(x,x'), \qquad \mathcal{E}_{x'} = x'\,\partial_{x'}\mathcal{W}(x,x'). \tag{5.3.70}$$

5.3.6. The connection formula for an equation with an apparent singularity

We have thus far examined Fuchsian equation with four or five punctures. In order to have a complete characterization of the energy-momentum tensor correlation functions, we need one more ingredient: an analysis of equations with an apparent singular point or puncture. We recall that an apparent puncture is a local where the indicial exponents of the two Frobenius solutions are integers. Naively, one expects a logarithmic branch of solutions. If this is absent, owing to a fine-tuning of the parameters, then we have an apparent puncture. Such a locus is,

in fact, an ordinary point, with Taylor series solutions and no monodromy. The wave equation for the scalar polarization of the energy-momentum tensor in a neutral black hole background will turn out to be of this form. We will therefore generalize our considerations to include this case.

Apparent singularities and higher degenerate representations: Consider the analog of an equation with five punctures, as discussed above. One of these punctures, which we designate as $\mathfrak{x}$, will be the apparent puncture. The normal form of the equation in this case will be as in (5.3.67), which with some relabeling we write as

$$\begin{aligned}\mathtt{T}(z) = \frac{\delta_0}{z^2} + \frac{\delta_1}{(z-1)^2} + \frac{\delta_x}{(z-x)^2} + \frac{\delta_{\mathfrak{x}}}{(z-\mathfrak{x})^2} + \frac{\delta_\infty - \delta_0 - \delta_1 - \delta_x - \delta_{\mathfrak{x}}}{z\,(z-1)} \\ + \frac{(x-1)\,\mathcal{E}_x}{z\,(z-1)\,(z-x)} + \frac{(\mathfrak{x}-1)\,\mathcal{E}_{\mathfrak{x}}}{z\,(z-1)\,(z-\mathfrak{x})}\,.\end{aligned} \tag{5.3.71}$$

The new feature is that we let $\theta_{\mathfrak{x}} \in \mathbb{Z}/2$.

Generically, when the exponent at a singularity satisfies $\theta_{\mathfrak{x}} \in \mathbb{Z}/2$, the local solution has logarithmic singularity and the local monodromy matrix takes a Jordan form. The special non-generic case where such singularity with $\theta_{\mathfrak{x}} \in \mathbb{Z}/2$ has trivial monodromy is called apparent singularity. The condition for apparent singularity involves an algebraic relation between the weights and accessory parameters. The case with $\theta_{\mathfrak{x}} = 3/2$ is the one relevant for the scalar polarization (sound channel) of the stress tensor.

To illustrate the apparent singularity condition explicitly, consider the following expansion of stress-tensor around $\mathfrak{x}$:

$$\mathtt{T}(z) = \sum_{m=0}^{\infty} \mathfrak{l}_{-m}\,(z-\mathfrak{x})^{m-2}\,, \qquad \mathfrak{l}_{-m} \coloneqq \mathrm{Res}_{z=\mathfrak{x}}\left[(z-\mathfrak{x})^{1-m}\mathtt{T}(z)\right]\,. \tag{5.3.72}$$

The apparent singularity conditions for $\theta_{\mathfrak{x}} = s/2$ can be expressed in terms of these expansion coefficients $\mathfrak{l}_{-m}$. Explicit forms for the first few values of s are given in table 5.1.

s	ASC_s (=0)
2	$\mathfrak{l}_{-1}^2 + \mathfrak{l}_{-2}$
3	$\frac{1}{4}\mathfrak{l}_{-1}^3 + \mathfrak{l}_{-1}\mathfrak{l}_{-2} + \mathfrak{l}_{-3}$
4	$\frac{1}{36}\mathfrak{l}_{-1}^4 + \frac{5}{18}\mathfrak{l}_{-1}^2\mathfrak{l}_{-2} + \frac{1}{4}\mathfrak{l}_{-2}^2 + \frac{2}{3}\mathfrak{l}_{-1}\mathfrak{l}_{-3} + \mathfrak{l}_{-4}$

Table 5.1.: The apparent singularity conditions (ASC) for $\theta_{\mathfrak{r}} = s/2$ tabulated for the first few non-trivial values of s.

To derive the connection formula in presence of such apparent singularity in the large-c CFT approach, we need to know the corresponding heavy CFT operator at this locus. The answer is the following:

$$\boxed{\text{Apparent singularity with } \theta_{\mathfrak{r}} = \frac{s}{2} \longleftrightarrow \text{Insertion of } V_{\langle 1,s\rangle}(\mathfrak{r})} \tag{5.3.73}$$

To justify this, a shortcut is to consider the fusion rule between the light probe $V_{\langle 2,1\rangle}$ and the heavy operator $V_{\langle 1,s\rangle}$ [GW12]:

$$V_{\langle 2,1\rangle} \times V_{\langle 1,s\rangle} = V_{\langle 2,s\rangle}. \tag{5.3.74}$$

As only one fusion is allowed, it must be that the monodromy is trivial. Alternatively, one can justify this by showing that the BPZ equation for $V_{\langle 1,s\rangle}$ in the semiclassical limit reproduces the apparent singularity condition ASC_s; see §5.A for more details.

Degenerate blocks with apparent punctures: Now that we identified the presence of an apparent singularity with a higher degenerate operator, we can examine the BPZ equation. To do so consider the following Virasoro blocks with insertion of both $V_{\langle 2,1\rangle}$ and $V_{\langle 1,s\rangle}$:

$$\mathcal{F}_{\epsilon}^{[0]}(z,x,\mathfrak{r}) := \tag{5.3.75}$$

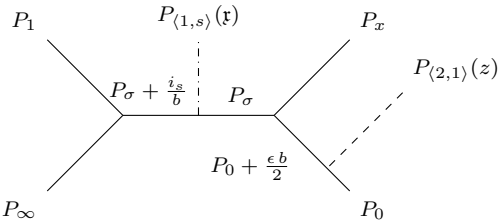

$$\mathcal{F}_{\epsilon}^{[x]}(z,x,\mathfrak{x}) \coloneqq$$ 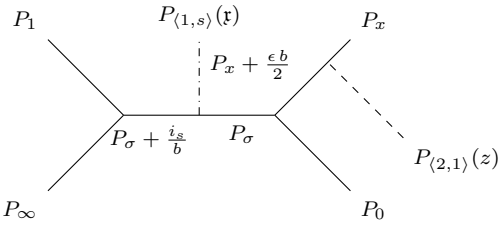

(5.3.76)

Here i_s takes s possible values $i_s = -\frac{s-1}{2}, \cdots, \frac{s-1}{2}$ due to fusion rule of $V_{\langle 1,s\rangle}$. Thanks to the locality of fusion transformation, the two Virasoro blocks are related by the same fusion matrix as before, viz.,

$$\mathcal{F}_{\epsilon}^{[0]}(z,x,\mathfrak{x}) = \sum_{\epsilon'=\pm} \mathsf{F}_{\epsilon\epsilon'}\left(P_0,P_x,P_\sigma\right)\, \mathcal{F}_{\epsilon'}^{[x]}(z,x,\mathfrak{x})\,, \tag{5.3.77}$$

where the fusion matrix F is the same as in (5.3.14). The BPZ equation for $V_{\langle 2,1\rangle}$ now reads

$$\left(b^{-2}\,\partial_z^2 + \mathcal{L}_{-2}\right)\mathcal{F}(z,x,\mathfrak{x}) = 0\,, \tag{5.3.78}$$

with the differential operator $\mathcal{L}_{-2}$ now taking the form

$$\begin{aligned}\mathcal{L}_{-2} = \frac{h_0}{z^2} + \frac{h_1}{(z-1)^2} + \frac{h_x}{(z-x)^2} + \frac{h_{\mathfrak{x}}}{(z-\mathfrak{x})^2} + \frac{h_\infty - h_{\langle 2,1\rangle} - h_0 - h_1 - h_x - h_{\mathfrak{x}}}{z(z-1)} \\ + \frac{x\,(x-1)}{z\,(z-1)\,(z-x)}\partial_x + \frac{\mathfrak{x}\,(\mathfrak{x}-1)}{z\,(z-1)\,(z-\mathfrak{x})}\partial_{\mathfrak{x}} \quad - \left(\frac{1}{z}+\frac{1}{z-1}\right)\partial_z\,.\end{aligned} \tag{5.3.79}$$

The connection formula from the semiclassical limit: We can now take the classical limit of (5.3.77) to derive the connection formula between $0, x$. The exponentiation of Virasoro block and heavy-light factorization is expected to hold here, even with the additional insertion of heavy degenerate operator (as in the standard case). The classical limit of the blocks now reads

$$\mathcal{F}_{\epsilon}^{[i]}(z,x,\mathfrak{x}) \quad \xrightarrow{\text{S.C.}} \quad \mathcal{N}_{\epsilon}^{[i]}\,\psi_{\epsilon}^{[i]}(z)\,\exp\left[b^{-2}\,\mathcal{W}(x,\mathfrak{x})\right]\,, \qquad i=0,\,x\,. \tag{5.3.80}$$

where the block in question is itself

$$\mathcal{W}(x,\mathfrak{x}) \coloneqq$$ 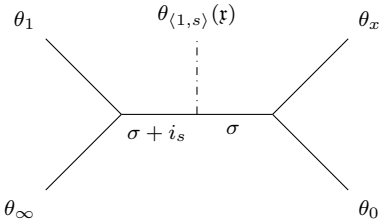

(5.3.81)

The normalization factor, as before, is

$$\mathcal{N}_{\epsilon}^{[i]} = \exp\left[\frac{\epsilon}{2}\,\partial_{\theta_i}\mathcal{W}(x,\mathfrak{x})\right]\,. \tag{5.3.82}$$

The identification of the wavefunctions $\psi_{\epsilon}^{[i]}$ with the normalized Frobenius solutions of the generalized Heun's equation (5.3.71) continues to hold, and the Zamolodchikov relation is generalized to

$$\mathcal{E}_x = x\,\partial_x\mathcal{W}(x,\mathfrak{x}), \qquad \mathcal{E}_{\mathfrak{x}} = \mathfrak{x}\,\partial_{\mathfrak{x}}\mathcal{W}(x,\mathfrak{x}). \tag{5.3.83}$$

The connection formula is then read off from the classical limit of (5.3.77) to be

$$\boxed{\begin{aligned}\mathsf{C}_{\epsilon\epsilon'} &= \mathsf{F}^{\rm cl}_{\epsilon\epsilon'}\left(\theta_0,\theta_x,\sigma\right)\,\frac{\mathcal{N}_{\epsilon'}^{[x]}}{\mathcal{N}_{\epsilon}^{[0]}}\\ &= \frac{\Gamma\left(1-2\,\epsilon\,\theta_0\right)\,\Gamma\left(2\,\epsilon'\theta_x\right)}{\Gamma\left(\frac{1}{2}-\epsilon\,\theta_0+\epsilon'\,\theta_x\pm\sigma\right)}\,\exp\left[\frac{1}{2}\left(\epsilon'\,\partial_{\theta_x}-\epsilon\,\partial_{\theta_0}\right)\mathcal{W}(x,\mathfrak{x})\right]\end{aligned}} \tag{5.3.84}$$

Now both σ and i_s need to be determined from the generalized Zamolodchikov relation.

5.4. Exact results for thermal 2-point functions and QNMs in AdS_5

We are now ready to apply the technology reviewed in §5.3 to obtain exact results for thermal 2-point functions of 4d holographic CFTs. These theories have a dual gravitational description in terms of Einstein-Hilbert gravity AdS_5. As a concrete example, one can view the results as being relevant for the thermal correlators of $\mathcal{N}=4$ SYM in the strong 't Hooft coupling regime.

While we will consider the correlation functions of scalar operators of such CFTs, our primary interest is in understanding correlation functions of the energy-momentum tensor. The stress tensor is dual to the bulk graviton. The latter has a universal low-energy description in terms of pure Einstein-Hilbert gravity in five dimensions, thanks to consistent truncation in string or supergravity compactifications. The results we derive for the stress tensor correlator are therefore are universally valid for the large class of (super)conformal holographic field theories. In this section, we will summarize the equations of interest, and relate them to the Fuchsian equations studied using 2d CFT techniques in §5.3. We illustrate the results with some examples along the way.

5.4.1. Black hole wave equations

Since we reviewed the technology for carrying out real-time computations in holography, we will present the wave equations in a form adapted to that discussion. We will later convert them to the form amenable to using the connection formulae. We also record these in general AdS_{d+1} black hole spacetimes, despite our focus on the $d = 4$ case.

The basic wave equation is a variation of the minimally coupled scalar wave equation, given by,

$$\frac{1}{r^{\mathcal{M}}}\mathbb{D}_+\left(r^{\mathcal{M}}\,\mathbb{D}_+\varphi\right)+\left(\omega^2-\lambda_\Sigma\, f-m^2\, r^2 f\right)\,\varphi=0\,. \tag{5.4.1}$$

Here λ_Σ is either $\ell(\ell+d-2)$ on $\mathbf{S}^{d-1}$ or k^2 on $\mathbb{R}^{d-1}$. For $\mathcal{M}=d-1$ and $m^2\neq 0$, we have a massive Klein-Gordon scalar, dual to a conformal primary of weight $\Delta=\frac{d}{2}+\sqrt{\frac{d^2}{4}+m^2\,\ell_{\text{AdS}}^2}$ of the boundary CFT.

The equation also captures polarizations of the stress tensor dual to components of the linearized graviton wave equations.

- The $\frac{1}{2}\,d\,(d-3)$ transverse tensor polarizations of stress tensor are obtained for $\mathcal{M}=d-1$ and $m^2=0$.
- The $d-2$ transverse vector polarizations of the stress tensor are obtained for $\mathcal{M}=1-d$ and $m^2=0$.

We also note that abelian conserved currents dual to bulk Maxwell fields are described by the equation with $m^2=0$; transverse vector polarizations have $\mathcal{M}=d-3$, while scalar polarization has $\mathcal{M}=3-d$ [GLPRSV21]. In the analysis below, we refer to the minimally coupled massive scalar as the Klein-Gordon scalar, and designate $\mathcal{M}\neq d-1$ as the designer massless scalar.

The scalar polarization of the stress tensor (the energy density operator), on the other hand, satisfies on $\mathbb{R}^{d-1,1}$ the following equation [HLRSV22]:

$$\begin{aligned} r^{d-3}\,\Lambda_k(r)^2\,\mathbb{D}_+\left(\frac{1}{r^{d-3}\,\Lambda_k(r)^2}\,\mathbb{D}_+\mathcal{Z}\right)+\left(\omega^2-k^2 f\left[1-\frac{d\,(d-2)\,r_+^d}{r^{d-2}\,\Lambda_k(r)}\right]\right)\mathcal{Z}=0\,,\\ \Lambda_k(r)=k^2+\frac{d-1}{2}\,r^3\,f'(r)\,. \end{aligned} \tag{5.4.2}$$

The corresponding equation for $\Sigma_{d-1} = \mathbf{S}^{d-1}$ is a bit more involved and can be found in [KI03]. For analogous equations in the case of charged black holes, see Appendix A of [LRV23] in the case of $\mathbb{R}^{d-1,1}$ and [KI04] for the spherically symmetric case.

5.4.2. Heun's oper from radial wave equation

The radial wave equation (5.4.1) in AdS_5, with complexified radial coordinate, can be generically mapped to Heun's oper on Riemann sphere $\mathbb{P}^1$ with four regular punctures, reproduced below for convenience:

$$\begin{aligned}
&\psi''(z) + \mathtt{T}(z)\,\psi(z) = 0\,,\\
&\mathtt{T}(z) = \frac{\delta_0}{z^2} + \frac{\delta_1}{(z-1)^2} + \frac{\delta_x}{(z-x)^2} + \frac{\delta_\infty - \delta_0 - \delta_1 - \delta_x}{z\,(z-1)} + \frac{(x-1)\,\mathcal{E}}{z\,(z-1)\,(z-x)}\,,\\
&\delta_i = \frac{1}{4} - \theta_i^2\,.
\end{aligned} \tag{5.4.3}$$

The punctures correspond to physical locations in the black hole geometry, such as the AdS boundary, the inner or outer horizons, curvature singularity, and additionally complex horizon loci due to complexification of radial coordinate. For a classification of the punctures, in the case of Schwarzschild-AdS_{d+1} and Reissner-Nordström-AdS_{d+1} black holes, we refer the reader to [LRV23]. In dimensions $d > 4$ one would encounter a larger number of punctures, but the CFT method should in principle apply as it relies solely on locality of fusion transformation. As noted, for concreteness and simplicity, we will focus on the AdS_5 case.

To recast the radial equation (5.4.1) to Heun's oper, we first pass to the static coordinates outside the horizon (viz., $t = v - \int \frac{dr}{r^2\,f(r)}$). We then perform the following coordinate transformation:

$$z = x\,\frac{r^2 - r_+^2}{r^2 - r_-^2}, \qquad x = \frac{r_{\rm c}^2 - r_-^2}{r_{\rm c}^2 - r_+^2}. \tag{5.4.4}$$

Here $r_{\rm c} \in i\mathbb{R}$ is the complex horizon satisfying $f(r_{\rm c}) = 0$, and $r_\pm$ are the outer and inner horizons, respectively. The transformation applies to both the neutral and charged black holes with spherical or planar horizons. The uncharged case corresponds to $r_- = 0$. The transformation recasts the radial equation (5.4.1) into a second-order ODE in z coordinate, $\Psi''(z) + p(z)\,\Psi'(z) + q(z)\,\Psi(z)$, with four regular singularities. The ODE is then transformed into the canonical Schrödinger form of Heun's oper by the standard transformation $\Psi(z) = \psi(z)\,e^{-\frac{1}{2}\int^z p(z')\,dz'}$,

with $\mathtt{T}(z) = q(z) - \frac{p^2(z)}{4} - \frac{p'(z)}{2}$.

General features: Before giving explicit expressions for Heun's parameters in various cases, let us take stock on some features. The physical meaning of the regular punctures differs between the charged and neutral black holes, but is independent of the horizon topology. For simplicity, in the case of the Klein-Gordon scalar with $\mathcal{M} = 3$, one has

$$\{0, x, 1, \infty\} \sim \begin{cases} \{r_+,\, \text{bdy},\, r_{\text{c}},\, \text{curv}\} & \text{uncharged black holes} \\ \{r_+,\, \text{bdy},\, r_{\text{c}},\, r_-\} & \text{charged black holes} \end{cases} \tag{5.4.5}$$

where curv denotes the curvature singularity. In particular, the curvature singularity does not appear as a puncture in Heun's oper for Klein-Gordon scalar around a charged AdS black hole. However, for $\mathcal{M} \neq 3$, we will indeed encounter an additional puncture in the charged case at the curvature singularity.

With a choice of sign conventions, the local monodromy exponents or classical Liouville momenta can be shown to have the following general features:

$$\theta_{r_\pm} \in i\omega\mathbb{R}_{\geq 0}, \qquad \theta_{\text{bdy}} \in \mathbb{R}_{\geq 0}, \qquad \theta_{r_{\text{c}}} \in \omega\mathbb{R}_{\geq 0}, \qquad \theta_{\text{curv}} \in \mathbb{R}_{\geq 0}\,. \tag{5.4.6}$$

In the following, we will also denote $\theta_{r_+} \equiv \theta_{\text{hor}}$. In particular,

$$\theta_{\text{hor}} = \frac{i\,\omega}{4\pi\,T}\,, \tag{5.4.7}$$

where T is the temperature of the black hole. The local solution with characteristic exponents $\frac{1}{2} \pm \theta_{\text{hor}}$ corresponds to outgoing and ingoing waves at the (outer) horizon. The local solutions with $\frac{1}{2} \pm \theta_{\text{bdy}}$ correspond to normalizable and non-normalizable modes at the boundary, respectively. For certain choices of matter, the conformal dimension of the dual operator Δ can be an integer, in which case our assumption of $\theta_i \notin \mathbb{Z}/2$ breaks down. We will treat these cases with a suitable limit procedure (this will of import for energy-momentum tensor correlators).

The angular or spatial momentum appears in the accessory parameter $\mathcal{E}$, which is generically

a degree two polynomial in frequency and momentum. The cross-ratio lies in the range

$$x \in [1/2, 1) \tag{5.4.8}$$

For the neutral Schwarzschild-AdS$_5$ black hole $x = \frac{1}{2}$. The t-channel OPE limit $x \to 1$ turns out to correspond to the small black hole or near-extremal limit. In particular, the s-channel OPE limit $x \to 0$ doesn't appear as a physical limit in the black hole perturbation problem.

In the following, we give explicit Heun's parameters in a few representative examples, to illustrate distinct features in the resulting Heun's opers to which the 2d CFT method will be universally applied. It is straightforward to obtain the Heun's parameters in more examples not listed below.

Planar black holes: For the planar black hole, i.e., in the large black hole limit, it is convenient to define the following dimensionless frequency and spatial momentum

$$\mathfrak{w} = \frac{\omega}{2\, r_+}, \quad \mathfrak{q} = \frac{|\mathbf{k}|}{2\, r_+}. \tag{5.4.9}$$

Neutral planar black hole: In this case, the metric function $f(r) = 1 - \frac{r_+^4}{r^4}$ has two pairs of roots at r_+ and $r_c = i r_+$, giving $x = \frac{1}{2}$. The parameters for the associated Heun's opers of Klein-Gordon and the designer massless scalar are listed in table 5.2. In particular, they have identical accessory parameters, only differing in $\theta_{\rm bdy}(x)$ and $\theta_{\rm curv}(\infty)$. We use the notation $\theta(\cdot)$ to denote the location of the puncture with Liouville momentum θ.

	$\theta_{\rm hor}(0)$	$\theta_{\rm bdy}(x)$	$\theta_{r_c}(1)$	$\theta_{\rm curv}(\infty)$	x	$\mathcal{E}$
Klein-Gordon scalar	$\frac{i\,\mathfrak{w}}{2}$	$\frac{\Delta-2}{2}$	$\frac{\mathfrak{w}}{2}$	0	$\frac{1}{2}$	$\mathfrak{q}^2 - \mathfrak{w}^2$
Designer massless scalar	-	$\frac{\lvert\mathbb{M}+1\rvert}{4}$	-	$\frac{\lvert\mathbb{M}-3\rvert}{4}$	-	-

Table 5.2.: Heun's parameters for a massive Klein-Gordon scalar and a designer massless scalar in uncharged planar Schwazschild-AdS$_5$ black hole, with $\theta(\cdot)$ used to denote the location of the puncture with Liouville momentum θ.

Charged planar black hole: The metric function $f(r)$ for the planar Reissner-Nordström-AdS$_5$

has three pairs of roots. We can parameterize it as

$$f(r) = \frac{(r^2 - r_+^2)\,(r^2 - r_-^2)\,(r^2 - r_{\rm c}^2)}{r^6}, \qquad r_{\rm c} = i\, r_i\,, \tag{5.4.10}$$

with $r_\pm, r_i \in \mathbb{R}_{\geq 0}$ related by

$$\frac{r_-}{r_+} = \sqrt{-\frac{1}{2} + \sqrt{\frac{1}{4} + Q^2}}, \qquad \frac{r_i}{r_+} = \sqrt{\frac{1}{2} + \sqrt{\frac{1}{4} + Q^2}}\,. \tag{5.4.11}$$

Here Q is a dimensionless parameter measuring the charge, and extremal limit is attained for $Q_{\rm ext} = \sqrt{2}$.

The cross-ratio x is now given by

$$x = \frac{r_i^2 + r_-^2}{r_i^2 + r_+^2} \;\in\; [1/2, 1)\,. \tag{5.4.12}$$

We see that the near-extremal limit $Q \to Q_{\rm ext}$, therefore, corresponds to the t-channel OPE limit $x \to 1$.

For completeness, we list below the Heun's parameters for a probe massive Klein-Gordon scalar dual to a boundary operator of dimension Δ (through the usual relation $m^2 = \Delta(\Delta - 4)$)

$$\begin{aligned}
\theta_{\rm hor}(0) &= \left|\frac{1}{r_+^2\, f'(r_+)}\right| i\,\omega = \frac{r_+^4}{(r_i^2 + r_+^2)(r_+^2 - r_-^2)}\, i\,\mathfrak{w}\,,\\
\theta_{\rm bdy}(x) &= \frac{\Delta - 2}{2}\,,\\
\theta_{r_{\rm c}}(1) &= \left|\frac{1}{r_{\rm c}^2 f'(r_{\rm c})}\right| \omega = \frac{r_i^3\, r_+}{(r_i^2 + r_+^2)\,(r_i^2 + r_-^2)}\,\mathfrak{w}\,,\\
\theta_{r_-}(\infty) &= \left|\frac{1}{r_-^2\; f'(r_-)}\right| i\,\omega = \frac{r_-^3\, r_+}{(r_i^2 + r_-^2)\,(r_+^2 - r_-^2)}\, i\,\mathfrak{w}\,,\\
\mathcal{E} &= \frac{1}{4\,(r_+^2 - r_-^2)}\Big[r_+^2\,\left(4\,\mathfrak{q}^2 - 4\,\mathfrak{w}^2 + m^2 + 2\right) - r_-^2\,(\Delta - 2)^2 - r_i^2\,\left(2 + m^2\right)\Big]\,.
\end{aligned} \tag{5.4.13}$$

One can indeed verify that setting $Q = 0$ reproduces the Heun's parameters in neutral case. The singular behavior of $\mathcal{E}$ as $Q \to Q_{\rm ext}$ is an artifact of the convention in Heun's oper (5.3.16) as $x \to 1$.

Global black holes: We can similarly recast the equations for global (i.e., spherically symmetric) black holes in AdS_5. For simplicity, we mainly focus on the Schwarzschild-AdS_5 case.

Neutral spherical black hole. In this case, the metric function reads

$$f(r) = \frac{\ell_{\text{AdS}}^2}{r^2}\left[1 + \frac{r^2}{\ell_{\text{AdS}}^2} - \frac{r_+^2}{r^2}\left(1 + \frac{r_+^2}{\ell_{\text{AdS}}^2}\right)\right]. \tag{5.4.14}$$

The $\ell_{\text{AdS}} \to 0$ limit recovers the planar black hole metric function. We set $\ell_{\text{AdS}} = 1$ hereafter for convenience. The complex horizon is located at $r_{\text{c}} = i\sqrt{1 + r_+^2}$, giving the cross-ratio

$$x = \frac{1 + r_+^2}{1 + 2\,r_+^2} \;\in\; [1/2, 1)\,. \tag{5.4.15}$$

The small black hole limit $r_+ \to 0$ therefore corresponds to t-channel OPE limit $x \to 1$, and the large black hole limit $r_+ \to \infty$ corresponds to the planar black hole value $x = \frac{1}{2}$.

Explicit expressions for the Heun's parameters for a massive Klein-Gordon scalar are

$$\begin{aligned}
\theta_{\text{hor}}(0) &= \frac{r_+}{2 + 4\,r_+^2}\, i\,\omega\,, \\
\theta_{\text{bdy}}(x) &= \frac{\Delta - 2}{2}\,, \\
\theta_{r_{\text{c}}}(1) &= \frac{\sqrt{1 + r_+^2}}{2 + 4\,r_+^2}\,\omega\,, \\
\theta_{\text{curv}}(\infty) &= 0\,, \\
\mathcal{E} &= \frac{\lambda_{\mathbf{S}^3} - \omega^2 - \Delta\,(\Delta - 4) - 2}{4\,r_+^2}\,.
\end{aligned} \tag{5.4.16}$$

The spherical harmonic eigenvalue is captured $\lambda_{\mathbf{S}^3} = l(l+2)$, and the mass has been traded for the conformal dimension Δ. The $r_+ \to \infty$ limit indeed recovers the planar black hole values. The singular behavior of $\mathcal{E}$ as $r_+ \to 0$ is once again an artifact of the convention in Heun's oper (5.3.16) as $x \to 1$.

5.4.3. Universal exact expressions for QNMs and holographic thermal 2-point functions

We are now ready to present an exact result for the holographic correlator at finite temperature. To this end, we recall from our review in §5.2.1 that the boundary 2-point function $K(\omega)$ is given by the solution to a connection problem (5.2.6). This version of the result, which we have argued is justified by a more careful contour prescription, is well-adapted to our differential equation analysis.

Let is start by noting that local Frobenius solutions at $z_{\rm hor} = 0$ corresponds to ingoing and outgoing solutions, respectively, which behave as

$$\psi_{\rm in/out}(z) = \psi_{\pm}^{[0]}(z) = z^{\frac{1}{2} \mp \theta_{\rm hor}} \, (1 + \cdots) \, . \tag{5.4.17}$$

On the other hand, the local Frobenius solutions at $z_{\rm bdy} = x$ correspond to the normalizable/non-normalizable solutions, and take the form

$$\psi_{\rm nor/nnor}(z) = \psi_{\mp}^{[x]}(z) = (z-x)^{\frac{1}{2} \pm \theta_{\rm bdy}} \, (1 + \cdots) \tag{5.4.18}$$

We have assumed $\theta_{\rm bdy} \notin \mathbb{Z}/2$ to keep the discussion generic.[8]

Consider the connection problem between the (outer) horizon and boundary. Fixing the ingoing solutions at the horizon, we have using the notation for connection matrix in §5.3

$$\psi_{\rm in}(z) = \mathsf{C}_{\rm in,nor} \, \psi_{\rm nor}(z) + \mathsf{C}_{\rm in,nnor} \, \psi_{\rm nnor}(z) = \mathsf{C}_{+-} \, \psi_{\rm nor}(z) + \mathsf{C}_{++} \, \psi_{\rm nnor}(z) \tag{5.4.19}$$

The retarded Greens function for holographic thermal two-point function and the quantization condition for QNMs are then defined by

$$\begin{aligned} K(\omega) &:= \mathfrak{f}\,(\theta_{\rm bdy}) \, \frac{\mathsf{C}_{\rm in,nor}}{\mathsf{C}_{\rm in,nnor}} = \mathfrak{f}\,(\theta_{\rm bdy}) \, \frac{\mathsf{C}_{+-}}{\mathsf{C}_{++}} \, , \\ \text{QNMs:} \quad & \mathsf{C}_{\rm in,nnor} = \mathsf{C}_{++} = 0 \, . \end{aligned} \tag{5.4.20}$$

We explicitly are using the observation that the QNMs are poles in the thermal retarded Green's

[8] For $\theta_{\rm bdy} \in \mathbb{Z}/2$ we would have a logarithmic branch to the solution. It will prove convenient to arrive at the result in this case by deforming Δ or equivalently $\theta_{\rm bdy}$.

function. The prefactor $\mathfrak{f}(\theta_{\rm bdy})$ needs to be determined by holographic renormalization. Since it depends solely on the scaling dimension Δ it has no effect on the analytic structure of the thermal correlation function.

Exact QNM and correlator in the s-channel: Having identified the relation between the black hole wave equation, which determines the thermal 2-point function and the connection formulae determined using 2d CFT techniques, we can now give the result for the thermal correlator. One can directly use s-channel connection formula explained in §5.3 to obtain

$$K(\omega)=\mathfrak{f}(\theta_{\rm bdy})\,\frac{\Gamma(-2\,\theta_{\rm bdy})}{\Gamma(2\,\theta_{\rm bdy})}\,\frac{\Gamma\left(\frac{1}{2}-\theta_{\rm hor}+\theta_{\rm bdy}\pm\sigma\right)}{\Gamma\left(\frac{1}{2}-\theta_{\rm hor}-\theta_{\rm bdy}\pm\sigma\right)}\,\exp\left[-\partial_{\theta_{\rm bdy}}\mathcal{W}^{s}(x)\right]\,. \tag{5.4.21}$$

We emphasize that the result holds when $\theta_{\rm bdy}\notin\frac{\mathbb{Z}}{2}$. We also are implicitly using the Zamolodchikov relation (5.3.46) for the accessory parameter. Finally, to be concrete, the s-channel semiclassical Virasoro block in this context itself is given by

$\mathcal{W}^{s}(x)=$ 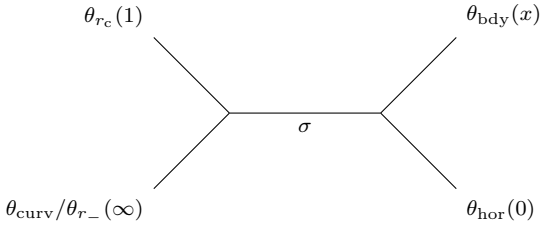

(5.4.22)

As explained earlier, the internal classical Liouville momentum σ needs to be determined from the Zamolodchikov relation (5.3.46). Using the inversion of Zamolodchikov relation, cf. §5.3, we are led to the following cross-ratio expansion for internal Liouville momentum σ:

$$\begin{aligned}\sigma\left(\boldsymbol{\theta},\mathcal{E}\right)&=\mathfrak{s}+\sum_{k=1}^{\infty}\sigma_{k}\left(\boldsymbol{\theta},\mathcal{E}\right)\,x^{k}\,,\\ \mathfrak{s}^{2}&=\theta_{\rm hor}^{2}+\theta_{\rm bdy}^{2}-\mathcal{E}-\frac{1}{4}\end{aligned} \tag{5.4.23}$$

The expansion coefficients $\sigma_k\left(\boldsymbol{\theta},\mathcal{E}\right)$ are fixed by the expansion coefficients $\mathcal{W}_k^s\left(\boldsymbol{\theta},\sigma\right)$ in classical Virasoro block. The first two terms can be found in (5.3.53). From the result, or directly from the definition of QNMs in terms of connection coefficient, we deduce an exact quantization condition for QNMs of the black hole. To wit,

$$\text{QNMs} = \left\{ \omega \;\middle|\; \frac{1}{2} - \theta_{\text{hor}} + \theta_{\text{bdy}} \pm \sigma\left(\boldsymbol{\theta}, \mathcal{E}\right) = -n, \quad n \in \mathbb{Z}_{\geq 0} \right\} \tag{5.4.24}$$

The universality of the answers (5.4.21) and thence (5.4.24) is manifest. Different types of holographic thermal correlators correspond to variations in the dependence of external classical Liouville momenta θ_i and accessory parameter $\mathcal{E}$. But this simply translates to deducing how to relate this data to the black hole parameters, which once done, solves the problem completely.

The logarithmic cases with $\theta_{\text{bdy}} \in \mathbb{Z}/2$: So far we have only defined thermal two-point functions and QNMs via (5.4.20) for $\theta_{\text{bdy}} \notin \mathbb{Z}/2$, and the results (5.4.21) and (5.4.24) are derived in this regime. Now we address the case $\theta_{\text{bdy}} \in \mathbb{Z}/2$, which in fact corresponds to most of the physical examples. The general mathematical properties in this situation with logarithmic solution were discussed in §5.3.2. In this situation, the normalizable/non-normalizable solutions at AdS boundary are the non-logarithmic/logarithmic solutions, respectively, viz.,

$$\psi_{\text{nor}}(z) = \psi_{\text{nlog}}(z)\,, \qquad \psi_{\text{nnor}}(z) = \psi_{\text{log}}(z)\,, \tag{5.4.25}$$

where the non-logarithmic and logarithmic solutions are as defined in §5.3.2, with two distinct cases. The connection problem relevant for our purpose is then,

$$\psi_{\text{in}}(z) = \mathsf{C}_{\text{in,nor}}\,\psi_{\text{nor}}(z) + \mathsf{C}_{\text{in,nnor}}\,\psi_{\text{nnor}}(z) = \mathsf{C}_{+\text{nlog}}\,\psi_{\text{nlog}}(z) + \mathsf{C}_{+\,\text{log}}\,\psi_{\text{log}}(z)\,. \tag{5.4.26}$$

As explained in §5.3.2, the connection coefficient $\mathsf{C}_{+\,\text{log}}$ is unambiguously defined in both cases, whereas $\mathsf{C}_{+\text{nlog}}$ has ambiguity in one of the cases. The QNMs can then be defined, in both logarithmic cases, as

$$\text{QNMs:} \quad \mathsf{C}_{\text{in,nnor}} = \mathsf{C}_{+\,\text{log}} = 0\,. \tag{5.4.27}$$

Claim 5.4.1. *The QNMs in logarithmic cases ($\theta_{\text{bdy}} \in \mathbb{Z}/2$), defined by (5.4.27), obey the same exact quantization condition (5.4.24) as in the non-logarithmic case ($\theta_{\text{bdy}} \notin \mathbb{Z}/2$).*

We have the following reasoning and evidence supporting this claim:

- *The analogue of the claim holds in the BTZ case (cf. §5.4.6).* In the familiar example of minimally-coupled scalar in BTZ background, the logarithmic cases correspond to $\Delta \in \mathbb{Z}$.

The analogue of the exact quantization condition (5.4.24) is a simple algebraic equation (cf. (5.4.56)) that holds in both non-logarithmic and logarithmic cases.

- *The exact quantization condition* (5.4.24) *is continuous in* θ_{bdy}*, and so is the QNM spectrum.* While the expression for exact two-point function (5.4.21) is singular at $\theta_{\text{bdy}} \in \mathbb{Z}/2$ due to the prefactor from degenerate fusion matrix, the associated semiclassical Virasoro block (5.4.22) is not, since in general Virasoro block is expected to be analytic in external weights. Therefore, the internal Liouville momentum σ appearing in the exact quantization condition (5.4.24) can still be defined from inverting Zamolodchikov relation, and hence the continuity of the condition (5.4.24) in θ_{bdy}. Physically, θ_{bdy} corresponds to a mass parameter, in which the QNM spectrum should be continuous.

- *The claim can be verified by explicit computation of QNMs.* In the following, we will perform explicit computation of QNMs using the exact quantization condition (5.4.24) in various examples with $\theta_{\text{bdy}} \in \mathbb{Z}/2$, and find good agreement with numerical data.

The situation for two-point function is more subtle in the logarithmic cases:

- **Case II** ($\theta_{\text{bdy}} = 0$)**:** In this case there is no ambiguity in $\mathsf{C}_{+\,\text{nlog}}$, and the two-point function can be defined as

$$K(\omega) \coloneqq \mathfrak{f}(\theta_{\text{bdy}}) \frac{\mathsf{C}_{\text{in,nor}}}{\mathsf{C}_{\text{in,nnor}}} = \mathfrak{f}(\theta_{\text{bdy}}) \frac{\mathsf{C}_{+\,\text{nlog}}}{\mathsf{C}_{+\,\log}} \tag{5.4.28}$$

- **Case III** ($\theta_{\text{bdy}} = \frac{n}{2}$, $n \in \mathbb{Z}_{>0}$)**:** In this case $\mathsf{C}_{+\,\text{nlog}}$ can no longer be unambiguously defined. The two-point function should instead be defined in terms of the fall-off coefficients defined in §5.3.2:

$$K(\omega) \coloneqq \mathfrak{f}(\theta_{\text{bdy}}) \frac{\mathcal{C}_{\text{in,nor}}}{\mathcal{C}_{\text{in,nnor}}} = \mathfrak{f}(\theta_{\text{bdy}}) \frac{\mathsf{C}_{+\,\text{nlog}} + \Psi_n\left(\lambda_-^{(n)}\right) \mathsf{C}_{+\,\log}}{\mathsf{C}_{+\,\log}} \tag{5.4.29}$$

  Here we remind that the combination $\mathsf{C}_{+\,\text{nlog}} + \Psi_n\left(\lambda_-^{(n)}\right) \mathsf{C}_{+\,\log}$ has no ambiguity.

As was done for QNMs, we would like to obtain the two-point functions in the logarithmic cases, defined by (5.4.28) and (5.4.29), from the non-logarithmic exact expression (5.4.21). The extra

subtlety compared to the QNM case is that, unlike the exact quantization condition (5.4.24), the expression (5.4.21) is no longer continuous in θ_{bdy}.

Claim 5.4.2. *The exact holographic thermal two-point functions in logarithmic cases ($\theta_{\text{bdy}} \in \mathbb{Z}/2$), defined by (5.4.28) and (5.4.29), can be obtained from the exact two-point function in non-logarithmic case ($\theta_{\text{bdy}} \notin \mathbb{Z}/2$) (5.4.21), by extracting the regular part in the singular limit $\theta_{\text{bdy}} \to \mathbb{Z}/2$.*

Our main evidence for the claim is that the analogous statement holds in the BTZ case, and that the additional semiclassical Virasoro block factor in (5.4.21) would not give extra singular behavior apart from the Gamma function factor as long as the internal Liouville momentum doesn't correspond to a degenerate representation, viz., $\sigma \in \mathbb{Z}/2$, which we assume to be the case.

Remark 5.4.1. It should be possible, and is desirable, to give a direct justification of Claim 5.4.1 by generalizing the CFT method discussed here to *logarithmic CFT*. Such a generalization could also facilitate direct evaluation of exact two-point functions in the logarithmic cases without the need for taking the singular limit as in Claim 5.4.2.

QNM expansion in s-channel: The s-channel exact quantization condition (5.4.24) can be used to solve QNMs as an expansion in the cross-ratio parameter x:

$$\omega_n = \sum_{k=0}^{\infty} \omega_n^{(k)}\, x^k, \qquad n \in \mathbb{Z}_{\geq 0}. \tag{5.4.30}$$

This is done by substituting the cross-ratio expansion (5.4.23) for σ and the QNM expansion (5.4.30) to the quantization condition (5.4.24) to solve $\omega_n^{(k)}$ order by order in x. In general, the leading coefficient $\omega_n^{(0)}$ is fixed by the OPE limit, and the higher-order coefficients are recursively determined in terms of $\omega_n^{(0)}$. The QNM expansion is thus fixed by semiclassical Virasoro block data.

Example 5.4.1 (Scalar fields in the planar Schwarzschild-AdS$_5$ black hole)**.** For concreteness, we present explicit forms of the first two terms of the QNM expansion for both Klein-Gordon and designer scalar fields propagating in the neutral black hole spacetime. For planar horizons,

we have $\theta_{\rm hor} = \frac{i\,\mathfrak{w}}{2}$, $\theta_{r_c} = \frac{\mathfrak{w}}{2}$, and $\mathcal{E} = \mathfrak{q}^2 - \mathfrak{w}^2$. The expansion coefficients as a function of overtone number n read

$$\begin{aligned}
\mathfrak{w}_n^{(0)} &= \frac{1}{2}\left[\pm\sqrt{1+3\,\mathfrak{n}^2+4\,\mathfrak{q}^2+6\,\mathfrak{n}\,\theta_{\rm bdy}-\theta_{\rm bdy}^2} - (\mathfrak{n}+\theta_{\rm bdy})\,i\right], \qquad \mathfrak{n} = n+\frac{1}{2}\,, \\
\mathfrak{w}_n^{(1)} &= \frac{i\left(1+2\,\mathfrak{q}^2-2\left(\mathfrak{w}_n^{(0)}\right)^2-4\,\theta_{\rm bdy}^2\right)\left(1+2\,\mathfrak{q}^2-2\left(\mathfrak{w}_n^{(0)}\right)^2-2\,\theta_{\rm bdy}^2+2\,\theta_{\rm curv}^2\right)}{\left(2+4\,\mathfrak{q}^2-3\left(\mathfrak{w}_n^{(0)}\right)^2-4\,\theta_{\rm bdy}^2\right)\left(-3\,i\,\mathfrak{w}_n^{(0)}+\sqrt{-1-4\,\mathfrak{q}^2+3\,\mathfrak{w}_n^{(0)}+4\,\theta_{\rm bdy}^2}\right)}\,.
\end{aligned} \tag{5.4.31}$$

As is the case for $\mathfrak{w}_n^{(1)}$, all higher-order expansion coefficients are recursively determined from the leading term $\mathfrak{w}_n^{(0)}$, which is fixed by OPE limit.

The s-channel OPE limit, per se, doesn't correspond to a physical limit in the QNM problem. Nevertheless, the QNM-type spectral problem is still well-defined if we take the limit $x \to 0$ in the Heun's oper associated with these scalar probes. The first two terms in the QNM expansion above can indeed be checked to agree with the numerical spectrum in the $x \to 0$ limit.

At the physical value $x = \frac{1}{2}$, the comparison between the QNM expansion and numerics is shown for

- A Klein-Gordon scalar with $\Delta = 4$ at $\mathfrak{q} = 0$ in table 5.3.
- Both Klein-Gordon scalar with $\Delta = 4$ and designer scalars with $\mathcal{M} = -1$ and $\mathcal{M} = -3$, respectively, at $\mathfrak{q} = 3$ in Fig. 5.2.

In those cases, we find good agreement with numerical results for the QNMs.

There, however, appears to be a convergence issue when applying the QNM expansion to designer scalars at small $\mathfrak{q}$, the regime where hydrodynamic modes enter the low-lying part of the QNM spectrum. This issue deserves further investigation.

n	$k_{\max}=2$	$k_{\max}=4$	$k_{\max}=6$	Num
0	$\pm 1.37-1.15i$	$\pm 1.47-1.29i$	$\pm 1.51-1.34i$	$\pm 1.56-1.37i$
1	$\pm 2.41-1.90i$	$\pm 2.49-2.14i$	$\pm 2.51-2.24i$	$\pm 2.58-2.38i$

Table 5.3.: Comparison between QNMs $\mathfrak{w}_n$ computed using QNM expansion (5.4.30) and known numerical values for a Klein-Gordon scalar in the planar Schwarzschild-AdS$_5$ background. We have chosen $\Delta=4, \mathfrak{q}=0$ for illustration. Here k_{max} is the order of truncation in the cross-ratio expansion (5.4.30). This data supports Claim 5.4.1 that the quantization condition (5.4.24) continues to holds for $\theta_{\rm bdy}\in\mathbb{Z}/2$. The numerical values can be found in, e.g., Table 1 of [NS03], or readily computed using numerical packages such as [Jan17].

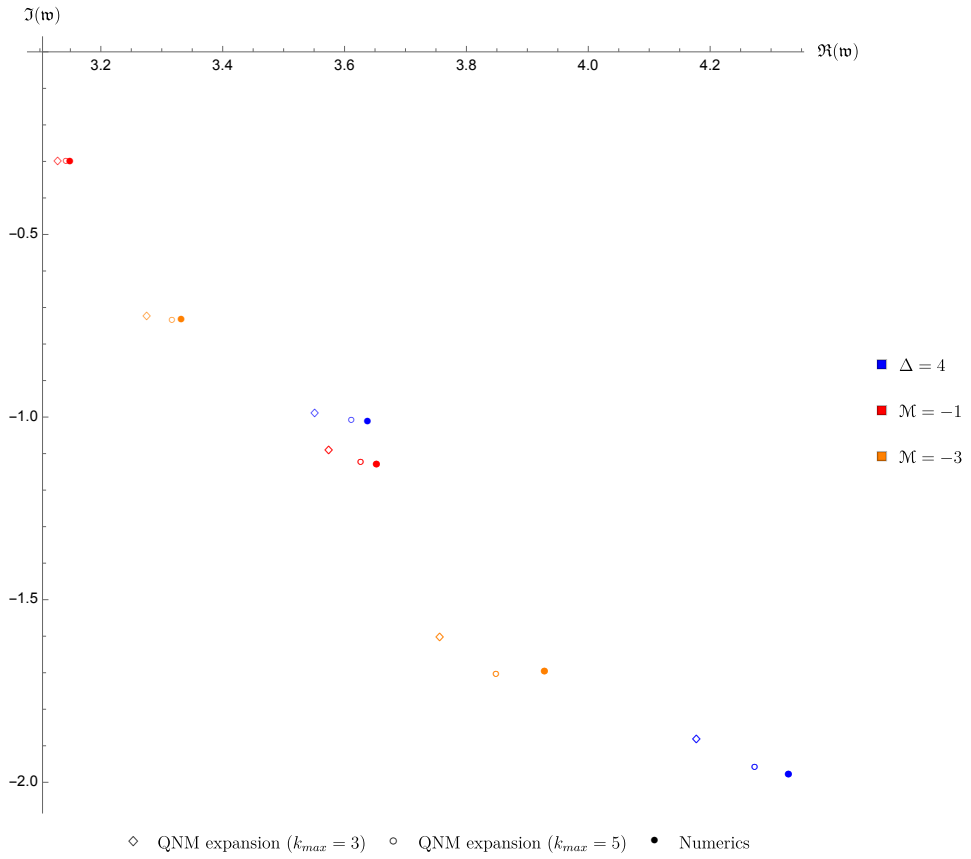

Figure 5.2.: Comparison between QNM expansion and numerics for the first two QNMs $(\mathfrak{w}_0,\mathfrak{w}_1)$ at $\mathfrak{q}=3$ for Klein-Gordon scalar with $\Delta=4$ (massless scalar perturbation), and designer scalars with $\mathcal{M}=-1$ (scalar polarization of gauge field perturbation) and $\mathcal{M}=-3$ (vector polarization of metric perturbation). Here k_{max} is the order of truncation in the cross-ratio expansion (5.4.30). The $\Re(\mathfrak{w})\geq 0$ part of the QNM spectrum is shown. This data again supports Claim 5.4.1 that the quantization condition (5.4.24) continues to holds for $\theta_{\rm bdy}\in\mathbb{Z}/2$.

Remark 5.4.2. Using the expansion of Virasoro block in terms of elliptic nome $q=e^{-\pi K(1-x)/K(x)}$ should allow faster convergence for the QNM expansion. It would also be useful to further study the convergence property of the QNM expansion.

Exact QNM and correlator: t-channel: We can equivalently use the t-channel connection formula obtained in §5.3. This yields

$$\boxed{K(\omega) = \mathfrak{f}\left(\theta_{\rm bdy}\right) \frac{\mathsf{A}\left(-\theta_{\rm bdy}\right)}{\mathsf{A}\left(\theta_{\rm bdy}\right)} \exp\left[-\partial_{\theta_{\rm bdy}} \mathcal{W}^t(x)\right]} \ , \tag{5.4.32}$$

where we defined

$$\mathsf{A}\left(\theta_{\rm bdy}\right) := \sum_{\kappa=\pm} \frac{\Gamma(1-2\,\theta_{\rm hor})\Gamma(2\,\kappa\,\sigma)}{\Gamma\left(\frac{1}{2}-\theta_{\rm hor}+\kappa\,\sigma\pm\theta_{\bullet}\right)} \frac{\Gamma(1+2\,\kappa\,\sigma)\Gamma(2\,\theta_{\rm bdy})}{\Gamma\left(\frac{1}{2}+\kappa\,\sigma+\theta_{\rm bdy}\pm\theta_{r_{\rm c}}\right)} \exp\left[\frac{\kappa}{2}\,\partial_\sigma \mathcal{W}^t(x)\right] \ . \tag{5.4.33}$$

Here $\theta_{\bullet} = \theta_{\rm curv}/\theta_{r_-}$ and we continue to assume that $\theta_{\rm bdy} \notin \frac{\mathbb{Z}}{2}$. The internal Liouville momentum σ is again implicitly defined via Zamolodchikov relation $\mathcal{E} = x\,\partial_x \mathcal{W}^t(x)$. The t-channel semiclassical Virasoro block here is

$\mathcal{W}^t(x) =$ 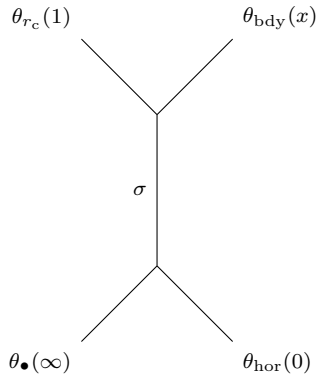

. (5.4.34)

From here, or directly from definition of QNMs in terms of connection coefficient, we deduce that in the t-channel exact quantization condition for QNMs is given by $\mathsf{A}\left(\theta_{\rm bdy}\right) = 0$, which can be written more explicitly as

$$\boxed{\begin{aligned} &\text{QNMs} = \left\{\omega \,\middle|\, \frac{\mathfrak{A}(\sigma)}{\mathfrak{A}(-\sigma)} = -\exp\left[-\partial_\sigma \mathcal{W}^t(x)\right]\right\} \ , \\ &\mathfrak{A}(\sigma) = \Gamma(2\,\sigma)\,\Gamma(1+2\,\sigma)\,\Gamma\left(\frac{1}{2}-\theta_{\rm hor}-\sigma\pm\theta_{\bullet}\right)\,\Gamma\left(\frac{1}{2}-\sigma+\theta_{\rm bdy}\pm\theta_{\bullet}\right) . \end{aligned}} \tag{5.4.35}$$

We are leaving the dependence of internal Liouville momentum σ on $\boldsymbol{\theta}, \mathcal{E}$ implicit for simplicity.

t-channel OPE limit: The t-channel expression for the exact quantization takes a more complicated form than its s-channel counterpart, but considerably simplifies in the OPE limit $x \to 1$.

In fact, the limit is physically more relevant for the black hole perturbation problem than the s-channel one. In this limit, using the solution to the internal momentum σ, cf. (5.3.65),

$$\sigma \to \mathfrak{s}, \quad \mathfrak{s}^2 = \theta_{r_c}^2 + \theta_{\text{bdy}}^2 + (1-x)\,\mathcal{E} - \frac{1}{4}. \tag{5.4.36}$$

As discussed in §5.3, if $\Re(\mathfrak{s}) \neq 0$, one of the terms in the sum over κ in connection matrix (C_{++} in this case) dominates in the OPE limit. With the sign convention $\Re(\mathfrak{s}) > 0$, the $\kappa = +$ term dominates. Alternatively, one can also directly observe that r.h.s. of the exact quantization condition in (5.4.35) scales as $(1-x)^{\mathfrak{s}} \to 0$ in the OPE limit. The QNM spectrum in the OPE limit is thus determined to be

$$\text{QNMs} \to \left\{ \omega \middle| \frac{1}{2} - \theta_{\text{hor}} + \mathfrak{s} \pm \theta_\bullet = -n \;\text{ or }\; \frac{1}{2} + \mathfrak{s} + \theta_{\text{bdy}} \pm \theta_{r_c} = -n, \quad n \in \mathbb{Z}_{\geq 0},\ \Re(\mathfrak{s}) > 0 \right\}. \tag{5.4.37}$$

There are two simple examples which illustrate these general considerations, the small neutral black hole limit, and the near-extermal limit. In both cases, we will examine the wave equation for a Klein-Gordon scalar with mass set by the dimension Δ.

Example 5.4.2 (Small black hole limit [DGIPZ22])**.** In the $x \to 1$ ($r_+ \to 0$) limit,

$$\theta_{\text{hor}} \to 0, \quad \theta_{r_c} \to \frac{\omega}{2}, \quad (1-x)\,\mathcal{E} \to \frac{\lambda_{\mathbf{S}^3} - \omega^2 - \Delta\,(\Delta-4) - 2}{4} \tag{5.4.38}$$

with $\theta_{\text{bdy}} = \frac{\Delta-2}{2}, \theta_{\text{curv}} = 0$. One then finds

$$\mathfrak{s} = \frac{l+1}{2}. \tag{5.4.39}$$

The first condition in (5.4.37) turns out not to have a solution. The second recovers the normal mode spectrum in AdS_5 at leading order,

$$\omega_n = \pm(2n + l + \Delta). \tag{5.4.40}$$

Example 5.4.3 (Near-extremal planar black hole)**.** Consider the Klein-Gordon equation for a massive uncharged scalar in the planar Reissner-Nordström-AdS_5 geometry. In the near-

extremal limit ($Q \to Q_{\rm ext} = \sqrt{2}$), the Heun parameters are

$$\begin{aligned} \theta_{\rm hor} &\to \frac{i\,\mathfrak{w}}{2\sqrt{2}\,(Q_{\rm ext}-Q)} + \frac{i\,\mathfrak{w}}{8}\,, \\ \theta_{r_{\rm c}} &\to \frac{2\sqrt{2}}{9}\,\mathfrak{w}\,, \\ \theta_{r_-} &\to \frac{i\,\mathfrak{w}}{2\sqrt{2}\,(Q_{\rm ext}-Q)} - \frac{19}{72}\,i\,\mathfrak{w}\,, \\ (1-x)\,\mathcal{E} &\to \frac{\mathfrak{q}^2}{3} - \frac{\mathfrak{w}^2}{3} - \frac{\Delta\,(\Delta-4)}{6} - \frac{1}{2}\,. \end{aligned} \tag{5.4.41}$$

with $\theta_{\rm bdy} = \frac{\Delta-2}{2}$. At finite $\mathfrak{w}$, this is a confluent limit leading to irregular puncture instead of a degenerate/OPE limit due to the divergence of $\theta_{\rm hor}, \theta_{r_-}$. In particular, one may check that in this limit the first few terms of the block coefficients scale as $\mathcal{W}_k^t \sim (Q_{\rm ext}-Q)^{-k} \sim (1-x)^{-k}$ and therefore cannot be ignored when solving the Zamolodchikov relation. However, we may take the $Q \to Q_{\rm ext}$ limit at small frequency $\mathfrak{w} = \mathcal{O}(Q_{\rm ext}-Q)$ so that all Liouville momenta are finite and the OPE analysis still applies.

One then finds

$$\mathfrak{s}^2 = -\frac{19}{81}\,\mathfrak{w}^2 + \frac{\mathfrak{q}^2}{3} + \frac{m^2}{12} + \frac{1}{4} \simeq \frac{\mathfrak{q}^2}{3} + \frac{\Delta\,(\Delta-4)}{12} + \frac{1}{4}. \tag{5.4.42}$$

where $\simeq$ denotes to leading order in $Q_{\rm ext}-Q$. Solving the first condition in (5.4.37) with a negative sign to the leading order in $Q_{\rm ext}-Q$, we find,

$$\mathfrak{w}_n = -i\frac{Q_{\rm ext}-Q}{\sqrt{2}}\left(2\,n+1+\sqrt{1+\frac{\Delta\,(\Delta-4)}{3}+\frac{4\,\mathfrak{q}^2}{3}}\right), \tag{5.4.43}$$

while other conditions in (5.4.37) don't admit solutions. To the best of our knowledge, the analytic form (5.4.43) of the purely decaying modes in near-extremal limit is new in the literature, and we find good agreement with numerics. The oscillation/Christmas-tree-type modes (cf. Fig. 5.3) are not visible in this OPE analysis, as they are at finite $\mathfrak{w}$ in the $Q \to Q_{\rm ext}$ limit.

5.4.4. An example with five punctures: conserved currents at finite density

As discussed in §5.4.1 the designer scalar equations in Reissner-Nordström-AdS$_5$ capture the dynamics of conserved currents. In particular, the scalar and vector polarization of gauge

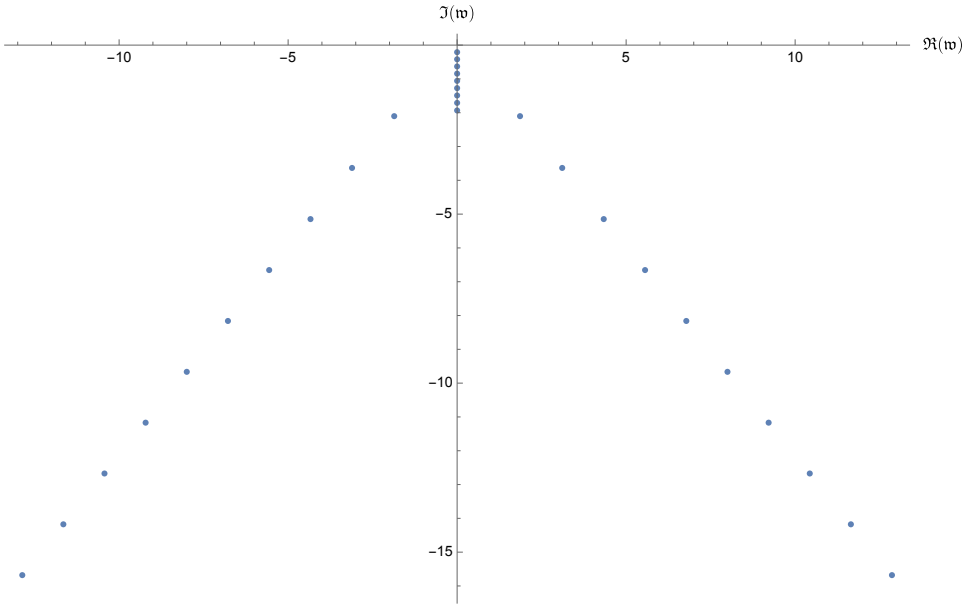

Figure 5.3.: Numerically computed QNM spectrum for massless uncharged scalar at zero momentum in near-extremal planar black hole background with $Q/Q_{\rm ext} = .9$. The purely decaying modes are well-described by (5.4.43) obtained via OPE analysis, equally spaced with gap $\sim Q_{\rm ext} - Q \sim T$. The oscillation/Christmas-tree-type modes at finite $\mathfrak{w}$ are not visible in the OPE analysis; see main text for more explanations. We also find good agreement between (5.4.43) and numerics for purely decaying modes in near-extremal limit at more generic masses and momenta. The numerical spectra were computed using the numerical package of [Jan17].

field perturbations, which are dual to the boundary global current, and the vector polarization of metric perturbation dual to the momentum flux operator, correspond to the radial wave equation (5.4.1) with $\mathcal{M} = -1, 1, -3$, respectively. The tensor polarization of energy-momentum tensor is equivalent to a massless Klein-Gordon scalar with $\mathcal{M} = 3$. Since there is a background charge, the equations capture the response of such currents at finite density.[9]

The radial wave equation (5.4.1) for designer scalar with $\mathcal{M} \neq 3$ on the planar Reissner-Nordström-AdS$_5$ black hole background is mapped to a (generalized) Heun's oper with five punctures, with aid of the transformation (5.4.4). The normal form of $\mathtt{T}(z)$ for this five punctured case can be found in (5.3.67).

The additional puncture at x' turns out to correspond to the curvature singularity. The two cross-ratios in this case lie in the range

$$x = \frac{r_i^2 + r_-^2}{r_i^2 + r_+^2} \in [1/2, 1)\,, \qquad x' = \frac{r_i^2 + r_-^2}{r_i^2 + r_+^2}\,\frac{r_+^2}{r_-^2} \in (1, \infty). \tag{5.4.44}$$

[9] In the case of gauge dynamics, the global current of the holographic CFT is different from the one that has background charge density. The equations for $\mathcal{M} = \pm 1$ should be viewed as that for a probe Maxwell field in the Reissner-Nordström-AdS$_5$ background, unrelated to the one sourcing the solution.

The near-extremal limit corresponds to both approaching unity, $x, x' \to 1$. The generalized Heun's parameters can be determined to be

$$\begin{aligned}
\theta_{\rm hor}(0) &= \left|\frac{1}{r_+^2 f'(r_+)}\right| i\,\omega = \frac{r_+^4}{(r_i^2+r_+^2)\,(r_+^2-r_-^2)}\, i\,\mathfrak{w}\,,\\
\theta_{\rm bdy}(x) &= \frac{|\mathcal{M}+1|}{4}\\
\theta_{r_{\rm c}}(1) &= \left|\frac{1}{r_{\rm c}^2 f'(r_{\rm c})}\right| \omega = \frac{r_i^3\, r_+}{(r_i^2+r_+^2)\,(r_i^2+r_-^2)}\,\mathfrak{w}\,,\\
\theta_{\rm curv}(x') &= \frac{|\mathcal{M}-5|}{4}\,,\\
\theta_{r_-}(\infty) &= \left|\frac{1}{r_-^2 f'(r_-)}\right| i\,\omega = \frac{r_-^3 r_+}{(r_i^2+r_-^2)\,(r_+^2-r_-^2)}\, i\,\mathfrak{w}\,,\\
\mathcal{E}_x &= \frac{1}{8\,(r_+^2-r_-^2)}\Big[2\,r_+^2\,\big(4\mathfrak{q}^2-4\mathfrak{w}^2+\mathcal{M}-1\big)-r_-^2\,\big(\mathcal{M}^2-1\big)-2\,r_i^2\,(\mathcal{M}-1)\Big]\,,\\
\mathcal{E}_{x'} &= \frac{\mathcal{M}-3}{8\,r_i^2\,\big(r_+^2-r_-^2\big)}\,\big(-2\,r_+^2\,r_-^2+2\,r_-^2\,r_i^2+(\mathcal{M}-5)\,r_+^2\,r_i^2\big)\,.
\end{aligned}$$

As a simple sanity check, we note that for $\mathcal{M}=3$, which corresponds to a Klein-Gordon scalar, the puncture at x' is removed.

The physical cases with $\mathcal{M}=-1,1,-3$ correspond to $\theta_{\rm bdy}\in\mathbb{Z}/2$, and therefore the connection formula for five punctures in §5.3 cannot be directly applied. Nonetheless, we can first consider generic $\mathcal{M}$ so that the connection formula can be applied to yield

$$K=\mathfrak{f}\,(\theta_{\rm bdy})\,\frac{\Gamma\,(-2\,\theta_{\rm bdy})}{\Gamma\,(2\,\theta_{\rm bdy})}\,\frac{\prod_\pm\Gamma\left(\frac{1}{2}-\theta_{\rm hor}+\theta_{\rm bdy}\pm\sigma\right)}{\prod_\pm\Gamma\left(\frac{1}{2}-\theta_{\rm hor}-\theta_{\rm bdy}\pm\sigma\right)}\exp\left[-\partial_{\theta_{\rm bdy}}\mathcal{W}(x,x')\right]\,,\quad \theta_{\rm bdy}\notin\frac{\mathbb{Z}}{2}.\tag{5.4.45}$$

Here the semiclassical Virasoro block is in the following channel

$$\mathcal{W}(x,x')=$$

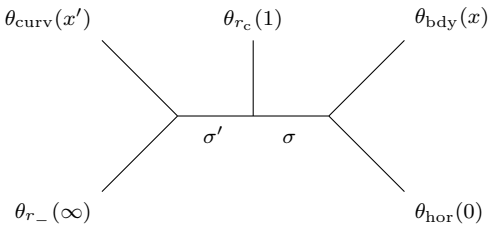

,

(5.4.46)

with σ, σ' defined implicitly by

$$\mathcal{E}_x = x\,\partial_x \mathcal{W}(x,x'), \quad \mathcal{E}_{x'} = x'\,\partial_{x'}\mathcal{W}(x,x'). \tag{5.4.47}$$

We again anticipate that the following exact quantization condition for QNMs does hold for physical values of $\mathcal{M}$ with $\theta_{\text{bdy}} \in \mathbb{Z}/2$. In any event, we predict the spectrum to be determined by

$$\boxed{\text{QNMs} = \left\{ \omega \middle| \frac{1}{2} - \theta_{\text{hor}} + \theta_{\text{bdy}} \pm \sigma\left(\boldsymbol{\theta}, \boldsymbol{\mathcal{E}}\right) = -n, \quad n \in \mathbb{Z}_{\geq 0} \right\}} \tag{5.4.48}$$

One again the dependence of σ on the parameters $\boldsymbol{\theta}, \boldsymbol{\mathcal{E}}$ is to be determined using the Zamolodchikov relations.

Remark 5.4.3. As in the case of scalar perturbation of the planar charged black hole, the near-extremal limit $x, x' \to 1$ is easier to study with a difference choice of channel than the current one, where the punctures at $1, x, x'$ sequentially fuse. We expect the near-extremal limit of purely decaying modes can be studied in such OPE limit as in the scalar case.

5.4.5. An example with apparent singularity: energy density correlators

The correlators of the energy density operator, which corresponds to scalar polarizations of the stress tensor, are determined from the equation (5.4.2). This differential equation was obtained by working with suitable gauge invariant variables to account for the diffeomorphism redundancies (see [KI03; HLRSV22] for details). Since the fluctuations of energy density correspond to sound propagation, this is also known as the sound channel equation.

The new feature in (5.4.2) is that it has an apparent singularity with $s = 3$. Its generalized Heun's parameters are listed in table 5.4. An added complication is that the exponent at the boundary vanishes, $\theta_{\text{bdy}} = 0$ (the asymptotic solutions are $\mathcal{Z} \sim c_1 + c_2 \log r$). Owing to this, the connection formula cannot be directly applied. As a simple trick, we will introduce, as in the designer scalar case, a one-parameter generalization of (5.4.2) where the connection formula does apply. We will then argue that the exact quantization condition for QNMs derived from the connection formula continues to hold as we limit to the $\theta_{\text{bdy}} = 0$ case.

One cannot naively deform the equation by simply changing θ_{bdy} alone. The reason being

that the apparent singularity condition involves a delicate cancelation of residues, which can fail if the equation is tweaked. Working with real $d \neq 4$ also doesn't address the issue. Instead, inspired by the structure in designer scalar case, we choose to deform both $\theta_{\rm bdy}$ and $\theta_{\rm curv}$ while keeping all other parameters fixed. The apparent singularity condition for $s = 3$ in this case evaluates to

$$\mathsf{ASC}_3 \propto 3\,(4\,\mathfrak{q}^4+9)\,\theta_{\rm bdy}^2 - 4\,\mathfrak{q}^4\,(4\,\mathfrak{q}^4-3)\,\theta_{\rm curv}^2 \tag{5.4.49}$$

where the proportionality factor only depends on $\mathfrak{q}$. We therefore introduce the following one-parameter generalization of the sound channel equation:

$$\begin{aligned} \theta_{\rm bdy} &= \Theta\,, \qquad\qquad \theta_{\rm curv} = \mathfrak{h}(\mathfrak{q})\,\Theta\,, \\ \mathfrak{h}^2(\mathfrak{q}) &= \frac{3\,(4\,\mathfrak{q}^4+9)}{4\,\mathfrak{q}^4\,(4\,\mathfrak{q}^4-3)}\,. \end{aligned} \tag{5.4.50}$$

In table 5.4 we record the generalized Heun's parameters for both (5.4.2) and the aforementioned modification.

	$\theta_{\rm hor}$	$\theta_{\rm bdy}$	θ_{r_c}	$\theta_{\rm curv}$	$\theta_{\mathfrak{x}}$	x	$\mathcal{E}_x$	$\mathfrak{x}$	$\mathcal{E}_{\mathfrak{x}}$
SC	$\frac{i\,\mathfrak{w}}{2}$	0	$\frac{\mathfrak{w}}{2}$	0	$\frac{3}{2}$	$\frac{1}{2}$	$\mathfrak{q}^2-\mathfrak{w}^2-\frac{3}{2\,\mathfrak{q}^2}$	$\frac{1}{2}+\frac{\mathfrak{q}^2}{3}$	$5+\frac{3}{2\mathfrak{q}^2}+\frac{12}{2\,\mathfrak{q}^2-3}$
SCg	-	Θ	-	$\mathfrak{h}(\mathfrak{q})\,\Theta$	-	-	-	-	-

Table 5.4.: Generalized Heun's parameters for sound channel (SC) equation (5.4.2) and its one-parameter generalization (SCg) as detailed by (5.4.50). Here $\mathfrak{x}$ is the apparent singularity occurring at the vanishing locus of the function Λ_k.

With this change, we can then readily apply the connection formula for an equation with apparent singularity (5.3.84). For the one-parameter deformation of (5.4.2) introduced herein, we have (assuming $\theta_{\rm bdy} \notin \frac{\mathbb{Z}}{2}$),

$$\boxed{K = \mathfrak{f}\,(\theta_{\rm bdy})\,\frac{\Gamma\,(-2\,\theta_{\rm bdy})}{\Gamma\,(2\,\theta_{\rm bdy})}\,\frac{\Gamma\left(\frac{1}{2}-\theta_{\rm hor}+\theta_{\rm bdy}\pm\sigma\right)}{\Gamma\left(\frac{1}{2}-\theta_{\rm hor}-\theta_{\rm bdy}\pm\sigma\right)}\exp\left[-\partial_{\theta_{\rm bdy}}\mathcal{W}(x,\mathfrak{x})\right]\,.} \tag{5.4.51}$$

The semiclassical Virasoro block here is

$$\mathcal{W}(x,\mathfrak{x}) = \quad (5.4.52)$$

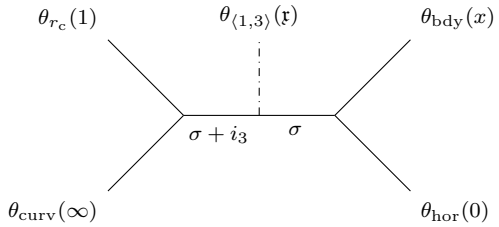

The internal Liouville momenta σ, i_3 need to be determined using the Zamolodchikov relations,

$$\mathcal{E}_x = x\,\partial_x \mathcal{W}(x,\mathfrak{x})\,, \qquad \mathcal{E}_{\mathfrak{x}} = \mathfrak{x}\,\partial_{\mathfrak{x}} \mathcal{W}(x,\mathfrak{x})\,. \quad (5.4.53)$$

The exact quantization condition for QNMs is given by

$$\text{QNMs} = \left\{ \omega \middle| \frac{1}{2} - \theta_{\rm hor} + \theta_{\rm bdy} \pm \sigma\left(\boldsymbol{\theta}, \boldsymbol{\mathcal{E}}\right) = -n, \quad n \in \mathbb{Z}_{\geq 0} \right\}. \quad (5.4.54)$$

5.4.6. Comparison with BTZ

The exact s-channel expressions for thermal two-point function (5.4.21) and QNMs (5.4.24) in the four-puncture case and their five-puncture generalization (5.4.48), have a formal structure analogous to the well-known BTZ answer, which corresponds to the three-puncture hypergeometric oper.

For minimally coupled massive scalar with $m^2 = \Delta(\Delta - 2)$ on planar BTZ background, standard manipulation recasts the radial wave equation to hypergeometric oper with

$$\begin{aligned} \mathtt{T}(z) &= \frac{\delta_0}{z^2} + \frac{\delta_1}{(z-1)^2} + \frac{\delta_\infty - \delta_0 - \delta_1}{z\,(z-1)}\,, \\ \theta_0 \equiv \theta_{\rm hor} &= \frac{i\,\mathfrak{w}}{2}, \quad \theta_1 \equiv \theta_{\rm bdy} = \frac{\Delta - 1}{2}, \quad \theta_\infty = \frac{i\,\mathfrak{q}}{2}\,. \end{aligned} \quad (5.4.55)$$

The well-known results for BTZ thermal two-point function and quantization condition for

QNMs read[10]

$$
\begin{aligned}
K &= \mathfrak{f}\left(\theta_{\text{bdy}}\right) \frac{\Gamma\left(-2\,\theta_{\text{bdy}}\right)}{\Gamma\left(2\,\theta_{\text{bdy}}\right)} \frac{\Gamma\left(\frac{1}{2}-\theta_{\text{hor}}+\theta_{\text{bdy}} \pm \theta_{\infty}\right)}{\Gamma\left(\frac{1}{2}-\theta_{\text{hor}}-\theta_{\text{bdy}} \pm \theta_{\infty}\right)}\,, \\
\text{QNMs} &= \left\{ \mathfrak{w} \middle| \frac{1}{2}-\theta_{\text{hor}}+\theta_{\text{bdy}} \pm \theta_{\infty} = -n, \quad n \in \mathbb{Z}_{\geq 0} \right\} \\
&= \left\{ \pm \mathfrak{q} - i\left(2\,n+\Delta\right) \middle| n \in \mathbb{Z}_{\geq 0} \right\}\,.
\end{aligned}
\tag{5.4.56}
$$

Therefore, compared with BTZ answer, the exact s-channel expressions in AdS_5 essentially replaces the external Liouville momentum θ_∞ by the interval momentum σ and has an additional factor of semiclassical Virasoro block in thermal two-point function. In particular, the momentum dependence no longer comes from an external Liouville momentum but arises from the accessory parameters that implicitly define the internal momentum σ via the Zamolodchikov relation. This similarity in structure indeed stems from locality of fusion transformation of the (degenerate) Virasoro block.

It is also the case in BTZ that the expression for K in (5.4.56) only holds for $\theta_{\text{bdy}} \notin \mathbb{Z}/2$ or $\Delta \notin \mathbb{Z}$[11], while the quantization condition for QMNs holds regardless of Δ being integer or not. This is analogous to Claim 5.4.1.

5.5. Relation with WKB period and Seiberg-Witten curve

It is well-known that there is a WKB regime of QNMs, either at large overtone number [MN03; NS04], or when the mass of the field (or momentum) gets large [FL09]. A natural question is therefore how to recover this WKB regime from the exact quantization condition in (5.4.24).

There is a useful way to realize this answer, but this involves using the gauge theory side of AGT relation [AGT10]. Recall that this correspondence links Liouville conformal blocks to the supersymmetric (Nekrasov) partition function of four-dimensional $\mathcal{N}=2$ superconformal field theories. For the four punctured case of interest, the WKB limit corresponds to the Seiberg-Witten (SW) limit of quasi-classical Virasoro block, where it reduces to the SW prepotential

[10] These expressions were originally derived from analytically continuing the Euclidean 2d CFT result in [Gub97]. The calculation in the AdS/CFT context was originally considered in [BSS02] and [SS02]. For a recent discussion in the context of the grSK geometry including generalization to the designer scalars, see [LRV22].

[11] In this case, it is straightforward to obtain the result of $K(\omega)$ for integer Δ by directly taking the limit of the correlator for non-integer conformal dimension.

of $\mathcal{N}=2, N_f=4$ gauge theory. By the AGT relation, the internal Liouville momentum σ is identified with the expectation value of the scalar a in the $\mathcal{N}=2$ multiplet, and therefore given by SW period in the SW limit. The SW period can furthermore be identified as WKB period from the known relation between $\mathcal{N}=2$ class $\mathcal{S}$ theories and WKB analysis [GMN13b; GMN13a; HRS21].

5.5.1. SW limit of semiclassical Virasoro block

To begin with, note that the semiclassical Virasoro block corresponds to the Nekrasov instanton partition in the Nekrasov-Shatashvili (NS) limit, which involves taking the deformation parameters $\epsilon_1=\hbar$ and $\epsilon_2=0$. To attain the SW limit, one is instructed to further take the large classical Liouville momenta limit in semiclassical Virasoro block and the associated Heun's equation. This is achieved by

$$\text{SW}:\hbar\to 0,\qquad \theta_i,\sigma\to\infty,\qquad \hbar\,\theta_i\to m_i,\qquad \hbar\,\sigma\to a,\qquad \hbar^2\,\mathcal{E}\to u\,. \tag{5.5.1}$$

Doing so, one obtains a "prepotential" from semiclassical Virasoro block as

$$\hbar^2\,\mathcal{W}\left(x|\boldsymbol{\theta},\sigma\right)\quad\xrightarrow{\text{SW}}\quad\mathcal{F}^{\text{Vir}}\left(x|\boldsymbol{m},a\right). \tag{5.5.2}$$

As indicated the Liouville parameters have been mapped to the corresponding SW data. In the aforementioned SW limit, the associated Heun's equation (5.3.16) reduces to a classical spectral curve, which is nothing but the SW curve. This can be seen from the limiting behavior of $\mathtt{T}(z)$

$$\begin{aligned}-\hbar^2\mathtt{T}(z)\quad&\xrightarrow{\text{SW}}\quad\phi_2(z)\\&=\frac{m_0^2}{z^2}+\frac{m_x^2}{(z-x)^2}+\frac{m_1^2}{(z-1)^2}+\frac{m_\infty^2-m_0^2-m_x^2-m_1^2}{z\,(z-1)}-\frac{u\,(x-1)}{z\,(z-1)\,(z-x)}\,,\end{aligned} \tag{5.5.3}$$

and the definition of the SW spectral curve

$$w^2=\phi_2(z)\,. \tag{5.5.4}$$

From the perspective of WKB analysis, the SW curve is nothing but the WKB curve for Heun's equation. The branched points in SW curve are the turning points in the WKB analysis. Furthermore, the Zamolodchikov relation (5.3.46) reduces to Matone-type relation for prepotential [Mat95]

$$u = x\,\partial_x \mathcal{F}^{\rm Vir}(x)\,. \tag{5.5.5}$$

There is yet another way to obtain the prepotential from the SW curve. One starts with the SW differential,

$$\lambda = w\,dz = \sqrt{\phi_2(z)}\,dz\,. \tag{5.5.6}$$

Recall that the SW equations can be expressed as the periods of λ around the A and B cycles of the torus. Explicitly, we have

$$a = \frac{1}{2\pi i}\oint_A \lambda, \qquad \partial_a \mathcal{F}^{\rm SW} = \frac{1}{2\pi i}\oint_B \lambda. \tag{5.5.7}$$

In principle, from calculating the A-period integral one can invert $a(u)$ as $u(a)$ and then plug it into the B-period integral to solve $\mathcal{F}^{\rm SW}$. The SW periods are then identified as WKB periods.

The two apparently different definitions of prepotential mentioned above are, in fact, equivalent:

$$\boxed{\mathcal{F}^{\rm Vir}\left(x|\boldsymbol{m},a\right) = \mathcal{F}^{\rm SW}\left(x|\boldsymbol{m},a\right)} \tag{5.5.8}$$

This is because: i) the SW prepotential can be extracted from Nekrasov instanton partition function in the $\epsilon_{1,2}\to 0$ limit [Nek03], and ii) from AGT relation, the $\epsilon_{1,2}\to 0$ limit of Nekrasov instanton partition function corresponds to taking the semiclassical limit (5.3.11) followed by the SW limit (5.5.1) of the Virasoro block. This relation is important for our purposes. It immediately allows one to identify, in the WKB regime of QNMs, the internal Liouville momentum σ appearing in the exact quantization condition (5.4.24) as a WKB period.

Computing the prepotential from SW curve through a recursion relation: It is instructive to verify (5.5.8) explicitly by directly computing $\mathcal{F}^{\rm SW}$ and comparing with $\mathcal{F}^{\rm Vir}$. Instead of directly computing A and B periods as described above, there is a more efficient way of computing SW prepotential. The trick is to expand the SW differential into a rational differential and use

Matone-type relation. This not only avoids the need to compute B-period, but also reduces the calculation of A-period to evaluation of residue. It eventually yields a recursion relation for the expansion coefficients of prepotential. This is explained, e.g., in Appendix A of [Tac13] for the $N_f = 0$, pure glue SU(2) theory.

We are interested in the somewhat more involved $N_f = 4$ case. To attain the result, we perform the following formal expansion in the quadratic differential $\phi_2(z)\, dz^2$:

$$\begin{aligned}
\phi_2(z) &= \phi_2(z)\Big|_{x=0} + \frac{1}{z^2}\sum_{n=1}^{\infty}\left[-u + (n+1)\, m_x^2\right]\left(\frac{x}{z}\right)^n \\
&= \frac{-u + m_0^2 + m_x^2}{z^2} + \frac{1}{z^2}\sum_{n=1}^{\infty}\left(-u + m_0^2 + n\, m_1^2 + m_x^2 - m_\infty^2\right) z^n \\
&\qquad + \frac{1}{z^2}\sum_{n=1}^{\infty}\left[-u + (n+1)\, m_x^2\right]\left(\frac{x}{z}\right)^n \\
&= \frac{-u + m_0^2 + m_x^2}{z^2}\left(1 + \sum_{n=1}^{\infty}\alpha_n(u,\boldsymbol{m})\, z^n + \beta_n(u,\boldsymbol{m})\, \left(\frac{x}{z}\right)^n\right),
\end{aligned} \tag{5.5.9}$$

with $\boldsymbol{m}$ collectively denoting the set of exponents m_i. The coefficients appearing in the above expansion are

$$\alpha_n(u,\boldsymbol{m}) = \frac{-u + m_0^2 + n m_1^2 + m_x^2 - m_\infty^2}{-u + m_0^2 + m_x^2}, \qquad \beta_n(u,\boldsymbol{m}) = \frac{-u + (n+1) m_x^2}{-u + m_0^2 + m_x^2}\,. \tag{5.5.10}$$

Using this series expression we find that the SW differential itself admits the following expansion:

$$\lambda = \frac{\sqrt{-u + m_0^2 + m_x^2}}{z}\sum_{k=0}^{\infty}\binom{\frac{1}{2}}{k}\left[\sum_{n=1}^{\infty}\alpha_n(u,\boldsymbol{m})\, z^n + \beta_n(u,\boldsymbol{m})\left(\frac{x}{z}\right)^n\right]^k dz\,. \tag{5.5.11}$$

Therefore, the A-period is given by residue at $z = 0$, i.e.,

$$a = \frac{1}{2\pi i}\oint_A \lambda \;=\; \sqrt{-u + m_0^2 + m_x^2}\sum_{k=0}^{\infty}\binom{\frac{1}{2}}{k}\gamma_k\left(x|\boldsymbol{m},u\right), \tag{5.5.12}$$

with

$$\gamma_k\left(x|\boldsymbol{m},u\right) = \left[\sum_{n=1}^{\infty}\alpha_n(u,\boldsymbol{m})\, z^n + \beta_n(u,\boldsymbol{m})\left(\frac{x}{z}\right)^n\right]^k\Bigg|_{\mathcal{O}(z^0)}. \tag{5.5.13}$$

In order to find a to order $x^{n_{\max}}$ the sum over k can be truncated at $k = 2n_{\max}$. One thus obtains a recursion relation for the expansion coefficients in the prepotential, viz.,

$$\mathcal{F}^{\rm SW}\left(x|\boldsymbol{m},a\right) = \left(-a^2+m_0^2+m_x^2\right)\,\log x + \sum_{k=1}^{\infty}\,\mathcal{F}_k^{\rm SW}\left(\boldsymbol{m},a\right)\,x^k\,, \tag{5.5.14}$$

This is achieved by substituting the Matone-type relation

$$u = x\partial_x\mathcal{F}^{\rm SW}\left(x|\boldsymbol{m},a\right) = -a^2+m_0^2+m_x^2+\sum_{k=1}^{\infty}\,k\,\mathcal{F}_k^{\rm SW}\left(\boldsymbol{m},a\right)\,x^k\,, \tag{5.5.15}$$

into (5.5.12) and solving order by order in x.

Carrying out this exercise, we find the first two coefficients to be given by

$$\mathcal{F}_1^{\rm SW}\left(\boldsymbol{m},a\right) = -\frac{\left(a^2+m_x^2-m_0^2\right)\left(a^2-m_\infty^2+m_1^2\right)}{2\,a^2} \tag{5.5.16}$$

and

$$\begin{aligned}\mathcal{F}_2^{\rm SW}\left(\boldsymbol{m},a\right) = \frac{1}{64\,a^6}\Big[&12\,a^2\left(a^2+2\,m_x^2-m_0^2\right)\left(a^2-m_\infty^2+m_1^2\right)^2+12\,a^2\,\left(a^2+m_x^2-m_0^2\right)^2\left(a^2-m_\infty^2+2\,m_1^2\right)\\&-21\left(a^2+m_x^2-m_0^2\right)^2\left(a^2-m_\infty^2+m_1^2\right)^2\\&-8\left(a^2+m_x^2-m_0^2\right)\left(a^2-m_\infty^2+m_1^2\right)\left(a^2\left(a^2+m_x^2-m_0^2\right)-\left(a^2+2\,m_x^2-2\,m_0^2\right)\left(a^2-m_\infty^2+m_1^2\right)\right)\\&-16\,a^4\left(a^2+2\,m_x^2-m_0^2\right)\left(a^2-m_\infty^2+2\,m_1^2\right)\Big]\end{aligned} \tag{5.5.17}$$

These can indeed be checked to agree with $\mathcal{F}_k^{\rm Vir}\left(\boldsymbol{m},a\right)$ from taking SW limit (5.5.1) of the expansion coefficients of quasi-classical Virasoro block.

5.5.2. The WKB regime of QNMs and the SW prepotential

We can now apply the SW prepotential to ascertain the asymptotic form of quasinormal modes. While we would like to do so by directly using the SW prepotential, for the present, we will instead confirm by a backward check that one indeed reproduces the WKS results. We comment at the end on prospects of directly obtaining the WKB asymptotics.

The asymptotic QNMs for massless scalar fields: By WKB analysis or direct numerical computation, one can show that the QNMs for both Klein-Gordon and designer scalars around a planar black hole background have the following asymptotic behavior at large overtone number [NS04; FL09]:

$$\mathfrak{w}_n = (\pm 1 - i)\, n + \mathcal{O}\big(n^0\big), \qquad n \to \infty\,. \tag{5.5.18}$$

Let us try to understand it from the exact quantization condition (5.4.24). The leading term should be the solution of the following large $\mathfrak{w}$ limit of (5.4.24):

$$-\frac{i\,\mathfrak{w}}{2} \pm \sigma(\mathfrak{w}) = -n, \quad n, \mathfrak{w} \to \infty \tag{5.5.19}$$

The asymptotic behavior (5.5.18) is obtained if $\sigma(\mathfrak{w}) = \frac{\mathfrak{w}}{2}$.

In the SW limit of semiclassical Virasoro block, the leading large $\mathfrak{w}$ limit corresponds to the SW curve with two massive punctures $(m_0, m_x, m_1, m_\infty) = (i\,\mu, 0, \mu, 0)$ and modulus $u = -4\,\mu^2$ at coupling $x = \frac{1}{2}$. Here $\mu = \frac{\hbar\,\mathfrak{w}}{2}$. To obtain (5.5.18), we therefore need to verify

$$a \stackrel{?}{=} \mu \tag{5.5.20}$$

in this set-up. We can check this by verifying the Matone-type relation

$$u = x\partial_x \mathcal{F}\Big(x\Big|\{i\,\mu, 0, \mu, 0\}, \mu\Big)\Big|_{x=\frac{1}{2}} \stackrel{?}{=} -4\,\mu^2\,. \tag{5.5.21}$$

Computing expansion coefficients of prepotential $\mathcal{F}_k\,(\boldsymbol{m}, a)$ using either semiclassical Virasoro block or SW curve (up to $k = 10$), we observe the following pattern:

$$\mathcal{F}_k\Big(\{i\mu, 0, \mu, 0\}, \mu\Big) = \frac{-2\,\mu^2}{k}. \tag{5.5.22}$$

We thus find

$$u = x\partial_x \mathcal{F}\Big(x\Big|\{i\,\mu, 0, \mu, 0\}, \mu\Big)\Big|_{x=\frac{1}{2}} = -2\,\mu^2(1 + x + x^2\cdots)\Big|_{x=\frac{1}{2}} = -4\,\mu^2\,. \tag{5.5.23}$$

This confirms that the asymptotic QNM spectrum is indeed reproduced by the exact quantiza-

tion condition (5.4.24) using SW limit of semiclassical Virasoro block.

QNMs at large Δ: The second limit where one expects a WKB formula to hold is for large dimension operators in the dual CFT. Consider a massive Klein-Gordon scalar in the planar black hole background at finite $\mathfrak{q}$. The QNMs at large Δ have the following asymptotic behavior [FL09]:

$$\mathfrak{w}_n = (\pm 1 - i)\left(\frac{\Delta}{2} + n\right) + \mathcal{O}(\Delta^0), \quad \Delta \to \infty\,. \tag{5.5.24}$$

In terms of the quantization condition (5.4.24), the leading term should be the solution of the following large $\mathfrak{w}, \Delta$ limit of

$$-\frac{i\,\mathfrak{w}}{2} + \frac{\Delta}{2} \pm \sigma(\mathfrak{w}, \Delta) = -n, \qquad \mathfrak{w}, \Delta \to \infty\,. \tag{5.5.25}$$

Once again $\sigma(\mathfrak{w}, \Delta) = \frac{\mathfrak{w}}{2}$ will reproduce the leading large Δ behavior.

The corresponding SW curve has three massive punctures $(m_0, m_x, m_1, m_\infty) = (i\,\mu, M, \mu, 0)$, with $\mu = \frac{\hbar\,\mathfrak{w}}{2}$ and $M = \frac{\hbar\Delta}{2}$. The moduli and coupling are still $u = -4\,\mu^2$ and $x = \frac{1}{2}$. We therefore need to verify

$$a \stackrel{?}{=} \mu\,, \tag{5.5.26}$$

in this set-up. We can again check this by verifying the Matone-type relation

$$u = x\partial_x \mathcal{F}\Big(x\Big|\{i\,\mu, M, \mu, 0\}, \mu\Big)\Big|_{x=\frac{1}{2}} \stackrel{?}{=} -4\,\mu^2. \tag{5.5.27}$$

Direct computation of prepotential coefficients (up to $k = 8$) now reveals the following pattern

$$\mathcal{F}_k\Big(\{im, M, m, 0\}, m\Big) = \frac{-2\,\mu^2 - M^2}{k}\,. \tag{5.5.28}$$

Using this we once again confirm the WKB regime of QNM from SW limit of semiclassical Virasoro block, for

$$\begin{aligned} u &= x\,\partial_x \mathcal{F}\Big(x\Big|\{i\,\mu, M, \mu, 0\}, \mu\Big)\Big|_{x=\frac{1}{2}} \\ &= -2\,\mu^2\,(1 + x + x^2 + \cdots) - M^2\,(-1 + x + x^2 \cdots)\Big|_{x=\frac{1}{2}} = -4\,\mu^2\,, \end{aligned} \tag{5.5.29}$$

indeed holds.

5.6. Energy-momentum tensor correlation functions in 4d holographic CFTs

We now turn to the correlation functions of the energy-momentum tensor in a 4d holographic CFT. The prototype example to keep in mind is the case of $\mathcal{N}=4$ SYM. We will work with the CFT on $\mathbb{R}^{3,1}$. To describe the results succinctly, we make the following kinematic choice. We pick the spatial momentum to be oriented along $\mathbf{k} = k\,\hat{\mathbf{e}}_z$. This allows us to decompose the stress tensor polarizations into physical components:

- The transverse traceless tensor polarizations (which are two in number) are exemplified by components, such as $T_{xy}(\omega,\mathbf{k})$ in our chosen kinematics. In the dual gravity theory, they are described by a massless Klein-Gordon scalar, i.e., by (5.4.1) with $\mathcal{M}=3$ on the planar-Schwarzschild-AdS$_5$ background. We write the asymptotic expansion of this scalar as

$$\varphi(r,\omega,\mathbf{k})\Big|_{\mathcal{M}=3,m^2=0} \sim \boldsymbol{\gamma}(\omega,\mathbf{k}) + \frac{1}{r^4}\,\langle\mathcal{O}(\omega,\mathbf{k})\rangle\ , \tag{5.6.1}$$

  which defines a boundary operator $\mathcal{O}$ of dimension $\Delta=4$, and its source $\boldsymbol{\gamma}$ (which are just the transverse traceless tensor components of the boundary metric). This implies that modulo a normalization factor one can write the result in terms of the correlator $\mathcal{O}$

$$\langle T_{xy}(-\omega,-\mathbf{k})\,T_{xy}(\omega,\mathbf{k})\rangle_{\rm ret} = i\,\mathfrak{N}\,\langle\mathcal{O}(-\omega,-\mathbf{k})\,\mathcal{O}(\omega,\mathbf{k})\rangle_{\rm ret}\ . \tag{5.6.2}$$

  The normalization factor $\mathfrak{N}$ itself can be deduced by comparing with the asymptotic expansion of the Einstein-Hilbert action as in [GLPRSV21]. It is given in terms of an effective central charge[12]

$$\mathfrak{N} = \pi^4\,T^4\,c_{\rm eff}\ . \tag{5.6.3}$$

  Using the expression for the correlator in the s-channel expansion, (5.4.21), and regulating

[12] The overall normalization factor of these correlators, consistent with large N scaling, is specified by $c_{\rm eff} = \frac{\ell^3_{\rm AdS}}{16\pi\,G_N}$. For the case of $\mathcal{N}=4$ SYM with gauge group SU(N) this normalization is $c_{\rm eff} = \frac{N^2}{8\pi^2}$.

$\Delta = 4 + \epsilon_c$ to ensure that $\theta_{\rm bdy} \notin \mathbb{Z}/2$, we have

$$\langle \mathcal{O}(-\omega,-\mathbf{k})\,\mathcal{O}(\omega,\mathbf{k})\rangle_{\rm ret} = \text{reg.}\lim_{\epsilon_c\to 0} \mathfrak{f}\,(1+\epsilon_c)\,\frac{\Gamma\,(-2-\epsilon_c)}{\Gamma\,(2+\epsilon_c)}\,\frac{\Gamma\left(\frac{3}{2}+\epsilon_c-\frac{i\,\mathfrak{w}}{2}\pm\sigma\right)}{\Gamma\left(\frac{1}{2}-\epsilon_c-\frac{i\,\mathfrak{w}}{2}\pm\sigma\right)}\,\exp\left[-\partial_{\theta_{\rm bdy}}\mathcal{W}^s_{\mathcal{O}}(x)\right]\,. \tag{5.6.4}$$

Here reg. denotes taking the regular part of the singular limit. The semiclassical block that we need in the above expression

$$\mathcal{W}^s_{\mathcal{O}}(x) = \tag{5.6.5}$$

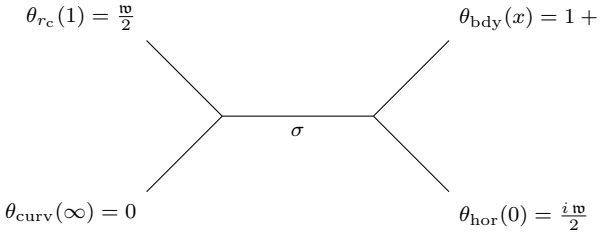

The intermediate Liouville momentum σ is fixed using the block

$$\mathfrak{q}^2-\mathfrak{w}^2 = x\,\partial_x\,\mathcal{W}^s_{\mathcal{O}}(x)\,, \tag{5.6.6}$$

and we set $x=\frac{1}{2}$ at the end of the day. For concreteness, we provide the first two terms in the cross-ratio expansion of $\sigma = \mathfrak{s} + \sum_{k=1}^{\infty}\sigma_k x^k$ to $\mathcal{O}(\epsilon_c^2)$:

$$\begin{aligned}
\mathfrak{s} &= \frac{1}{2}\sqrt{-4\,\mathfrak{q}^2+3\,\mathfrak{w}^2+3}+\frac{2}{\sqrt{-4\,\mathfrak{q}^2+3\,\mathfrak{w}^2+3}}\,\epsilon_c+\mathcal{O}\big(\epsilon_c^2\big)\\
\sigma_1 &= -\frac{\left(-4\,\mathfrak{q}^2+2\,\mathfrak{w}^2+2\right)\left(-4\,\mathfrak{q}^2+4\,\mathfrak{w}^2+6\right)}{8\left(-4\,\mathfrak{q}^2+3\,\mathfrak{w}^2+2\right)\sqrt{-4\,\mathfrak{q}^2+3\,\mathfrak{w}^2+3}}\\
&\quad-\frac{4\left(9\,\mathfrak{w}^6+2\left(11-18\,\mathfrak{q}^2\right)\mathfrak{w}^4+\left(50\,\mathfrak{q}^4-55\,\mathfrak{q}^2+16\right)\mathfrak{w}^2-3\,\left(2\mathfrak{q}^2-1\right)^3\right)}{\left(-4\,\mathfrak{q}^2+3\,\mathfrak{w}^2+2\right)^2\left(-4\,\mathfrak{q}^2+3\,\mathfrak{w}^2+3\right)^{3/2}}\,\epsilon_c+\mathcal{O}\big(\epsilon_c^2\big)\,.
\end{aligned} \tag{5.6.7}$$

- The transverse vector polarizations, also comprise two components, the momentum density $T_{zx}(\omega,\mathbf{k})$ and the momentum current $T_{vx}(\omega,\mathbf{k})$. In the gravitational description they are described by a massless designer scalar with $\mathcal{M}=-3$, i.e., again through (5.4.1) in the planar-Schwarzschild-AdS$_5$ background. Such a field has an asymptotic behavior,

$$\varphi(r,\omega,\mathbf{k})\Big|_{\mathcal{M}=-3} \sim\ \langle\mathcal{P}(\omega,\mathbf{k})\rangle + r^2\,\boldsymbol{\alpha}(\omega,\mathbf{k})\,. \tag{5.6.8}$$

Notice that the constant mode of the field in this case defines the dual boundary operator's expectation value. The mode that is growing as r^2 picks out the transverse vector component of the boundary metric.

The correlation functions can thus be read off from those of the designer scalar, which we refer to as the shear mode scalar $\mathcal{P}$ are given by

$$\begin{aligned}
\langle T_{vx}(-\omega,-\mathbf{k})\,T_{vx}(\omega,\mathbf{k})\rangle_{\text{ret}} &= -i\,4\,\mathfrak{N}\,\mathfrak{q}^2\ \langle \mathcal{P}(-\omega,-\mathbf{k})\,\mathcal{P}(\omega,\mathbf{k})\rangle_{\text{ret}}\ ,\\
\langle T_{vx}(-\omega,-\mathbf{k})\,T_{zx}(\omega,\mathbf{k})\rangle_{\text{ret}} &= i\,4\,\mathfrak{N}\,\mathfrak{w}\,\mathfrak{q}\ \langle \mathcal{P}(-\omega,-\mathbf{k})\,\mathcal{P}(\omega,\mathbf{k})\rangle_{\text{ret}}\ ,\\
\langle T_{xy}(-\omega,-\mathbf{k})\,T_{xy}(\omega,\mathbf{k})\rangle_{\text{ret}} &= -i\,4\,\mathfrak{N}\,\mathfrak{w}^2\ \langle \mathcal{P}(-\omega,-\mathbf{k})\,\mathcal{P}(\omega,\mathbf{k})\rangle_{\text{ret}}\ .
\end{aligned} \tag{5.6.9}$$

The correlation function of $\mathcal{P}$ itself is given by (taking $\mathcal{M}=-3+2\,\epsilon_c$)

$$\langle \mathcal{P}(-\omega,-\mathbf{k})\,\mathcal{P}(\omega,\mathbf{k})\rangle_{\text{ret}} = \text{reg.}\lim_{\epsilon_c\to 0}\ \mathfrak{f}\left(\frac{1-\epsilon_c}{2}\right)\frac{\Gamma\left(-1+\epsilon_c\right)}{\Gamma\left(1-\epsilon_c\right)}\,\frac{\Gamma\left(-\epsilon_c-\frac{i\,\mathfrak{w}}{2}\pm\sigma\right)}{\Gamma\left(\frac{1}{2}-\epsilon_c-\frac{i\,\mathfrak{w}}{2}\pm\sigma\right)}\ \exp\left[-\partial_{\theta_{\text{bdy}}}\mathcal{W}^s_{\mathcal{P}}(x)\right]\ . \tag{5.6.10}$$

The semiclassical block that we need in the above expression

$$\mathcal{W}^s_{\mathcal{P}}(x) = \tag{5.6.11}$$

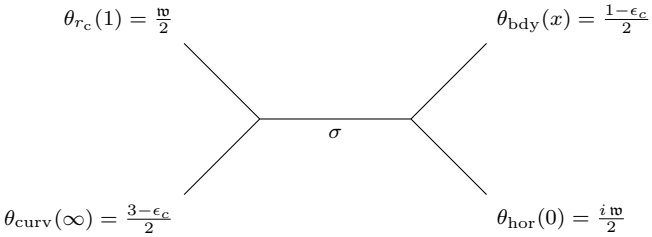

Now we fix σ by solving

$$\mathfrak{q}^2-\mathfrak{w}^2 = x\,\partial_x\,\mathcal{W}^s_{\mathcal{P}}(x)\,, \tag{5.6.12}$$

and set $x=\frac{1}{2}$ at the end. The first two terms in the expansion $\sigma=\mathfrak{s}+\sum_{k=1}^{\infty}\sigma_k x^k$ are

$$\begin{aligned}
\mathfrak{s} &= \frac{1}{2}\,\sqrt{-4\,\mathfrak{q}^2+3\,\mathfrak{w}^2}-\frac{2}{\sqrt{-4\,\mathfrak{q}^2+3\,\mathfrak{w}^2}}\,\epsilon_c+\mathcal{O}\big(\epsilon_c^2\big)\\
\sigma_1 &= \frac{(\mathfrak{q}-\mathfrak{w})(\mathfrak{q}+\mathfrak{w})\left(2\,\mathfrak{q}^2-\mathfrak{w}^2+5\right)}{\left(4\,\mathfrak{q}^2-3\,\mathfrak{w}^2+1\right)\sqrt{3\,\mathfrak{w}^2-4\,\mathfrak{q}^2}}\\
&\quad-\frac{18\,\mathfrak{w}^6-\left(63\,\mathfrak{q}^2+4\right)\mathfrak{w}^4+2\left(35\,\mathfrak{q}^4-4\,\mathfrak{q}^2-5\right)\mathfrak{w}^2+3\,\mathfrak{q}^2\left(-8\,\mathfrak{q}^4+6\,\mathfrak{q}^2+5\right)}{\left(4\,\mathfrak{q}^2-3\,\mathfrak{w}^2+1\right)^2\left(3\,\mathfrak{w}^2-4\,\mathfrak{q}^2\right)^{3/2}}\epsilon_c+\mathcal{O}\big(\epsilon_c^2\big)\,.
\end{aligned} \tag{5.6.13}$$

A few comments are in order. Firstly, the field φ with $\mathcal{M} = -3$ is quantized in the bulk with Neumann boundary conditions. This is not only natural given the asymptotic fall-offs (5.6.8), but it also follows the bulk Einstein-Hilbert dynamics. In particular, the parametrization of metric fluctuations in terms of $\varphi_{\mathcal{M}=-3}$ involves radial derivatives. These are responsible for converting the Dirichlet boundary condition imposed on the bulk metric into Neumann boundary conditions for $\varphi_{\mathcal{M}=-3}$. The prefactors involving momentum and frequency arise from the map between the physical stress tensor components and the designer scalar used to parameterize the dual gravitational fluctuations. For details regarding these statements, see [GLPRSV21].[13] We should also note that the aforementioned reference phrase the answer not for the generating function of $\mathcal{P}$ correlators, but in terms of its Legendre transform, the effective action parameterized by $\langle \mathcal{P} \rangle$ (denoted $\breve{\mathcal{P}}$ there).

- Finally, the single scalar polarization, which encompasses the energy density $T_{vv}(\omega, \mathbf{k})$ and other scalar components, $\{T_{zz}(\omega, \mathbf{k}), T_{vz}(\omega, \mathbf{k}), T_{xx}(\omega, \mathbf{k}) + T_{yy}(\omega, \mathbf{k})\}$ can be mapped to another designer scalar $\mathcal{Z}$ with $\mathcal{M} = -1$, albeit with a more involved equation (5.4.2). This field has asymptotics[14]

$$\mathcal{Z} = \langle \mathcal{Z} \rangle + \boldsymbol{\zeta} \, \log r \, . \tag{5.6.14}$$

  In particular, the holographic extrapolate dictionary relates the expectation value energy density operator to the operator $\breve{\mathcal{O}}_{\mathcal{Z}}$ dual to the field $\mathcal{Z}$ as

$$T^v_v \sim -\frac{k^2}{3} \, \mathcal{Z} \, . \tag{5.6.15}$$

We fix the correlation function of the energy density operator and then use flat spacetime Ward identities (energy-momentum tensor conservation) to fix the correlators of the other polarizations following [PSS02]. The result can be succinctly expressed in terms of a (kinematic)

[13] The dimensionless frequencies and momenta used there differ from our current conventions by a factor of 2; specifically, $\{\mathfrak{w}, \mathfrak{q}\}_{\text{there}} = 2\,\{\mathfrak{w}, \mathfrak{q}\}_{\text{here}}$.

[14] This is true for non-vanishing spatial momentum. At zero spatial momentum $\mathcal{Z}$ satisfies a massless Klein-Gordon equation. Relatedly, the apparent singularity in (5.4.2) is absent. The physical reason for this change in behavior is due to the enhanced gauge symmetry in the dual gravity description at $k = 0$, cf. [HLRSV22] for a detailed discussion.

tensor, $\mathfrak{G}_{\mu\nu,\rho\sigma}(\omega,\mathbf{k})$ which is polynomial in ω and k

$$\langle T_{\mu\nu}(-\omega,-\mathbf{k})\,T_{\rho\sigma}(\omega,\mathbf{k})\rangle_{\rm ret} = \frac{16\,\mathfrak{q}^4}{9}\,\mathfrak{G}^{\mu\nu,\rho\sigma}(\omega,\mathbf{k})\,\langle \mathcal{Z}(-\omega,-\mathbf{k})\,\mathcal{Z}(\omega,\mathbf{k})\rangle_{\rm ret}\ . \tag{5.6.16}$$

Explicit expressions for the kinematic tensor can be found in [HLRSV22] (modulo a convention change of $\{\mathfrak{w},\,\mathfrak{q}\}_{\rm there} = 2\,\{\mathfrak{w},\mathfrak{q}\}_{\rm here}$).

The new ingredient here is that the $\mathcal{Z}$ equation has an apparent singular point of order $s=3$. We cure it as described in §5.4.5 by introducing a regulator deforming the indicial exponents at the horizon and curvature singularity (5.4.50). Once this is done, the correlation function of $\mathcal{Z}$ itself is given by (taking $\Theta=\epsilon_c$ for convenience)

$$\langle \mathcal{Z}(-\omega,-\mathbf{k})\,\mathcal{Z}(\omega,\mathbf{k})\rangle_{\rm ret} = \text{reg.}\lim_{\epsilon_c\to 0}\ \mathfrak{f}\,(\epsilon_c)\,\frac{\Gamma\,(-2\,\epsilon_c)}{\Gamma\,(2\,\epsilon_c)}\,\frac{\Gamma\left(\frac{1}{2}+\epsilon_c-\frac{i\,\mathfrak{w}}{2}\pm\sigma\right)}{\Gamma\left(\frac{1}{2}-\epsilon_c-\frac{i\,\mathfrak{w}}{2}\pm\sigma\right)}\,\exp\left[-\partial_{\theta_{\rm bdy}}\mathcal{W}^s_{\mathcal{Z}}(x,x)\right]\ . \tag{5.6.17}$$

The semiclassical block that we need in this case is a five-point block

$$\mathcal{W}_{\mathcal{Z}}(x,\mathfrak{x}) = \tag{5.6.18}$$

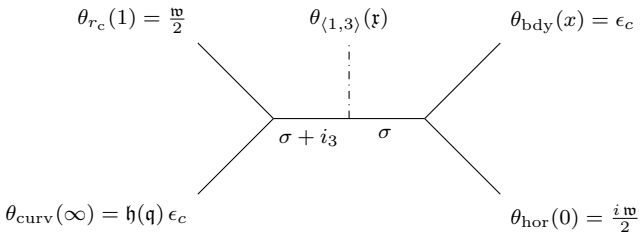

The internal Liouville momenta σ, i_3 are determined by solving

$$\mathfrak{q}^2-\mathfrak{w}^2-\frac{3}{2\,\mathfrak{q}^2} = x\,\partial_x\mathcal{W}(x,\mathfrak{x})\,,\qquad 5+\frac{3}{2\,\mathfrak{q}^2}+\frac{12}{2\,\mathfrak{q}^2-3} = \mathfrak{x}\,\partial_{\mathfrak{x}}\mathcal{W}(x,\mathfrak{x})\,. \tag{5.6.19}$$

and setting $x=\frac{1}{2}$ and $\mathfrak{x}=\frac{1}{2}+\frac{\mathfrak{q}^2}{3}$.

To obtain the result for the $\mathcal{Z}$ correlation function, we quantize the field with Neumann boundary condition. The reason is similar to that for $\varphi_{\mathfrak{M}=-3}$ mentioned above, but the details, which can be found in [HLRSV22], are more involved. That work, which was interested in the low-energy limit, $\mathfrak{w},\mathfrak{q}\ll 1$, obtained results in a gradient expansion. We need not restrict to this low-energy regime, and do stay away from $\mathfrak{q}\neq 0$ to avoid the complications alluded to in footnote 14.

5.7. Discussion

The primary focus of the chapter was to exploit the connection between wave equations in AdS black hole backgrounds, and the BPZ equation for degenerate Virasoro conformal blocks, to analyze thermal correlation functions of holographic CFTs. These correlators are meromorphic, with the location of the poles being associated with the quasinormal modes (QNMs) of the black hole. The QNMs themselves are solutions to the connection problem of the aforesaid differential equation, and can be directly obtained using an exact quantization condition.

While these insights have been discussed in the literature, we have argued for a simpler formula for the thermal 2-point function. This was achieved by working with a different s-channel expansion of the semiclassical Virasoro blocks. In particular, our final result for the 2-point function bears striking resemblance to the answers obtained in a thermal CFT_2. Specifically,

$$\begin{aligned} K(\omega,k)\Big|_{\text{CFT}_4} &\propto \frac{\Gamma\left(\frac{1-i\,\mathfrak{w}}{2}+\frac{\Delta-2}{2}+\sigma\right)\Gamma\left(\frac{1-i\,\mathfrak{w}}{2}+\frac{\Delta-2}{2}-\sigma\right)}{\Gamma\left(\frac{1-i\,\mathfrak{w}}{2}-\frac{\Delta-2}{2}+\sigma\right)\Gamma\left(\frac{1-i\,\mathfrak{w}}{2}-\frac{\Delta-2}{2}-\sigma\right)}\,, \\ K(\omega,k)\Big|_{\text{CFT}_2} &\propto \frac{\Gamma\left(\frac{1-i\,\mathfrak{w}}{2}+\frac{\Delta-1}{2}+\frac{i\,\mathfrak{q}}{2}\right)\Gamma\left(\frac{1-i\,\mathfrak{w}}{2}+\frac{\Delta-1}{2}-\frac{i\,\mathfrak{q}}{2}\right)}{\Gamma\left(\frac{1-i\,\mathfrak{w}}{2}-\frac{\Delta-1}{2}+\frac{i\,\mathfrak{q}}{2}\right)\Gamma\left(\frac{1-i\,\mathfrak{w}}{2}-\frac{\Delta-1}{2}-\frac{i\,\mathfrak{q}}{2}\right)}\,. \end{aligned} \tag{5.7.1}$$

Apart from a shift of the conformal dimension, we see that $\sigma = \frac{i\,\mathfrak{q}}{2}$ is elementary in CFT_2 (holographic or otherwise), but is a more involved function of $\sigma(\mathfrak{w},\mathfrak{q},\Delta)$ in higher dimensional holographic CFTs. In the latter case, one needs to determine σ from the semiclassical Virasoro block. This form of the result not only holds for scalar conformal primaries of the holographic CFT, but also for the conserved currents. In order to determine the latter, we have generalized the formalism to include equations with apparent singular points. In the auxiliary 2d CFT these correspond to heavy degenerate operator insertions.

One useful result we have been able to derive using this formalism is an exact quantization condition for purely decaying QNMs in a near-extremal black hole background. Schematically, this result takes the form

$$\mathfrak{w}_n = -i\,T\,(2\,n+\Delta_{\text{near-horizon}})\,, \qquad n\in\mathbb{Z}_{\geq 0}\,. \tag{5.7.2}$$

Here $\Delta_{\text{near-horizon}}$ is the conformal dimension of the operator in the near-horizon AdS_2 throat

present in the extremal limit. We have derived this expression for a neutral scalar primary of the holographic CFT, but expect it to hold more generally. One reason for this expectation is based on the structure of correlators in the AdS_2 throat region [FLMV11]. We comment further on this result below.

There are several directions in which our results can be generalized, some of which we outline below.

Conserved current correlators: A natural extension of our analysis would be to carry out an analogous exercise for correlation functions in a finite density system. For instance, by analyzing the fluctuations of gravitons and photons in the Reissner-Nordström-AdS_5 background, one can extract the correlation functions of the energy-momentum and charge current in $\mathcal{N} = 4$ SYM. This example also has the advantage of teaching us about thermal correlation functions in the presence of 't Hooft anomalies using holography. This problem has recently been analyzed in a series of works [HLRV22b; HLRV22a] and there are even results for anomaly induced correlation functions [RVZ23]. Another interesting analysis in this context would be to consider charged fermionic operators along the lines of [LRSS21; MS24].

One aspect we have not discussed is the low energy gradient expansion of the correlation functions. One of the motivations for analyzing the equations for us originated from the recent understanding of open effective field theories for quantum systems coupled to conserved currents of a thermal environment. The presence of long-lived hydrodynamic modes in such thermal environments leads to non-Markovian open system dynamics. This class of problems was analyzed for neutral holographic environments in [GLPRSV21; HLRSV22] and for charged holographic environments in [HLRV22b; HLRV22a]. These works derived the 2-point retarded thermal Green's functions in a low frequency and momentum expansion, both for conserved charged currents and the energy-momentum tensor. Our results are complementary in that we have not attempted to directly analyze this low energy regime. It would also be interesting to understand the connection to the recent work [AABGT23], who argue for an expansion in terms of multiple polylogarithms, for a similar structure originates in the gradient expansion in the aforementioned works.

Asymptotic QNMs: The SW limit of the exact quantization condition allows one to obtain the asymptotic QNMs at large overtone number. As discussed in §5.5 it would be desirable to directly deduce the asymptotic behaviour from the SW prepotential. In particular, it would be interesting to apply this to determine the asymptotic gap in QNMs (for both purely decaying and the so-called Christmas-tree type with a non-vanishign real part) around charged black hole backgrounds. Based on numerical results, we expect the asymptotic gap for the purely decaying mode to go from linear to temperature in the near-extremal limit to infinity in the neutral black hole.

Another interesting question to analyze is to analytically determine purely decaying QNMs for all channels of scalar, gauge field, and metric perturbations in near-extremal black hole backgrounds. As we noted above, we expect a result analogous to (5.7.2). The calculation ought to be doable as near-extremal limit at small frequency corresponds to certain OPE or degeneration limit of four or five-punctured sphere to three-punctured sphere. The latter corresponds to the hypergeometric oper, which is natural given the emergence of a long AdS_2 throat and thus an $SL(2,\mathbb{R})$ isometry in the extremal limit.

One loop determinants around black holes: The determination of an analytic formula for purely decaying QNMs around near-extremal black holes, has interesting implications for black hole thermodynamics. It is now well understood that the Bekenstein-Hawking result for the near-extremal thermodynamics receives corrections [GMT20; IT21; IMT22] owing to gapless modes localized in the near-horizon region. This result is derived by computing the one-loop partition function around the black hole background, and realizing that these gapless modes lead to a temperature dependent one-loop determinant. The connection with QNMs arises owing to an elegant formula for the black hole determinant over the set of QNMs (and their conjugate anti-QNMs) [DHS10]. We believe it should be possible to explicitly deduce this temperature dependent contribution from these purely decaying QNMs, and hope to report on it in the near-future (for another perspective, see [Kol24]). See also [ABT24] for a recent application of the connection coefficients method discussed here to black hole determinant.

Higher point functions: Our discussion has primarily focused on thermal 2-point functions, which have the nice feature of being directly related to the connection problem. However, as reviewed in §5.2.2 it is more natural to work with the Schwinger-Keldysh formalism for real-time computations. The essential ingredient in that case is the ingoing boundary-to-bulk Green's function G_{in}, in terms of which we can obtain all the correlation functions using bulk Witten diagrams on the grSK geometry. Therefore, should one be able to compute G_{in} from the auxiliary 2d CFT description, we would be in a position to compute any desired holographic thermal correlator that can be obtained with the Schwinger-Keldysh time-ordering. This ingoing Green's function is an on-shell solution to the black hole wave equation subject to non-normalizable boundary conditions at the AdS boundary, and is ingoing at the horizon. In our language, this is given by the wavefunction $\psi_{\text{in}}(z)$, which can be obtained from the Virasoro block $\mathcal{F}(z,x)$. In particular, taking the ratio of the full degenerate Virasoro block and its heavy part in the semiclassical limit gives us $\psi_{\text{in}}(z)$, cf. (5.3.43). While obtaining the degenerate Virasoro block, and its semiclassical limit, is still a challenging proposition, doing so would allow us to extend the formalism to computing higher point thermal correlation functions.

Generalization to logarithmic CFT: Technically, the CFT method discussed here only applies to black hole perturbation problems holographically dual to CFT operators with non-integer conformal dimensions, with the integer cases involving logarithmic solutions. In fact, the integer cases correspond to most of the physically relevant examples, especially when the dual CFT operators are conserved currents. While, as advocated in Claims 5.4.1 and 5.4.2, the answers for the integer cases can in principle be extracted from taking a suitable limit from the non-integer case, the procedure is not particularly straightforward for calculating the two-point function, where regularization of a singular limit is required. It is thus desirable to give a direct description of the integer cases without the need for taking such limit. As already mentioned in Remark 5.4.1, we expect that this can be achieved by generalizing the current CFT method to logarithmic CFT.

The origins of the auxiliary 2d CFT: While one might have guessed at a formula as in (5.7.1) for holographic CFTs from the knowledge of the analytic structure, it is intriguing that this

form of the answer is naturally suggested by viewing the black hole wave equation as the BPZ Ward identity for a higher-point function in an auxiliary 2d CFT. Thus far, the origin of this auxiliary 2d CFT appears somewhat empirical to us. Knowing that the wave equations in black hole backgrounds are Fuchsian, one can identify this auxiliary CFT as a tool to help solve the equation, or at least deduce the physical features of interest such as the QNMs. However, it is interesting to ask why this relation arises in the first place.

Consider computing the thermal correlator of strongly coupled planar CFT, and imagine that we are unaware of a holographic dual. Could one deduce from the structure of the thermal 2-point function that there is an auxiliary 2d CFT lurking in the background? Note that this question is intimately tied with bulk locality in the holographic context, since the BPZ equation of the auxiliary CFT is the radial wave equation. Therefore, being able to show that a relation to the auxiliary CFT exists would introduce naturally the bulk radial coordinate, a feature that is a priori not visible in just the thermal correlator. This is a fascinating question that we think deserves further attention. For instance, one could ask if a similar result would hold away from the classical gravity regime. Would, for example, thermal correlation functions of $\mathcal{N}=4$ SYM at large N, but finite 't Hooft coupling continue to be related to a connection problem, which can be interpreted in terms of an auxiliary 2d CFT?

5.A. Further details on apparent singularities and their CFT description

Consider a second order Fuchsian equation in normal form, with apparent singularities at $\{w_\alpha\}$:

$$\begin{gathered}\psi''(z)+\mathtt{T}(z)\psi(z)=0\,,\\ \mathtt{T}(z)=\sum_i\left(\frac{\delta_i}{(z-z_i)^2}+\frac{c_i}{z-z_i}\right)+\sum_\alpha\left(\frac{\delta_\alpha}{(z-w_\alpha)^2}+\frac{d_\alpha}{z-w_\alpha}\right)\,,\\ \delta_i=\frac{1}{4}-\theta_i^2,\quad \delta_\alpha=\frac{1-s_\alpha^2}{4},\quad s_\alpha\in\mathbb{Z}\,.\end{gathered}\tag{5.A.1}$$

The exponents are $\frac{1}{2}\pm\theta_i$ at $\{z_i\}$, and $\frac{1}{2}\pm\frac{s_\alpha}{2}$ at $\{w_\alpha\}$. For $\{w_\alpha\}$ to be apparent singularities without logarithmic branch, additional conditions on $\mathtt{T}(z)$ are needed.

A useful property: A basis of solution $\psi_\pm(z)$ of the Fuchsian equation satisfies,

$$\left\{\frac{\psi_+}{\psi_-}, z\right\} = 2\,\mathtt{T}(z) \tag{5.A.2}$$

where $\{\cdot, z\}$ denote Schwarzian derivative w.r.t. z.

5.A.1. The apparent singularity condition

At each w_α, define the expansion

$$\mathtt{T}(z) = \sum_{m=0} \mathfrak{l}_{-m}^{(w_\alpha)}\,(z-w_\alpha)^{m-2}\,, \qquad \mathfrak{l}_{-m}^{(w_\alpha)} = \mathrm{Res}_{z=w_\alpha}\left[(z-w_\alpha)^{1-m}\,\mathtt{T}(z)\right]\,. \tag{5.A.3}$$

The coefficients themselves are

$$\begin{aligned}
&\mathfrak{l}_0^{(w_\alpha)} = \delta_\alpha\,, \qquad \mathfrak{l}_{-1}^{(w_\alpha)} = d_\alpha\,,\\
&\mathfrak{l}_{-m}^{(w_\alpha)} = \frac{1}{(m-2)!}\,\partial_z^{m-2}\mathtt{T}^{(\bar\alpha)}(z)\Big|_{z=w_\alpha}\,, \qquad m\geq 2\\
&\qquad = \sum_i \frac{(m-1)\,\delta_i}{(z_i-w_\alpha)^m} - \frac{c_i}{(z_i-w_\alpha)^{m-1}} + \sum_{\beta\neq\alpha}\frac{(m-1)\,\delta_\beta}{(w_\beta-w_\alpha)^m} - \frac{d_\beta}{(w_\beta-w_\alpha)^{m-1}}\,,
\end{aligned} \tag{5.A.4}$$

where $\mathtt{T}^{(\bar\alpha)}(z)$ denotes $\mathtt{T}(z)$ with singular terms at w_α excluded.

The apparent singularity condition with exponent difference n is an algebraic equation between $\mathfrak{l}_{-1}, \cdots, \mathfrak{l}_{-n}$. The condition can be extracted from the Schwarzian derivative of $\frac{\psi_+}{\psi_-} = (z-w)^n\,F(z)$.

Example 5.A.1 (n=3)**.** Using (5.A.2) and (5.A.3), we compute $\mathfrak{l}_{-1}$, $\mathfrak{l}_{-2}$, $\mathfrak{l}_{-3}$ from Schwarzian derivative of $\frac{\psi_+}{\psi_-} = (z-w)^3\,F(z)$:

$$\begin{aligned}
\mathfrak{l}_{-1} &= -\frac{4}{3}\,\frac{F'(w)}{F(w)}\,,\\
\mathfrak{l}_{-2} &= \frac{8\,F'(w)^2 - 15\,F(w)\,F''(w)}{18\,F(w)^2}\\
\mathfrak{l}_{-3} &= \frac{32\,F'(w)^3 - 30\,F(w)\,F'(w)\,F''(w)}{27\,F(w)^3}.
\end{aligned} \tag{5.A.5}$$

We note the absence of $F^{(3)}(w)$ in $\mathfrak{l}_{-3}$. This allows one to write $\mathfrak{l}_{-3}$ in terms of $\mathfrak{l}_{-1}$ and $\mathfrak{l}_{-2}$ by first solving $\frac{F'(w)}{F(w)}$ and $\frac{F''(w)}{F(w)}$ using the first two conditions.

This procedure continues to work for higher n where $F^{(n)}(w)$ is absent from l_{-n}. The first few apparent singularity conditions (ASCs) were listed in table 5.1.

5.A.2. Degenerate Virasoro representations

To understand what the ASC means, we recall from §5.3.1 that the Liouville theory has a set of degenerate representations $V_{\langle r,s\rangle}$ with conformal weights $h_{\langle r,s\rangle}$. In the Hilbert space, we have null states $\left|\chi_{\langle r,s\rangle}\right\rangle$ at level rs:

$$\left|\chi_{\langle r,s\rangle}\right\rangle = L_{\langle r,s\rangle}\left|h_{\langle r,s\rangle}\right\rangle. \tag{5.A.6}$$

The null states at the first few levels are collated in table 5.5.

rs	$\langle r,s\rangle$	$L_{\langle r,s\rangle}$
1	$\langle 1,1\rangle$	L_{-1}
2	$\langle 1,2\rangle$	$b^2\,L_{-1}^2 + L_{-2}$
	$\langle 2,1\rangle$	$b^{-2}\,L_{-1}^2 + L_{-2}$
3	$\langle 1,3\rangle$	$\frac{b^4}{2\,(2-b^2)}\,L_{-1}^3 + \frac{2\,b^2}{2-b^2}\,L_{-1}\,L_{-2} + L_{-3}$
	$\langle 3,1\rangle$	$\frac{1}{2\,b^2(2\,b^2-1)}\,L_{-1}^3 + \frac{2}{2\,b^2-1}\,L_{-1}\,L_{-2} + L_{-3}$
4	$\langle 1,4\rangle$	$\frac{b^6}{6\,(6-4\,b^2+b^4)}\,L_{-1}^4 + \frac{5\,b^4}{3\,(6-4\,b^2+b^4)}\,L_{-1}^2\,L_{-2} + \frac{3\,b^2}{2\,(6-4\,b^2+b^4)}\,L_{-2}^2 + \frac{b^2\,(12-5\,b^2)}{3\,(6-4\,b^2+b^4)}\,L_{-1}\,L_{-3} + L_{-4}$
	$\langle 4,1\rangle$	$\frac{1}{6\,(b^2-4\,b^4+6\,b^6)}\,L_{-1}^4 + \frac{5}{3(1-4\,b^2+6\,b^4)}\,L_{-1}^2\,L_{-2} + \frac{3\,b^2}{2-8\,b^2+12\,b^4}\,L_{-2}^2 + \frac{(12\,b^2-5)}{3\,(1-4\,b^2+6\,b^4)}\,L_{-1}\,L_{-3} + L_{-4}$
	$\langle 2,2\rangle$	$\frac{b^2}{3\,(-1+b^2)^2}\,L_{-1}^4 + \frac{2\,(1+b^4)}{3\,(-1+b^2)^2}\,L_{-1}^2\,L_{-2} + \frac{(1+b^2)^2}{3\,b^2}\,L_{-2}^2 - \frac{2\,(1-3\,b^2+b^4)}{3\,(-1+b^2)^2}\,L_{-1}\,L_{-3} + L_{-4}$

Table 5.5.: Null vectors at first few levels.

5.A.3. Apparent singularities from degenerate representations

Consider the following degenerate Virasoro block in any channel

$$\mathcal{F}\,(z,\mathbf{z},\mathbf{w}) = \left\langle V_{\langle 2,1\rangle}(z)\,\prod_i V_{P_i}(z_i)\,\prod_\alpha V_{\langle r_\alpha,s_\alpha\rangle}(w_\alpha)\right\rangle, \quad s_\alpha \neq 1. \tag{5.A.7}$$

The operator $V_{\langle 2,1\rangle}(z)$ is singled out, while the other degenerate operators $V_{\langle r_\alpha,s_\alpha\rangle}(w_\alpha)$ are inserted at locations w_α, which we will identify with the location of apparent singularties.

The degenerate block satisfies BPZ null vector decoupling equations for each of the degenerate

representations involved, viz.,

$$\begin{aligned} \mathcal{L}^{(z)}_{\langle 2,1\rangle}\mathcal{F} &= 0 \\ \mathcal{L}^{(w_\alpha)}_{\langle r_\alpha,s_\alpha\rangle}\mathcal{F} &= 0 \quad \forall\alpha. \end{aligned} \tag{5.A.8}$$

The differential operator $\mathcal{L}^{(\zeta)}_{\langle r,s\rangle}$ is induced from $L_{\langle r,s\rangle}$, with action of each Virasoro generator given by

$$\mathcal{L}^{(\zeta)}_{-n} = \sum_I \frac{(n-1)\,h_I}{(\zeta_I-\zeta)^n} - \frac{1}{(\zeta_I-\zeta)^{n-1}}\,\partial_{\zeta_I} \tag{5.A.9}$$

where the sum is over all other operators in the correlation function. In particular,

$$\mathcal{L}^{(\zeta)}_{-1} = -\sum_I \partial_{\zeta_I} = \partial_\zeta. \tag{5.A.10}$$

We now consider the semiclassical limit (5.3.11) of this degenerate block, which we record here for convenience

$$b\to 0, \quad P_i\to\infty, \quad bP_i\to\theta_i \ (b^2h_i\to\delta_i) \tag{5.A.11}$$

In this limit, $V_{\langle 2,1\rangle}$ is light with $\mathcal{O}\big(b^0\big)$ weight, while other operators have $\mathcal{O}\big(b^{-2}\big)$ weights, including the other degenerate operators with $s_\alpha\neq 1$. This motivates the heavy-light factorization ansatz:

$$\mathcal{F}_{\rm cl}(z,\mathbf{z},\mathbf{w}) = \psi(z|\mathbf{z},\mathbf{w})\; e^{b^{-2}\,\mathcal{W}(\mathbf{z},\mathbf{w})}. \tag{5.A.12}$$

The BPZ equation $\mathcal{L}^{(z)}_{\langle 2,1\rangle}\mathcal{F}_{\rm cl}=0$ leads to

$$\begin{gathered} b^{-2}\Big[\psi''(z)+\mathtt{T}(z)\psi(z)\Big]+\mathcal{O}\big(b^0\big)=0\,, \\ \mathtt{T}(z)=\sum_i\left(\frac{\delta_i}{(z-z_i)^2}+\frac{\partial_{z_i}\mathcal{W}}{z-z_i}\right)+\sum_\alpha\left(\frac{\delta_\alpha}{(z-w_\alpha)^2}+\frac{\partial_{w_\alpha}\mathcal{W}}{z-w_\alpha}\right), \\ \delta_i=\frac{1}{4}-\theta_i^2, \quad \delta_\alpha=\frac{1-s_\alpha^2}{4}\,. \end{gathered} \tag{5.A.13}$$

Note that one has the following identification between accessory parameters and derivatives of classical conformal block:

$$c_i=\partial_{z_i}\mathcal{W}\,, \qquad d_\alpha=\partial_{w_\alpha}\mathcal{W}. \tag{5.A.14}$$

For the other BPZ equations $\mathcal{L}^{(w_\alpha)}_{\langle r_\alpha, s_\alpha\rangle}\mathcal{F}_{\rm cl}=0$, consider the action of each Virasoro generato r at level m:

$$\mathcal{L}^{(w_\alpha)}_{-m}\mathcal{Z}_{\rm cl}=b^{-2}\left[\sum_i\frac{(m-1)\,\delta_i}{(z_i-w_\alpha)^m}-\frac{\partial_{z_i}\mathcal{W}}{(z_i-w_\alpha)^{m-1}}+\sum_{\beta\neq\alpha}\frac{(m-1)\delta_\beta}{(w_\beta-w_\alpha)^m}-\frac{\partial_{w_\beta}\mathcal{W}}{(w_\beta-w_\alpha)^{m-1}}\right]\mathcal{Z}_{\rm cl}$$
$$+\mathcal{O}\big(b^0\big) \tag{5.A.15}$$

Recalling relations (5.A.4) and (5.A.14), we therefore have

$$\boxed{\mathcal{L}^{(w_\alpha)}_{-m}\mathcal{F}_{\rm cl}\;=\;b^{-2}\,\mathfrak{l}^{(w_\alpha)}_{-m}\mathcal{F}_{\rm cl}+\mathcal{O}\big(b^0\big),\qquad m\geq 1\,.} \tag{5.A.16}$$

In other words, in the classical limit $\mathcal{Z}_{\rm cl}$ acts as a common eigenfunction for all (raising) Virasoro generators. Each BPZ equation $\mathcal{L}^{(w_\alpha)}_{\langle r_\alpha, s_\alpha\rangle}\mathcal{F}_{\rm cl}=0$ then gives the following constraint on $\mathfrak{l}^{(w_\alpha)}_{-m}$:

$$\boxed{\lim_{b\to 0}L_{\langle r,s\rangle}\Big|_{L_{-m}\to b^{-2}\,\mathfrak{l}_{-m}}=0,\qquad s\neq 1\,.} \tag{5.A.17}$$

So we have two constraints for $\mathcal{Z}_{\rm cl}$, one which is a second order equation (5.A.13), which is of the form we seek to solve for holographic correlators, and another which constraints the accessory parameters

$$\sum_i\frac{(m-1)\,\delta_i}{(z_i-w_\alpha)^m}-\frac{c_i}{(z_i-w_\alpha)^{m-1}}+\sum_{\beta\neq\alpha}\frac{(m-1)\,\delta_\beta}{(w_\beta-w_\alpha)^m}-\frac{d_\beta}{(w_\beta-w_\alpha)^{m-1}}=0 \tag{5.A.18}$$

From tables 5.1 and 5.5, we see that, up to $n=4$, the apparent singularity conditions for exponent difference n are precisely recovered from the classical limits of BPZ equations for degenerate representations $V_{\langle 1,n\rangle}$.

Bibliography

[AABGT23] Gleb Aminov, Paolo Arnaudo, Giulio Bonelli, Alba Grassi, and Alessandro Tanzini. "Black hole perturbation theory and multiple polylogarithms". In: *JHEP* 11 (2023), p. 059. DOI: 10.1007/JHEP11(2023)059. arXiv: 2307.10141 [hep-th] (cit. on pp. 120, 186).

[ABT24] Paolo Arnaudo, Giulio Bonelli, and Alessandro Tanzini. "One loop effective actions in Kerr-(A)dS Black Holes". In: (May 2024). arXiv: 2405.13830 [hep-th] (cit. on p. 187).

[ACHP18] Raúl E. Arias, Horacio Casini, Marina Huerta, and Diego Pontello. "Entropy and modular Hamiltonian for a free chiral scalar in two intervals". In: *Phys. Rev. D* 98.12 (2018), p. 125008. DOI: 10.1103/PhysRevD.98.125008. arXiv: 1809.00026 [hep-th] (cit. on pp. 6, 93).

[AF98] G. E. Arutyunov and S. A. Frolov. "Virasoro amplitude from the S**N R**24 orbifold sigma model". In: *Theor. Math. Phys.* 114 (1998), pp. 43–66. DOI: 10.1007/BF02557107. arXiv: hep-th/9708129 (cit. on pp. 54, 56, 68, 73).

[AGH22] Gleb Aminov, Alba Grassi, and Yasuyuki Hatsuda. "Black Hole Quasinormal Modes and Seiberg–Witten Theory". In: *Annales Henri Poincare* 23.6 (2022), pp. 1951–1977. DOI: 10.1007/s00023-021-01137-x. arXiv: 2006.06111 [hep-th] (cit. on pp. 120, 128).

[AGT10] Luis F. Alday, Davide Gaiotto, and Yuji Tachikawa. "Liouville Correlation Functions from Four-dimensional Gauge Theories". In: *Lett. Math. Phys.* 91 (2010), pp. 167–197. DOI: 10.1007/s11005-010-0369-5. arXiv: 0906.3219 [hep-th] (cit. on pp. 5, 120, 131, 173).

[AH23] David Avis and Sergio Hernández-Cuenca. "On the foundations and extremal structure of the holographic entropy cone". In: *Applications Math.* 328 (2023), p. 16. DOI: 10.1016/j.dam.2022.11.016. arXiv: 2102.07535 [math.CO] (cit. on pp. 10, 12, 19, 27).

[AHR21] Chris Akers, Sergio Hernández-Cuenca, and Pratik Rath. "Quantum Extremal Surfaces and the Holographic Entropy Cone". In: *JHEP* 11 (2021), p. 177. DOI: 10.1007/JHEP11(2021)177. arXiv: 2108.07280 [hep-th] (cit. on p. 10).

[BBT03] Olivier Babelon, Denis Bernard, and Michel Talon. *Introduction to Classical Integrable Systems*. Cambridge Monographs on Mathematical Physics. Cambridge University Press, 2003. DOI: 10.1017/CBO9780511535024 (cit. on p. 58).

[BC20] Pablo Bueno and Horacio Casini. "Reflected entropy, symmetries and free fermions". In: *JHEP* 05 (2020), p. 103. DOI: 10.1007/JHEP05(2020)103. arXiv: 2003.09546 [hep-th] (cit. on pp. 97, 100).

[BCHS20a] Ning Bao, Newton Cheng, Sergio Hernández-Cuenca, and Vincent P. Su. "The Quantum Entropy Cone of Hypergraphs". In: *SciPost Phys.* 9.5 (2020), p. 5. DOI: 10.21468/SciPostPhys.9.5.067. arXiv: 2002.05317 [quant-ph] (cit. on p. 10).

[BCHS20b] Ning Bao, Newton Cheng, Sergio Hernández-Cuenca, and Vincent Paul Su. "A Gap Between the Hypergraph and Stabilizer Entropy Cones". In: (June 2020). arXiv: 2006.16292 [quant-ph] (cit. on p. 10).

[BCHS22] Ning Bao, Newton Cheng, Sergio Hernández-Cuenca, and Vincent Paul Su. "Topological Link Models of Multipartite Entanglement". In: *Quantum* 6 (2022), p. 741. DOI: 10.22331/q-2022-06-20-741. arXiv: 2109.01150 [quant-ph] (cit. on p. 10).

[BCS09] Emanuele Berti, Vitor Cardoso, and Andrei O. Starinets. "Quasinormal modes of black holes and black branes". In: *Class. Quant. Grav.* 26 (2009), p. 163001. DOI: 10.1088/0264-9381/26/16/163001. arXiv: 0905.2975 [gr-qc] (cit. on p. 117).

[BDK20] Mert Beşken, Shouvik Datta, and Per Kraus. "Semi-classical Virasoro blocks: proof of exponentiation". In: *JHEP* 01 (2020), p. 109. DOI: 10.1007/JHEP01(2020)109. arXiv: 1910.04169 [hep-th] (cit. on p. 133).

[BGZ14] Leonardo Banchi, Paolo Giorda, and Paolo Zanardi. "Quantum information-geometry of dissipative quantum phase transitions". In: *Phys. Rev. E* 89 (2 Feb. 2014), p. 022102. DOI: 10.1103/PhysRevE.89.022102. URL: https://link.aps.org/doi/10.1103/PhysRevE.89.022102 (cit. on p. 99).

[BIPT23] Giulio Bonelli, Cristoforo Iossa, Daniel Panea Lichtig, and Alessandro Tanzini. "Irregular Liouville Correlators and Connection Formulae for Heun Functions". In: *Commun. Math. Phys.* 397.2 (2023), pp. 635–727. DOI: 10.1007/s00220-022-04497-5. arXiv: 2201.04491 [hep-th] (cit. on p. 119).

[BJLR17] Avinash Baidya, Chandan Jana, R. Loganayagam, and Arnab Rudra. "Renormalization in open quantum field theory. Part I. Scalar field theory". In: *JHEP* 11 (2017), p. 204. DOI: 10.1007/JHEP11(2017)204. arXiv: 1704.08335 [hep-th] (cit. on p. 118).

[BM18] Ning Bao and Márk Mezei. "On the Entropy Cone for Large Regions at Late Times". In: (Oct. 2018). arXiv: 1811.00019 [hep-th] (cit. on p. 10).

[BNOSSW15] Ning Bao, Sepehr Nezami, Hirosi Ooguri, Bogdan Stoica, James Sully, and Michael Walter. "The Holographic Entropy Cone". In: *JHEP* 09 (2015), p. 130. DOI: 10.1007/JHEP09(2015)130. arXiv: 1505.07839 [hep-th] (cit. on pp. 10, 12, 19).

[BP02] H.P. Breuer and F. Petruccione. *The theory of open quantum systems*. Oxford University Press, 2002 (cit. on p. 118).

[BPZ84] A. A. Belavin, Alexander M. Polyakov, and A. B. Zamolodchikov. "Infinite Conformal Symmetry in Two-Dimensional Quantum Field Theory". In: *Nucl. Phys. B* 241 (1984). Ed. by I. M. Khalatnikov and V. P. Mineev, pp. 333–380. DOI: 10.1016/0550-3213(84)90052-X (cit. on p. 4).

[BSS02] Danny Birmingham, Ivo Sachs, and Sergey N. Solodukhin. "Conformal field theory interpretation of black hole quasinormal modes". In: *Phys. Rev. Lett.* 88 (2002), p. 151301. DOI: 10.1103/PhysRevLett.88.151301. arXiv: hep-th/0112055 (cit. on pp. 119, 173).

[BW76] J. J Bisognano and E. H. Wichmann. "On the Duality Condition for Quantum Fields". In: *J. Math. Phys.* 17 (1976), pp. 303–321. DOI: 10.1063/1.522898 (cit. on pp. 89, 105).

[Car86] John L. Cardy. "Operator Content of Two-Dimensional Conformally Invariant Theories". In: *Nucl. Phys. B* 270 (1986), pp. 186–204. DOI: 10.1016/0550-3213(86)90552-3 (cit. on p. 5).

[CC04] Pasquale Calabrese and John L. Cardy. "Entanglement entropy and quantum field theory". In: *J. Stat. Mech.* 0406 (2004), P06002. DOI: 10.1088/1742-5468/2004/06/P06002. arXiv: hep-th/0405152 (cit. on pp. 5, 53, 54, 57, 73, 75, 86, 88).

[CCCJLS19] Bidisha Chakrabarty, Joydeep Chakravarty, Soumyadeep Chaudhuri, Chandan Jana, R. Loganayagam, and Akhil Sivakumar. "Nonlinear Langevin dynamics via holography". In: (2019). arXiv: 1906.07762 [hep-th] (cit. on p. 117).

[CCL19] Bidisha Chakrabarty, Soumyadeep Chaudhuri, and R. Loganayagam. "Out of Time Ordered Quantum Dissipation". In: *JHEP* 07 (2019), p. 102. DOI: 10.1007/JHEP07(2019)102. arXiv: 1811.01513 [cond-mat.stat-mech] (cit. on p. 127).

[CCT09] Pasquale Calabrese, John Cardy, and Erik Tonni. "Entanglement entropy of two disjoint intervals in conformal field theory". In: *J. Stat. Mech.* 0911 (2009), P11001. DOI: 10.1088/1742-5468/2009/11/P11001. arXiv: 0905.2069 [hep-th] (cit. on pp. 6, 54, 84).

[CCT12] Pasquale Calabrese, John Cardy, and Erik Tonni. "Entanglement negativity in quantum field theory". In: *Phys. Rev. Lett.* 109 (2012), p. 130502. DOI: 10.1103/PhysRevLett.109.130502. arXiv: 1206.3092 [cond-mat.stat-mech] (cit. on p. 54).

[CCY19] Minjae Cho, Scott Collier, and Xi Yin. "Genus Two Modular Bootstrap". In: *JHEP* 04 (2019), p. 022. DOI: 10.1007/JHEP04(2019)022. arXiv: 1705.05865 [hep-th] (cit. on p. 54).

[CD19] Bartlomiej Czech and Xi Dong. "Holographic Entropy Cone with Time Dependence in Two Dimensions". In: *JHEP* 10 (2019), p. 177. DOI: 10.1007/JHEP10(2019)177. arXiv: 1905.03787 [hep-th] (cit. on p. 10).

[CFMP22] Dario Consoli, Francesco Fucito, Jose Francisco Morales, and Rubik Poghossian. "CFT description of BH's and ECO's: QNMs, superradiance, echoes and tidal responses". In: *JHEP* 12 (2022), p. 115. DOI: 10.1007/JHEP12(2022)115. arXiv: 2206.09437 [hep-th] (cit. on p. 119).

[CH09] H. Casini and M. Huerta. "Reduced density matrix and internal dynamics for multicomponent regions". In: *Class. Quant. Grav.* 26 (2009), p. 185005. DOI: 10.1088/0264-9381/26/18/185005. arXiv: 0903.5284 [hep-th] (cit. on pp. 6, 93).

[CHHHSW19] Shawn X. Cui, Patrick Hayden, Temple He, Matthew Headrick, Bogdan Stoica, and Michael Walter. "Bit Threads and Holographic Monogamy". In: *Commun. Math. Phys.* 376.1 (2019), pp. 609–648. DOI: 10.1007/s00220-019-03510-8. arXiv: 1808.05234 [hep-th] (cit. on p. 10).

[CHM11] Horacio Casini, Marina Huerta, and Robert C. Myers. "Towards a derivation of holographic entanglement entropy". In: *JHEP* 05 (2011), p. 036. DOI: 10.1007/JHEP05(2011)036. arXiv: 1102.0440 [hep-th] (cit. on pp. 89, 105).

[CHMY15] Horacio Casini, Marina Huerta, Robert C. Myers, and Alexandre Yale. "Mutual information and the F-theorem". In: *JHEP* 10 (2015), p. 003. DOI: 10.1007/JHEP10(2015)003. arXiv: 1506.06195 [hep-th] (cit. on p. 26).

[CM16] Renzo Cavalieri and Eric Miles. "Riemann Surfaces and Algebraic Curves: A First Course in Hurwitz Theory". In: 2016 (cit. on p. 62).

[CMM17] John Cardy, Alexander Maloney, and Henry Maxfield. "A new handle on three-point coefficients: OPE asymptotics from genus two modular invariance". In:

JHEP 10 (2017), p. 136. DOI: 10.1007/JHEP10(2017)136. arXiv: 1705.05855 [hep-th] (cit. on p. 54).

[CMMT20] Scott Collier, Alexander Maloney, Henry Maxfield, and Ioannis Tsiares. "Universal dynamics of heavy operators in CFT_2". In: *JHEP* 07 (2020), p. 074. DOI: 10.1007/JHEP07(2020)074. arXiv: 1912.00222 [hep-th] (cit. on p. 5).

[CMST18] Horacio Casini, Raimel Medina, Ignacio Salazar Landea, and Gonzalo Torroba. "Renyi relative entropies and renormalization group flows". In: *JHEP* 09 (2018), p. 166. DOI: 10.1007/JHEP09(2018)166. arXiv: 1807.03305 [hep-th] (cit. on p. 99).

[CP21] Bidisha Chakrabarty and Aswin P. M. "Open effective theory of scalar field in rotating plasma". In: *JHEP* 08 (2021), p. 169. DOI: 10.1007/JHEP08(2021)169. arXiv: 2011.13223 [hep-th] (cit. on p. 117).

[CS21] Bartlomiej Czech and Sirui Shuai. "Holographic Cone of Average Entropies". In: (Dec. 2021). arXiv: 2112.00763 [hep-th] (cit. on pp. 19, 40).

[CT16] John Cardy and Erik Tonni. "Entanglement hamiltonians in two-dimensional conformal field theory". In: *J. Stat. Mech.* 1612.12 (2016), p. 123103. DOI: 10.1088/1742-5468/2016/12/123103. arXiv: 1608.01283 [cond-mat.stat-mech] (cit. on pp. 7, 89, 105).

[CW23] Bartlomiej Czech and Yunfei Wang. "A holographic inequality for N = 7 regions". In: *JHEP* 01 (2023), p. 101. DOI: 10.1007/JHEP01(2023)101. arXiv: 2209.10547 [hep-th] (cit. on pp. 10, 40).

[DE20] Andrea Dei and Lorenz Eberhardt. "Correlators of the symmetric product orbifold". In: *JHEP* 01 (2020), p. 108. DOI: 10.1007/JHEP01(2020)108. arXiv: 1911.08485 [hep-th] (cit. on pp. 54, 55, 90, 92).

[DF21] Souvik Dutta and Thomas Faulkner. "A canonical purification for the entanglement wedge cross-section". In: *JHEP* 03 (2021), p. 178. DOI: 10.1007/JHEP03(2021)178. arXiv: 1905.00577 [hep-th] (cit. on pp. 54, 84).

[DFMS87] Lance J. Dixon, Daniel Friedan, Emil J. Martinec, and Stephen H. Shenker. "The Conformal Field Theory of Orbifolds". In: *Nucl. Phys. B* 282 (1987), pp. 13–73. DOI: 10.1016/0550-3213(87)90676-6 (cit. on pp. 54, 56, 68, 70, 72, 73, 75–77, 84, 89).

[DGIPZ22] Matthew Dodelson, Alba Grassi, Cristoforo Iossa, Daniel Panea Lichtig, and Alexander Zhiboedov. "Holographic thermal correlators from supersymmetric instantons". In: (June 2022). arXiv: 2206.07720 [hep-th] (cit. on pp. 120, 129, 166).

[DHS10] Frederik Denef, Sean A. Hartnoll, and Subir Sachdev. "Black hole determinants and quasinormal modes". In: *Class. Quant. Grav.* 27 (2010), p. 125001. DOI: 10.1088/0264-9381/27/12/125001. arXiv: 0908.2657 [hep-th] (cit. on p. 187).

[DIKZ24] Matthew Dodelson, Cristoforo Iossa, Robin Karlsson, and Alexander Zhiboedov. "A thermal product formula". In: *JHEP* 01 (2024), p. 036. DOI: 10.1007/JHEP01(2024)036. arXiv: 2304.12339 [hep-th] (cit. on p. 117).

[DLR16] Xi Dong, Aitor Lewkowycz, and Mukund Rangamani. "Deriving covariant holographic entanglement". In: *JHEP* 11 (2016), p. 028. DOI: 10.1007/JHEP11(2016)028. arXiv: 1607.07506 [hep-th] (cit. on p. 4).

[DMS97] P. Di Francesco, P. Mathieu, and D. Senechal. *Conformal Field Theory*. Graduate Texts in Contemporary Physics. New York: Springer-Verlag, 1997. ISBN: 978-0-387-94785-3, 978-1-4612-7475-9. DOI: 10.1007/978-1-4612-2256-9 (cit. on pp. 130, 131).

[Ebe20] Lorenz Eberhardt. "AdS_3/CFT_2 at higher genus". In: *JHEP* 05 (2020), p. 150. DOI: 10.1007/JHEP05(2020)150. arXiv: 2002.11729 [hep-th] (cit. on p. 77).

[EGG20] Lorenz Eberhardt, Matthias R. Gaberdiel, and Rajesh Gopakumar. "Deriving the AdS_3/CFT_2 correspondence". In: *JHEP* 02 (2020), p. 136. DOI: 10.1007/JHEP02(2020)136. arXiv: 1911.00378 [hep-th] (cit. on p. 54).

[Eyn18] Bertrand Eynard. "Lectures notes on compact Riemann surfaces". In: *arXiv: Mathematical Physics* (2018) (cit. on p. 63).

[Fay73] John D. Fay. "Theta Functions on Riemann Surfaces". In: 1973 (cit. on p. 63).

[FG21] Davide Fioravanti and Daniele Gregori. "A new method for exact results on Quasinormal Modes of Black Holes". In: (Dec. 2021). arXiv: 2112.11434 [hep-th] (cit. on p. 120).

[FH22] Matteo Fadel and Sergio Hernández-Cuenca. "Symmetrized holographic entropy cone". In: *Phys. Rev. D* 105.8 (2022), p. 086008. DOI: 10.1103/PhysRevD.105.086008. arXiv: 2112.03862 [quant-ph] (cit. on pp. 19, 40).

[FKW14] A. Liam Fitzpatrick, Jared Kaplan, and Matthew T. Walters. "Universality of Long-Distance AdS Physics from the CFT Bootstrap". In: *JHEP* 08 (2014), p. 145. DOI: 10.1007/JHEP08(2014)145. arXiv: 1403.6829 [hep-th] (cit. on p. 119).

[FL09] Guido Festuccia and Hong Liu. "A Bohr-Sommerfeld quantization formula for quasinormal frequencies of AdS black holes". In: *Adv. Sci. Lett.* 2 (2009), pp. 221–235. DOI: 10.1166/asl.2009.1029. arXiv: 0811.1033 [gr-qc] (cit. on pp. 173, 178, 179).

[FLMV11] Thomas Faulkner, Hong Liu, John McGreevy, and David Vegh. "Emergent quantum criticality, Fermi surfaces, and AdS(2)". In: *Phys. Rev. D* 83 (2011), p. 125002. DOI: 10.1103/PhysRevD.83.125002. arXiv: 0907.2694 [hep-th] (cit. on p. 186).

[FV63] R.P. Feynman and Jr. Vernon F.L. "The Theory of a general quantum system interacting with a linear dissipative system". In: *Annals Phys.* 24 (1963), pp. 118–173. DOI: 10.1016/0003-4916(63)90068-X (cit. on p. 118).

[GCL18] Paolo Glorioso, Michael Crossley, and Hong Liu. "A prescription for holographic Schwinger-Keldysh contour in non-equilibrium systems". In: (2018). arXiv: 1812.08785 [hep-th] (cit. on pp. 117, 125).

[GGKM21] Matthias R. Gaberdiel, Rajesh Gopakumar, Bob Knighton, and Pronobesh Maity. "From symmetric product CFTs to AdS_3". In: *JHEP* 05 (2021), p. 073. DOI: 10.1007/JHEP05(2021)073. arXiv: 2011.10038 [hep-th] (cit. on p. 54).

[GIL12] O. Gamayun, N. Iorgov, and O. Lisovyy. "Conformal field theory of Painlevé VI". In: *JHEP* 10 (2012). [Erratum: JHEP 10, 183 (2012)], p. 038. DOI: 10.1007/JHEP10(2012)038. arXiv: 1207.0787 [hep-th] (cit. on pp. 84, 93).

[GIL19] P. Gavrylenko, N. Iorgov, and O. Lisovyy. "Higher rank isomonodromic deformations and W-algebras". In: *Lett. Math. Phys.* 110.2 (2019), pp. 327–364. DOI: 10.1007/s11005-019-01207-6. arXiv: 1801.09608 [math-ph] (cit. on pp. 84, 93).

[GKP98] S. S. Gubser, Igor R. Klebanov, and Alexander M. Polyakov. "Gauge theory correlators from noncritical string theory". In: *Phys. Lett. B* 428 (1998), pp. 105–114. DOI: 10.1016/S0370-2693(98)00377-3. arXiv: hep-th/9802109 (cit. on p. 2).

[GLPRSV21] Jewel K. Ghosh, R. Loganayagam, Siddharth G. Prabhu, Mukund Rangamani, Akhil Sivakumar, and V. Vishal. "Effective field theory of stochastic diffusion from gravity". In: *JHEP* 05 (2021), p. 130. DOI: 10.1007/JHEP05(2021)130. arXiv: 2012.03999 [hep-th] (cit. on pp. 152, 180, 183, 186).

[GM16] P. Gavrylenko and A. Marshakov. "Exact conformal blocks for the W-algebras, twist fields and isomonodromic deformations". In: *JHEP* 02 (2016), p. 181. DOI: 10.1007/JHEP02(2016)181. arXiv: 1507.08794 [hep-th] (cit. on pp. 63, 82, 93, 102, 112).

[GMN13a] Davide Gaiotto, Gregory W. Moore, and Andrew Neitzke. "Spectral networks". In: *Annales Henri Poincare* 14 (2013), pp. 1643–1731. DOI: 10.1007/s00023-013-0239-7. arXiv: 1204.4824 [hep-th] (cit. on p. 174).

[GMN13b] Davide Gaiotto, Gregory W. Moore, and Andrew Neitzke. "Wall-crossing, Hitchin systems, and the WKB approximation". In: *Adv. Math.* 234 (2013), pp. 239–403. DOI: 10.1016/j.aim.2012.09.027. arXiv: 0907.3987 [hep-th] (cit. on p. 174).

[GMT20] Animik Ghosh, Henry Maxfield, and Gustavo J. Turiaci. "A universal Schwarzian sector in two-dimensional conformal field theories". In: *JHEP* 05 (2020), p. 104. DOI: 10.1007/JHEP05(2020)104. arXiv: 1912.07654 [hep-th] (cit. on p. 187).

[Gub97] Steven S. Gubser. "Absorption of photons and fermions by black holes in four-dimensions". In: *Phys. Rev. D* 56 (1997), pp. 7854–7868. DOI: 10.1103/PhysRevD.56.7854. arXiv: hep-th/9706100 (cit. on p. 173).

[GW12] Davide Gaiotto and Edward Witten. "Knot Invariants from Four-Dimensional Gauge Theory". In: *Adv. Theor. Math. Phys.* 16.3 (2012), pp. 935–1086. DOI: 10.4310/ATMP.2012.v16.n3.a5. arXiv: 1106.4789 [hep-th] (cit. on p. 149).

[Har13] Thomas Hartman. "Entanglement Entropy at Large Central Charge". In: (Mar. 2013). arXiv: 1303.6955 [hep-th] (cit. on pp. 54, 84, 96, 119).

[HB21] John Harnad and Ferenc Balogh. *Tau Functions and their Applications*. Cambridge Monographs on Mathematical Physics. Cambridge University Press, 2021. DOI: 10.1017/9781108610902 (cit. on p. 58).

[Her19] Sergio Hernández-Cuenca. "Holographic entropy cone for five regions". In: *Phys. Rev. D* 100.2 (2019), p. 026004. DOI: 10.1103/PhysRevD.100.026004. arXiv: 1903.09148 [hep-th] (cit. on p. 10).

[HH00] Gary T. Horowitz and Veronika E. Hubeny. "Quasinormal modes of AdS black holes and the approach to thermal equilibrium". In: *Phys. Rev.* D62 (2000), p. 024027. DOI: 10.1103/PhysRevD.62.024027. arXiv: hep-th/9909056 [hep-th] (cit. on p. 117).

[HHH19] Temple He, Matthew Headrick, and Veronika E. Hubeny. "Holographic Entropy Relations Repackaged". In: *JHEP* 10 (2019), p. 118. DOI: 10.1007/JHEP10(2019)118. arXiv: 1905.06985 [hep-th] (cit. on pp. 9, 16, 32, 34).

[HHJ23] Sergio Hernández-Cuenca, Veronika E. Hubeny, and Hewei Frederic Jia. "Holographic Entropy Inequalities and Multipartite Entanglement". In: (Sept. 2023). arXiv: 2309.06296 [hep-th] (cit. on pp. ix, 34).

[HHK23] Temple He, Sergio Hernández-Cuenca, and Cynthia Keeler. "Beyond the Holographic Entropy Cone via Cycle Flows". In: (Dec. 2023). arXiv: 2312.10137 [hep-th] (cit. on p. 10).

[HHLR14] Matthew Headrick, Veronika E. Hubeny, Albion Lawrence, and Mukund Rangamani. "Causality & holographic entanglement entropy". In: *JHEP* 12 (2014), p. 162. DOI: 10.1007/JHEP12(2014)162. arXiv: 1408.6300 [hep-th] (cit. on p. 21).

[HHM13] Patrick Hayden, Matthew Headrick, and Alexander Maloney. "Holographic Mutual Information is Monogamous". In: *Phys. Rev. D* 87.4 (2013), p. 046003. DOI: 10.1103/PhysRevD.87.046003. arXiv: 1107.2940 [hep-th] (cit. on pp. 11, 18, 28).

[HHR] Temple He, Veronika Hubeny, and Massimiliano Rota. "Algorithmic derivation of SSA-compatible extreme rays of the subadditivity cone and the $\mathcal{N} = 6$ solution". In: (). In preparation (cit. on p. 41).

[HHR20] Temple He, Veronika E. Hubeny, and Mukund Rangamani. "Superbalance of Holographic Entropy Inequalities". In: *JHEP* 07 (2020), p. 245. DOI: 10.1007/JHEP07(2020)245. arXiv: 2002.04558 [hep-th] (cit. on pp. 10, 13, 25, 29).

[HHR22a] Temple He, Veronika E. Hubeny, and Massimiliano Rota. "On the relation between the subadditivity cone and the quantum entropy cone". In: (Nov. 2022). arXiv: 2211.11858 [hep-th] (cit. on pp. 10, 40).

[HHR22b] Sergio Hernández-Cuenca, Veronika E. Hubeny, and Massimiliano Rota. "The holographic entropy cone from marginal independence". In: *JHEP* 09 (2022), p. 190. DOI: 10.1007/JHEP09(2022)190. arXiv: 2204.00075 [hep-th] (cit. on pp. 9, 10, 40, 41).

[HHR23] Temple He, Veronika E. Hubeny, and Massimiliano Rota. "A gap between holographic and quantum mechanical extreme rays of the subadditivity cone". In: (July 2023). arXiv: 2307.10137 [hep-th] (cit. on pp. 10, 40).

[HHR24] Temple He, Veronika E. Hubeny, and Massimiliano Rota. "Inner bounding the quantum entropy cone with subadditivity and subsystem coarse grainings". In: *Phys. Rev. A* 109.5 (2024), p. 052407. DOI: 10.1103/PhysRevA.109.052407. arXiv: 2312.04074 [quant-ph] (cit. on p. 40).

[HHRR19] Sergio Hernández-Cuenca, Veronika E. Hubeny, Mukund Rangamani, and Massimiliano Rota. "The quantum marginal independence problem". In: (Dec. 2019). arXiv: 1912.01041 [quant-ph] (cit. on pp. 9, 10, 40).

[HJPW04] Patrick Hayden, Richard Jozsa, Denes Petz, and Andreas Winter. "Structure of States Which Satisfy Strong Subadditivity of Quantum Entropy with Equality". In: *Commun. Math. Phys.* 246.2 (Apr. 2004), pp. 359–374. ISSN: 1432-0916. DOI: 10.1007/s00220-004-1049-z. URL: http://dx.doi.org/10.1007/s00220-004-1049-z (cit. on p. 11).

[HK21] Yasuyuki Hatsuda and Masashi Kimura. "Spectral Problems for Quasinormal Modes of Black Holes". In: *Universe* 7.12 (2021), p. 476. DOI: 10.3390/universe7120476. arXiv: 2111.15197 [gr-qc] (cit. on pp. 117, 120).

[HLRSV22] Temple He, R. Loganayagam, Mukund Rangamani, Akhil Sivakumar, and Julio Virrueta. "The timbre of Hawking gravitons: an effective description of energy transport from holography". In: *JHEP* 09 (2022), p. 092. DOI: 10.1007/JHEP09(2022)092. arXiv: 2202.04079 [hep-th] (cit. on pp. 152, 170, 183, 184, 186).

[HLRV22a] Temple He, R. Loganayagam, Mukund Rangamani, and Julio Virrueta. "An effective description of charge diffusion and energy transport in a charged plasma from holography". In: (May 2022). arXiv: 2205.03415 [hep-th] (cit. on p. 186).

[HLRV22b] Temple He, R. Loganayagam, Mukund Rangamani, and Julio Virrueta. "An effective description of momentum diffusion in a charged plasma from holography". In: *JHEP* 01 (2022), p. 145. DOI: 10.1007/JHEP01(2022)145. arXiv: 2108.03244 [hep-th] (cit. on p. 186).

[HP83] S. W. Hawking and Don N. Page. "Thermodynamics of Black Holes in anti-De Sitter Space". In: *Commun. Math. Phys.* 87 (1983), p. 577. DOI: 10.1007/BF01208266 (cit. on p. 3).

[HRR18] Veronika E. Hubeny, Mukund Rangamani, and Massimiliano Rota. "Holographic entropy relations". In: *Fortsch. Phys.* 66.11-12 (2018), p. 1800067. DOI: 10.1002/prop.201800067. arXiv: 1808.07871 [hep-th] (cit. on pp. 10, 22, 23).

[HRR19] Veronika E. Hubeny, Mukund Rangamani, and Massimiliano Rota. "The holographic entropy arrangement". In: *Fortsch. Phys.* 67.4 (2019), p. 1900011. DOI: 10.1002/prop.201900011. arXiv: 1812.08133 [hep-th] (cit. on pp. 10, 13, 16, 18, 26–28).

[HRS21] Lotte Hollands, Philipp Rüter, and Richard J. Szabo. "A geometric recipe for twisted superpotentials". In: *JHEP* 12 (2021), p. 164. DOI: 10.1007/JHEP12(2021)164. arXiv: 2109.14699 [hep-th] (cit. on p. 174).

[HRT07a] Veronika E. Hubeny, Mukund Rangamani, and Tadashi Takayanagi. "A Covariant holographic entanglement entropy proposal". In: *JHEP* 07 (2007), p. 062. DOI: 10.1088/1126-6708/2007/07/062. arXiv: 0705.0016 [hep-th] (cit. on p. 3).

[HRT07b] Veronika E. Hubeny, Mukund Rangamani, and Tadashi Takayanagi. "A Covariant holographic entanglement entropy proposal". In: *JHEP* 07 (2007), p. 062. DOI: 10.1088/1126-6708/2007/07/062. arXiv: 0705.0016 [hep-th] (cit. on pp. 21, 96).

[HS03] C. P. Herzog and D. T. Son. "Schwinger-Keldysh propagators from AdS/CFT correspondence". In: *JHEP* 03 (2003), p. 046. DOI: 10.1088/1126-6708/2003/03/046. arXiv: hep-th/0212072 [hep-th] (cit. on p. 125).

[HS17] Stefan Hollands and Ko Sanders. "Entanglement measures and their properties in quantum field theory". In: (Feb. 2017). arXiv: 1702.04924 [quant-ph] (cit. on p. 5).

[HT07] Matthew Headrick and Tadashi Takayanagi. "A Holographic proof of the strong subadditivity of entanglement entropy". In: *Phys. Rev. D* 76 (2007), p. 106013. DOI: 10.1103/PhysRevD.76.106013. arXiv: 0704.3719 [hep-th] (cit. on p. 4).

[IKSY91] Katsunori Iwasaki, Hironobu Kimura, Shun Shimomura, and Masaaki Yoshida. *From Gauss to Painlevé: A Modern Theory of Special Functions*. 1st ed. Aspects of Mathematics. Vieweg+Teubner Verlag Wiesbaden, June 1991, pp. XII, 347. ISBN: 978-3-322-90165-1. DOI: 10.1007/978-3-322-90163-7 (cit. on p. 135).

[ILT13] N. Iorgov, O. Lisovyy, and Yu. Tykhyy. "Painlevé VI connection problem and monodromy of $c = 1$ conformal blocks". In: *JHEP* 12 (2013), p. 029. DOI: 10.1007/JHEP12(2013)029. arXiv: 1308.4092 [hep-th] (cit. on p. 5).

[ILT15] N. Iorgov, O. Lisovyy, and J. Teschner. "Isomonodromic tau-functions from Liouville conformal blocks". In: *Commun. Math. Phys.* 336.2 (2015), pp. 671–694. DOI: 10.1007/s00220-014-2245-0. arXiv: 1401.6104 [hep-th] (cit. on pp. 5, 84, 93).

[IMT22] Luca V. Iliesiu, Sameer Murthy, and Gustavo J. Turiaci. "Revisiting the Logarithmic Corrections to the Black Hole Entropy". In: (Sept. 2022). arXiv: 2209.13608 [hep-th] (cit. on p. 187).

[IT21] Luca V. Iliesiu and Gustavo J. Turiaci. "The statistical mechanics of near-extremal black holes". In: *JHEP* 05 (2021), p. 145. DOI: 10.1007/JHEP05(2021)145. arXiv: 2003.02860 [hep-th] (cit. on p. 187).

[Jan17] Aron Jansen. "Overdamped modes in Schwarzschild-de Sitter and a Mathematica package for the numerical computation of quasinormal modes". In: *Eur. Phys. J. Plus* 132.12 (2017), p. 546. DOI: 10.1140/epjp/i2017-11825-9. arXiv: 1709.09178 [gr-qc] (cit. on pp. 164, 168).

[Jia23a] Hewei Frederic Jia. "Twist operator correlator revisited and tau function on Hurwitz space". In: (July 2023). arXiv: 2307.03729 [hep-th] (cit. on pp. ix, 86, 87, 89).

[Jia23b] Hewei Frederic Jia. "Twist operator correlators and isomonodromic tau functions from modular Hamiltonians". In: (Aug. 2023). arXiv: 2308.16839 [hep-th] (cit. on p. ix).

[JLR20] Chandan Jana, R. Loganayagam, and Mukund Rangamani. "Open quantum systems and Schwinger-Keldysh holograms". In: *JHEP* 07 (2020), p. 242. DOI: 10.1007/JHEP07(2020)242. arXiv: 2004.02888 [hep-th] (cit. on pp. 117, 118, 126, 127).

[JMU81] M. Jimbo, T. Miwa, and a K. Ueno. "Monodromy Preserving Deformations Of Linear Differential Equations With Rational Coefficients. 1." In: *Physica D* 2 (1981), pp. 407–448 (cit. on pp. 58, 81, 87).

[JN20] Saebyeok Jeong and Nikita Nekrasov. "Opers, surface defects, and Yang-Yang functional". In: *Adv. Theor. Math. Phys.* 24.7 (2020), pp. 1789–1916. DOI: 10.4310/ATMP.2020.v24.n7.a4. arXiv: 1806.08270 [hep-th] (cit. on p. 121).

[JR24] Hewei Frederic Jia and Mukund Rangamani. "Holographic thermal correlators and quasinormal modes from semiclassical Virasoro blocks". In: (Aug. 2024). arXiv: 2408.05208 [hep-th] (cit. on p. ix).

[KI03] Hideo Kodama and Akihiro Ishibashi. "A Master equation for gravitational perturbations of maximally symmetric black holes in higher dimensions". In: *Prog. Theor. Phys.* 110 (2003), pp. 701–722. DOI: 10.1143/PTP.110.701. arXiv: hep-th/0305147 (cit. on pp. 153, 170).

[KI04] Hideo Kodama and Akihiro Ishibashi. "Master equations for perturbations of generalized static black holes with charge in higher dimensions". In: *Prog. Theor. Phys.* 111 (2004), pp. 29–73. DOI: 10.1143/PTP.111.29. arXiv: hep-th/0308128 (cit. on p. 153).

[KK03] A. Kokotov and D. Korotkin. *Tau-function on Hurwitz spaces*. 2003. arXiv: math-ph/0202034 [math-ph] (cit. on pp. 58–60, 68–70, 75, 79, 83, 84).

[KK04] A. Kokotov and D. Korotkin. "Tau-functions on Hurwitz Spaces". In: *Mathematical Physics, Analysis and Geometry* 7.1 (Mar. 2004), pp. 47–96. ISSN:

1572-9656. DOI: 10.1023/B:MPAG.0000022835.68838.56. URL: https://doi.org/10.1023/B:MPAG.0000022835.68838.56 (cit. on pp. 5, 87, 89).

[Kni87] V. G. Knizhnik. "Analytic Fields on Riemann Surfaces. 2". In: *Commun. Math. Phys.* 112 (1987), pp. 567–590. DOI: 10.1007/BF01225373 (cit. on p. 54).

[Kol24] Kolanowski, Maciej and Rakic, Ilija and Rangamani, Mukund, and Turiaci, Gustavo J. "Looking at extremal black holes from very far away". In: *to appear* (2024) (cit. on p. 187).

[Kor03] D. Korotkin. *Solution of matrix Riemann-Hilbert problems with quasi-permutation monodromy matrices*. 2003. arXiv: math-ph/0306061 [math-ph] (cit. on pp. 58, 59, 69, 80, 81, 84).

[Kor04] D. Korotkin. "Solution of matrix Riemann-Hilbert problems with quasi-permutation monodromy matrices". In: *Mathematische Annalen* 329.2 (June 2004), pp. 335–364. ISSN: 1432-1807. DOI: 10.1007/s00208-004-0528-z. URL: https://doi.org/10.1007/s00208-004-0528-z (cit. on p. 87).

[KS99] Kostas D. Kokkotas and Bernd G. Schmidt. "Quasinormal modes of stars and black holes". In: *Living Rev. Rel.* 2 (1999), p. 2. DOI: 10.12942/lrr-1999-2. arXiv: gr-qc/9909058 (cit. on p. 117).

[KSS05] P. Kovtun, Dan T. Son, and Andrei O. Starinets. "Viscosity in strongly interacting quantum field theories from black hole physics". In: *Phys. Rev. Lett.* 94 (2005), p. 111601. DOI: 10.1103/PhysRevLett.94.111601. arXiv: hep-th/0405231 (cit. on p. 3).

[Kud23] Jonah Kudler-Flam. "Rényi Mutual Information in Quantum Field Theory". In: *Phys. Rev. Lett.* 130.2 (2023), p. 021603. DOI: 10.1103/PhysRevLett.130.021603. arXiv: 2211.01392 [hep-th] (cit. on p. 6).

[KW20] Sumeet Khatri and Mark M. Wilde. "Principles of Quantum Communication Theory: A Modern Approach". In: (Nov. 2020). arXiv: 2011.04672 [quant-ph] (cit. on p. 6).

[KZ11] R. A. Konoplya and A. Zhidenko. "Quasinormal modes of black holes: From astrophysics to string theory". In: *Rev. Mod. Phys.* 83 (2011), pp. 793–836. DOI: 10.1103/RevModPhys.83.793. arXiv: 1102.4014 [gr-qc] (cit. on p. 117).

[Las14] Nima Lashkari. "Relative Entropies in Conformal Field Theory". In: *Phys. Rev. Lett.* 113 (2014), p. 051602. DOI: 10.1103/PhysRevLett.113.051602. arXiv: 1404.3216 [hep-th] (cit. on p. 5).

[LLNZ14] Alexey Litvinov, Sergei Lukyanov, Nikita Nekrasov, and Alexander Zamolodchikov. "Classical Conformal Blocks and Painleve VI". In: *JHEP* 07 (2014), p. 144. DOI: 10.1007/JHEP07(2014)144. arXiv: 1309.4700 [hep-th] (cit. on pp. 5, 119).

[LM01] Oleg Lunin and Samir D. Mathur. "Correlation functions for M**N / S(N) orbifolds". In: *Commun. Math. Phys.* 219 (2001), pp. 399–442. DOI: 10.1007/s002200100431. arXiv: hep-th/0006196 (cit. on pp. 53–56, 70, 71, 75–77, 86, 87, 89).

[LM13] Aitor Lewkowycz and Juan Maldacena. "Generalized gravitational entropy". In: *JHEP* 08 (2013), p. 090. DOI: 10.1007/JHEP08(2013)090. arXiv: 1304.4926 [hep-th] (cit. on p. 4).

[LM24] R. Loganayagam and Godwin Martin. "An Exterior EFT for Hawking Radiation". In: (Mar. 2024). arXiv: 2403.10654 [hep-th] (cit. on pp. 117, 127).

[LN22] O. Lisovyy and A. Naidiuk. "Perturbative connection formulas for Heun equations". In: *J. Phys. A* 55.43 (2022), p. 434005. DOI: 10.1088/1751-8121/ac9ba7. arXiv: 2208.01604 [math-ph] (cit. on pp. 119, 129, 139, 147).

[Lon19] Jiang Long. "Correlation function of modular Hamiltonians". In: *JHEP* 11 (2019), p. 163. DOI: 10.1007/JHEP11(2019)163. arXiv: 1907.00646 [hep-th] (cit. on p. 112).

[LRS20] R. Loganayagam, Krishnendu Ray, and Akhil Sivakumar. "Fermionic Open EFT from Holography". In: (Nov. 2020). arXiv: 2011.07039 [hep-th] (cit. on p. 117).

[LRSS21] R. Loganayagam, Krishnendu Ray, Shivam K. Sharma, and Akhil Sivakumar. "Holographic KMS relations at finite density". In: *JHEP* 03 (2021), p. 233. DOI: 10.1007/JHEP03(2021)233. arXiv: 2011.08173 [hep-th] (cit. on pp. 117, 186).

[LRV22] R. Loganayagam, Mukund Rangamani, and Julio Virrueta. "Holographic open quantum systems: Toy models and analytic properties of thermal correlators". In: (Nov. 2022). arXiv: 2211.07683 [hep-th] (cit. on pp. 117, 118, 127, 173).

[LRV23] R. Loganayagam, Mukund Rangamani, and Julio Virrueta. "Holographic thermal correlators: a tale of Fuchsian ODEs and integration contours". In: *JHEP* 07 (2023), p. 008. DOI: 10.1007/JHEP07(2023)008. arXiv: 2212.13940 [hep-th] (cit. on pp. 117, 119, 128, 134, 153).

[LX18] Roberto Longo and Feng Xu. "Relative Entropy in CFT". In: *Adv. Math.* 337 (2018), pp. 139–170. DOI: 10.1016/j.aim.2018.08.015. arXiv: 1712.07283 [math.OA] (cit. on p. 6).

[LZ03] Sergei K. Lando and Alexander Zvonkin. "Graphs on Surfaces and Their Applications". In: 2003 (cit. on p. 61).

[Mal98] Juan Martin Maldacena. "The Large N limit of superconformal field theories and supergravity". In: *Adv. Theor. Math. Phys.* 2 (1998), pp. 231–252. DOI: 10.4310/ATMP.1998.v2.n2.a1. arXiv: hep-th/9711200 (cit. on p. 2).

[Mat95] Marco Matone. "Instantons and recursion relations in N=2 SUSY gauge theory". In: *Phys. Lett. B* 357 (1995), pp. 342–348. DOI: 10.1016/0370-2693(95)00920-G. arXiv: hep-th/9506102 (cit. on p. 175).

[MN03] Lubos Motl and Andrew Neitzke. "Asymptotic black hole quasinormal frequencies". In: *Adv. Theor. Math. Phys.* 7.2 (2003), pp. 307–330. DOI: 10.4310/ATMP.2003.v7.n2.a4. arXiv: hep-th/0301173 (cit. on p. 173).

[MPS20] Alex May, Geoff Penington, and Jonathan Sorce. "Holographic scattering requires a connected entanglement wedge". In: *JHEP* 08 (2020), p. 132. DOI: 10.1007/JHEP08(2020)132. arXiv: 1912.05649 [hep-th] (cit. on p. 41).

[MRW17] Donald Marolf, Massimiliano Rota, and Jason Wien. "Handlebody phases and the polyhedrality of the holographic entropy cone". In: *JHEP* 10 (2017), p. 069. DOI: 10.1007/JHEP10(2017)069. arXiv: 1705.10736 [hep-th] (cit. on p. 10).

[MS24] Godwin Martin and Shivam K. Sharma. "Open EFT for Interacting Fermions from Holography". In: (Mar. 2024). arXiv: 2403.10604 [hep-th] (cit. on p. 186).

[MS89a] Gregory W. Moore and Nathan Seiberg. "Classical and Quantum Conformal Field Theory". In: *Commun. Math. Phys.* 123 (1989), p. 177. DOI: 10.1007/BF01238857 (cit. on pp. 4, 133).

[MS89b] Gregory W. Moore and Nathan Seiberg. "LECTURES ON RCFT". In: *1989 Banff NATO ASI: Physics, Geometry and Topology*. Sept. 1989 (cit. on p. 133).

[MSY22] Alex May, Jonathan Sorce, and Beni Yoshida. "The connected wedge theorem and its consequences". In: *JHEP* 11 (2022), p. 153. DOI: 10.1007/JHEP11(2022)153. arXiv: 2210.00018 [hep-th] (cit. on p. 41).

[Nek03] Nikita A. Nekrasov. "Seiberg-Witten prepotential from instanton counting". In: *Adv. Theor. Math. Phys.* 7.5 (2003), pp. 831–864. DOI: 10.4310/ATMP.2003.v7.n5.a4. arXiv: hep-th/0206161 (cit. on p. 175).

[Nek17] Nikita Nekrasov. "BPS/CFT correspondence V: BPZ and KZ equations from qq-characters". In: (Nov. 2017). arXiv: 1711.11582 [hep-th] (cit. on p. 121).

[Nis18] Tatsuma Nishioka. "Entanglement entropy: holography and renormalization group". In: *Rev. Mod. Phys.* 90.3 (2018), p. 035007. DOI: 10.1103/RevModPhys.90.035007. arXiv: 1801.10352 [hep-th] (cit. on pp. 5, 88).

[NS03] Alvaro Nunez and Andrei O. Starinets. "AdS / CFT correspondence, quasinormal modes, and thermal correlators in N=4 SYM". In: *Phys. Rev. D* 67 (2003), p. 124013. DOI: 10.1103/PhysRevD.67.124013. arXiv: hep-th/0302026 (cit. on p. 164).

[NS04] Jose Natario and Ricardo Schiappa. "On the classification of asymptotic quasi-normal frequencies for d-dimensional black holes and quantum gravity". In: *Adv. Theor. Math. Phys.* 8.6 (2004), pp. 1001–1131. DOI: 10.4310/ATMP.2004.v8.n6.a4. arXiv: hep-th/0411267 (cit. on pp. 173, 178).

[Pes03] Ingo Peschel. "Calculation of reduced density matrices from correlation functions". In: *Journal of Physics A: Mathematical and General* 36.14 (Mar. 2003), pp. L205–L208. DOI: 10.1088/0305-4470/36/14/101. URL: https://doi.org/10.1088%2F0305-4470%2F36%2F14%2F101 (cit. on pp. 6, 90, 97).

[PRR09] Ari Pakman, Leonardo Rastelli, and Shlomo S. Razamat. "Diagrams for Symmetric Product Orbifolds". In: *JHEP* 10 (2009), p. 034. DOI: 10.1088/1126-6708/2009/10/034. arXiv: 0905.3448 [hep-th] (cit. on pp. 54, 55, 90, 92).

[PSS01] G. Policastro, Dan T. Son, and Andrei O. Starinets. "The Shear viscosity of strongly coupled N=4 supersymmetric Yang-Mills plasma". In: *Phys. Rev. Lett.* 87 (2001), p. 081601. DOI: 10.1103/PhysRevLett.87.081601. arXiv: hep-th/0104066 [hep-th] (cit. on p. 3).

[PSS02] Giuseppe Policastro, Dam T. Son, and Andrei O. Starinets. "From AdS / CFT correspondence to hydrodynamics. 2. Sound waves". In: *JHEP* 12 (2002), p. 054. DOI: 10.1088/1126-6708/2002/12/054. arXiv: hep-th/0210220 (cit. on p. 183).

[PT99] B. Ponsot and J. Teschner. "Liouville bootstrap via harmonic analysis on a noncompact quantum group". In: (Nov. 1999). arXiv: hep-th/9911110 (cit. on pp. 4, 133).

[Ree09] Balt C. van Rees. "Real-time gauge/gravity duality and ingoing boundary conditions". In: *Nucl. Phys. Proc. Suppl.* 192-193 (2009), pp. 193–196. DOI: 10.1016/j.nuclphysbps.2009.07.078. arXiv: 0902.4010 [hep-th] (cit. on p. 125).

[Rib14] Sylvain Ribault. "Conformal field theory on the plane". In: (June 2014). arXiv: 1406.4290 [hep-th] (cit. on pp. 130, 131).

[RT06a] Shinsei Ryu and Tadashi Takayanagi. "Holographic derivation of entanglement entropy from AdS/CFT". In: *Phys. Rev. Lett.* 96 (2006), p. 181602. DOI: 10.1103/PhysRevLett.96.181602. arXiv: hep-th/0603001 (cit. on p. 3).

[RT06b] Shinsei Ryu and Tadashi Takayanagi. "Holographic derivation of entanglement entropy from AdS/CFT". In: *Phys. Rev. Lett.* 96 (2006), p. 181602. DOI: 10.1103/PhysRevLett.96.181602. arXiv: hep-th/0603001 (cit. on pp. 19, 96).

[RVZ23] Mukund Rangamani, Julio Virrueta, and Shuyan Zhou. "Anomalous hydrodynamics effective actions from holography". In: *JHEP* 11 (2023), p. 044. DOI: 10.1007/JHEP11(2023)044. arXiv: 2306.01055 [hep-th] (cit. on p. 186).

[RW18] Massimiliano Rota and Sean J. Weinberg. "New constraints for holographic entropy from maximin: A no-go theorem". In: *Phys. Rev. D* 97.8 (2018), p. 086013. DOI: 10.1103/PhysRevD.97.086013. arXiv: 1712.10004 [hep-th] (cit. on p. 10).

[SMJ79] M. Sato, T. Miwa, and M. Jimbo. "Holonomic Quantum Fields. II. The Riemann-hilbert Problem". In: *Publ. Res. Inst. Math. Sci. Kyoto* 15 (1979), pp. 201–278. DOI: 10.2977/prims/1195188429 (cit. on p. 83).

[SR08] Kostas Skenderis and Balt C. van Rees. "Real-time gauge/gravity duality". In: *Phys. Rev. Lett.* 101 (2008), p. 081601. DOI: 10.1103/PhysRevLett.101.081601. arXiv: 0805.0150 [hep-th] (cit. on p. 117).

[SR09] Kostas Skenderis and Balt C. van Rees. "Real-time gauge/gravity duality: Prescription, Renormalization and Examples". In: *JHEP* 05 (2009), p. 085. DOI: 10.1088/1126-6708/2009/05/085. arXiv: 0812.2909 [hep-th] (cit. on p. 117).

[SS02] Dam T. Son and Andrei O. Starinets. "Minkowski space correlators in AdS / CFT correspondence: Recipe and applications". In: *JHEP* 09 (2002), p. 042. DOI: 10.1088/1126-6708/2002/09/042. arXiv: hep-th/0205051 [hep-th] (cit. on pp. 117, 119, 125, 128, 173).

[Sus95] Leonard Susskind. "The World as a hologram". In: *J. Math. Phys.* 36 (1995), pp. 6377–6396. DOI: 10.1063/1.531249. arXiv: hep-th/9409089 (cit. on p. 2).

[t H93] Gerard 't Hooft. "Dimensional reduction in quantum gravity". In: *Conf. Proc. C* 930308 (1993), pp. 284–296. arXiv: gr-qc/9310026 (cit. on p. 2).

[Tac13] Yuji Tachikawa. *N=2 supersymmetric dynamics for pedestrians*. Dec. 2013. DOI: 10.1007/978-3-319-08822-8. arXiv: 1312.2684 [hep-th] (cit. on p. 176).

[Tes16] Jörg Teschner. "Exact Results on $\mathcal{N} = 2$ Supersymmetric Gauge Theories". In: *New Dualities of Supersymmetric Gauge Theories*. Ed. by Jörg Teschner. 2016, pp. 1–30. DOI: 10.1007/978-3-319-18769-3_1. arXiv: 1412.7145 [hep-th] (cit. on p. 5).

[Tes17] Joerg Teschner. "Classical conformal blocks and isomonodromic deformations". In: (July 2017). arXiv: 1707.07968 [hep-th] (cit. on p. 119).

[Wal14] Aron C. Wall. "Maximin Surfaces, and the Strong Subadditivity of the Covariant Holographic Entanglement Entropy". In: *Class. Quant. Grav.* 31.22 (2014), p. 225007. DOI: 10.1088/0264-9381/31/22/225007. arXiv: 1211.3494 [hep-th] (cit. on p. 4).

[Wit18] Edward Witten. "APS Medal for Exceptional Achievement in Research: Invited article on entanglement properties of quantum field theory". In: *Rev. Mod. Phys.* 90.4 (2018), p. 045003. DOI: 10.1103/RevModPhys.90.045003. arXiv: 1803.04993 [hep-th] (cit. on pp. 5, 92).

[Wit98] Edward Witten. "Anti-de Sitter space and holography". In: *Adv. Theor. Math. Phys.* 2 (1998), pp. 253–291. DOI: 10.4310/ATMP.1998.v2.n2.a2. arXiv: hep-th/9802150 (cit. on p. 2).

[Zam86] Al B Zamolodchikov. "Two-dimensional conformal symmetry and critical four-spin correlation functions in the Ashkin-Teller model". In: *Soviet Journal of Experimental and Theoretical Physics* 63.5 (1986), p. 1061 (cit. on pp. 119, 133).

[Zam87] A. B. Zamolodchikov. “Conformal Scalar Field on the Hyperelliptic Curve and Critical Ashkin-teller Multipoint Correlation Functions”. In: *Nucl. Phys. B* 285 (1987), pp. 481–503. DOI: 10.1016/0550-3213(87)90350-6 (cit. on pp. 63, 84).

[ZCZW19] Bei Zeng, Xie Chen, Duan-Lu Zhou, and Xiao-Gang Wen. *Quantum Information Meets Quantum Matter: From Quantum Entanglement to Topological Phases of Many-Body Systems*. Quantum Science and Technology. Springer, 2019. ISBN: 978-1-4939-9082-5, 978-1-4939-9084-9. DOI: 10.1007/978-1-4939-9084-9. arXiv: 1508.02595 [cond-mat.str-el] (cit. on p. 5).